REMARKS

Objection to the specification

The specification is objected to for misspelling "adjuvans" and for the term "galenicals".

Although, the term is clearly defined at page 4, lines 13-16 of the present specification, this does indeed seem to be a misspelling or mistranslation of the term "adjuvants.". With this amendment, the spelling of the term "adjuvans" has been corrected to "adjuvant."

Regarding the term "galenicals," although the term is somewhat archaic, a dictionary definition of the term is available to anyone. Examples of dictionary definitions of the term are attached herewith as Attachment A. Further clarification is found in the discussion following the use of the term in the last paragraph on page 9.

In view of Applicants' arguments, withdrawal of all objections to the specification is respectfully requested.

Rejection under 35 U.S.C. § 112, first paragraph

Claims 1 and 15 are rejected under 35 U.S.C. § 112, first paragraph as containing subject matter which is not described in the specification in such a way so as to enable one skilled in the art to which it pertains to make and/or use the invention.

The Examiner argues that the present claims are not enabled because the prior art teaches that tumor cells are less phenotypically stable than normal cells and escape the immune response of the host by various mechanisms. The Office Action cites an Immunology text by Paul which teaches that tumor cells escape immune detection by deficient antigen presentation (Office action, page 4, lines 10-page 5, line 1). Although the Examiner acknowledges that the specification teaches induction of cytotoxic T cells against tumor cells in vitro (Office Action, page 3, line 21-22), the Office Action posits that the claimed peptide would not be effective against a tumor in situ (Office Action, page 5, lines 1-3).

In response, Applicants submit clinical results using SEQ ID NOS:1 & 2 of the present application as published by P. Brossart, one of the inventors of the present application, and colleagues (Wierecky J, Mueller M, Brossart P. *Dendritic cell-based cancer immunotherapy targeting MUC-1*. Cancer Immunol Immunother. 2005 (Attachment B). The publication demonstrates that objective clinical responses (1 complete response, 2 partial responses) can be

achieved in late-stage patients (stage IV renal cell carcinoma). This evidence directly rebuts the Examiner's assertion that the claimed peptide would not be effective against a tumor in situ.

The following discussion addresses points raised in the Office Action. References referred to are found in Attachment C, unless otherwise specified.

The Examiner appears to think that the present invention lacks enablement due to an escape of the cells by deficient antigen presentation (page 4, with respect to Paul et al.), i.e. that an antigen presentation would be required. This is not completely correct. The aberrant post-translational modification of MUC1 in cancer cells leads to an intracellular accumulation of MUC1, without a secretion thereof. In carcinomas, MUC1 overexpression is found in tumors from breast, lung, kidney, and thyroid and correlates with an aggressive tumor and increased metastasis. A recent immunohistological study of 71 breast carcinomas, coupled with a review of the literature, indicates that it is actually the aberrant localization of intracellular MUC1 that is associated with a worse prognosis for the patient. The expression of MUC1-protein at the cellular surface is <u>irrelevant</u> for the recognition of the tumor cells by either CD8+ or CD4+ T-cells, which recognize peptides in conjunction with HLA class I or HLA class II molecules, respectively. It is crucial that short peptides of MUC1, such as the one that is claimed, are generated from intracellular sources of polypeptides proteins. Such a generation of peptides is based on processes such as translation-stop-products (DRiPs, "defective ribosomal products", see Schubert U, Anton LC, Gibbs J, Norbury CC, Yewdell JW, Bennink JR. *Rapid degradation of a large fraction of newly synthesized proteins by proteasomes.* Nature. 2000 Apr 13;404(6779):770-4) that serve as source for MHC-class-I-associated peptides (Princiotta MF, Finzi D, Qian SB, Gibbs J, Schuchmann S, Buttgereit F, Bennink JR, Yewdell JW. *Quantitating protein synthesis, degradation, and endogenous antigen processing.* Immunity. 2003 Mar;18(3):343-54.) and complete intracellular proteins. Furthermore, it was shown that in HLA-A*02-transgenic mice, T-cells being specific for A*02-associated peptides from MUC1 protect the mice from the development of tumors derived from injected tumor cells expressing MUC1 (Heukamp LC, van der Burg SH, Drijfhout JW, Melief CJ, Taylor-Papadimitriou J, Offringa R. *Identification of three non-VNTR MUC1-derived HLA-A*0201-restricted T-cell epitopes that induce protective anti-tumor immunity in HLA-A2/K(b)-transgenic mice.* Int J Cancer. 2001 Feb 1;91(3):385-92.).

As discussed above, clinical results with exactly the two MUC1 peptides disclosed by Applicants including the claimed peptide were published by P. Brossart and colleagues (Wierecky J, Mueller M, Brossart P. *Dendritic cell-based cancer immunotherapy targeting MUC-1*. Cancer Immunol Immunother. 2005; see Attachment B for this reference), demonstrating that objective clinical responses (1 complete response, 2 partial responses) can be achieved in late-stage patients (stage IV renal cell carcinoma).

The Office Action also refers to "tumor escape"-mechanisms, such as, for example as mentioned in Paul et al., "Fundamental Immunology". Nevertheless, the interpretation and conclusions of the Examiner with respect to the existence of such mechanisms and their effects on the invention are incorrect. As is the case in other prominent cancer therapeutics, the present invention does not provide a cure for cancer based on the provision of MUC1-peptide, but provides a treatment for the disease, e.g., a slow-down of the progression of the disease, an increase in overall survival, an improved time to treatment failure by either toxicity or death, an increase in progression-free survival (clinical efficacy in oncology trials is usually demonstrated in randomized phase II clinical trials based on clinical endpoints such as, e.g., "time to disease progression", "median survival time", "2-year survival rate", "5-year-survival rate", "overall survival", "disease-free survival", "objective response rate", "progression-free survival", or "time to treatment failure") and/or an improved "quality of life", which can, e.g., be measured in "Quality-adjusted life years (QALY)". Thus, the present invention relates to a treatment of cancer, and is not directed to a cure. Nevertheless, the present invention and the active, i.e. T-cell-based immunotherapy as such can be employed with success, as can be seen, for example in Provenge™ of the Dendreon Corp. in the field of prostate cancer (Phase III-results show a significant increase of survival in the treatment arm vs. the placebo arm, published by Dendreon Corp. on 17 February 2005. The corresponding scientific publication for earlier phase II results are found in Burch PA, Croghan GA, Gastineau DA, Jones LA, Kaur JS, Kylstra JW, Richardson RL, Valone FH, Vuk-Pavlovic S. *Immunotherapy (APC8015, Provenge) targeting prostatic acid phosphatase can induce durable remission of metastatic androgen-independent prostate cancer: a Phase 2 trial*. Prostate. 2004 Aug 1;60(3):197-204.). Another example of successful T-cell based immunotherapy is found with autologous lysates in the field of renal cancer (Liponova, published phase III-results in Jocham D, Richter A, Hoffmann L, Iwig K, Fahlenkamp D,

Zakrzewski G, Schmitt E, Dannenberg T, Lehmacher W, von Wietersheim J, Doehn C. *Adjuvant autologous renal tumour cell vaccine and risk of tumour progression in patients with renal-cell carcinoma after radical nephrectomy: phase III, randomised controlled trial.* Lancet. 2004 Feb 21; 363 (9409): 594-9), and with BLP25 of Biomira Inc. in the field of non-small cell lung carcinoma (results of a phase IIb-study presented at the 2005 ASCO Meeting on 14 May 2005 as a poster titled "A Liposomal MUC1 Vaccine for Treatment of Non-Small Cell Lung Cancer (NSCLC); Updated Survival Results from Patients with Stage IIIB Disease", Murray, et al. Abstract No. 7037) using a 25-mer-peptide from MUC1. Accordingly, successful cancer vaccines are known including the vaccine peptide claimed by Applicants.

The Office Action also states that the pharmaceutical composition of claim 15 does not include co-stimulators although the specification teaches that they are required. These co-stimulators are dendritic cells (professional antigen presenting cells that are presenting the peptides, i.e. cells that are provided in vivo by the body). Dendritic cells may be recruited to the site of injection of a pharmaceutical product containing peptides as the sole active pharmaceutical ingredient by previous injection of a chemoattractant for dendritic cells such as, e.g., granulocyte-macrophage colony-stimulating factor (GM-CSF), or a classical adjuvant such as, e.g., Montanide-ISA-51. It has been shown previously by others (G. Gaudernack et al., *Clinical trials of a peptide based vaccine targeting telomerase*, 2003 ASCO Meeting, abstract no. 666 and presentation) that this approach is feasible. It can make sense to apply an adjuvant in order to further activate and/or recruit dendritic cells (as mentioned on page 4 of the description), nevertheless, this is not mandatory in order to achieve an effective pharmaceutical preparation.

Scientific results that show the suitability of HLA-A*02-restricted peptides as vaccines in cancer-immunotherapy, are published, for example, in Banchereau et al. (Banchereau J, Palucka AK, Dhodapkar M, Burkeholder S, Taquet N, Rolland A, Taquet S, Coquery S, Wittkowski KM, Bhardwaj N, Pineiro L, Steinman R, Fay J. *Immune and clinical responses in patients with metastatic melanoma to CD34(+) progenitor-derived dendritic cell vaccine.* Cancer Res. 2001 Sep 1;61(17):6451-8). It was shown in 1997 in the case of T-cell-reactivities against multiple myeloma-cells that MUC1 is an antigen on myeloma cells that is recognized both by CD8-positive as well as CD4-positive T-cells (Noto H, Takahashi T, Makiguchi Y, Hayashi T, Hinoda Y, Imai K. *Cytotoxic T lymphocytes derived from bone marrow mononuclear cells of multiple*

myeloma patients recognize an underglycosylated form of MUC1 mucin. Int Immunol. 1997 May;9(5):791-8).

In summary, and in contrast to the opinion of the Examiner, the person skilled in the art would be able to practice the claimed invention based upon the description in the specification. The clinical evidence in Attachment B, obtained using the peptide of the claimed invention, directly rebuts the Examiner's position that the clamed invention is not enabled for in vivo disease treatment. MUC1 represents an antigen that is over-expressed in tumors on the level of protein, from which peptides can be derived in amounts that are suitable for a stimulation/expansion of specific, MHC class I-restricted, in particular HLA-A*02-restricted, T-cells. These T-cells that recognize peptides from MUC1 on MHC class I-molecules (in particular HLA-A*02-molecules) are suitable to mediate protective immunity in vivo as shown in HLA-A*02-transgenic mice against MUC1-expressing tumor cells of epithelial tumors (see papers above) and were shown in patients to be associated with objective clinical responses (see papers above). Thus, the presently claimed MUC1-peptide as well as its use in a pharmaceutical preparation is completely enabled by the present specification.

In view of Applicants' arguments which are supported by the references provided in Attachments B & C, reconsideration and withdrawal of this ground of rejection is respectfully requested.

Rejoinder

Claims 1 and 15 are now believed to be in condition for allowance in view of the arguments presented above. Accordingly, Applicants respectfully request rejoinder of claims 21, 24, 27, 29, and 31.

CONCLUSION

In view of Applicants' amendments to the specification and the foregoing Remarks, it is respectfully submitted that the present application is in condition for allowance. Should the Examiner have any remaining concerns which might prevent the prompt allowance of the application, the Examiner is respectfully invited to contact the undersigned at the telephone number appearing below.

Please charge any additional fees, including any fees for additional extension of time, or credit overpayment to Deposit Account No. 11-1410.

Respectfully submitted,

KNOBBE, MARTENS, OLSON & BEAR, LLP

Dated: July 18, 2005

By: _Che S. Chereskin_

Che Swyden Chereskin, Ph.D.
Registration No. 41,466
Agent of Record
Customer No. 20,995
(949) 760-0404

1787939
062405

msn Encarta®

> > **Subscribe**

Reference | **Enc**

Dictionary

Find

galenical   in   [Dictionary]

Click here to search all of MSN Encarta

Advertisement

Dictionary   Thesaurus   Translations *

BEST AVAILABLE COPY

galenical

galax
Galaxy
galaxy
galaxy cluster
galbanum
gale
galea
galena
▶ **galenical**
galenite
galère
Galesburg
galette
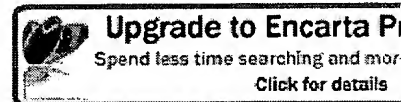gali
Galibi
Galilean (1)
Galilean (2)

ga·len·i·cal [gə lé′enik′l]

noun (*plural* ga·len·i·cals)

natural drug: any medicinal preparation that is made from plant or animal tissue, especially vegetable matter, rather than being created synthetically

adjective

not synthetic: made from plant or animal tissue rather than synthesized

[Mid-17th century. Formed from Galen, because he prescribed such remedies.]

Print Preview

See pronunciation key

Search for **"galenical"** in all of MSN Encarta

Download the MSN Encarta Right-Click Dictionary

Our Partners

- Amazon: Buy books
- ClassesUSA.com: Compare onlin
- CollegeBound Network: ReadyS
- hq|education: Career education
- Kaplan Test Prep and Admission:
- The Princeton Review
- Sylvan Learning Center

Also on Encarta

- Finish that degree: Nursing, bac MBA, and more
- You're smart, right? Help us mal better
- Special: Helping kids succeed at

More Links from Our Advertisers

SAT Prep	**Tutoring**
Distance Learning	**Online MBA**
Education Online	**Textbook**

Also on MSN

- Supervolcano on the Discovery (
- Tired of your job? Train to be a (
  designer, Web master ...
- Travel Central: Heroes of Africa

MSN Shopping

**Arrow Striped Poplin Shirt -
$32.00 Sale $19.2**
Kohl's
More Men's Casual Button-D(

infoplease®

All the knowledge you need.

Enter search term | in | All Infoplease | Search

Daily Almanac for Apr. 12, 2005

Home   Almanacs   Atlas   Encyclopedia   Dictionary   Thesaurus   White Pages

World & News

United States

History & Gov't

Biography

Sports

Arts & Ent.

Business

Society & Culture

Health & Science

Homework Center

Fact Monster
Kid's reference,
games, quizzes

RSS Daily Almanac

This Day in History

Today's Birthday

Word of the Day

Editor's Favorites

Poetry Month

British Royalty

Pope John Paul II

Titanic Anniversary

Earth Day

Quotations

2005 Calendar

Timelines

Infoplease Tools

Periodic Table

Conversion Tool

Perpetual Calendar

Year by Year

Help | Site Map

Career Center

Job Search

Post Your Resume

Continuing Ed.

Dictionary

ga•len•i•cal

Pronunciation: (gā-len'i-kul, gu-), [key]
—*n.*
1. an herb or other vegetable drug, distinguished from a mineral or chemical drug.
2. a crude drug, tincture, or decoction, distinguished from a preparation that has been refined.

—*adj.*
1. galenic.
2. (*cap.*) Galenic (def. 1).
3. Galenic (def. 2).

Random House Unabridged Dictionary, Copyright © 1997, by Random House, Inc., on Infoplease

PAGE TOOLS: CITE | PRINT | EMAIL | HOTWORDS

galenic

Galenic pharmacy

more . . .

Search: Infoplease

[ ] go!
Info search tips

Search: Biographies

[ ] go!
Bio search tips

Symposium Paper

Dendritic cell-based cancer immunotherapy targeting MUC-1

J. Wierecky[1], M. Mueller[1] and P. Brossart[1] ✉

(1) Department of Oncology, Hematology, Immunology, and Rheumatology, Medizinische Klinik, University of Tuebingen Medical Center, Otfried-Mueller-Str. 10, Tuebingen, 72076, Germany

✉ P. Brossart
Email: peter.brossart@med.uni-tuebingen.de
Fax: +49-7071-295709

Abstract Vaccination therapy using dendritic cells (DC) as antigen presenting cells (APC) has shown significant promise in laboratory and animal studies as a potential treatment for malignant diseases. Pulsing of autologous DCs with tumor-associated antigens (TAA) is a method often used for antigen delivery and choice of suitable antigens plays an important role in designing an effective vaccine. We identified two HLA-A2 binding novel 9-mer peptides of the TAA MUC1, which is overexpressed on various hematological and epithelial malignancies. Cytotoxic T cells generated after pulsing DC with these peptides were able to induce lysis of tumor cells expressing MUC1 in an antigen-specific and HLA-restricted fashion. Within two clinical studies, we demonstrated that vaccination of patients with advanced cancer using DCs pulsed with MUC1 derived peptides is well tolerated without serious side effects and can induce immunological responses. Of 20 patients with metastatic renal cell carcinoma, 6 patients showed regression of metastases with 3 objective responses (1 CR, 2 PR). Furthermore, we found that in patients responding to treatment T cell responses for antigens not used for treatment occurred suggesting that antigen spreading in vivo might be a possible mechanism of mediating antitumor effects. These results demonstrate that immunotherapy in patients with advanced malignancies using autologous DCs pulsed with MUC1 derived peptides can induce immunological and clinical responses. However, further clinical studies are needed to identify the most potent treatment regimen that can consistently mediate an antitumor immune response in vivo.

This article is a symposium paper from the conference "Progress in Vaccination against Cancer 2004 (PIVAC 4)", held in Freudenstadt-Lauterbad, Black Forest, Germany, on 22–25 September 2004.

Introduction

The development of effective cancer vaccines relies not only on the identification of tumor-associated antigens (TAA), but also on the choice of antigen source as well as the optimal route of antigen delivery and using of adjuvants [1]. One of the most promising approaches to cancer immunotherapy is the administration of antigen-presenting cells (APC) such as dendritic cells (DC) loaded with TAA. DCs are the most potent APCs expressing high levels of major histocompatibility complex (MHC) and various immunomodulatory proteins and capable of sensitizing T cells to new and recall antigens [2]. Several techniques were established to load DCs with TAA. Peptides derived from endocytosed tumor lysates can be presented on MHC molecules after proteolytic processing [3]. RNA encoding for TAA or derived from tumor cells can be used to generate TAA in DC themselves [4]. One of the most common ways of generating tumor-specific immune responses is pulsing of DC with human leukocyte antigen (HLA) class I- and class II binding peptides, which are able to bind directly to the MHC molecule on the cell surface [5, 6].

MUC1 mucins are highly glycosylated type I glycoproteins expressed by various normal and malignant epithelial cells such as breast, kidney and ovarian cancers and hematologic malignancies including acute myelogenous leukemia (AML), multiple myeloma and some B-cell lymphoma [7–9]. The complex molecule is anchored within the cell surface by a transmembrane domain. The largest part is a unique extracellular domain with a variable number of tandem repeats (VNTR) of 20 amino acids [10, 11]. The overexpression of MUC1 in many malignancies makes it an attractive and broadly applicable target for cancer vaccination therapies [12, 13]. Previous studies have shown that the tandem repeat of MUC 1 is highly immunogenic and that peptides derived from this domain are recognized by cytotoxic T cells [14, 15]. Furthermore, it has been demonstrated that epitopes derived from this domain can initiate antibody-mediated immune responses [16, 17].

The majority of known TAA epitopes are presented within MHC class I molecules and are recognized by cytotoxic T cells (CTL), whereas a small number of TAA peptides are presented in association with MHC class II molecules and recognized by CD4+ T cells [18–20]. Most of TAA peptides used in cancer vaccination trials bind HLA-A2, the most common MHC class I molecule among Caucasians. The characterization of MHC class I allele-specific motifs to define epitopes contained within a given antigen was an important step in the development of effective cancer vaccines [21, 22].

Identification of MUC1 derived epitopes

For identification of MUC1 derived epitopes, which can be used for dendritic cell-based vaccination therapies, we screened the MUC1 protein for HLA-A2-binding peptides using a computer-assisted analysis [23, 24]. Two novel 9-mer peptides, M1.1 and M1.2, could be identified. Both peptides showed a high binding probability to HLA-A2. The M1.1 peptide is derived from the tandem repeat region of the MUC1 protein whereas M1.2 is localized within the signal sequence of MUC1 [25, 26]. To analyze whether these epitopes are presented by tumor cells endogenously expressing MUC1, we induced MUC1 peptide-specific CTL responses by

primary in vitro immunization and used these CTL to determine the presentation of MUC1 epitopes on human tumor lines. DC were pulsed with M1.1 and M1.2 and demonstrated a high ability to initiate an MUC1-specific CTL responses. Incubation with the Pan-DR binding peptide PADRE was able to amplify the antigen-specific cytotoxic activity of the induced CTL [27].

In previous studies, it was shown that pulsing human lymphocytes with a liposome-encapsulated MUC1 peptides consisting of 25 amino acids from the VNTR could induce cytotoxic T-cell responses [28]. Comparable to the results obtained in our experiments MUC1 peptide-specific cytotoxic T-cell responses as well as the secretion of IFN-gamma were detected when the in vitro induced CTL were analyzed for their effector functions. In our study, we demonstrated that CTL were able to recognize tumor cells endogenously expressing the MUC1 protein in an HLA-A2-restricted manner and lysed cell lines of breast, pancreatic and renal cell cancer expressing MUC1 and HLA-A2. The cytotoxicity against tumor cells could be inhibited by cold HLA-A2+ targets pulsed with the cognate peptide in a cold-target inhibition assay and by anti-HLA-A2 MoAb.

An increased expression and secretion of the MUC1 protein is an independent predictor of poor prognosis and early metastatic disease in cancer patients [29, 30]. It was shown that the MUC1 protein can induce apoptosis of activated T cells in vitro [31]. Furthermore, it has been demonstrated that cancer associated MUC1 inhibits T-cell proliferation [32]. This inhibition was mediated by the whole MUC1 protein or large synthetic tandem repeats of the MUC1 core peptide and was reversible by addition of IL-2, anti-CD28 MoAb or short 16-amino acid MUC1 peptide, indicating that vaccination therapy using short synthetic peptides in combination with DC and/or IL-2 may overcome the observed immunosuppression in cancer patients. These findings were supported by studies with MUC1 transgenic mice, where the tolerance to human MUC1 antigen could be reversed by immunizing the animals with fusions of DC- and MUC1-expressing tumor cells [33].

Our results showed that the use of MUC1-derived peptides for a DC-based active specific immunotherapy could reverse the observed immunosuppression and MUC1 tolerance in cancer patients and provide an additional, broadly applicable approach to established therapies of epithelial malignancies, such as renal cell, breast, and pancreatic carcinoma.

Vaccinations with peptide pulsed dendritic cells. Clinical and immunological responses

In a phase I/II study, we analyzed the feasibility and efficacy of HER-2/neu or MUC1 peptide-pulsed "mature" monocyte derived DC vaccinations in heavily pretreated patients with metastatic cancer [34]. All patients had histologically confirmed metastatic breast or ovarian cancer that expressed HER-2/neu or MUC1. Ten patients with advanced diseases that were pretreated by multiple cycles of chemotherapy, including high-dose chemotherapy and autologous stem cell transplantation were included in this study. DC were pulsed with two HLA-A2 binding peptides deduced from MUC1 and two derived from the HER-2/neu protein (E75 and GP2) [35, 36]. Vaccinations were performed sc every 2 weeks four times and repeated

afterwards monthly until tumor progression. The vaccinations were tolerated with no side effects. After three vaccinations, peptide-specific CTL could be detected in 5 of 10 patients in the peripheral blood using both intracellular IFN-gamma staining and ^{51}Cr-release assays, suggesting that even after high-dose chemotherapy TAA-pulsed DCs can induce antigen-specific immune responses. The main immunologic responses in vivo were induced with the HER-2/neu-derived E75 and the MUC1-derived M1.2 peptide, which lasted for more than 6 months, suggesting that these two peptides might be immunodominant. In one patient treated with MUC-1 peptide-pulsed DC, CEA- and MAGE-3 peptide-specific T-cell responses were detected after several vaccinations and MUC1 peptide-specific T cells were observed in another patient after seven immunizations with HER-2/neu-derived peptides, suggesting that antigen spreading in vivo might occur after successful immunization with a single T cell epitope.

One possible mechanism for this kind of antigen spreading might be the induction of other tumor antigen-specific CTL as a result of the destruction of the malignant cells by the in vivo-induced CTL and uptake and processing of the killed cells by APC, such as DC or macrophages [37–39]. In this report, we showed for the first time that vaccination therapy using DC pulsed with HER-2/neu- or MUC1-derived peptides can induce immunologic responses in patients with advanced metastatic breast and ovarian cancers.

In the subsequent study, we analyzed the clinical and immunological responses in patients with metastatic renal cell carcinoma (RCC) using autologous mature monocyte derived DC pulsed with the HLA-A2 binding MUC1 peptides.

Therapy of metastatic RCC is still challenging because of its resistance to conventional therapies such as radiation or chemotherapy [40]. In view of the observed spontaneous remissions of advanced RCC and infiltration of cancer tissue with lymphocytes and dendritic cells, immune mechanisms have been suggested to play a role in the natural disease course of RCC and immunotherapy strategies like interleukin-2 (IL-2) and interferon-α (IFN-α) were developed [41, 42]. However, therapy is often only moderately tolerated and response rates of 20–30% remain unsatisfactory [43].

This has lead to a proliferation of clinical trials testing the effectiveness of DC-based immunotherapy in patients with advanced RCC [44–47]. We vaccinated 20 patients with metastatic RCC with DC loaded with the MUC1 derived peptides M1.1. and M1.2. For the activation of CD4+ T-helper lymphocytes, DC were further incubated with the PAN-HLA-DR binding peptide PADRE.

Vaccinations were performed sc every 2 weeks four times and repeated afterwards monthly until tumor progression. After the fifth DC injection, patients additionally received three injections/week of low dose IL-2 (1Mio IE/m^2) sc. In six patients, regression of metastases was induced with 3 objective responses (1 CR, 2 PR) and two mixed responses. Four patients had a stabilization of the disease. The enhancement of T cell precursor was monitored using IFN-γ

ELISPOT and ^{51}Cr-release assays. MUC1 peptide specific T cell responses in vivo were detected in the PBMC of all patients with objective responses. These in vivo induced CTL were able to recognize target cells pulsed with the cognate peptide or matched allogeneic tumor cells of the cell line A498 (RCC, MUC1+, HLA-A2+) constitutively expressing MUC1 in an antigen and HLA restricted manner after in vitro restimulation. Similar to the preceding study, we could

demonstrate that patients responding to the treatment developed T cell responses to HLA-A2 restricted epitopes not used for vaccinations like adipophilin, telomerase or OFA indicating that epitope spreading might occur. Proliferative responses to the PADRE peptide were detectable in 11 out of 16 analyzed patients, in some patients already after the first 2–3 vaccinations.

Conclusion

DC-based vaccination therapy for patients with malignant diseases has been a focus of intense research over the last years. Several different techniques of antigen loading of DC were established, the most widely used being incubation of DC with HLA-binding tumor-associated peptides. We were able to identify two HLA-A2 restricted peptides from the MUC1 protein and generated MUC-1 specific CTL, which lysed tumor cell endogenously expressing MUC1 in an HLA-A2 restricted fashion in vitro. We demonstrated that vaccination therapy in patient with advanced RCC can induce immunological and clinical responses. Irrespective of the small number of patients treated in these trials, the findings are encouraging and warrant further studies of tumor vaccination, particularly in patients with limited disease.

References

1. Mullins DW, Sheasley SL, Ream RM, Bullock TN, Fu YX, Engelhard VH (2003) Route of immunization with peptide-pulsed dendritic cells controls the distribution of memory and effector T cells in lymphoid tissues and determines the pattern of regional tumor control. J Exp Med 198:1023–1034

2. Lanzavecchia A, Sallusto F. (2001) Regulation of T cell immunity by dendritic cells. Cell 106:263–266

3. Banchereau J, Schuler-Thurner B, Palucka AK, Schuler G (2001) Dendritic cells as vectors for therapy. Cell 106:271–274

4. Muller MR, Tsakou G, Grunebach F, Schmidt SM, Brossart P (2004) Induction of chronic lymphocytic leukemia (CLL)-specific CD4- and CD8-mediated T-cell responses using RNA-transfected dendritic cells. Blood 103:1763–1769

5. Brossart P, Stuhler G, Flad T, Stevanovic S, Rammensee HG, Kanz L, Brugger W (1998) Her-2/neu-derived peptides are tumor-associated antigens expressed by human renal cell and colon carcinoma lines and are recognized by in vitro induced specific cytotoxic T lymphocytes. Cancer Res 58:732–736

6. Schmidt SM, Schag K, Muller MR, Weck MM, Appel S, Kanz L, Grunebach F, Brossart P (2003) Survivin is a shared tumor-associated antigen expressed in a broad variety of malignancies and recognized by specific cytotoxic T cells. Blood 102:571–576

[ChemPort] [PubMed]

7. Gendler SJ, Spicer AP (1995) Epithelial mucin genes. Annu Rev Physiol 57:607–634

[ChemPort] [PubMed]

8. Brossart P, Schneider A, Dill P, Schammann T, Grunebach F, Wirths S, Kanz L, Buhring HJ, Brugger W (2001) The epithelial tumor antigen MUC1 is expressed in hematological malignancies and is recognized by MUC1-specific cytotoxic T-lymphocytes. Cancer Res 61:6846–6850

[ChemPort] [PubMed]

9. Gendler S, Taylor-Papadimitriou J, Duhig T, Rothbard J, Burchell J (1988) Highly immunogenic region of a human polymorphic epithelial mucin expressed by carcinomas is made up of tandem repeats. J Biol Chem 263:12820–12823

[ChemPort] [PubMed]

10. Siddiqui J, Abe M, Hayes D, Shani E, Yunis E, Kufe D (1988) Isolation and sequencing of a cDNA coding for the human DF3 breast carcinoma-associated antigen. Proc Natl Acad Sci U S A 85 (7):2320–2323

[ChemPort] [PubMed]

11. Taylor-Papadimitriou J, Burchell J, Miles DW, Dalziel M (1999) MUC1 and cancer. Biochim Biophys Acta 1455:301–313

[ChemPort] [PubMed]

12. Finn OJ, Jerome KR, Henderson RA, Pecher G, Domenech N, Magarian-Blander J, Barratt-Boyes SM (1995) MUC-1 epithelial tumor mucin-based immunity and cancer vaccines. Immunol Rev 145:61–89

[ChemPort] [PubMed]

13. Apostolopoulos V, McKenzie IF (1994) Cellular mucins: targets for immunotherapy. Crit Rev Immunol 14:293–309

[ChemPort] [PubMed]

14. Ioannides CG, Fisk B, Jerome KR, Irimura T, Wharton JT, Finn OJ (1993) Cytotoxic T cells from ovarian malignant tumors can recognize polymorphic epithelial mucin core peptides. J Immunol 51:3693–3703

15. Takahashi T, Makiguchi Y, Hinoda Y, Kakiuchi H, Nakagawa N, Imai K, Yachi A (1994) Expression of MUC1 on myeloma cells and induction of HLA-unrestricted CTL against MUC1 from a multiple myeloma patient. J Immunol 153:2102–2109

[ChemPort] [PubMed]

16. Kotera Y, Fontenot JD, Pecher G, Metzgar RS, Finn OJ (1994) Humoral immunity against a tandem repeat epitope of human mucin MUC-1 in sera from breast, pancreatic, and colon cancer patients.

Cancer Res 54:2856–2860
ChemPort PubMed

17. Karanikas V, Hwang LA, Pearson J, Ong CS, Apostolopoulos V, Vaughan H, Xing PX, Jamieson G, Pietersz G, Tait B, Broadbent R, Thynne G, McKenzie IF (1997) Antibody and T cell responses of patients with adenocarcinoma immunized with mannan-MUC1 fusion protein. J Clin Invest 100:2783–2792
ChemPort PubMed

18. Renkvist N, Castelli C, Robbins PF, Parmiani G (2001) A listing of human tumor antigens recognized by T cells. Cancer Immunol Immunother 50:3–15
ChemPort PubMed

19. Topalian SL, Gonzales MI, Parkhurst M, Li YF, Southwood S, Sette A, Rosenberg SA, Robbins PF (1996) Melanoma-specific CD4+ T cells recognize nonmutated HLA-DR-restricted tyrosinase epitopes. J Exp Med 183:1965–1971
ChemPort PubMed

20. Brossart P, Bevan MJ (1997) Presentation of exogenous protein antigens on major histocompatibility complex class I molecules by dendritic cells: pathway of presentation and regulation by cytokines. Blood 90:1594–1599
ChemPort PubMed

21. Rammensee HG, Falk K, Rotzschke O (1993) Peptides naturally presented by MHC class I molecules. Annu Rev Immunol 11:213–244
ChemPort PubMed

22. Davenport MP, Ho Shon IA, Hill AV (1995) An empirical method for the prediction of T-cell epitopes. Immunogenetics 42:392–397
ChemPort PubMed

23. Rammensee H, Bachmann J, Emmerich NP, Bachor OA, Stevanovic S (1999) SYFPEITHI: database for MHC ligands and peptide motifs. Immunogenetics 50:213–219
ChemPort PubMed

24. Domenech N, Henderson RA, Finn OJ (1995) Identification of an HLA-A11-restricted epitope from the tandem repeat domain of the epithelial tumor antigen mucin. J Immunol 155:4766–4774
ChemPort PubMed

25. Apostolopoulos V, Karanikas V, Haurum JS, McKenzie IF (1997) Induction of HLA-A2-restricted CTLs to the mucin 1 human breast cancer antigen. J Immunol 159:5211–5218
ChemPort PubMed

26. Brossart P, Heinrich KS, Stuhler G, Behnke L, Reichardt VL, Stevanovic S, Muhm A, Rammensee HG, Kanz L, Brugger W (1999) Identification of HLA-A2-restricted T-cell epitopes derived from the MUC1 tumor antigen for broadly applicable vaccine therapies. Blood 93:4309–4317
ChemPort PubMed

27. Alexander J, Sidney J, Southwood S, Ruppert J, Oseroff C, Maewal A, Snoke K, Serra HM, Kubo RT, Sette A (1994) Development of high potency universal DR-restricted helper epitopes by modification of high affinity DR-blocking peptides. Immunity 1:751–761
[ChemPort] [PubMed]

28. Agrawal B, Krantz MJ, Reddish MA, Longenecker BM (1998) Rapid induction of primary human CD4+ and CD8+ T cell responses against cancer-associated MUC1 peptide epitopes. Int Immunol 10:1907–1916
[ChemPort] [PubMed]

29. Kobayashi H, Terao T, Kawashima Y (1992) Serum sialyl Tn as an independent predictor of poor prognosis in patients with epithelial ovarian cancer. J Clin Oncol 10:95–101
[ChemPort] [PubMed]

30. Fung PY, Longenecker BM (1991) Specific immunosuppressive activity of epiglycanin, a mucin-like glycoprotein secreted by a murine mammary adenocarcinoma (TA3-HA). Cancer Res 51:1170–1176
[ChemPort] [PubMed]

31. Gimmi CD, Morrison BW, Mainprice BA, Gribben JG, Boussiotis VA, Freeman GJ, Park SY, Watanabe M, Gong J, Hayes DF, Kufe DW, Nadler LM (1996) Breast cancer-associated antigen, DF3/MUC1, induces apoptosis of activated human T cells. Nat Med 2:1367–1370
[ChemPort] [PubMed]

32. Agrawal B, Krantz MJ, Reddish MA, Longenecker BM (1998) Cancer-associated MUC1 mucin inhibits human T-cell proliferation, which is reversible by IL-2. Nat Med 4:43–49
[ChemPort] [PubMed]

33. Gong J, Chen D, Kashiwaba M, Li Y, Chen L, Takeuchi H, Qu H, Rowse GJ, Gendler SJ, Kufe D (1998) Reversal of tolerance to human MUC1 antigen in MUC1 transgenic mice immunized with fusions of dendritic and carcinoma cells. Proc Natl Acad Sci U S A 95:6279–6283
[ChemPort] [PubMed]

34. Brossart P, Wirths S, Stuhler G, Reichardt VL, Kanz L, Brugger W (2000) Induction of cytotoxic T-lymphocyte responses in vivo after vaccinations with peptide-pulsed dendritic cells. Blood 96:3102–3108
[ChemPort] [PubMed]

35. Fisk B, Blevins TL, Wharton JT, Ioannides CG (1995) Identification of an immunodominant peptide of HER-2/neu protooncogene recognized by ovarian tumor-specific cytotoxic T lymphocyte lines. J Exp Med 181:2109–2117
[ChemPort] [PubMed]

36. Brossart P, Stuhler G, Flad T, Stevanovic S, Rammensee HG, Kanz L, Brugger W (1998) Her-2/neu-derived peptides are tumor-associated antigens expressed by human renal cell and colon carcinoma lines and are recognized by in vitro induced specific cytotoxic T lymphocytes. Cancer Res 58:732–736
[ChemPort] [PubMed]

37. Bevan MJ (1976) Cross-priming for a secondary cytotoxic response to minor H antigens with H-2 congenic cells which do not cross-react in the cytotoxic assay. J Exp Med 143:1283–1288
ChemPort   PubMed

38. Kovacsovics-Bankowski M, Rock KL (1995) A phagosome-to-cytosol pathway for exogenous antigens presented on MHC class I molecules. Science 267:243–246
ChemPort   PubMed

39. Brossart P, Bevan MJ (1997) Presentation of exogenous protein antigens on major histocompatibility complex class I molecules by dendritic cells: pathway of presentation and regulation by cytokines. Blood 90:1594–1599
ChemPort   PubMed

40. Glaspy JA (2002) Therapeutic options in the management of renal cell carcinoma. Semin Oncol 29(3 Suppl 7):41–46
ChemPort

41. Belldegrun A, Muul LM, Rosenberg SA (1988) Interleukin 2 expanded tumor-infiltrating lymphocytes in human renal cell cancer: isolation, characterization, and antitumor activity. Cancer Res 48:206–214
ChemPort   PubMed

42. Thurnher M, Radmayr C, Ramoner R, Ebner S, Bock G, Klocker H, Romani N, Bartsch G (1996) Human renal-cell carcinoma tissue contains dendritic cells. Int J Cancer 68:1–7
ChemPort   PubMed

43. Atzpodien J, Kirchner H, Jonas U, Bergmann L, Schott H, Heynemann H, Fornara P, Loening SA, Roigas J, Muller SC, Bodenstein H, Pomer S, Metzner B, Rebmann U, Oberneder R, Siebels M, Wandert T, Puchberger T, Reitz M (2004) Interleukin-2- and interferon alfa-2a-based immunochemotherapy in advanced renal cell carcinoma: a prospectively randomized trial of the German Cooperative Renal Carcinoma Chemoimmunotherapy Group (DGCIN). J Clin Oncol 22:1188–1194
ChemPort   PubMed

44. Su Z, Dannull J, Heiser A, Yancey D, Pruitt S, Madden J, Coleman D, Niedzwiecki D, Gilboa E, Vieweg J (2003) Immunological and clinical responses in metastatic renal cancer patients vaccinated with tumor RNA-transfected dendritic cells. Cancer Res 63:2127–2133
ChemPort   PubMed

45. Holtl L, Zelle-Rieser C, Gander H, Papesh C, Ramoner R, Bartsch G, Rogatsch H, Barsoum AL, Coggin JH Jr, Thurnher M (2002) Immunotherapy of metastatic renal cell carcinoma with tumor lysate-pulsed autologous dendritic cells. Clin Cancer Res 8:3369-3376
ChemPort   PubMed

46. Oosterwijk-Wakka JC, Tiemessen DM, Bleumer I, de Vries IJ, Jongmans W, Adema GJ, Debruyne FM, de Mulder PH, Oosterwijk E, Mulders PF (2002) Vaccination of patients with metastatic renal cell carcinoma with autologous dendritic cells pulsed with autologous tumor antigens in combination with interleukin-2: a phase 1 study. J Immunother 25:500–508
ChemPort   PubMed

47. Marten A, Renoth S, Heinicke T, Albers P, Pauli A, Mey U, Caspari R, Flieger D, Hanfland P, Von Ruecker A, Eis-Hubinger AM, Muller S, Schwaner I, Lohmann U, Heylmann G, Sauerbruch T, Schmidt-Wolf I G (2003) Allogeneic dendritic cells fused with tumor cells: preclinical results and outcome of a clinical phase I/II trial in patients with metastatic renal cell carcinoma. Hum Gene Ther 14:483–494
PubMed

ATTACHMENT C

shp1-1 allele; amplification using the oligos 5'-GTGACGGAAGGAGGGTTGACG-3' and 5'-GTCTACTGATGAGTTGTCACTAGG-3' yields an 871-bp product in plants with a wild-type allele of *SHP1*, and no product in plants homozygous for the *shp1-1* allele. Amplification using the oligos 5'-GAGGATAGAGAACACTACGAATCGTC-3' and 5'-CAGGTCAAGTCAATAGATTCCCTAC-3' yields a 1.5-kb product in plants with a wild-type allele of *SHP2*, and a single 2.8-kb product in plants homozygous for the *shp2-1* allele.

Generation of transgenic plants

A full-length *SHP1* complementary DNA was created by fusing the *Eco*RI fragments of pCIT2241 and pCIT4219 (ref. 10). The *SHP1* cDNA was then cloned into the *Bam*HI site of pCGN18 (ref. 29), to place *SHP1* transcription under the control of the viral 35S promoter[25]. A full-length *SHP2* cDNA was PCR amplified with the oligos 5'-GGAGATCTGAATTCAT CTTCCCCATCC-3' and 5'-CCGGTACCTCAAACAAGTTG-CAGAGGTGGTTGG TCTTGGTTGGAGGAATTCTGATTCGGTTCAAG-3', using pCIT2242 (ref. 10) as template. After cloning this product into the TA vector (Invitrogen), a *Bgl*II/*Kpn*I fragment containing the *SHP2* cDNA was cloned into the plant transformation vector pMON530 (Monsanto). The resulting construct also places *SHP2* transcription under control of the 35S promoter. Transgenic plants were selected on kanamycin after *Agrobacterium*-mediated transformation. 35S::*SHP1* plants are in the Landsberg *erecta* ecotype, whereas 35S::*SHP2* plants are in the Columbia ecotype. 35S::*SHP1* and 35S::*SHP2* plants were crossed to each other; in the F1 generation, 35S::*SHP1* 35S::*SHP2* plants were identified by PCR genotyping using *SHP1* transgene-specific (5'-GAAGGTGGGAGTAGTCACGAC-3' and 5'-CGGAAGGAGGGTTGACGGCA-3') and *SHP2* transgene-specific (5'-GGTGGTGCGAGTAATGAAGTA-3' and 5'-TGGTCGGAGGGTTAACGGCG-3') oligos.

Scanning electron microscopy

Fruit from wild-type (Columbia ecotype), *shp1 shp2* mutants and 35S::*SHP1* 35S::*SHP2* plants were fixed for approximately 4 h at 25 °C in FAA (50% ethanol, 5% glacial acetic acid, 3.7% formaldehyde) and prepared for scanning electron microscopy[27]. Samples were examined in a Cambridge S360 scanning electron microscope using an accelerating voltage of 10 kV.

Histological staining

Tissue from wild-type (Columbia ecotype), *shp1 shp2* and 35S::*SHP1* 35S::*SHP2* plants was fixed, sectioned and stained with toluidine blue[26] with minor modifications. For lignin analyses, sections were stained for 2 min in a 2% phloroglucinol solution in 95% ethanol, then photographed in 50% hydrochloric acid.

Molecular marker analyses

The YJ36 enhancer trap line was generated by *Agrobacterium*-mediated transformation with the plasmid pOCA-28-15-991 (ref. 21). Transgenic plants containing YJ36 or GT140 (ref. 20) were crossed to *shp1 shp2* plants. Among the F2 population, plants with a *shp1 shp2* phenotype that also carried the respective molecular marker were selected for further study. F1 plants from marker crosses to 35S::*SHP1* 35S::*SHP2* plants were genotyped for both transgenes, and analysed further. For β-glucuronidase expression analyses, fruit from GT140, *shp1 shp2* GT140, 35S::*SHP1* 35S::*SHP2* GT140, YJ36, *shp1 shp2* YJ36 and 35S::*SHP1* 35S::*SHP2* YJ36 plants were fixed, sectioned and stained as described[30] with minor modifications.

1. Jenkins, E. S. *et al.* Characterization of an mRNA encoding a polygalacturonase expressed during pod development in oilseed rape (*Brassica napus* L.). *J. Exp. Bot.* **47**, 111–115 (1996).
2. Petersen, M. *et al.* Isolation and characterisation of a pod dehiscence zone-specific polygalacturonase from *Brassica napus. Plant Mol. Biol.* **31**, 517–527 (1996).
3. Coupe, S. A., Taylor, J. E., Isaac, P. G. & Roberts, J. A. Identification and characterization of a proline-rich mRNA that accumulates during pod development in oilseed rape (*Brassica napus* L.). *Plant Mol. Biol.* **23**, 1223–1232 (1993).
4. Child, R. D., Chauvaux, N., John, K., Ulvskov, P. & Onckelen, H. A. Ethylene biosynthesis in oilseed rape pods in relation to pod shatter. *J. Exp. Bot.* **49**, 829–838 (1998).
5. MacLeod, J. in *Oilseed Rape Book* 107–119 (Cambridge Agricultural, Cambridge, 1981).
6. Riechmann, J. L. & Meyerowitz, E. M. MADS domain proteins in plant development. *J. Biol. Chem.* **378**, 1079–1101 (1997).
7. Purugganan, M. D. The MADS-box floral homeotic gene lineages predate the origin of seed plants: phylogenetic and molecular clock estimates. *J. Mol. Evol.* **45**, 392–396 (1997).
8. Bowman, J. L., Alvarez, J., Weigel, D., Meyerowitz, E. M. & Smyth, D. R. Control of flower development in *Arabidopsis thaliana* by *APETALA1* and interacting genes. *Development* **119**, 721–743 (1993).
9. Kempin, S. A., Savidge, B. & Yanofsky, M. F. Molecular basis of the *cauliflower* phenotype in *Arabidopsis. Science* **267**, 522–525 (1995).
10. Ma, H., Yanofsky, M. F. & Meyerowitz, E. M. *AGL1–AGL6*, an *Arabidopsis* gene family with similarity to floral homeotic and transcription factor genes. *Genes Dev.* **5**, 484–495 (1991).
11. Flanagan, C. A., Hu, Y. & Ma, H. Specific expression of *AGL1* MADS-box gene suggests regulatory functions in *Arabidopsis* gynoecium and ovule development. *Plant J.* **10**, 343–353 (1996).
12. Savidge, B., Rounsley, S. D. & Yanofsky, M. F. Temporal relationship between the transcription of two *Arabidopsis* MADS box genes and the floral organ identity genes. *Plant Cell* **7**, 721–733 (1995).
13. Spence, J. *Development of the Silique of* Arabidopsis thaliana. Thesis, Univ. Durham (1992).
14. Spence, J., Vercher, Y., Gates, P. & Harris, N. 'Pod shatter' in *Arabidopsis thaliana, Brassica napus* and *B. juncea. J. Microsc.* **181**, 195–203 (1996).
15. Bowman, J. L., Baum, S. F., Eshed, Y., Putterill, J. & Alvarez, J. Molecular genetics of gynoecium development in Arabidopsis. *Curr. Top. Dev. Biol.* **45**, 155–205 (1999).
16. Ferrándiz, C., Pelaz, S. & Yanofsky, M. Control of carpel and fruit development in Arabidopsis. *Annu. Rev. Biochem.* **68**, 321–354 (1999).
17. Rollins, R. C. *The Cruciferae of Continental North America—Systematics of the Mustard Family from the Arctic to Panama* (Stanford Univ. Press, Stanford, 1993).
18. Meakin, P. & Roberts, J. Dehiscence of fruit in oilseed rape (*Brassica napus* L.) I. Anatomy of pod dehiscence. *J. Exp. Bot.* **41**, 995–1002 (1990).
19. Kempin, S. A. *et al.* Targeted disruption in *Arabidopsis. Nature* **389**, 802–803 (1997).
20. Sundaresan, V. *et al.* Patterns of gene action in plant development revealed by enhancer trap and gene trap transposable elements. *Genes Dev.* **9**, 1797–1810 (1995).
21. Eshed, Y., Baum, S. F. & Bowman, J. L. Distinct mechanisms promote polarity establishment in carpels of *Arabidopsis. Cell* **99**, 199–209 (1999).
22. Yanofsky, M. F. *et al.* The protein encoded by the *Arabidopsis* homeotic gene *agamous* resembles transcription factors. *Nature* **346**, 35–40 (1990).
23. Rounsley, S. D., Ditta, G. S. & Yanofsky, M. F. Diverse roles for MADS box genes in *Arabidopsis* development. *Plant Cell* **7**, 1259–1269 (1995).
24. Bowman, J. L., Drews, G. N. & Meyerowitz, E. M. Expression of the *Arabidopsis* floral homeotic gene *AGAMOUS* is restricted to specific cell types late in flower development. *Plant Cell* **3**, 749–758 (1991).
25. Benfey, P. N. & Chua, N.-H. The cauliflower mosaic virus 35S promoter: combinatorial regulation of transcription in plants. *Science* **250**, 959–966 (1990).
26. Mizukami, Y. & Ma, H. Ectopic expression of the floral homeotic gene *AGAMOUS* in transgenic *Arabidopsis* plants alters floral organ identity. *Cell* **71**, 119–131 (1992).
27. Gu, Q., Ferrándiz, C., Yanofsky, M. & Martienssen, R. The *FRUITFULL* MADS-box gene mediates cell differentiation during *Arabidopsis* fruit development. *Development* **125**, 1509–1517 (1998).
28. Mandel, A. M. & Yanofsky, M. F. The *Arabidopsis AGL8* MADS-box gene is expressed in inflorescence meristems and is negatively regulated by *APETALA1. Plant Cell* **7**, 1763–1771 (1995).
29. Jack, T., Fox, G. L. & Meyerowitz, E. M. *Arabidopsis* homeotic gene *APETALA3* ectopic expression: transcriptional and post-transcriptional regulation determine floral organ identity. *Cell* **76**, 703–716 (1994).
30. Blázquez, M. A., Soowal, L. N., Lee, I. & Weigel, D. *LEAFY* expression and flower initiation in *Arabidopsis. Development* **124**, 3835–3844 (1997).

Rapid degradation of a large fraction of newly synthesized proteins by proteasomes

Ulrich Schubert*†, Luis C. Antón*, James Gibbs*, Christopher C. Norbury*, Jonathan W. Yewdell* & Jack R. Bennink*

* *Laboratory of Viral Diseases, National Institute of Allergy and Infectious Diseases, Bethesda, Maryland, USA*
† *Heinrich-Pette Institute, University of Hamburg, Hamburg, Germany*

MHC class I molecules function to present peptides eight to ten residues long to the immune system. These peptides originate primarily from a cytosolic pool of proteins through the actions of proteasomes[1], and are transported into the endoplasmic reticulum, where they assemble with nascent class I molecules[2]. Most peptides are generated from proteins that are apparently metabolically stable. To explain this, we previously proposed that peptides arise from proteasomal degradation of defective ribosomal products (DRiPs). DRiPs are polypeptides that never attain native structure owing to errors in translation or post-translational processes necessary for proper protein folding[3]. Here we show, first, that DRiPs constitute upwards of 30% of newly synthesized proteins as determined in a variety of cell types; second, that at least some DRiPs represent ubiquitinated proteins; and last, that ubiquitinated DRiPs are formed from human immunodeficiency virus Gag polyprotein, a long-lived viral protein that serves as a source of antigenic peptides.

Reasoning that proteasomes should be the principal consumer of DRiPs, we examined the effects of the proteasome inhibitors carbobenzoxyl-LeuLeu-leucinal (zLLL) and lactacystin on the recovery of proteins from HeLa cells pulse-radiolabelled with [35S]methionine ([35S]Met) for 30 seconds and chased for up to 60 min. Lactacystin is a highly specific inhibitor of the proteasome[4], whereas zLLL inhibits proteasomes and other proteases[5]. Radiolabelled cells were either directly boiled in SDS–polyacrylamide gel electrophoresis (PAGE) sample buffer (Fig. 1, 'All'), or lysed by freeze–thawing and fractionated by centrifugation into soluble cytosolic ('Cyto') and insoluble (pellet; 'Ins') fractions before boiling in sample buffer. Radiolabelled proteins were resolved by SDS–PAGE and the quantities of radioactivity in dried gels were measured. For all matched inhibitor-treated and untreated samples, identical amounts of cellular protein were loaded per lane. Greater cellular equivalents were loaded for fractionated than for unfractionated samples; 'All' lanes therefore contained less radioactivity than the sum of the 'Cyto' and 'Ins' lanes.

In the absence of proteasome inhibitors, the amount of protein recovered reached plateau values within 10 min following pulse radiolabelling (Fig. 1a, b). This lag presumably reflects the time needed to utilize [35S]Met-charged tRNA. Incubation of cells with lactacystin/zLLL progressively increased the amount of protein recovered in the 'All' fraction, reaching threefold the amount recovered from untreated cells by 60 min. This cannot be attributed

to an increased rate of translation or [35S]Met incorporation because first, all of the increase occurred in the insoluble fraction, and second, the increase was biased towards slower-migrating proteins. The simplest interpretation of these findings is that a large fraction (two-thirds) of proteins synthesized under these conditions are degraded during or rapidly after translation by proteases sensitive to lactacystin/zLLL. On the basis of additional evidence presented below, we believe that they consist largely of DRiPs and refer to them as such in what follows.

The consequences of preincubating cells for increasing durations with lactacystin/zLLL before radiolabelling were monitored by acid precipitation of extracts on filter paper as well as by SDS–PAGE (Fig. 1c). The enhancing effect of lactacystin/zLLL on protein recovery was maximal when the inhibitors were added 10 min before radiolabelling; preincubation for 30 min resulted in a slight (10%) decrease in the effect. Pretreating cells for 60 min had only a minor effect on protein recovery, whereas treating for 2 or 4 h profoundly decreased protein synthesis. SDS–PAGE analysis of insoluble fractions revealed that an increased recovery of proteins of relative molecular mass (M_r) 46,000–250,000 (46K–250K) was observed only for cells exposed to lactacystin/zLLL for 10 or 30 min before radiolabelling. In an additional experiment (not shown), exposure of cells to 50 μM zLLL immediately after pulse radiolabelling did not enhance protein recovery or modify the size or distribution of proteins. Thus, the optimal detection of DRiPs
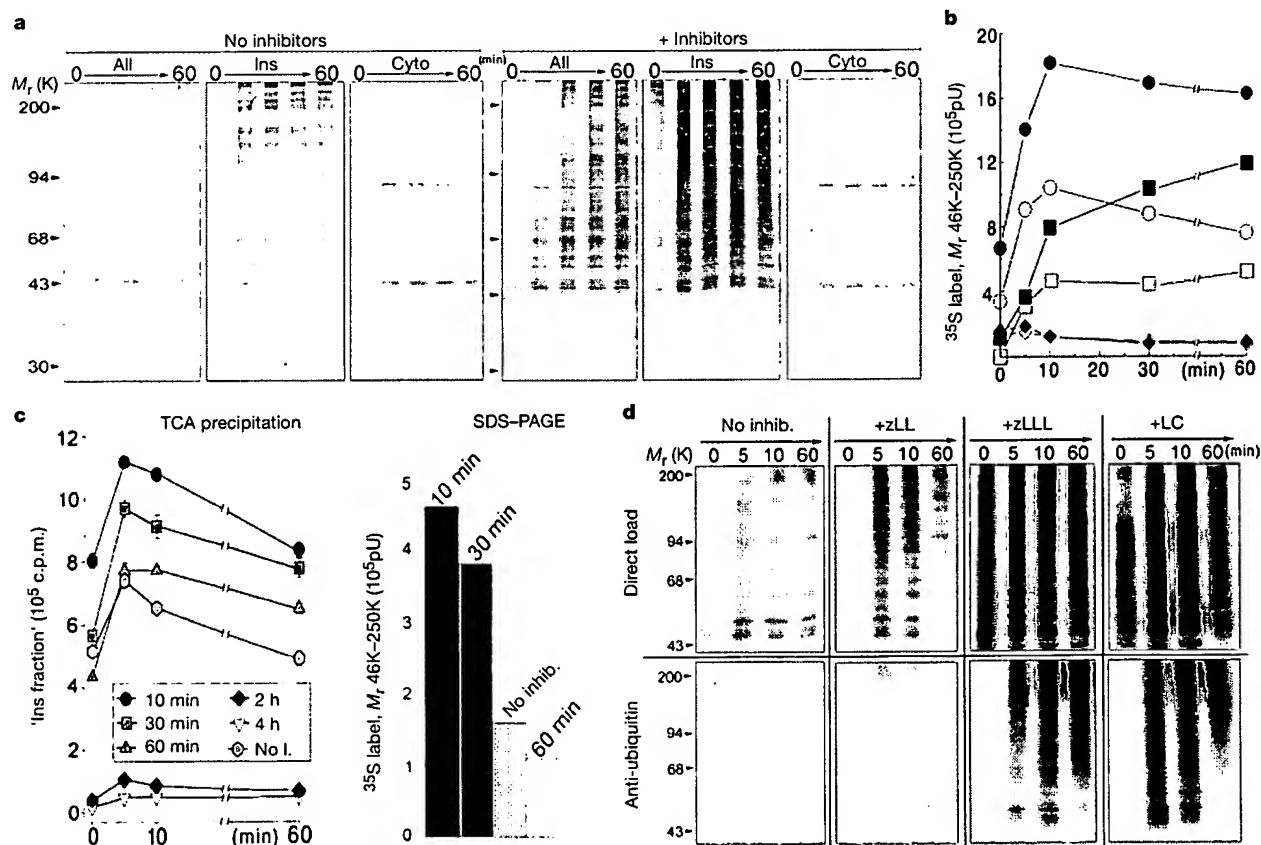

Figure 1 Detection of cellular DRiPs. HeLa cells treated with 50 μM of zLLL/lactacystin each during the final 30 min of a 60-min starvation in Met-free media were radiolabelled for 30 s and chased for up to 60 min. **a**, Fluorographs of fraction samples separated by SDS–PAGE. All, total proteins; Ins, insoluble fraction; Cyto, cytoplasmic fraction.
b, Quantification of the 35S-labelled proteins in the M_r 46K–250K range plotted in Phosphorlmager units (pU). Filled circles, insoluble fraction plus inhibitors; open circles, insoluble fraction without inhibitors; filled squares, total proteins plus inhibitors; open squares, total proteins without inhibitors; filled diamonds, cytoplasmic fraction plus

inhibitors; open diamonds, cytoplasmic fraction without inhibitors. **c**, HeLa cells were treated with zLLL/lactacystin for the indicated durations and radiolabelled proteins recovered in the 'Ins' fraction by precipitation with TCA were quantified in triplicate. 'Ins' fractions from the 60-min chase samples were analysed by SDS–PAGE and quantified as in **a**. No inhib., no inhibitors. **d**, HeLa cells were pulse-radiolabelled after incubation with 50 μM zLL, zLLL or lactacystin (LC) starting 15 min before the pulse. The 'Ins' fraction was analysed by SDS–PAGE directly or after extraction with SDS, renaturation and binding of material to ubiquitin-specific antibodies.

© 2000 Macmillan Magazines Ltd

requires a narrow window of exposure time to proteasome inhibitors, just long enough, in fact, to block proteasomes before protein synthesis. In an additional experiment we examined the influence of Met starvation on DRiP formation by pulse radiolabelling for 2.5 min with or without prior incubation in Met-deficient medium. Prior Met starvation doubled the quantities of DRiPs detected, possibly owing to protein misfolding induced by limitations in Met-charged tRNA.

If DRiPs truly represent misfolded or unpartnered proteins, it is expected that at least a fraction of DRiPs are ubiquitinated. This was examined by immunoprecipitation of SDS extracts from fractionated [35S]Met-labelled HeLa cells with ubiquitin-specific antibodies. Cells were treated with either 50 μM zLLL, lactacystin or carbobenzoxyl-Leu-leucinal (zLL), which like zLLL is a potent inhibitor of thiol proteases but does not detectably inactivate proteasomes at the concentration used[6]. Figure 1d shows the effects of the inhibitors on the recovery of proteins in the post-nuclear 150,000g pellet, where it is seen that zLLL and lactacystin have similar effects on protein recovery when used individually (as in

Fig. 1a–c). zLL has no significant effect on DRiP recovery, strongly implicating proteasomes in DRiP degradation. Quantification of immunoprecipitated material showed that lactacystin and zLLL increase by ~4.5-fold the recovery of ubiquitinated material relative to untreated or zLL-treated cells. As after direct loading on gels, most anti-ubiquitin-reactive material migrated at $M_r > 43K$.

We next examined whether we could detect DRiPs generated from a specific gene product, the Pr55 Gag polyprotein precursor of human immunodeficiency virus type 1 (HIV-1), which is the source of a large variety of class I antigenic peptides. HeLa cells were transfected with an infectious molecular clone of HIV-1, and the soluble material in high-detergent-concentration extracts from pulse-radiolabelled cells that bound to a mixture of antibodies raised against the major Pr55 processing product capsid (CA), was analysed by SDS–PAGE (Fig. 2a). In cells treated with zLLL/lactacystin just before labelling we detected, in addition to the expected Gag precursor protein Pr55, an increasing intensity of individual diffuse bands in addition to a smear of proteins between them migrating from M_r 60K to the top of the stacking gel. The magnitude of the increase (Fig. 2b) suggests that ~40% of the specific radioactivity recovered by anti-CA antibodies consists of high-M_r Gag-DRiPs. The smear recovered by anti-CA antibodies was not recovered under the same conditions from cells transfected with a control plasmid nor when non-transfected [35S]Met-labelled cells were mixed with unlabelled HIV-1-expressing cells before extraction (not shown). This strongly suggests that the smear truly represents Gag-DRiPs and not cellular proteins that bind non-specifically to Gag–anti-Gag immune complexes. In the same experiment there was also a large increase in the amount of radiolabelled polyubiquitinated proteins that bound to a monoclonal antibody, FK2, specific for polyubiquitinated proteins[7] (Fig. 2c). We next demonstrated that the high-M_r smear recovered with HIV-specific antibodies from cells treated with proteasome inhibitors represents polyubiquitinated viral proteins by showing that the material reacted in western blots with the FK2 monoclonal antibody (Fig. 2d). This was a specific effect, requiring that cells both express HIV proteins and be exposed to proteasome inhibitors. These findings show that ubiquitinated forms of a defined long-lived viral gene product are produced rapidly after synthesis and are destroyed by proteasomes.

If DRiPs are abundant and largely ubiquitinated, then blocking protein synthesis should rapidly deplete polyubiquitinated protein pools. This prediction was confirmed when HeLa cells were treated
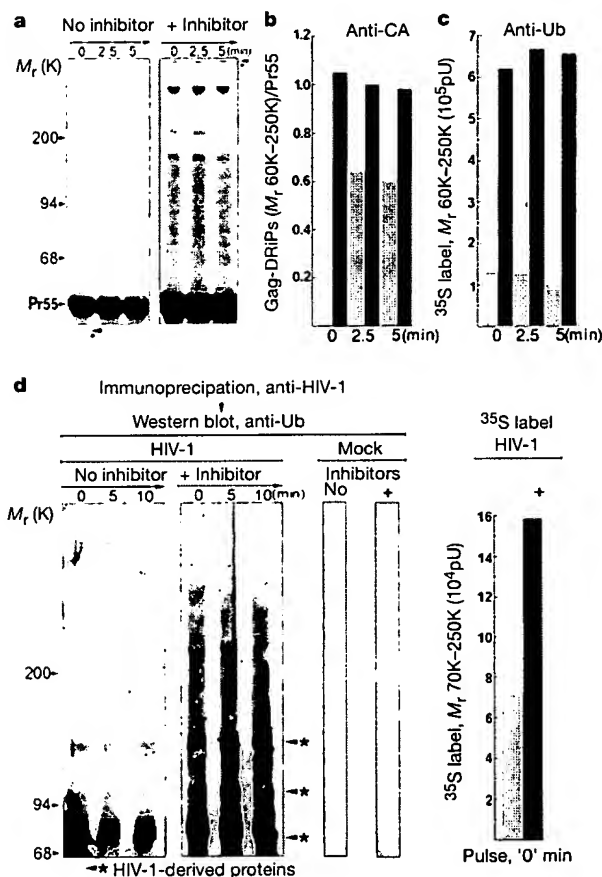

Figure 2 Detection of viral DRiPs. HeLa cells transfected with HIV-1 clone pNL4-3 were treated with 25 μM lactacystin/zLLL before being radiolabelled as in Fig. 1. Material recovered with anti-CA antibodies was separated by SDS–PAGE (**a**) and quantified as the ratio of counts recovered in the M_r 60K–250K smear relative to counts recovered as Pr55 Gag precursor protein (**b**). **c**, Enhanced amounts of high-M_r polyubiquitinated proteins were recovered from the same lysates by using the FK2 monoclonal antibody. **d**, Lysates of a pulse–chase similar to that shown in **a** with pNL4-3 and mock-transfected HeLa cells were immunoprecipitated with anti-HIV antibodies, and polyubiquitinated proteins present in the immunoprecipitates were detected by western blotting with FK-1 monoclonal antibody. Major bands migrating in the M_r range 70K–160K labelled with an asterisk represent HIV-specific proteins that reacted with FK-2. Relative amounts of 35S-labelled HIV-DRiPs migrating in the M_r range 70K–250K were quantified for the pulse time point (right panel). In **b**, **c** and **d**, grey columns, no inhibitors; black columns, with inhibitors.
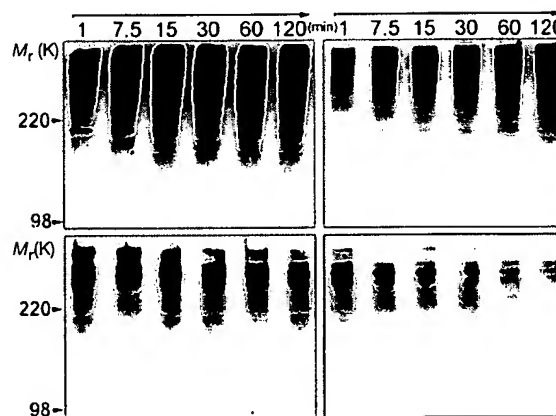
Figure 3 Dependence of polyubiquitinated proteins on continuing protein synthesis. HeLa cells were treated with or without protein synthesis inhibitors in the presence or absence of 25 μM zLLL for up to 120 min. The relative levels of polyubiquitinated proteins were detected by western blotting of total cell lysates with the FK-2 monoclonal antibody specific for polyubiquitin. Left panels, with protein synthesis; lower panels, without protein synthesis; top panels, with zLLL; lower panels, without zLLL.

with protein synthesis inhibitors in the presence or absence of proteasome inhibitors, and levels of polyubiquitinated proteins were determined in western blots with the FK2 monoclonal antibody. In zLLL-treated cells, blocking protein synthesis retarded the accumulation of polyubiquitinated proteins (Fig. 3). This echoes earlier findings that protein synthesis is required for the accumulation of ubiquitin at the microtubule-organizing centre[8], now known to be a specialized location for protein degradation[9,10]. Importantly, in the absence of proteasome inhibitors, blocking protein synthesis rapidly depletes polyubiquitinated proteins, providing evidence for the existence of DRiPs in cells not exposed to proteasome inhibitors. These data suggest that DRiPs are a significant source of ubiquitinated proteins and that a substantial proportion of DRiPs are polyubiquitinated. Given the high level of DRiP ubiquitination, it was

possible that a significant fraction of the signal detected in the high-M_r ^{35}S-labelled DRiPs emanated from Met residues in ubiquitin synthesized *de novo*. This possibility was eliminated by detecting DRiPs after labelling with [35S]Cys, a residue not present in ubiquitin (data not shown).

The experiments described so far used HeLa cells, which are highly aneuploid. We extended these results to dendritic cells, which are believed to function *in vivo* to present endogenously synthesized viral antigens to naive T cells[11]. With the use of a dendritic cell line derived from mouse bone marrow, DRiPs also constituted a significant fraction of newly synthesized proteins (see Supplementary Information). Although it is not technically feasible to label cells *in vivo*, we approached this ideal by also measuring DRiPs in lymph node cells as quickly as possible after their removal from mice (Fig. 4a). The results completely recapitulated the findings made with dendritic and HeLa cells, with the added feature that, after preservation of the stacking gel in this experiment, it was clear that DRiPs were also present as high-M_r material that barely entered the stacking gel. We estimate that, under these conditions, DRiPs constitute 30% of newly synthesized proteins on the basis of the differences in total radioactivity detected for each time point in fluorograms of Fig. 4a.

We tested the prediction that DRiPs are a significant source of peptide ligands for class I molecules by examining the effect of blocking protein synthesis on the transport of mouse class I molecules H-2D[b] and H2K[b] class I molecules from the endoplasmic reticulum, which is known to be controlled by the availability of suitable peptide ligands[12]. The export of nascent class I molecules was assessed by collecting class I molecules pulse-radiolabelled with [35S]Met and tracking the decreased electrophoretic mobility associated with the sialylation of N-linked oligosaccharides in the *trans*-Golgi complex (Fig. 4b). As reported previously[13], K[b] is exported more rapidly than D[b]. Notably, the export of both allomorphs is slowed 2–3-fold by blocking protein synthesis immediately after labelling. In contrast, the export of the transferrin receptor was unaffected, showing that the effect on class I molecules is not due to general retardation in membrane protein export from the endoplasmic reticulum.

We believe that this is the first study to examine the overall efficiency of protein biogenesis. Using the most physiological cell system (lymph node cells *ex vivo*) under the most physiological conditions (no Met starvation), one-third of newly synthesized proteins are rapidly destroyed by proteasomes. We note that the precise proportion of DRiPs relative to truly short-lived proteins, as well as the relative contributions of errors in mRNA synthesis, processing and translation versus errors in protein folding remain to be directly established. But these findings, in conjunction with others[14], firmly link the generation of class I peptide ligands to continuing protein synthesis. The fact that self peptides recovered from class I molecules in sufficient quantities for chemical identification demonstrate no apparent molar bias towards derivation from short-lived proteins[15,16] indicates strongly that most of the rapidly degraded proteins that we identify in the present study are in fact DRiPs derived mostly from long-lived proteins. The 70% efficiency for protein biosynthesis compares favourably to an estimated 50% efficiency for producing functional mRNA from heterogeneous nuclear RNA[17]. The remarkably high abundance of proteasomes (constituting 1% of total cellular protein) is consistent with a high constitutive level of DRiPs requiring disposal. We expect that some proteins are more disposed than others towards becoming DRiPs, on the basis of size and inherent difficulties in folding or assembly. If DRiPs maintain some elements of native structure, they might act in a dominant-negative manner to interfere with the function of proteins that associate with normally folded domains of DRiPs, as seems to occur with HIV-1 Gag (U.S., unpublished data). If under some conditions DRiP degradation were delayed, this could contribute to disease processes. □
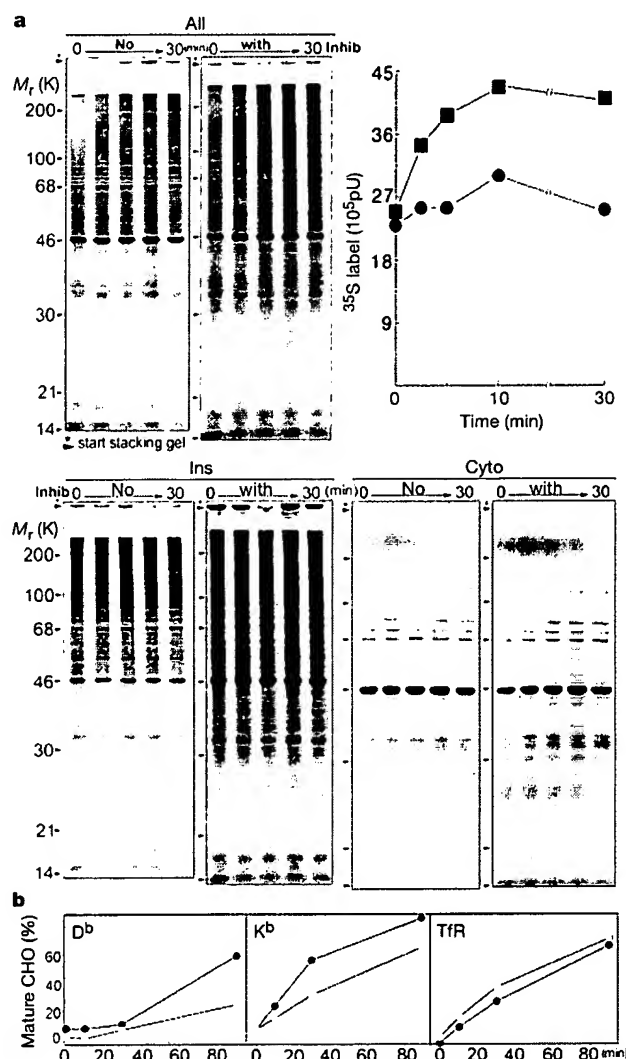

Figure 4 DRiP formation in lymph node cells and effect of protein synthesis inhibitors on class I transport. **a**, Lymph node cells were radiolabelled for 2.5 min in the absence or presence of 10 μM zLLL, 10 μM lactacystin and 1 μM clasto-lactacystin β-lactone. Total ('All') or fractionated ('Ins' and 'Cyto') cell lysates were separated by SDS–PAGE; in the graph the relative amounts of proteins in the M_r range 14K–250K detected in the 'All' fraction are plotted against the duration of the chase. Circles, no inhibitors; squares, with inhibitors. **b**, Pulse-radiolabelled RMA cells were chased for the indicated durations in the presence (open circles) and absence (filled circles) of protein synthesis inhibitors, and K[b], D[b] and transferrin receptor (TfR) molecules were recovered with specific monoclonal antibodies. Each class I specific monoclonal antibody was used twice sequentially to insure quantitative recovery. Shown is a time-dependent shift in mobility in SDS–PAGE quantified by PhosphorImager analysis. CHO, N-linked carbohydrate.

773

Methods

The cultivation of RMA and HeLa cell lines, as well as the generation of dendritic and lymph node cells are described in detail elsewhere (see Supplementary Information). Different cells vary considerably in their sensitivities to the various proteasome inhibitors, in terms of efficacy and adverse effects (decreased protein synthesis and viability). The amounts and concentrations of inhibitors used for different cells were optimized. For pulse–chase experiments, cells were incubated at 37 °C for up to 60 min in Met-free, serum-free RPMI (M⁻RPMI) before being radiolabelled. Cells (usually ~10⁷) were pelleted, resuspended in 150 μl M⁻RPMI prewarmed to 37 °C and radiolabelled by adding prewarmed [³⁵S]methionine (Amersham Life Science) to a final concentration of 5 mCi ml⁻¹. After incubation of cells at 37 °C for 30 or 150 s, 1 ml ice-cold Iscove's DMEM with 10% fetal bovine serum (I⁺) and supplemented with 10 mM Met (M⁺I⁺) was added, and cells were microcentrifuged for 10 s at 8,000*g*, aliquoted into 1 ml prewarmed M⁺I⁺, and incubated on a rotating platform at 37 °C during the chase period. In experiments in which cells were pulse-labelled for 30 s, cells were washed and aliquoted in ice-cold M⁺I⁺. Cells were lysed by 3 cycles of freeze–thawing (37 °C water bath alternated with solid CO₂) in isotonic buffer (0.25 M sucrose, 10 mM triethanolamine, 1 mM EDTA, 20 mM acetic acid pH 7.4) containing 1 mM phenylmethylsulphonyl fluoride (PMSF), 5 mM N-ethyl maleimide, 20 μM zLLL, 20 μM lactacystin, 100 units ml⁻¹ DNase I and Complete protease inhibitor cocktail (Boehringer Mannheim). Insoluble material was separated from the soluble cytosolic fraction by centrifugation of cell lysates at 150,000*g* for 2 h at 4 °C. For the experiment shown in Fig. 1d, nuclei were removed before ultracentrifugation by centrifugation at 3,000*g* for 10 min at 4 °C.

Aliquots of unfractionated cells resuspended in isotonic buffer before freeze–thawing ('All' fraction) were immediately mixed with boiling sample buffer (2% (w/v) SDS, 1% (v/v) 2-mercaptoethanol, 1% (v/v) glycerol, 65 mM Tris-HCl pH 6.8, 20 μM zLLL, 20 μM lactacystin). Pellets of insoluble material after ultracentrifugation were resuspended in Chaps-deoxycholate buffer (50 mM Tris-HCl pH 8.0, 5 mM EDTA, 100 mM NaCl, 0.5% (w/v) Chaps, 0.2% (w/v) deoxycholate) containing inhibitors as above, and equivalent amounts of soluble and insoluble samples were injected into boiling sample buffer. Samples were separated in 12.5% (w/v) Acryl aide Prosieve gels (FMC Bioproducts). Gels were fixed for 30 min in 40% (v/v) methanol, 10% (v/v) acetic acid, rinsed with water, soaked in 1 M sodium salicylic acid for 3 h, and dried. Radioactivity in gels was quantified with a PhosphorImager (Molecular Dynamics). For precipitations with trichloroacetic acid (TCA), aliquots of cell lysates were spotted onto DEAE-cellulose, washed with 10% (w/v) TCA and twice more with 70% ethanol then dried; radioactivity was then determined with a β-plate counter (MicroBeta 1450 Trilux; Wallac Oy). All estimations were done in triplicate.

Immunoprecipitation with ubiquitin-specific antibodies (mixture of polyclonal rabbit IgGs from several commercial sources) prebound to Protein G–Sepharose was performed on protein samples that had been denatured in SDS under non-reducing conditions, precipitated with acetone, resuspended in Chaps-deoxycholate buffer containing inhibitors as above, and renatured in Triton buffer (300 mM NaCl, 50 mM Tris-HCl pH 7.4, 0.1% (v/v) Triton X-100, 1 mM PMSF). For western blot analysis, HeLa cells were cultured in six-well plates and treated with a mixture of protein synthesis inhibitors (25 μg ml⁻¹ cycloheximide, 25 μg ml⁻¹ emetine and 25 μg ml⁻¹ puromycine) or proteasome inhibitors. Cells were lysed while attached on the plate with Chaps-deoxycholate buffer containing inhibitors as above. Aliquots of lysates were separated in 8% Prosieve gels, electrotransferred to Immobilon P membranes (Millipore), probed with mouse monoclonal antibody specific for polyubiquitin (clone FK-1; Nippon Bio-Test Laboratories), and developed by using the ECL system (Pierce).

For detection of HIV-1 Gag-DRiPs HeLa cells were transfected with pNL4-3 (ref. 18) by using LipofectAMINE 2000 (Gibco BRL) and a standard pulse–chase was conducted 24 h later. After the chase, cells were frozen in solid CO₂, thawed and instantly lysed in Chaps buffer containing 1% deoxycholate and protease inhibitors as above. After being precleared with preimmune serum, aliquots of lysates were immunoprecipitated with γ-globulin from pooled plasma of HIV-1 donors (NIH AIDS Research and Reference Reagent Program, catalogue number 192) and a cocktail of six monoclonal and three polyclonal antibodies directed against various epitopes of HIV-1 CA derived from native, recombinant and synthetic HIV-1 Gag proteins (catalogue numbers 287, 384, 1238, 1239, 1241, 1244, 4121 and 4250), as well as against full-length recombinant CA produced in *Escherichia coli* (Seramun GmbH). Polyubiquitinated forms of anti-HIV-1 immunoprecipitates separated in 6% Acryl aide gels were transferred to membranes and probed with the FK-1 monoclonal antibody. The pulse–chase experiment and the analysis of class I transport in RMA cells are described in detail elsewhere (see Supplementary Information).

1. Rock, K. L. & Goldberg, A. L. Degradation of cell proteins and the generation of MHC class I-presented peptides. *Annu. Rev. Immunol.* 17, 739–779 (1999).
2. Pamer, E. & Cresswell, P. Mechanisms of MHC class I restricted antigen processing. *Annu. Rev. Immunol.* 16, 323–358 (1998).
3. Yewdell, J. W., Antón, L. C. & Bennink, J. R. Defective ribosomal products (DRiPs). A major source of antigenic peptides for MHC class I molecules? *J. Immunol.* 157, 1823–1826 (1996).
4. Fenteany, G. *et al.* Inhibition of proteasome activities and subunit-specific amino-terminal threonine modification by lactacystin. *Science* 268, 726–731 (1995).
5. Rock, K. L. *et al.* Inhibitors of the proteasome block the degradation of most cell proteins and the generation of peptides presented on MHC class I molecules. *Cell* 78, 761–771 (1994).
6. Vinitsky, A., Michaud, C., Powers, J. C. & Orlowski, M. Inhibition of the chymotrypsin-like activity of the pituitary multicatalytic proteinase complex. *Biochemistry* 31, 9421–9428 (1992).
7. Fujimuro, M., Sadada, H. & Yokosawa, H. Production and characterization of monoclonal antibodies specific to multi-ubiquitin chains of polyubiquitinated proteins. *FEBS Lett.* 349, 173–180 (1994).
8. Wojcik, C., Schroeter, D., Wilk, S., Lamprecht, J. & Paweletz, N. Ubiquitin-mediated proteolysis centers in HeLa cells: indication from studies of an inhibitor of the chymotrypsin-like activity of the proteasome. *Eur. J. Cell Biol.* 71, 311–318 (1996).
9. Johnston, J. A., Ward, C. L. & Kopito, R. R. Aggresomes: a cellular response to misfolded proteins. *J. Cell. Biol.* 143, 1883–1898 (1998).
10. Anton, L. C. *et al.* Intracellular localization of proteasomal degradation of a viral antigen. *J. Cell Biol.* 146, 113–124 (1999).
11. Steinman, R. M. in *Fundamental Immunology* (ed. Paul, W. E.) 547–604 (Lippincott–Raven, Philadelphia, 1998).
12. Townsend, A. *et al.* Association of class I major histocompatibility heavy and light chains induced by viral peptides. *Nature* 340, 443–448 (1989).
13. Degen, E. & Williams, D. B. Participation of a novel 88-kD protein in the biogenesis of murine class I histocompatibility molecules. *J. Cell Biol.* 112, 1099–1115 (1991).
14. Reits, E. A. J., Vos, J. C., Grommé, M. & Neefjes, J. The major substrates for TAP *in vivo* are derived from newly synthesized proteins. *Nature* 404, 774–778 (2000).
15. Rammensee, H. -G., Bachmann, J. & Stevanovic, S. *MHC Ligands and Peptide Motifs* (Landes Bioscience, Austin, 1997).
16. Engelhard, V. H. Structures of peptides associated with class I and class II MHC molecules. *Annu. Rev. Immunol.* 12, 181–207 (1994).
17. Alberts, B. *et al. Molecular Biology of the Cell* (Garland, New York, 1994).
18. Adachi, A. *et al.* Production of acquired immunodeficiency syndrome-associated retrovirus in human and nonhuman cells transfected with an infectious molecular clone. *J. Virol.* 59, 284–291 (1986).

The major substrates for TAP *in vivo* are derived from newly synthesized proteins

Eric A. J. Reits, Jan C. Vos, Monique Grommé & Jacques Neefjes

Division of Tumor Biology, The Netherlands Cancer Institute, Plesmanlaan 121, 1066 CX Amsterdam, The Netherlands

The transporter associated with antigen processing (TAP) is a member of the family of ABC transporters that translocate a large variety of substrates across membranes[1]. TAP transports peptides from the cytosol into the endoplasmic reticulum for binding to MHC class I molecules and for subsequent presentation to the immune system[2]. Here we follow the lateral mobility of TAP in living cells. TAP's mobility increases when it is inactive and decreases when it translocates peptides. Because TAP activity is dependent on substrate, the mobility of TAP is used to monitor the intracellular peptide content *in vivo*. Comparison of the diffusion rates in peptide-free and peptide-saturated cells indicates that normally about one-third of all TAP molecules actively translocate peptides. However, during an acute influenza infection TAP becomes fully employed owing to the production and degradation of viral proteins. Furthermore, TAP activity depends on continuing protein translation. This implies that MHC class I molecules mainly sample peptides that originate from newly synthesized proteins, to ensure rapid presentation to the immune system.

TAP is composed of two subunits, TAP1 and TAP2, that form a structure consisting of a transmembrane domain, a peptide-binding domain and two nucleotide-binding domains[3,4]. To investigate whether conformational changes in TAP would affect its lateral

Quantitating Protein Synthesis, Degradation, and Endogenous Antigen Processing

Michael F. Princiotta,[1] Diana Finzi,[1]
Shu-Bing Qian,[1] James Gibbs,[1]
Sebastian Schuchmann,[2] Frank Buttgereit,[2]
Jack R. Bennink,[1] and Jonathan W. Yewdell[1,*]
[1]Laboratory of Viral Diseases
National Institute of Allergy
  and Infectious Diseases
Bethesda, Maryland 20892
[2]Department of Rheumatology
  and Clinical Immunology
Charité University Hospital
Humboldt University
10117 Berlin
Germany

Summary

Using L929 cells, we quantitated the macroeconomics of protein synthesis and degradation and the microeconomics of producing MHC class I associated peptides from viral translation products. To maintain a content of 2.6×10^9 proteins, each cell's 6×10^6 ribosomes produce 4×10^6 proteins min^{-1}. Each of the cell's 8×10^5 proteasomes degrades 2.5 substrates min^{-1}, creating one MHC class I-peptide complex for each 500–3000 viral translation products degraded. The efficiency of complex formation is similar in dendritic cells and macrophages, which play a critical role in activating T cells in vivo. Proteasomes create antigenic peptides at different efficiencies from two distinct substrate pools: rapidly degraded newly synthesized proteins that clearly represent defective ribosomal products (DRiPs) and a less rapidly degraded pool in which DRiPs may also predominate.

Introduction

Contemporary cell biology is dominated by reductionist approaches. Faced with the daunting complexity of cells, cell and molecular biologists typically examine isolated components of systems without accounting for their place in the larger scheme. Despite the fact that quantitative aspects of systems are critical to their understanding, they are frequently ignored.

A case in point is protein synthesis and degradation, clearly two of the more important tasks performed by cells. There has been remarkable progress toward understanding how proteins are degraded by eukaryotic cells (Hershko and Ciechanover, 1998; Rock and Goldberg, 1999). Scant attention has been paid, however, to quantitative aspects of degradation. Clearly, protein synthesis and degradation must be balanced for cells to maintain viability. The degradative machinery must have sufficient baseline capacity to dispose of damaged or defective proteins produced by cells under normal conditions and sufficient excess capacity to cope with

*Correspondence: jyewdell@nih.gov

various forms of physical or chemical stress that rapidly increase protein turnover. Cell growth or activation is also expected to increase the protein disposal rate due to increased rates of protein synthesis and also the redistribution of cellular resources to new tasks.

Extending the previous work of Wheatley (1989), we recently provided evidence that a significant fraction (upwards of 30%) of proteins are degraded by proteasomes shortly after their synthesis, presumably due in large part to their inability to achieve a functional state (we have termed such proteins defective ribosomal products [DRiPs]) (Schubert et al., 2000). One explanation for the apparent inefficiency in protein synthesis is that it is less costly for cells to degrade a high fraction of defective proteins than it is to synthesize proteins more efficiently. To evaluate the costs, we need to know the rate of protein synthesis and its energetic costs. We also need to know the number of proteasomes and the turnover rates required for degradation of such a large fraction of nascent proteins.

The importance of understanding protein degradation in quantitative terms is heightened by its contribution to immune surveillance. The vertebrate immune system uses the peptide products of proteasomal degradation to monitor the presence of viruses and other intracellular parasites (Rock et al., 2002). A fraction of proteasomal peptides find their way to class I molecules of the major histocompatibility complex (MHC) which display them on the cell surface for perusal by T cell receptors on $CD8^+$ T cells (T_{CD8+}).

Many quantitative aspects of antigen processing are uncertain. What fraction of viral peptides derives from DRiPs? What is the efficiency of generating peptides from proteasomal substrates? Do these numbers vary widely between different substrates? What are the rates of peptide generation and class I transport? What is the capacity of the class I presentation system?

In this study we provide answers to these questions, show that the rate of class I peptide complex formation can be used to estimate the rate of DRiP formation (referred to henceforth as the "DRiP rate") of a given substrate, and relate the economics of antigen processing to the overall protein and energy economies of the cell.

Results

The Protein Economy of L-K^b Cells

In the studies that follow we primarily use mouse L929 cells. To employ the 25-D1.16 mAb for quantitating peptide class I complexes (Porgador et al., 1997), we used cells transfected with a cDNA encoding the mouse H-2 K^b class I molecule (termed L-K^b cells).

Our first (and easiest) step in characterizing the protein economy of L-K^b cells was to determine their protein content. This amounted to 200 pg cell^{-1} as determined by the Biorad DC protein assay or 2.6×10^9 copies cell^{-1} of a typical protein defined as consisting of 466 amino acid residues (the average length in the EMBL human

A <u>Ribosomes</u>

<u>Purified x 10³</u>   <u>Cells x 10²</u>

100 50 25 12.5 6.3   100 50 25

B <u>Proteasomes</u>

<u>Purified x 10⁸</u>   <u>Cells x 10²</u>

100 50 25 12.5 6.3 100 50 25 12.5

C

D <u>NP Molecules x 10³</u> <u>rVV Infected L-Kᵇ Cells</u>

50   25   12.5   6.3   NP KEKE-NP R-NP

E <u>rVV Infected L-Kb Cells x 10²</u>

<u>NP Molecules x 10⁹</u>   <u>NP</u>   <u>KEKE-NP</u>

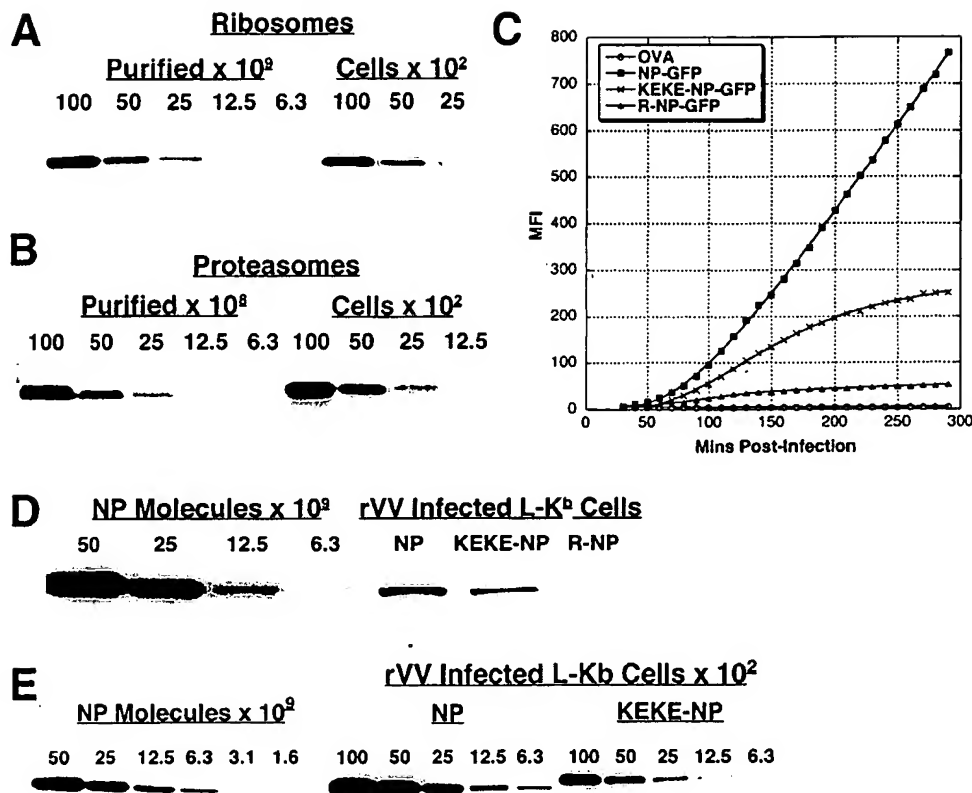50 25 12.5 6.3 3.1 1.6   100 50 25 12.5 6.3   100 50 25 12.5 6.3

Figure 1. Determination of Protein Concentrations in L-Kᵇ Cells

(A and B) Two-fold serial dilutions of lysates from L-Kᵇ cells infected with rVV-expressing NP-GFP or uninfected control cells were immunoblotted for ribosomes (A) or proteasomes (B). Purified ribosome and proteasome preparations were used to generate standard curves to determine proteasome and ribosome concentrations.
(C) Accumulation of chimeric NP-GFP molecules in L-Kᵇ cells infected with rVV-expressing NP-GFP (squares), KEKE-NP-GFP (X), R-NP-GFP (triangles), or OVA (circles). Note that nonfluorescent OVA defines autofluorescence levels.
(D) (Right side) L-Kᵇ cells (10⁴ cells/lane) infected with rVV-expressing chimeric NP-GFP 2.5 hr p.i. and immunoblotted with NP-specific antibodies. (Left side) Purified influenza nucleoprotein added to uninfected cell lysates was run on the same gel to generate a standard curve.
(E) (Right side) L-Kᵇ cells (cell number per lane indicated) infected with rVV-expressing NP-GFP or KEKE-NP-GFP 5 hr p.i. and immunoblotted with anti-NP antibodies. Uninfected cell lysates were added to samples to maintain 10⁴ cell equivalents per lane. (Left side) Same as for (D).

proteome). Next, we used quantitative Western blotting in conjunction with purified ribosome and proteasome standards to determine copy numbers. L-Kᵇ cells possess 6×10^6 ribosomes and 10^6 proteasomes cell^{-1} (Figures 1A and 1B). We need to correct these figures to account for subunits that are not present in functional assemblies. For ribosomes, this should be minimal since the half-life of assembled ribosomes (10 d) is much longer than their assembly time (Nissen-Meyer and Eikhom, 1976). There is no comparable data for proteasomes in L929 cells, but it has been reported that 75%–80% of proteasome subunits are present in functional assemblies in a rapidly dividing mouse cell line (Nandi et al., 1997). Extrapolating this result to L-Kᵇ cells results in a copy number of $\sim 8 \times 10^5$ functional proteasomes cell^{-1}.

We next measured the rate of protein synthesis by measuring the incorporation of ^{3}H-Leu into TCA insoluble material by L-Kᵇ cells labeled in normal growth media (see Experimental Procedures). The apparent rate of protein synthesis was 3.3×10^6 proteins min^{-1}. This does not account for DRiPs, however, some of which are degraded during pulse labeling (Schubert et al., 2000). To estimate the fraction of newly synthesized proteins degraded under these conditions, we radiolabeled cells in the presence and absence of proteasome inhibitors. These data indicate that the true rate of protein synthesis is $\sim 25\%$ greater than the measured rate in the absence of proteasome inhibitors, or $\sim 4 \times 10^6$ proteins min^{-1}. This value is consistent with the ribosome count; given a typical translation rate of 5 amino acid residues s^{-1} (Palmiter, 1975), each ribosome can produce a typical protein every 93 s, which amounts to 3.9×10^6 proteins cell^{-1} min^{-1} if all ribosomes are translating proteins at this rate. Our data indicate that there are few idle ribosomes in L-Kᵇ cells.

Can we account for the fate of the 4×10^6 proteins produced each min? Based on recovery of TCA insoluble material in pulse-chase experiments, we find that 1.3×10^6 proteins min^{-1} are degraded by proteasomes within the first 2 hr of their synthesis (1×10^6 min^{-1} in the first 10 min), 4.7×10^5 proteins min^{-1} are secreted

Table 1. Chimeric Protein Construct Names and Descriptions

Name	Protein	Description
NP-GFP	NP-SIINFEKL-EGFP	Stable, nuclear form of protein
R-NP-GFP	Ub-R-NP-SIINFEKL-EGFP	Posttranslationally degraded ($t_{1/2} \sim$ 10 min)
KEKE-NP-GFP	NP-KEKE-SIINFEKL-EGFP	Misfolded NP; forms an unstable cellular pool of protein ($t_{1/2} \sim$ 70 min)
OVA	Chicken egg ovalbumin	Full-length ovalbumin; secreted protein; no cellular protein pool accumulates
MSIINFEKL	SIINFEKL peptide	Minimal K^b binding peptide with amino terminal met from initiating AUG

or released from cells within an hour of their synthesis, and a further 5×10^5 proteins min^{-1} are degraded over the next 22 hr based on a measured turnover rate of 1.1% of long-lived proteins per hour (see Experimental Procedures). This would leave 1.7×10^6 proteins min^{-1} to create a daughter L-K^b cell, which is remarkably close to the number of proteins (1.8×10^6 min^{-1}) needed to double cellular protein content to support a cell division time of 24 hr.

We next determined the energetic cost of protein synthesis in L-K^b cells. When protein synthesis was blocked by adding cycloheximide to cells, oxygen consumption was reduced by 34%. We measured the efficiency of producing ATP from O_2 under these conditions to be 75% (using oligomycin to block the mitochondrial ATPase), meaning that protein synthesis consumes $\sim$45% of cellular ATP supplies. This is a minimal estimate of the cellular energy that is devoted to protein synthesis since, using the medium required for measuring ATP consumption, protein synthesis was diminished relative to cells incubated in growth medium. This underscores the high price that cells pay for protein synthesis, $\sim$5 ATP per peptide bond or 2300 ATP per typical protein. The cost of DRiPs in energetic terms is correspondingly high: a DRiP rate of 25% corresponds to $\sim$11% of total cellular energy usage.

In addition, we found that treating L-K^b cells with the proteasome inhibitor lactacystin did not result in any detectable reduction in oxygen consumption (data not shown). Although proteasome mediated protein degradation consumes ATP, the amount of ATP used would have to be on the order of 150 ATPs substrate^{-1} to account for even a 1% reduction in oxygen consumption, given a proteasome-mediated degradation rate of 1.8×10^6 proteins min^{-1}. A 1% reduction in oxygen consumption is below the sensitivity of detection of the method used. Even if proteasome ATP consumption is larger than this, it might not be inhibited by proteasome inhibitors, since the energy is expended by the 19S subunit which may continue to function while attached to inactivated 20S proteasomes.

Quantitating Antigen Processing in L-K^b Cells
Step 1: Quantitating Substrate Synthesis
Several recent studies suggest that a large portion of the peptides presented by MHC class I molecules on the cell surface are derived from nascent proteins (Schubert et al., 2000; Reits et al., 2000; Khan et al., 2001). To gain a more quantitative understanding of peptide generation, we used a panel of recombinant vaccinia viruses (rVV) that express chimeric proteins containing influenza nucleoprotein (NP), a 498 residue protein with an extremely high metabolic stability as measured by standard means (Table 1).

The first construct expresses NH_2-terminal NP fused with the chicken egg ovalbumin-derived K^b binding SIINFEKL peptide and enhanced green fluorescence protein (GFP) at the COOH terminus (this chimera is termed NP-GFP). In the second chimera, a sequence consisting largely of repeated Lys-Glu residues is inserted into NP-GFP (KEKE-NP-GFP) (Antón et al., 1999). The KEKE motif causes NP-GFP to misfold and is degraded by the ubiquitin (Ub)-proteasome system with a $t_{1/2}$ of $\sim$70 min in L-K^b cells (data not shown). In the third chimera, the initiating Met of NP-GFP is replaced by Arg fused at the COOH terminus of Ub (R-NP-GFP). Ub is cotranslationally cleaved by Ub hydrolases, and the remaining protein is degraded by proteasomes with a $t_{1/2}$ of 10 min in L-K^b cells (data not shown).

Following infection of L-K^b cells with rVVs, GFP synthesis was monitored by flow cytometry at 10 min intervals for 5 hr. Between 50 and 60 min after adding VV-NP-GFP to cells, we first detected GFP, whose rate of accumulation accelerated until peaking approximately 30 min later (Figure 1C). Detection of the modified NP-GFP chimeras displayed similar kinetics, but with a gentler slope that eventually decelerated as the rate of degradation matched the rate of synthesis. The character of these curves is completely consistent with the measured biochemical half-lives of the respective proteins (Figure 1D).

We measured the amount of NP-GFP fusion proteins by quantitative Western blotting (Figure 1E). This revealed that 1 fluorescent unit corresponds to 1×10^4 molecules, and therefore the cellular concentration of NP-GFP 5 hr after infection is 8×10^6 molecules cell^{-1}. Starting at $\sim$90 min postinfection, NP-GFP accumulates at a rate of 2.2×10^6 molecules hr^{-1}.

We confirmed the validity of these figures by metabolic radiolabeling. VV-NP-GFP infected cells were radiolabeled with [^{35}S]-Met. After resolving [^{35}S]-Met labeled proteins via SDS-PAGE, we used a PhosphorImager to determine the fraction of radioactivity incorporated in NP-GFP. Taking into account the Met content of NP-S-GFP, we calculated that NP-GFP production ranged from 1.4% to 2.5% of the total protein synthesis in rVV-infected L-K^b cells in several different experiments. Based on the overall rate of protein synthesis determined using [^{3}H]-Leu to label a different aliquot of cells in the same experiment, we calculated that cells produced between $2.1–3.8 \times 10^6$ NP-GFP molecules hr^{-1}, which agrees with the Western blot data.

Radiolabeling further revealed that the rate of NP-GFP synthesis attained maximal levels approximately 30 min earlier than fluorescence as determined by flow cytometry. The acquisition of fluorescence by GFP expressed in bacteria under anaerobic conditions upon exposure to oxygen demonstrates similar kinetics ($t_{1/2}$ = 27 min) (Heim et al., 1995), suggesting that the rate-limiting step
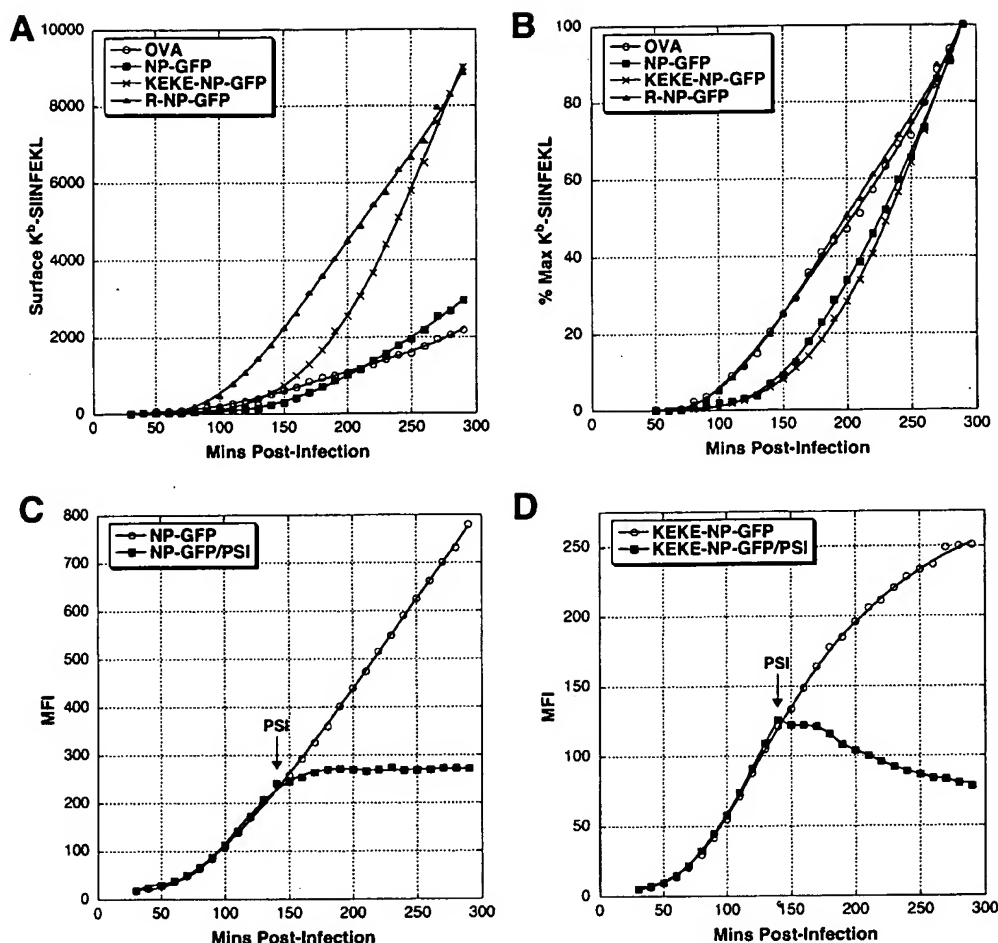
Figure 2. K^b-SIINFEKL and Chimeric NP-GFP Levels in rVV-Infected L-K^b Cells

(A) L-K^b cells were infected with rVVs expressing NP-GFP (squares), KEKE-NP-GFP (X), R-NP-GFP (triangles), or OVA (circles). Surface K^b-SIINFEKL complexes were quantitated by direct staining with Alexa Fluor 647-conjugated 25-D1.16 mAb.

(B) Surface K^b-SIINFEKL levels from (A) expressed as the percent of maximum expression for each construct. Graph symbols are the same as for (A).

(C and D) GFP levels in L-K^b cells infected with rVV-expressing NP-GFP (C) or KEKE-NP-GFP (D) and treated 140 min p.i. with protein synthesis inhibitors (squares) or left untreated (circles).

in GFP maturation in eukaryotic cells is also oxidation of the fluorophore.

Step 2: Quantitating Peptide Class I Complexes

We quantitated K^b-SIINFEKL complexes (hereafter referred to as complexes) using 25-D1.16 mAb conjugated to Alexa Fluor 647. By relating fluorescence intensity to a standard curve, we could determine the number of complexes present on the surface of rVV-infected cells shown in Figure 1C. In addition to the rVVs described above, we used rVVs encoding chicken egg ovalbumin (OVA) (the source of SIINFEKL) or MSIINFEKL.

As seen in Figure 2A, ~3 × 10^3 complexes are generated after a 5 hr infection with either VV-NP-GFP or VV-OVA. Although R-NP-GFP is degraded rapidly, the number of complexes increases only 3-fold. By 5 hr postinfection a similar number of complexes are produced from KEKE-NP-GFP as from R-NP-GFP. Interestingly, the kinetics of peptide-class I complex generation markedly differs between these two substrates. While

the rate of complex formation from R-NP-GFP plateaus at ~110 min postinfection, the rate of complex formation from KEKE-NP-GFP accelerates throughout the infection period. This suggests that complexes are derived from two pools of KEKE-NP-GFP, one that is degraded rapidly and the other more slowly. As the latter pool accumulates, the absolute rate of degradation increases, and the rate of complex generation increases in step.

Note that the peptide generation curves for R-NP-GFP and KEKE-NP-GFP eventually cross. Since the rates of synthesis of the two proteins are similar (if anything, slightly more R-NP-GFP is synthesized) (data not shown), this indicates that the efficiency of generating SIINFEKL from the two proteins differs. Calculation of the slopes reveals that by 4 hr postinfection (p.i.), SIINFEKL is generated at twice the efficiency from KEKE-NP-GFP than from R-NP-GFP. This cannot be attributed to differences in local flanking sequences, since the proteins differ only

by the Ub extension (which is removed immediately) and the insertion of the KEKE sequence 165 residues upstream from SIINFEKL.

In Figure 2B, K^b-SIINFEKL levels are replotted as a percentage of the maximum surface levels at the end of the infection, revealing that the kinetics of K^b-SIINFEKL production from OVA and R-NP-GFP are remarkably similar. Following a lag period of 90 min p.i., rates rapidly reach maximal levels in parallel. This strongly suggests that nearly all peptides from OVA derive from DRiPs. By contrast, the relative rate of complex formation from NP-GFP is highly similar to KEKE-NP-GFP. This suggests that, as with KEKE-NP-GFP, peptides are derived from rapidly and slowly degraded forms of NP-GFP, with the latter being the more efficient source.

Contribution of Newly Synthesized Proteins to Antigen Processing

We further examined the contribution of nascent proteins to complex formation by treating cells with protein synthesis inhibitors (PSI) 140 min after the start of infection. Protein synthesis halted within a minute of adding PSI to cells, as determined by cessation of incorporation of [^{35}S]-Met. There was an immediate retardation in the rate of GFP accumulation. GFP continued, however, to accumulate at a lower rate for 40 min. This is consistent with the lag between radiolabeling and fluorescence noted above.

Importantly, the level of NP-GFP fluorescence remained essentially unchanged for the remainder of the 2.5 hr incubation period (Figure 2C). By contrast, the addition of PSI resulted in an immediate leveling off of KEKE-NP-GFP fluorescence for ~30 min, which then declined with a $t_{1/2}$ of 180 min (Figure 2D). We interpret the plateau to indicate a balance between the acquisition of fluorescence by nascent GFP and degradation. Notably, the fluorescent $t_{1/2}$ is considerably longer than the measured biochemical $t_{1/2}$ of KEKE-NP-GFP (~70 min). This indicates that there is heterogeneity of KEKE-NP-GFP with regard to fluorescence and, further, that fluorescence is associated with greater metabolic stability.

We examined complex formation in the same experiment. In cells expressing R-NP-GFP, addition of PSI did not affect complex generation for 50 min, when it abruptly ceased (Figure 3A). Since peptides are generated rapidly from this substrate, this demonstrates that 50 min are required for peptide processing, complex formation, and transporting complexes to the cell surface. This is in close agreement with the lag between the times required to achieve the maximal synthetic rate of VV-encoded proteins (90–100 min) and the maximal rate of peptide generation from R-NP-GFP (140–150 min). OVA behaved identically to R-NP-GFP (Figure 3B), demonstrating that, for this protein, peptides are derived nearly exclusively from a newly synthesized pool.

The production of complexes from NP-GFP and KEKE-NP-GFP demonstrated a different behavior. Like R-NP-GFP and OVA, both demonstrated the 50 min lag in which complex formation continued identically to untreated cells. However, rather than stopping at this time, complexes accumulated at a reduced rate for the next 90 min (Figures 3C and 3D). This demonstrates that the abrupt abrogation of complex formation from R-NP-GFP

and OVA is not simply due to general effects of PSI on antigen processing or K^b availability or export. Normalization of the data reveals that the relative rates of production of complexes from NP-GFP and KEKE-NP-GFP are highly similar, reaching a rate of complex formation half of that observed in untreated cells (Figure 3E). This suggests that these peptides derive nearly equally from rapidly and slowly degraded substrate pools at this time postinfection.

Time Required for Peptide Generation and Trafficking

We further examined the kinetics of antigen processing using the rVV-expressing MSIINFEKL. Although it is not technically feasible to measure the translation rate of this peptide, it is under the control of the same VV promoter as the other inserted genes, and its rate of translation should be similar. The peak rate of complex formation from MSIINFEKL is ~5-fold higher than that of R-NP-GFP. Thus, even the near complete degradation of R-NP-GFP does not come close to producing saturating amounts of peptide.

Complex formation from MSIINFEKL ceases 30 min after the addition of PSI (Figure 3F). Since peptides are degraded rapidly unless protected by MHC class I molecules (Malarkannan et al., 1995; Reits et al., 2003), association must occur within a few minutes of their synthesis. Consequently, virtually all complexes exit the endoplasmic reticulum (ER) and transit the secretory pathway within 30 min of their formation. Notably, the PSI-induced cessation of complex formation from R-NP-GFP (and OVA) demonstrated a 20 min lag relative to MSIINFEKL. This is consistent with the 10 min half-life of R-NP-GFP and suggests that OVA DRiPs are degraded with similar kinetics.

Quantitating Antigen Processing in Professional Antigen-Presenting Cells

We next studied the efficiency of antigen processing in VV-infected professional antigen-presenting cells (pAPC): bone marrow dendritic cells (BMDCs), the DC-like cell line DC2.4 (Shen et al., 1997), and macrophages (Mϕ). CD11c$^+$ BMDCs and DC2.4 cells expressed NP-GFP with similar kinetics and at similar levels as L-K^b cells, while CD11b$^+$ macrophages present in peritoneal exudates expressed NP-GFP at ~45% of the levels achieved in L-K^b and DCs (Figure 3G; data for L-K^b cells are replotted from Figure 1 for purposes of comparison). Notably, the generation of K^b-SIINFEKL complexes from NP-GFP now demonstrated nearly linear kinetics (Figure 3H) strongly suggesting that peptides derive principally from DRiPs. The efficiency of generating K^b-SIINFEKL complexes from NP-GFP, R-NP-GFP (Figure 3I), KEKE-NP-GFP (data not shown), and OVA (data not shown) by DCs and Mϕs was similar to L-K^b cells, as determined by calculating the ratio of cell surface complexes generated per quantity of protein substrate biosynthesized.

Discussion

Macroeconomics of Protein Synthesis and Degradation

We have measured rates of protein synthesis and degradation and the numbers of ribosomes and proteasomes in a model-cultured cell (Table 2). Although several of
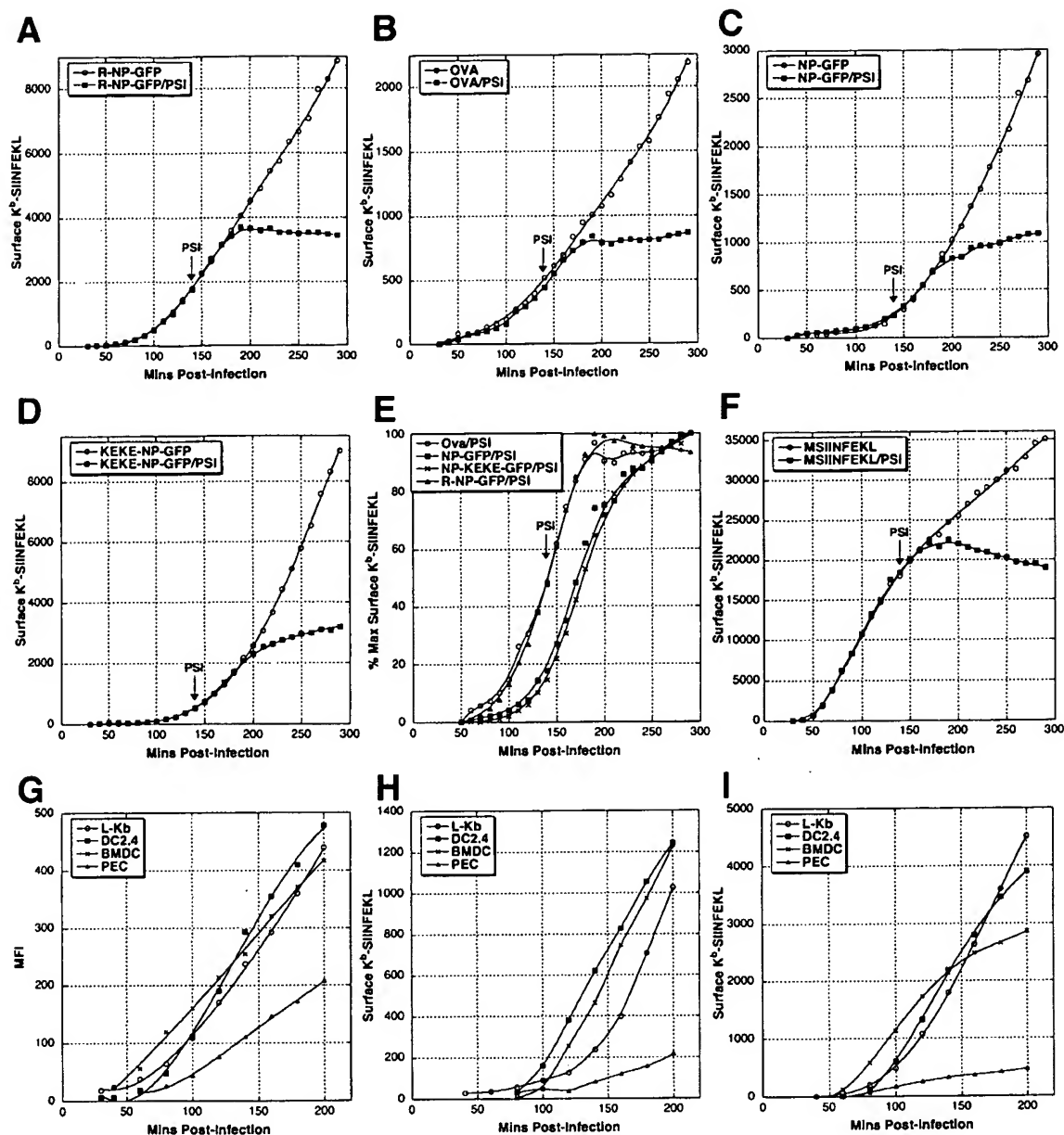
Figure 3. Generation of Surface K^b-SIINFEKL Complexes on rVV-Infected Cells

(A–D and F) Surface K^b-SIINFEKL levels on L-K^b cells infected with rVVs expressing OVA (A), R-NP-GFP (B), NP-GFP (C), KEKE-NP-GFP (D), or MSIINFEKL (F) and treated 140 min p.i. with protein synthesis inhibitors (squares) or left untreated (circles).

(E) Surface K^b-SIINFEKL levels on cells expressing OVA (circles), NP-GFP (squares), KEKE-NP-GFP (X), and R-NP-GFP (triangles) following treatment with protein synthesis inhibitors 140 min p.i. Surface K^b-SIINFEKL levels are expressed as the percent of maximum 25-D1.16 staining for each construct.

(G–I) DC-like DC2.4 cells (squares), bone marrow-derived dendritic cells (BMDC) (X), and peritoneal exudate macrophages (PEC) (triangles) were infected with rVV-expressing NP-GFP (G and H) or R-NP-GFP (I). GFP levels (G) and K^b-SIINFEKL complexes (H and I) were quantitated as described for L-K^b cells. GFP and surface K^b-SIINFEKL levels for L-K^b cells (circles) are replotted from Figures 1 and 2 for the purpose of comparison.

these values have been published before, it has always been in a piecemeal manner (separate laboratories working with different cells) that prevents integrating the data in anything but a theoretical manner (Yewdell, 2001). Remarkably, the theoretical values correlate rea-

sonably well with the actual values we have determined. These values have some interesting implications.

Using textbook values relating the rRNA:tRNA or cellular protein:tRNA ratios (Alberts et al., 1994), we can calculate that L-K^b cells possess ~10–25 copies of tRNA

Table 2. The Protein Economy of L-K^b Cells

Production	
Proteins per cell	2.6×10^9
Ribosomes per cell	6×10^6
Translation rate	4×10^8 min^{-1}
% Required for cell division (24 hr)	43%
% Secreted or released	12%
% Ribosomes engaged in translation	>95%
tRNA per ribosome	10–25
% Cellular metabolism devoted to protein synthesis	45%
Destruction	
Proteasomes per cell	8×10^5
Overall degradation rate	1.8×10^6 min^{-1}
Newly synthesized proteins	1.3×10^6 min^{-1}
Long-lived proteins	5×10^5 min^{-1}
Proteasome activity	2.5 substrates degraded min^{-1}
Creative destruction	
Efficiency of SIINFEKL-K^b complex production	1/440–1/3000 substrates degraded per complex created

per ribosome. Since a complete set of tRNA comprises 32 species whose abundance differs by 10-fold, it means that the lower abundance tRNAs may be present at a ratio of 1 copy for every 20 ribosomes. The low ratio of tRNA to ribosomes makes it easy to understand how codon usage governs translation rates (Sharp and Li, 1986; Liljenstrom and von Heijne, 1987). If ribosomes translate proteins in compartments that limit access to tRNA, as evidence suggests (Stapulionis and Deutscher, 1995), then such compartments must contain multiple ribosomes. We can estimate that there must be ~20 ribosomes per compartment for each compartment to contain at least one of each tRNA species.

We find that L-K^b cells possess approximately eight times as many functional ribosomes as proteasomes. This precludes the pairing of a proteasome with each ribosome to create a translation/degradation complex. To the extent that proteins are truly degraded cotranslationally (Turner and Varshavsky, 2000), this means that proteasomes must be recruited to ribosomes. Given the density of ribosomes in the cytosol, the inter-proteasome-ribosome distance should never be much greater than the diameter of ribosomes, and given the velocity of proteasome diffusion in the cytosol (Reits et al., 1997), the time will be very short relative to the speed of translation.

Dividing the number of substrates degraded min^{-1} (2×10^6) by the number of functional proteasomes (8×10^5) reveals that each proteasome degrades an average of ~2.5 substrates min^{-1}. Taking the average size of a peptide generated by the proteasome as 7–8 residues (Kisselev et al., 1999) and the average size of a protein as 466 amino acids, the proteasome must be capable of cleaving at least 150 peptide bonds min^{-1}. This represents a minimal estimate of the turnover rate, since proteasomes (whose levels can only be increased relatively slowly due to their slow assembly times), must have residual capacity for degrading proteins when cells are damaged by chemical or physical stress.

Similar to other cells (Schubert et al., 2000), 25% of proteins synthesized by L-K^b cells appear to represent DRiPs. Since protein synthesis accounts for 45% of ATP utilization, this means that DRiP production consumes 11% of cellular energy and whatever additional energy costs (probably minor in comparison) are incurred during DRiP destruction. Protein synthesis is believed to consume between ~20% of the energy generated by adult mammals and a higher fraction in growing juveniles (Rolfe and Brown, 1997). A 25%–30% DRiP rate translates into wasting >6% of food consumption due to inefficient protein biosynthesis. On top of this must be added the energy devoted to creating the infrastructure for synthesizing (ribosomes, chaperones, tRNA, etc.) and destroying (proteasomes, Ub, etc.) DRiPs.

Could this be? As discussed previously (Yewdell et al., 2001), the true DRiP rate in vivo may be considerably lower than we measure in vitro. We must entertain the possibility, however, that high DRiP rates are a general feature of cells. Protein biosynthesis may simply be a difficult task, and investments in increasing efficiency may not be worth the cost. Alternatively (and risking heresy), perhaps we overvalue efficiency in biological systems. Only ~2% of the human genome encodes proteins. Though some noncoding DNA must be essential, retro transposons seem to be a clear-cut case of inefficiency. Rube Goldberg would be proud of mitochondria, which maintain a complete translation system and genome to produce just 13 proteins. Ultimately, selection pressure in evolution is exerted by other similarly inefficient organisms and not arbitrary standards of efficiency conjured by human intelligence.

Microeconomics of MHC Peptide Ligand Generation

Obtaining a valid estimate of the efficiency of generating class I ligands from protein substrates requires accurate knowledge of the numbers of complexes formed and substrates degraded. Obtaining the latter number is not a simple task for proteins traditionally thought of as metabolically stable, due to the uncertain proportion of nascent protein diverted to the DRiP pool. Montoya and del Val (1999) estimated the efficiency of generating an antigenic peptide from VV-encoded β-galactosidase but limited their analysis to the amount of protein synthesized as determined by enzymatic activity compared to purified β-galactosidase. They did not attempt to determine the DRiP fraction of β-galactosidase, leaving open

Table 3. Processing Efficiency and DRiP Rate

Experiment	Cell Type	Protein Molecules Degraded per Surface K^b-SIINFEKL Complex	DRiP Rate
1	L-K^b	1638	18.7%
2	L-K^b	1214	25.4%
3	L-K^b	994	31.5%
4	L-K^b	2292	20.9%
5	L-K^b	2031	27.8%
6	L-K^b	1772	29.0%
7	L-K^b	3122	37.4%
8	L-K^b	2872	30.9%
9	L-K^b	2026	22.6%
Avg		1995	27.1%
1	DC2.4	1780	44.8%
2	DC2.4	1226	23.0%
3	DC2.4	1211	25.7%
Avg		1406	31.2%
1	BMDC	1464	40.4%
2	BMDC	4400	55.8%
Avg		2932	48.1%
1	PEC	6481	42.6%
2	PEC	2960	22.0%
Avg		4720	32.3%

the question of the efficiency of peptide generation per substrate.

Determining the true DRiP fraction for any given protein poses technical hurdles (Yewdell et al., 2001). This is much less of a problem, however, for R-NP-GFP, which in being nearly completely degraded within minutes of its synthesis exhibits a DRiP rate of nearly 100%. Since NP-GFP, R-NP-GFP, and KEKE-NP-GFP are synthesized at comparable rates, we can use NP-GFP as a reference protein to calculate the rate of R-NP-GFP synthesis. Although an uncertain amount of newly synthesized NP-GFP is diverted to DRiPs, this can be accounted for by calculating the difference in the rate of K^b-SIINFEKL complex formation from the two proteins and dividing this by the difference in the rates of synthesis of stable proteins, which is essentially equal to the apparent rate of NP-GFP synthesis. By taking these rates shortly after the rate of production of complexes from R-NP-GFP peaks, we can minimize the contribution of peptides from the slowly degraded cellular NP-GFP pool.

Examination of Figure 3 shows that between 160 and 180 min postinfection, 970 complexes are generated from R-NP-GFP by L-K^b cells. Over the same period, 306 complexes were generated from NP-GFP. The corresponding increase in stable NP-GFP protein, which must be taken 50 min earlier (110–130 min postinfection) to allow for processing and transport of peptide-class I complexes, was 6.6×10^5 molecules synthesized. Thus, 6.6×10^5 more R-NP-GFP molecules were degraded than NP-GFP over this time period to generate an additional 664 K^b-SIINFEKL complexes. We can therefore calculate the efficiency of complex generation:

$$\frac{970 - 306}{6.6 \times 10^5} = 1/994. \tag{1}$$

Over nine independent experiments this number was relatively constant, ranging between 1/994 and 1/3122

(Table 3), with an average efficiency of 1 complex generated per 1995 R-NP-GFP molecules degraded. The efficiency of peptide generation was similar in pAPCs (Table 3), averaging 1 per 1406 substrates degraded by DC2.4 cells, 1 per 2932 substrates degraded by BMDC and 1 per 4720 substrates degraded by Mϕs.

The findings with VV-MSIINFEKL in L-K^b cells help explain this low efficiency. The much higher levels of K^b-SIINFEKL complex formation observed using this rVV demonstrates that TAP or MHC class I molecules are not limiting in the processing of NP-GFP constructs. The maximal rate of complex formation from MSIINFEKL (200 complexes min^{-1}) was achieved by 50 to 60 min postinfection. Given the 30 min delay for complex appearance at the cell surface, this means that peptide achieves near saturating levels between 20 and 30 min postinfection. At this time, MSIINFEKL peptide is expressed at a rate of $\sim$10,000 molecules min^{-1} based on comparison to NP-GFP synthetic rates. Therefore, the observed $\sim$200 complexes min^{-1} are created with an efficiency of $\sim$2%.

Since 1 of every 50 peptides synthesized survives to form a stable surface K^b-SIINFEKL complex whereas complexes are generated from protein with an efficiency of 1 in 2000, this suggests the rate of suitable peptide production from protein is $\sim$1 in 40. Cascio et al. (2001) reported that the efficiency of producing SIINFEKL or N-extended forms that can be further trimmed (cells are rich in amino exopeptidase activity against oligopeptides but lack carboxypeptidase activity) from OVA by incubation with standard or immunoproteasomes is approximately 1/16.

Given some wiggle room then, we can account for the efficiency of SIINFEKL production—proteasomes produce appropriate precursor peptides $\sim$2.5% of the time, and only $\sim$2% of these will survive the perils of the cytosol and voyage into the ER to find class I molecules, a net efficiency of .05% or 1/2000. Although the comparative data set is limited, SIINFEKL is produced
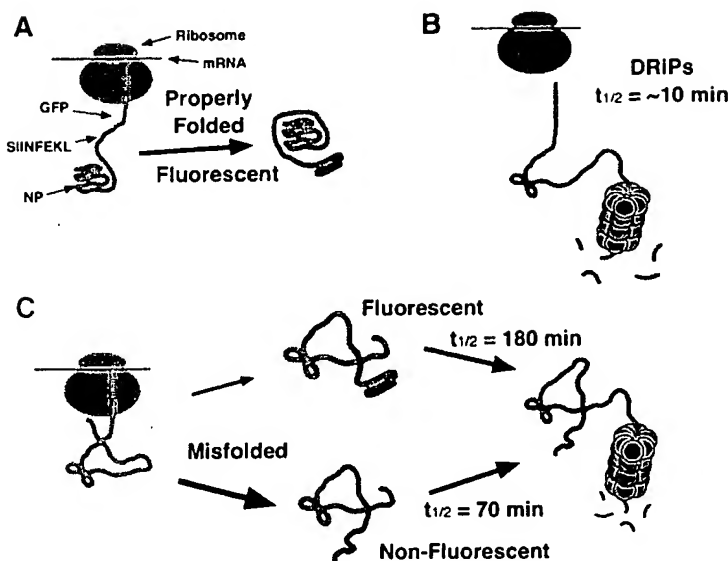
Figure 4. Possible Fates of Newly Synthesized Protein Molecules

(A) Properly folded nascent protein molecule. Stable, with long $t_{1/2}$. Protein is fluorescent due to properly folded GFP moiety. Represented by non-DRiP fraction of NP construct.
(B) Defective ribosomal product. Highly unstable, with $t_{1/2}$ = 10 min. Targeted for rapid degradation by the proteasome. Virtually all R-NP behaves as a DRiP, as well as a fraction of newly synthesized NP and KEKE-NP molecules.
(C) Improperly folded nascent protein molecule. Protein fails to fold to native conformation. GFP moiety may or may not fold properly, resulting in fluorescent and nonfluorescent protein populations. Unstable, with $t_{1/2}$ = 70–180 min. Predominant fate of non-DRiP fraction of KEKE-NP.

more efficiently than other defined determinants expressed under similar circumstances (Antón et al., 1997, 1998; Montoya and del Val, 1999). This is consistent with previous calculations, indicating that the overall efficiency of peptide generation from degraded molecules is on the order of 1/10,000 (Yewdell, 2001).

This is a far cry from previous determinations of the efficiency of proteasome-mediated peptide generation from bacterial proteins secreted into the cytosol of infected J774 cells (a Mϕ-like reticulum cell sarcoma), which was determined to be as high as one class I peptide complex generated for every three L. monocytogenes p60 proteins degraded (Villanueva et al., 1994; Sijts et al., 1996). What could account for this discrepancy? Probably real differences in processing efficiency combined with experimental errors. It is unlikely that macrophages are generally more adept at processing endogenous antigens, since we find that peritoneal Mϕs are actually less efficient than L-K^b cells and DCs in generating K^b-SIINFEKL complexes from R-NP-GFP. It is possible, however, that Mϕs possess specialized machinery that enables high efficiency processing of bacteria and other phagocytosed antigens. It was recently reported that phagosomes fuse with portions of the ER in Mϕs (Gagnon et al., 2002). Since proteasomes appear to participate in the processing of p60 (Zwickey and Potter, 1999), any gains in processing efficiency would have to entail export of bacterial peptides to the cytosol from the ER-phagosome and their reimportation into the ER-phagosome or ER.

Fully acknowledging the seminal importance of the quantitative studies by Pamer and colleagues, we note that they may have overestimated the number of peptides produced and underestimated the amount of protein degraded. Differences between naturally processed peptides and their synthetic counterparts will lead to an overestimation of the number of peptides generated by cells if, as is often the case, T_{CD8+} preferentially recognize the naturally processed versions. Side chain modification can often only be detected by mass spectroscopic

analysis, which was not used to demonstrate the identity of synthetic and natural Listeria-derived peptides. The amount of p60 introduced into the cytosol was not determined directly but was based on the rate of secretion of p60 by extracellular bacteria. This was measured using antibodies that may not recognize all forms of secreted p60. Notably, the $t_{1/2}$ of p60 in J774 cells measured using these antibodies was 90 min while peptide loading of class I molecules was virtually complete within 30 min of addition of a bacterial protein synthesis inhibitor. This suggests a discrepancy between the antibody reactive-p60 and p60 that provides antigenic peptides.

Although the efficiency of peptide generation from endogenous viral proteins appears to be relatively low, it may still be sufficient to serve the purposes of the immune system. A key feature of many viral infections is the nearly complete replacement of host mRNA translation with viral mRNA. Since T_{CD8+} require only tens to hundreds of class I peptide complexes for activation, this, in combination with a high DRiP rate, should enable T_{CD8+} recognition of infected cells in a time frame that enables lysis of infected cells prior to completion of the infectious cycle.

Biosynthesized Proteins as Sources of Peptide

Khan et al. (2001) reported that generation of an antigenic peptide from a protein requires continued production of mRNA encoding the protein, as shown over the course of hours after blocking transcription. We show that the kinetics of K^b-SIINFEKL complex generation from OVA (its natural protein source) under normal conditions and after blocking protein synthesis behaves exactly as predicted for a short-lived DRiP. This provides conclusive evidence for the validity of the DRiP hypothesis for the generation of peptides from a specific, genetically unmodified gene product.

Unlike OVA, SIINFEKL production from NP-GFP continues at a reduced rate after blocking protein synthesis. Over the same interval, GFP levels remain virtually constant when measured with an extremely high degree

of precision in individual cells by flow cytometry. We interpret this to mean that peptides derive from a nonfluorescent subpopulation of NP-GFP that is degraded relatively slowly. This interpretation is fully consistent with the acceleration of peptide production as the infection period proceeds. In this manner NP-GFP behaves like KEKE-NP-GFP, which provides a model for a slowly degraded substrate. (Figure 4 illustrates the possible conformational states and fates of the chimeric NP proteins we utilized.) Even KEKE-NP-GFP demonstrates two forms, since its biochemical decay is significantly faster than its decay in fluorescence when protein synthesis is halted. The nonfluorescent form of NP-GFP may never have been properly folded, in which case it can be considered a slowly degraded DRiP. The absolute stability of NP-GFP fluorescence in the presence of PSI suggests that this is the case, but we cannot rule out the possibility that peptides derive from a pool of native NP-GFP that unfolded well after translation.

If class I peptide complexes are produced with similar efficiency from rapidly degraded NP-GFP DRiPs and R-NP-GFP, we can calculate the percentage of nascent NP-GFP that is diverted to this pool. To limit the contribution of the more slowly degraded cellular substrate pool, we use the number of complexes generated between 110 and 130 min postinfection with NP-GFP:

$$(306 \text{ complexes}) \times (994 \text{ substrates/complex}) =$$

$$3.04 \times 10^5 \text{ substrates.} \tag{2}$$

Dividing the number of rapidly degraded proteins by the total number of NP-GFP molecules synthesized gives us the DRiP rate:

$$\frac{(3.04 \times 10^5 \text{ substrates})}{(6.6 \times 10^5 \text{ NP}) + (3.04 \times 10^5 \text{ DRiPs})} = 31.5\%. \tag{3}$$

As seen in Table 3, this ranged from 19% to 37% over nine experiments for L-K^b cells, with an average value of 27%—remarkably similar to the overall DRiP rate of 25%. Similar calculations for pAPCs reveal a comparable range of DRiP rates.

As can be seen in Figure 2A, the rate of K^b-SIINFEKL production from KEKE-NP-GFP accelerates as the size of the cellular KEKE-NP-GFP pool increases, eventually overtaking the rate of production from R-NP-GFP. This is only possible if K^b-SIINFEKL complexes are generated from the cellular KEKE-NP-GFP pool more efficiently than from the short-lived DRiPs.

The efficiency of K^b-SIINFEKL generation from the long-lived KEKE-NP-GFP pool can be calculated by taking advantage of the fact that the rates of KEKE-NP-GFP synthesis and degradation approach equilibrium by 5 hr postinfection. At this time the rate of synthesis is 3.2×10^6 molecules hr^{-1}. If 31.5% of these molecules ($1 \times 10^6 \text{ hr}^{-1}$) are short-lived DRiPs, then the net synthetic rate is $2.2 \times 10^6 \text{ hr}^{-1}$, which equals the degradation rate. The rate of K^b-SIINFEKL production at this time is 6×10^3 complexes hr^{-1}. Of these, we calculate that 1×10^3 are generated from the short-lived DRiP fraction (1×10^6 DRiPs degraded with an efficiency of 1 complex per 994 substrates). The remaining 5×10^3 complexes should be derived from the 2.2×10^6 molecules of KEKE-NP-GFP degraded hr^{-1} from the long-lived pool. This

yields a calculated efficiency of 1 K^b-SIINFEKL complex generated per 440 KEKE-NP-GFP molecules degraded.

If this efficiency applies to the pool of nonfluorescent NP-GFP discussed above, we can calculate that the 447 complexes generated from the slowly degraded pool in the last hour of infection (1365 total complexes minus the 918 complexes from rapidly degraded DRiPs using the initial rate) would represent the degradation of 2.0×10^5 substrates, which represents $\sim$2.5% of the total NP pool at this time.

We can use these values to bolster our conclusion that after blocking protein synthesis complexes are generated from nonfluorescent NP-GFP. Over the last 100 min of the infection in the presence of protein synthesis inhibitors (when GFP levels are stable), 300 complexes were generated, which would represent degradation of $300 \times 440 = 1.3 \times 10^5$ substrates. If these molecules were fluorescent, this would represent 13 fluorescent units, which is well within the precision of our measurements.

The more efficient generation of class I peptide complexes from KEKE-NP-GFP than from R-NP-GFP suggests that proteasomes display heterogeneity in their capacity to generate class I peptide ligands. Little is known about functional differences between proteasomes—given their abundance and involvement in myriad cellular processes it is likely that proteasomes display considerable heterogeneity in function, in addition to those attributed to the alterations associated with immunoproteasomes.

Experimental Procedures

Cells and Viruses
L-K^b and DC2.4 cells were provided, respectively, by Sheil (West Virginia University, Morgantown, WV) and Rock (University of Massachusetts Medical School, Worcester, MA). Mϕs elicited from C57BL/6 mice by intraperitoneal injection of 1 ml 3% (w/v) thioglycollate solution were harvested 5–6 days postinjection and used immediately. BMDC obtained from femurs were propagated in media supplemented with 20% FBS and 10% supernatant from X63 cells transfected with murine GM-CSF. Nonadherent cells were removed on days 2 and 4. Adherent cells were used for assays on days 6–7 after harvest.

rVVs expressing SIINFEKL-containing proteins have been described (Antón et al., 1999). NP-GFP fusion proteins contain SIINFEKL peptide at the C terminus of NP followed by ARDPPVAT followed by EGFP. Cells were infected at a multiplicity of infection (MOI) of 10 for 15 min at 37°C with constant agitation in balanced salt solution containing 0.1% bovine serum albumin (BSS/BSA). Cells were then incubated at 37°C in growth media for the remainder of the assay in the presence of 25 μg/ml cytosine arabinoside. Protein synthesis was inhibited by the addition of cycloheximide and emetine (Sigma, St. Louis, MO) to a final concentration of 25 μg /ml each.

Immunoblotting
L-K^b cells (5×10^5) were lysed in 1 ml 95°C SDS-PAGE sample buffer and boiled for 10 min. Serial 2-fold dilutions were made into sample buffer containing uninfected L-K^b cell lysates (5×10^5 cells/ml) to maintain a constant protein concentration in samples. Samples were separated in 10%–12.5% SDS-PAGE gels and transferred to PVDF membranes. Immunoblots were incubated with rabbit antibodies raised to a synthetic peptide corresponding to NP$_{2-13}$. Proteasome immunoblots were probed with a mouse mAb that binds the p29K α-subunit (ICN Biomedicals, Costa Mesa, CA). Ribosome immunoblots were probed with human anti-ribosomal P autoimmune serum (Immunovision, Springdale, AK). Blots were developed with horseradish peroxidase-coupled antibodies using a chemilumines-

cent peroxide substrate. Luminescence was recorded on Biomax MR film (Eastman Kodak, Rochester, NY), digitized, and analyzed using ImageQuant software (Molecular Dynamics Inc., Sunnyvale, CA). Standard curves were used to determine concentrations of corresponding proteins in samples containing lysates from rVV-infected L-K^b cells.

NP-GFP standards were prepared by determining the total protein concentration in purified preparations of influenza virus A/Puerto Rico/8/34. The percentage NP-GFP of total viral protein was determined by SDS-PAGE. Purified proteasomes and ribosomes were the kind gifts, respectively, of DeMartino (University of Texas Southwestern Medical Center, Dallas, TX) and Nicchitta (Duke University Medical Center, Durham, NC).

Cytofluorography

K^b-SIINFEKL levels were determined by incubating cells for 30 min on ice with the 25-D1.16 antibody (Porgador et al., 1997) conjugated to Alexa Fluor 647 (Molecular Probes, Eugene, OR). Cellular GFP and Alexa Fluor 647 levels were determined on a FACScalibur cytofluorograph (Beckton Dickinson, San Jose, CA) using CellQuest (Beckton Dickinson) software, and data were analyzed using FlowJo (Tree Star, San Carlos, CA) software.

Purified 25-D1.16 mAb was conjugated to either fluorescein isothiocyanate (FITC) (Roche) or Alexa Fluor 647, and fluorescence to protein ratios (F:P) for each conjugate were determined. Antibody preparations were titrated against SIINFEKL peptide L-K^b cells to ensure that all staining was performed with saturating concentrations of Ab. To quantitate surface K^b-SIINFEKL levels, L-K^b cells were incubated with 2-fold dilutions of SIINFEKL peptide and stained with 25-D1.16 conjugated to either FITC or Alexa Fluor 647, and fluorescence levels were determined by cytofluorography. Fluorescence levels for FITC-coated calibration beads (DAKO) were determined in parallel and used to construct a standard curve of FITC molecules versus mean fluorescence intensity (MFI). The F:P for FITC-conjugated 25-D1.16 was then used to calculate the number of antibody molecules bound per cell. Calibration standards for Alexa Fluor 647 are not commercially available; therefore, the ratio of MFI to bound antibody for Alexa Fluor 647-conjugated 25-D1.16 was determined by direct comparison with FITC-25-D1.16-stained L-K^b cells.

Peritoneal macrophages, BMDC, and DC2.4 were incubated with 2.4G2 culture supernatant for 20 min on ice to block Fc-receptor-mediated binding prior to staining with 25-D1.16.

Pulse Labeling of Cellular Proteins

L-K^b cells were labeled at 37°C for 10 min with 100 μCi [^{3}H]-Leu (153 Ci/mM) (Amersham) in 180 μl of I$^+$ (which contains 0.802 mM Leu). Labeling was stopped by adding ice-cold media containing excess (10 mM) Leu, and cell pellets were washed once in this same medium. Cell pellets were frozen on dry ice, thawed briefly, and lysed in SDS-PAGE sample buffer at 95°C. Cell lysates were transferred onto filter paper, and protein was precipitated with 10% TCA and then washed extensively with 70% ethanol. Radioactivity was measured by scintillation counting. Labeling of L-K^b cells with [^{35}S]-Met (Amersham) was performed as described for [^{3}H]-Leu. Cell lysates were separated in 10% SDS-polyacrylamide gels. Gels were dried and then scanned on a Typhoon 8600 imager, and digitized images were analyzed using ImageQuant software. To measure secretion of newly synthesized proteins from L-K^b cells, [^{35}S]-Met labeled cells were chased for up to 2 hr containing nonradiolabeled Met. Cell pellets and supernatants from each time point were collected, lysed, and transferred to filter paper and quantitated by scintillation counting as described above.

In preliminary experiments we established that incorporation of [^{3}H]-Leu into proteins with time was absolutely linear under these conditions with no detectable lag following incubation for as short as 1 min. For reasons we do not understand fully, labeling of proteins with [^{35}S]-Met resulted in ~1/10 of the specific activity obtained with [^{3}H]-Leu, which precluded the use of [^{35}S]-Met for absolute determination of protein synthesis rates. Due to the low sensitivity of detecting [^{3}H]-Leu with PhosphorImager screens, we used [^{35}S]-Met to determine the fraction of total protein allotted to NP synthesis.

ATP Consumption

The proportion of cellular energy devoted to protein synthesis in L-K^b cells was determined by measuring O_2 consumption in the presence or absence of protein synthesis inhibitors as previously described (Buttgereit et al., 1992).

References

Alberts, B., Bray, D., Lewis, J., Raff, M., Roberts, K., and Watson, J.D. (1994). Molecular Biology of the Cell (New York: Garland Publishing).

Antón, L.C., Yewdell, J.W., and Bennink, J.R. (1997). MHC class I-associated peptides produced from endogenous gene products with vastly different efficiencies. J. Immunol. 158, 2535–2542.

Antón, L.C., Snyder, H.L., Bennink, J.R., Vinitsky, A., Orlowski, M., Porgador, A., and Yewdell, J.W. (1998). Dissociation of proteasomal degradation of biosynthesized viral proteins from generation of MHC class I-associated antigenic peptides. J. Immunol. 160, 4859–4868.

Antón, L.C., Schubert, U., Bacik, I., Princiotta, M.F., Wearsch, P.A., Gibbs, J., Day, P.M., Realini, C., Rechsteiner, M.C., Bennink, J.R., and Yewdell, J.W. (1999). Intracellular localization of proteasomal degradation of a viral antigen. J. Cell Biol. 146, 113–124.

Buttgereit, F., Brand, M.D., and Muller, M. (1992). ConA induced changes in energy metabolism of rat thymocytes. Biosci. Rep. 12, 109–114.

Cascio, P., Hilton, C., Kisselev, A.F., Rock, K.L., and Goldberg, A.L. (2001). 26S proteasomes and immunoproteasomes produce mainly N-extended versions of an antigenic peptide. EMBO J. 20, 2357–2366.

Gagnon, E., Duclos, S., Rondeau, C., Chevet, E., Cameron, P.H., Steele-Mortimer, O., Paiement, J., Bergeron, J.J., and Desjardins, M. (2002). Endoplasmic reticulum-mediated phagocytosis is a mechanism of entry into macrophages. Cell 110, 119–131.

Heim, R., Cubitt, A.B., and Tsien, R.Y. (1995). Improved green fluorescence. Nature 373, 663–664.

Hershko, A., and Ciechanover, A. (1998). The ubiquitin system. Annu. Rev. Biochem. 67, 425–479.

Khan, S., de Giuli, R., Schmidtke, G., Bruns, M., Buchmeier, M., van Den, B.M., and Groettrup, M. (2001). Cutting edge: neosynthesis is required for the presentation of a T cell epitope from a long-lived viral protein. J. Immunol. 167, 4801–4804.

Kisselev, A.F., Akopian, T.N., Woo, K.M., and Goldberg, A.L. (1999). The sizes of peptides generated from protein by mammalian 26 and 20 S proteasomes. Implications for understanding the degradative mechanism and antigen presentation. J. Biol. Chem. 274, 3363–3371.

Liljenstrom, H., and von Heijne, G. (1987). Translation rate modification by preferential codon usage: intragenic position effects. J. Theor. Biol. 124, 43–55.

Malarkannan, S., Goth, S., Buchholz, D.R., and Shastri, N. (1995). The role of MHC class I molecules in the generation of endogenous peptide/MHC complexes. J. Immunol. 154, 585–598.

Montoya, M., and del Val, M. (1999). Intracellular rate-limiting steps in MHC class I antigen processing. J. Immunol. 163, 1914–1922.

Nandi, D., Woodward, E., Ginsburg, D.B., and Monaco, J.J. (1997). Intermediates in the formation of mouse 20S proteasomes: implications for the assembly of precursor beta subunits. EMBO J. 16, 5363–5375.

Nissen-Meyer, J., and Eikhom, T.S. (1976). An excess of the small ribosomal subunits and a higher rate of turnover of the 60 S than of the 40 S ribosomal subunits in L cells grown in suspension culture. J. Mol. Biol. 101, 211–221.

Palmiter, R.D. (1975). Quantitation of parameters that determine the rate of ovalbumin synthesis. Cell 4, 189.

Porgador, A., Yewdell, J.W., Deng, Y., Bennink, J.R., and Germain, R.N. (1997). Localization, quantitation, and in situ detection of specific peptide-MHC class I complexes using a monoclonal antibody. Immunity 6, 715–726.

Reits, E.A.J., Benham, A.M., Plougastel, B., Neefjes, J., and Trowsdale, J. (1997). Dynamics of proteasome distribution in living cells. EMBO J. 16, 6087–6094.

Reits, E.A., Vos, J.C., Gromme, M., and Neefjes, J. (2000). The major substrates for TAP in vivo are derived from newly synthesized proteins. Nature 404, 774–778.

Reits, E., Griekspoor, A., Neijssen, J., Groothuis, T., Jalink, K., van Veelen, P., Janssen, H., Calafat, J., Drijfhout, J.W., and Neefjes, J. (2003). Peptide diffusion, protection, and degradation in nuclear and cytoplasmic compartments before antigen presentation by MHC class I. Immunity 18, 97–108.

Rock, K.L., and Goldberg, A.L. (1999). Degradation of cell proteins and the generation of MHC class I-presented peptides. Annu. Rev. Immunol. 17, 739–779.

Rock, K.L., York, I.A., Saric, T., and Goldberg, A.L. (2002). Protein degradation and the generation of MHC class I-presented peptides. Adv. Immunol. 80, 1–70.

Rolfe, D.F., and Brown, G.C. (1997). Cellular energy utilization and molecular origin of standard metabolic rate in mammals. Physiol. Rev. 77, 731–758.

Schubert, U., Anton, L.C., Gibbs, J., Norbury, C.C., Yewdell, J.W., and Bennink, J.R. (2000). Rapid degradation of a large fraction of newly synthesized proteins by proteasomes. Nature 404, 770–774.

Sharp, P.M., and Li, W.H. (1986). An evolutionary perspective on synonymous codon usage in unicellular organisms. J. Mol. Evol. 24, 28–38.

Shen, Z., Reznikoff, G., Dranoff, G., and Rock, K.L. (1997). Cloned dendritic cells can present exogenous antigens on both MHC class I and class II molecules. J. Immunol. 158, 2723–2730.

Sijts, A.J., Neisig, A., Neefjes, J., and Pamer, E.G. (1996). Two Lysteria monocytogenes epitopes are processed from the same antigen with different efficiencies. J. Immunol. 156, 683–692.

Stapulionis, R., and Deutscher, M.P. (1995). A channeled tRNA cycle during mammalian protein synthesis. Proc. Natl. Acad. Sci. USA 92, 7158–7161.

Turner, G.C., and Varshavsky, A. (2000). Detecting and measuring cotranslational protein degradation in vivo. Science 289, 2117–2120.

Villanueva, M.S., Fischer, P., Feen, K., and Pamer, E.G. (1994). Efficiency of MHC class I antigen processing: a quantitative analysis. Immunity 1, 479–489.

Wheatley, D.N. (1989). Protein turnover in relation to growth status and the cell cycle in cultured mammalian cells. Revis. Biol. Celular 21, 377–400.

Yewdell, J.W. (2001). Not such a dismal science: the economics of protein synthesis, folding, degradation and antigen processing. Trends Cell Biol. 11, 294–297.

Yewdell, J.W., Schubert, U., and Bennink, J.R. (2001). At the crossroads of cell biology and immunology: DRiPs and other sources of peptide ligands for MHC class I molecules. J. Cell Sci. 114, 845–851.

Zwickey, H.L., and Potter, T.A. (1999). Antigen secreted from noncytosolic Listeria monocytogenes is processed by the classical MHC class I processing pathway. J. Immunol. 162, 6341–6350.

IDENTIFICATION OF THREE NON-VNTR MUC1-DERIVED HLA-A*0201-RESTRICTED T-CELL EPITOPES THAT INDUCE PROTECTIVE ANTI-TUMOR IMMUNITY IN HLA-A2/K^b-TRANSGENIC MICE

Lukas C. Heukamp[1], Sjoerd H. van der Burg[2], Jan-Wouter Drijfhout[2], Cornelis J.M. Melief[2], Joyce Taylor-Papadimitriou[1]* and Rienk Offringa[2]

[1]*Imperial Cancer Research Fund, Breast Cancer Biology Group, Guy's Hospital, London, United Kingdom*
[2]*Department of Immunohematology and Blood Transfusion, Leiden University Medical Center, Leiden, The Netherlands*

The human epithelial mucin MUC1 is over-expressed in more than 90% of carcinomas of the breast, ovary, and pancreas as well as in some other tumours, making it a potential target for tumour immunotherapy. We have identified several MUC1-derived peptides mapping outside the variable number tandem repeat region that comply with the peptide-binding motif for HLA-A*0201 and that become processed into stable major histocompatibility complex-peptide complexes as assessed by *in vitro* assays. In A2/K^b transgenic mice, 3 peptides, namely MUC$_{79–87}$ (TLAPATEPA), MUC$_{167–175}$ (ALGSTAPPV) and MUC$_{264–272}$ (FLSFHISNL) elicit peptide-specific cytotoxic T lymphocyte (CTL) immunity, which protects these mice against a challenge with MUC1, A2/K^b-expressing tumour cells. These peptides therefore represent naturally processed MUC1-derived CTL epitopes that could be used as components in peptide-based vaccines and for the analysis of anti-MUC1 CTL responses in A*0201-positive patients with MUC1-expressing tumours.
© 2001 Wiley-Liss, Inc.

Key words: *MUC1; CTL-epitope; HLA-A*0201; HLA-transgenic mice*

The human epithelial mucin, MUC1, is a heavily O-glycosylated type 1 transmembrane protein expressed on the luminal surface of most glandular epithelial tissues and on a subset of lymphoid cells.[1–3] Expression of MUC1 is dramatically increased in more than 90% of breast, pancreatic and ovarian carcinomas as well as in a proportion of colon and lung cancers,[4–6] B-cell lymphomas and multiple myelomas.[7] Thus, as a widely expressed tumour-associated antigen, MUC1 is under intensive investigation, in both pre-clinical and clinical studies, as a potential target antigen for immunotherapy of cancer.[8]

The extracellular domain of MUC1 consists largely of tandem repeats of 20 amino acids (PDTRPAPGSTAPPAHGVTSA)[5] and the number of repeats varies between 25 and 100, making this region an expressed VNTR (variable number of tandem repeats). Each repeat contains 5 potential O-glycosylation sites and the O-glycans added in some cancers are different from those added in the corresponding normal tissues.[9,10] The aberrant glycosylation in this region results in the exposure of epitopes in the tandem repeat that are normally masked so that the cancer mucin can be recognised as antigenically distinct by B cells. This result has been supported by a large body of data describing antibodies directed against the VNTR that are specific for the tumour-associated altered glycosylation pattern.[6] In addition, non-classical major histocompatibility complex (MHC)-unrestricted T-cell responses have been described that depend on aberrant glycosylation of the VNTR.[7,11–13]

In searching for classical T-cell epitopes, again the focus has been on the VNTR of the molecule, which has been considered to be immunodominant due to the large number of repeats. Thus the VNTR-derived peptide sequence STAPPAHGV has been found to constitute a target for both HLA-A*1101 and HLA-A*0201-restricted cytotoxic T lymphocytes (CTL).[12,14] However, this peptide does not comply fully with the regular binding-motifs for these human leukocyte antigen (HLA) molecules and shows relatively poor binding compared with many other known epitopes, suggest-

ing that it interacts with these HLA molecules in a non-conventional manner.[14]

Although it may seem attractive to focus on HLA-restricted CTL epitopes in the VNTR region, the expression of MUC1 by normal epithelia, albeit at a lower level, needs to be considered. Because the VNTR constitutes an abundant source of antigenic peptides, these could be presented by normal cells, as well as by professional antigen-presenting cells that have taken up significant quantities of antigen derived from MUC1-expressing tissues.[15] As seen with several transgenic mouse models expressing artificial auto-antigens in a tissue-specific manner, high expression can result in T-cell tolerance at a thymic and/or peripheral level. Moreover, the degree of tolerance may relate to the level of antigen expression.[16,17] On the other hand, expression of such tissue-specific auto-antigens may be ignored by T cells, and breaking of this T-cell ignorance by a strong antigenic stimulus can result in T-cell-mediated destruction of the tissues expressing the auto-antigen.[18,19]

The sequences outside the MUC1 VNTR constitute a less abundant source of antigen than those derived from the VNTR. Consequently, the T-cell immune system is less likely to have become tolerised for epitopes mapping to this part of the MUC1 protein. Furthermore, such epitopes are more likely to provide a window for discrimination by effector T cells between the MUC1-over-expressing tumour and normal MUC1 tissue expressing lower amounts. Finally, the VNTR does not harbour peptide sequences that comply well with the binding motifs for the most common HLA-A molecules, whereas these motifs predict a vast quantity of potential epitopes in other areas of the MUC1 sequence.

In an attempt to find HLA-A*0201-restricted immunogenic epitopes in the non-VNTR areas of the MUC1 sequence, we first identified MUC1 peptides that bind well to HLA-A*0201 and tested these for their ability to elicit specific anti-tumour immunity in HLA-A2/K^b mice. These experiments resulted in the identification of 3 MUC1-derived HLA-A*0201-binding epitopes that could serve as targets for the anti-tumour CTL response against MUC1-over-expressing tumours.

MATERIAL AND METHODS

Cell culture

All cell lines were cultured in Iscove's modified Dulbecco's medium (IMDM) (Bio Whittaker, Verviers, Belgium) supplemented with penicillin (100 IU/ml, Brocades Pharma, Leiderdorp, the Netherlands), L-glutamine (2 mM, ICN Biochemicals, Costa Mesa, CA), 8% heat inactivated fetal calf serum (Hyclone, Logan,

*Correspondence to: Imperial Cancer Research Fund, Breast Cancer Biology Group, 3rd floor, Thomas Guy House, Guy's Hospital, London, SE1 9RT, UK. Fax: (44)0207-955-2027. E-mail: papadimi@icrf.icnet.uk

UT) and 20 μM 2-mercaptoethanol (Merck, Darmstadt, Germany) unless otherwise stated.

Jurkat-A2/K^b cells were derived from the human T-cell line Jurkat upon transfection with the chimeric HLA-A*0201/K^b (A2/K^b) gene[20] and cultured in normal culture medium supplemented with 500 μg/ml G418 (Life Technologies, Paisly, UK). B16-MUC1-A2/K^b were derived from the mouse melanoma B16 F1 by transfection with MUC1 cDNA under control of the β-actin promoter[21] and the HLA-A*0201/K^b gene and cultured with 500 μg/ml G418 and 50 μg/ml puromycine (Clonetech, Westburg, NL). Surface expression of MUC1 and A2/K^b was measured by fluorescence-activated cell sorting (FACS) analysis with human MUC1-specific antibodies 12C10 and HMFG2 and with HLA-A*0201-specific antibody BB7.2, respectively (antibodies provided by Imperial Cancer Research Fund). Jurkat-A2/K^b cells, the A2/K^b plasmid and A2/K^b transgenic mice were kindly provided by Dr. L. Sherman (The Scripps Research Institute, Dept. of Immunology, La Jolla, CA) The chimeric A2/K^b gene has the α$_3$ domain of the heavy chain replaced by the corresponding murine H-2 K^b domain while the HLA-A*0201 α$_1$ and α$_2$ domains are left in place.[20] This procedure allows interaction of the mouse CD8 molecule with the mouse α$_3$ domain, while peptide-binding characteristics associated with α$_1$ and α$_2$ domains are retained.

Synthetic peptides

Peptides were made by Fmoc chemistry with a Syro II peptide synthesiser (Multisyntech, Witten, Germany). Peptides were analysed by reversed-phase high performance liquid chromatography that showed over 90% purity. They were then lyophilised and weighed. For MHC binding studies the peptides were dissolved in DMSO (Merck) at 100 mg/ml and stored at −20°C. From this stock solution peptides were diluted in phosphate-buffered saline (PBS) to relevant concentrations. Fluorescent (FL)-labelled reference (FLPSDC(-FL)FPSV) peptide was synthesised as described previously by cystein labelling with 4-(iodoacetamido)-fluorescein (Fluka, Buchs, Switzerland).[22]

Peptide binding assay

Peptide binding to HLA-A*0201 was analysed using B lymphoblastoid JY cells that were homozygous for HLA-A*0201, in a semi-quantitative competition assay as described previously.[22] The assay is based on competitive binding of a test peptide and a fluorescently labelled reference peptide to HLA-A*0201 molecules. Briefly, peptides were stripped off HLA-A*0201-peptide complexes on JY cells, by exposing them for 90 sec to ice-cold citric acid buffer at pH 3.2. Subsequently, cells were washed twice in IMDM and resuspended in IMDM supplemented with 1 μg/ml β$_2$-microglobulin (Nuclilab). In a 96-well U-bottomed plate 150 nM FL-labelled reference peptide (FLPSDC(-FL)FPSV) and titrated amounts of competitor peptide were incubated with 7 × 10^5 acid-stripped JY cells for 24 hr at 4°C. Cells were washed in PBA1% (PBS with 1% bovine serum albumin), fixed with 0.5% paraformaldehyde and analysed on FACScan (Becton Dickinson, Mountain View, CA). The mean fluorescence (MF) obtained in the absence of competitor peptide was regarded as maximal binding and equated to 0% inhibition; the MF obtained without reference peptide was equated to 100% inhibition. The percentage inhibition was calculated using the formula:

$$\{1 - \frac{(\text{MF } 150 \text{ nM reference and competitor peptide} - \text{MF no reference peptide})}{(\text{MF } 150 \text{ nM reference peptide} - \text{MF no reference peptide})} \times 100\%$$

The binding capacity of competitor peptides is expressed as the concentration (μM) needed to inhibit 50% of binding of the FL-labelled reference peptide (IC$_{50}$).

Measurement of MHC-peptide complex stability at 24°C

To measure MHC-peptide complex stability the above peptide binding assay was carried out at room temperature (24°C) for 3 and 24 hr and IC$_{50}$ values were obtained in a similar manner.[23] Peptide-MHC complexes were regarded as relatively stable if significant peptide binding (IC$_{50}$ < 50) was detectable even after prolonged (24 hr) incubation at elevated temperature (24°C).

Immunisations, T cell cultures, cytotoxicity assays

To assess immunogenicity of the peptides, transgenic mice expressing the product of the A2/K^b chimeric gene were used. A2K^b transgenic mice were used to assess immunogenicity of identified HLA-A*0201 binding peptides. Mice were kept under standard clean experimental conditions. Groups of A2/K^b transgenic mice were immunised subcutaneously (s.c.) on the left flank with 100 μg of MUC1 peptide emulsified in IFA in the presence of 140 μg of the H-2 I-A^b-restricted HBV core antigen-derived T-helper epitope (HBV$_{128-140}$ TPPAYRPPNAPIL).[24] After a minimum period of 2 weeks the mice were boosted using same protocol. Two weeks after the last immunisation, mice were sacrificed and spleen cells (30 × 10^6 cell in 10 ml) were restimulated with peptide-pulsed syngeneic irradiated lipopolysaccharide-elicited B-cell lymphoblasts (ratio 3:1) and 1 μg/ml MUC1-derived peptide in complete medium in T75 flasks. On day 7 of *in vitro* culture, the cells were passed over a Ficoll gradient and CTL reactivity was tested in a standard chromium (^{51}Cr) release assay. As a target, peptide-pulsed Jurkat-A2/K^b cells were used. Labelled target cells were pulsed for 20 min with peptide (10 μg/ml) and incubated at constant number with a titrated amount of effector cells for at least 5 hr at 37°C. Spontaneous and maximum release were measured in multiples of 6 wells. Bulks were scored specific when target cell lysis was at least 20% higher than background at a minimum of 2 E:T ratios.

Dendritic cell (DC) preparation

Spleen-derived dendritic cells (scDC) were prepared as described previously.[25] In short, single cell suspensions were made after spleens were incubated with 400 U/ml of collagenase (Sigma) for 15 min at 37°C. After a density bovine serum albumin gradient, cells in the alpha band were plated on 36-mm glass dishes and left to adhere for 2 hr. Non-adherent cells were washed away and the remaining cells were incubated overnight at 37°C, 5% CO$_2$. The following day non-adhered cells were collected, peptide loaded (10 μg/ml, 1 hr) washed in PBA1% and injected intravenously (i.v.) in PBS (5 × 10^5 DC per mouse).

RESULTS

Selection of MUC1 peptides for their HLA-A*0201 binding capacity

Computer programs[26,27] were used to scan the entire MUC1 protein sequence for peptides that matched the motifs for HLA-A*0201 to select peptides for biochemical synthesis. The MUC1 sequence comprising two tandem repeats (TR)[1] was searched for 9 amino acid long peptides complying with the anchor residue motifs for HLA-A*0201. Ninemers in the top 10% of the scoring data for HLA-A*0201 were synthesised and tested for binding to HLA-A*0201. In addition the VNTR-derived peptide MUC1$_{130-138}$ STAPPAHGV was tested, as it had been described previously to constitute an HLA-A*0201-restricted T-cell epitope.[14]

Peptide binding to HLA-A*0201 was analysed using HLA-A*0201$^+$ B lymphoblastoid JY cells in a semi-quantitative competition assay.[22] All peptides were tested in at least 3 independent experiments. Of 90 peptides tested, 5 were able to compete for HLA-A*0201 binding with the fluorescently labelled reference peptide to 50% at concentrations lower than 15 μM (Table IB). This range of binding capacity has been observed for known naturally processed epitopes (see Flu-M1$_{58-66}$ in Table IA).[25] In addition, we identified 6 peptides, including the VNTR-derived peptide MUC1$_{130-138}$ STAPPAHGV, that showed measurable but weaker binding to HLA-A*0201 (Table IC). None of the remaining peptides exhibited any detectable binding to HLA-A*0201 (data not shown).

TABLE I – SUMMARY OF THE PARAMETERS CHARACTERISING THE 11 BEST HLA-A*0201 BINDING PEPTIDES

	Peptide	Sequence	Motif[1]	Motif[2]	IC_{50}[3]	Stability	CTL response[4]	Tumour protection[5]
A	FLU-M1[58-66]	GILGFVFTL	54	55[1]	3[2]	+	N.T.	N.T.[5]
	HPV16 E6	KLPQLCTEL			9	−		
B	MUC[264-272]	FLSFHISNL	59	226	7	+	3/7	+
	MUC[460-468]	SLSYTNPAV	62	69	8	+	0/6	−
	MUC[13-21]	LLLTVLTVV	63	412	6	+	0/4	−
	MUC[167-175]	ALGSTAPPV	64	69	10	+	4/6	+
	MUC[79-87]	TLAPATEPA	58	2	11	+	4/6	+
C	MUC[107-115]	ALGSTTPPA	56	5	25	+/−	N.T.	N.T.
	MUC[257-265]	STGVSFFFL	45	17	50	−	N.T.	N.T.
	MUC[353-361]	NLTISDVSV	57	69	85	−	N.T.	N.T.
	MUC[130-138]	STAPPAHGV	51	1	> 100	−	N.T.	N.T.
	MUC[170-178]	STAPPVHNV	53	2	> 100	−	N.T.	N.T.
	MUC[12-20]	LLLLTVLTV	64	1006	> 100	−	N.T.	N.T.

Positive control peptides (A), strong MUC1 binders (B) and weak MUC1 binders (C).–[1]Motif score derived using motif published by D'Amaro et al.[26]–[2]Motif score derived using http://bimas.cit.nih.gov/molbio/hla_bind/index.html.[27]–[3]IC_{50} represents the amount of peptide (μM) required for 50% inhibition of binding of the fluorescein-labeled reference peptide.–[4]Fraction of mice that mounted a peptide-specific response. (20% specific lysis over control targets in two E:T ratios.)–[5]+, peptides protecting mice against MUC1-expressing tumours, −, peptides failing to show protection; N.T., not tested.

TABLE II – STABILITY OF PEPTIDE BINDING TO HLA-A*0201

	IC_{50} (μM)			
Peptide stability	4°C		24°C	
	3hr	24hr	3hr	24hr
FLU-M1[58-66]	1	3	2	3
HPV16 E6	26	9	27	55
MUC[264-272]	6	7	4	35
MUC[460-468]	8	8	7	17
MUC[13-21]	20	6	6	25
MUC[167-175]	27	10	13	25
MUC[79-87]	20	11	7	12
MUC[107-115]	20	25	24	45
MUC[257-265]	100	50	20	> 100
MUC[353-361]	40	85	40	> 100
MUC[130-138]	80	> 100	> 100	> 100
MUC[170-178]	35	> 100	45	> 100
MUC[12-20]	> 100	> 100	> 100	> 100

Stability of the peptides was tested by the HLA-A*0201 binding assay incubating the cells with peptide at 4°C or 24°C for 3 or 24 hr.

Because the peptide-binding assay is performed at 4°C, it measures the capacity of peptides to bind MHC while ignoring the influence of higher physiological temperature on the stability of MHC-peptide complexes. The latter parameter was shown to correlate more accurately with immunogenicity than binding capacity per se.[23,28] We therefore tested the stability of the strong and intermediate binding peptides at 24°C as well as 4°C after 3 and 24 hr (Table II). All 5 peptides that exhibited strong binding also formed stable MHC-peptide complexes (Table IB). Of the 6 peptides with lower binding capacity, only MUC[107-115] bound well enough to permit stability analysis. As shown in Table II, this peptide formed poorly stable complexes with HLA-A*0201. Its binding characteristics were comparable to that of several other peptides that were previously shown to be non-immunogenic.[23] Peptide HPV16 E6 is included as an example of a peptide that binds well but does not form stable complexes with HLA-A*0201 and is not immunogenic.[23]

Immunogenicity of MUC1-derived peptides in A2/K[b] transgenic mice

The 5 peptides that were selected on basis of the binding assays (Table IB) were tested for their capacity to induce peptide-specific CTL immunity *in vivo*. Mice transgenic for a chimeric HLA-A*0201/K[b] molecule (A2/K[b]),[20] which have been used successfully by many researchers including ourselves to identify HLA-A*0201-restricted CTL epitopes derived from tumour antigens

(*e.g.*, Ressing *et al.*[24]), were immunised with the synthetic peptides emulsified in IFA. Bulk splenocyte cultures taken from these mice 2 weeks after the last immunisation were tested for cytotoxic activity after 1 week of *in vitro* restimulation against peptide-loaded Jurkat-A2/K[b] cells.

Three of the 5 peptides, namely MUC[79-87], MUC[167-175] and MUC[264-272], were found to be immunogenic in A2/K[b] transgenic mice, in that they reproducibly induced strong peptide-specific CTL responses. In contrast peptides MUC[13-21] and MUC[460-468] did not induce peptide-specific responses in any of the immunised mice, even though their binding to HLA-A*0201 was comparable to that of the other peptides (Table I; Fig. 1). A2/K[b] transgenic mice expressed, in addition to the transgene-encoded A2/K[b] molecule, 2 endogenous class I MHC molecules: H-2D[b] and H-2K[b]. Importantly, we tested the *in vitro* reactivity of the peptide-induced CTL against Jurkat-A2/K[b] cells that lack either of these murine class I molecules, ensuring that the CTL reactivity detected in these assays is indeed A2/K[b]-restricted. Furthermore, parallel analysis of the MUC1 sequence for peptides binding to H-2D[b] and H-2K[b] resulted in selection of a set of peptides that did not include MUC[79-87], MUC[167-175] and MUC[264-272]. Moreover, the latter 3 peptides were not found to be a target of the MUC1-specific CTL response in non-A2/K[b]-transgenic mice (our additional unpublished data). Taken together, our data therefore indicate that peptides MUC[79-87], MUC[167-175] and MUC[264-272] represent immunogenic targets in the context of HLA-A2/K[b].

Peptide immunisation induces MUC1-specific anti-tumour immunity in A2/K[b]-transgenic mice

The data in Figure 1, although showing that peptides MUC[79-87], MUC[167-175] and MUC[264-272] are highly immunogenic, do not address the question whether CTL raised against these peptides are capable of reacting against MUC1 and A2/K[b]-positive tumour cells that present physiological quantities of naturally processed epitopes at their surface. We therefore carried out experiments to analyse whether the *in vivo* induced peptide-specific CTL responses are capable of killing MUC1-over-expressing tumours. A tumour model in the A2/K[b] transgenic mice was developed by transfection of the highly tumourigenic mouse melanoma B16 F1 with the MUC1 cDNA and the HLA-A2/K[b] gene. From these transfections clone B16-MUC1-HLA-A2/K[b] was derived (Fig. 2). MUC1 expression levels on B16-MUC1-A2/K[b] were similar to those on HeLa human cervical carcinoma cells and T47D human breast carcinoma cells (Fig. 2a–f). A2/K[b] expression on B16-MUC1-A2/K[b] was low but detectable on routinely cultured cells, and strongly increased when cells were cultured in the presence of interferonγ (IFNγ) (Fig. 2g,h). Strong up-regulation of class I MHC by IFNγ is a common phenomenon
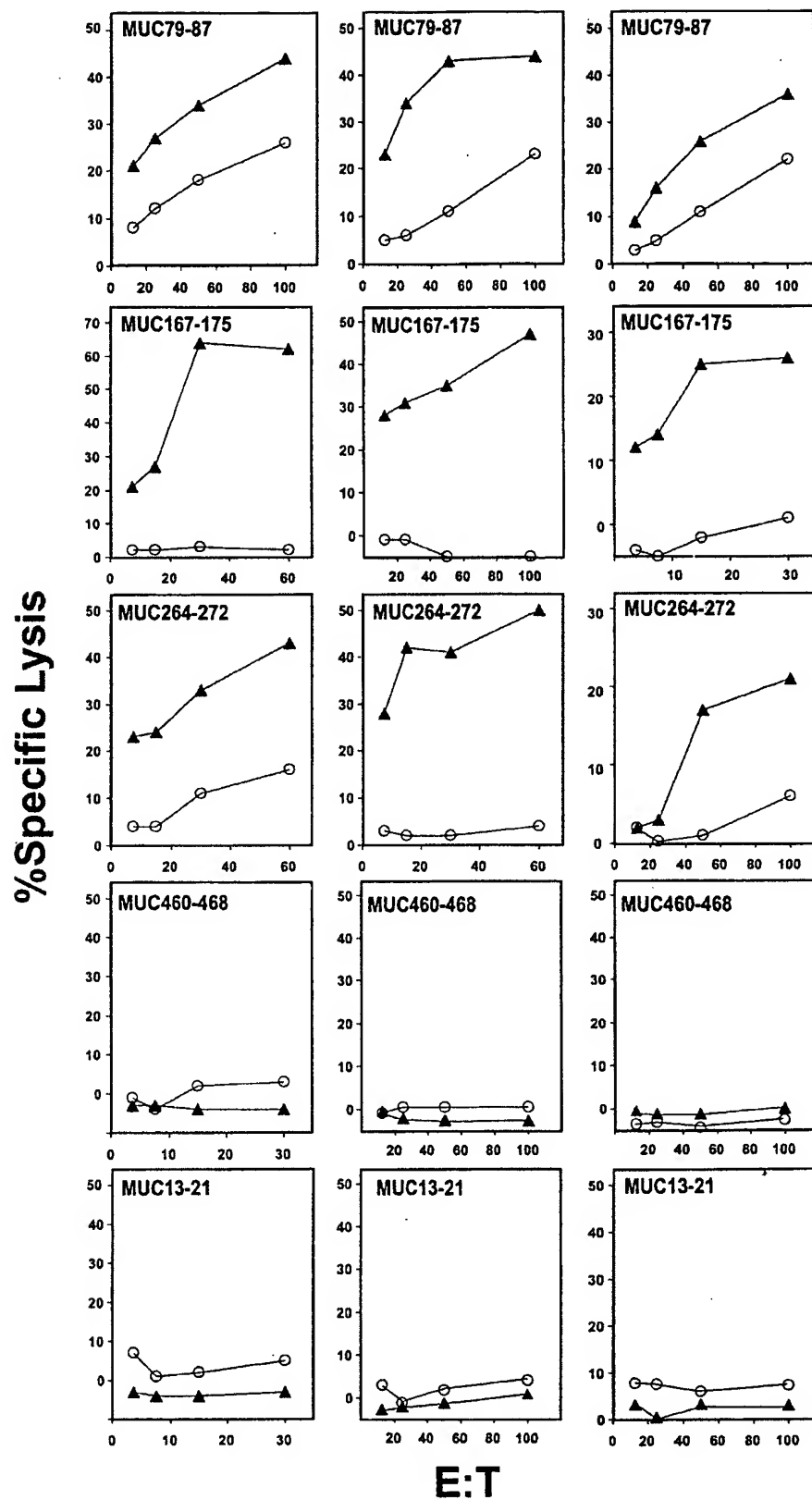
FIGURE 1 – MUC1-derived HLA-A*0201 binding peptides induce peptide-specific cytotoxic T lymphocyte (CTL) responses. A2/K^b transgenic mice were immunised twice with 100 μg of MUC1 peptide in incomplete Freund's adjuvant and 140 μg of the H-2 I-A^b-restricted HBV core antigen-derived T-helper epitope (HBV$^{128-140}$ TPPAYRPPNAPIL) day −28 and −14, as described previously.[24] On day 0 single cell splenocytes suspensions were restimulated in vitro for one week with peptide loaded syngeneic LPS-elicited lymphoblasts and tested for cytotoxicity of peptide loaded Jurkat-A2/K^b. Groups of A2/K^b transgenic mice were immunised with either of the peptides MUC1$_{264-272}$, MUC1$_{460-468}$, MUC1$_{13-21}$, MUC1$_{167-175}$ or MUC1$_{79-87}$. CTL bulk cultures were tested against Jurkat-A2/K^b cells loaded with the cognate peptide (filled triangles) or irrelevant influenza matrix control peptide (open circles). For each peptide data from 3 mice are shown. A summary of all results is provided in Table I.
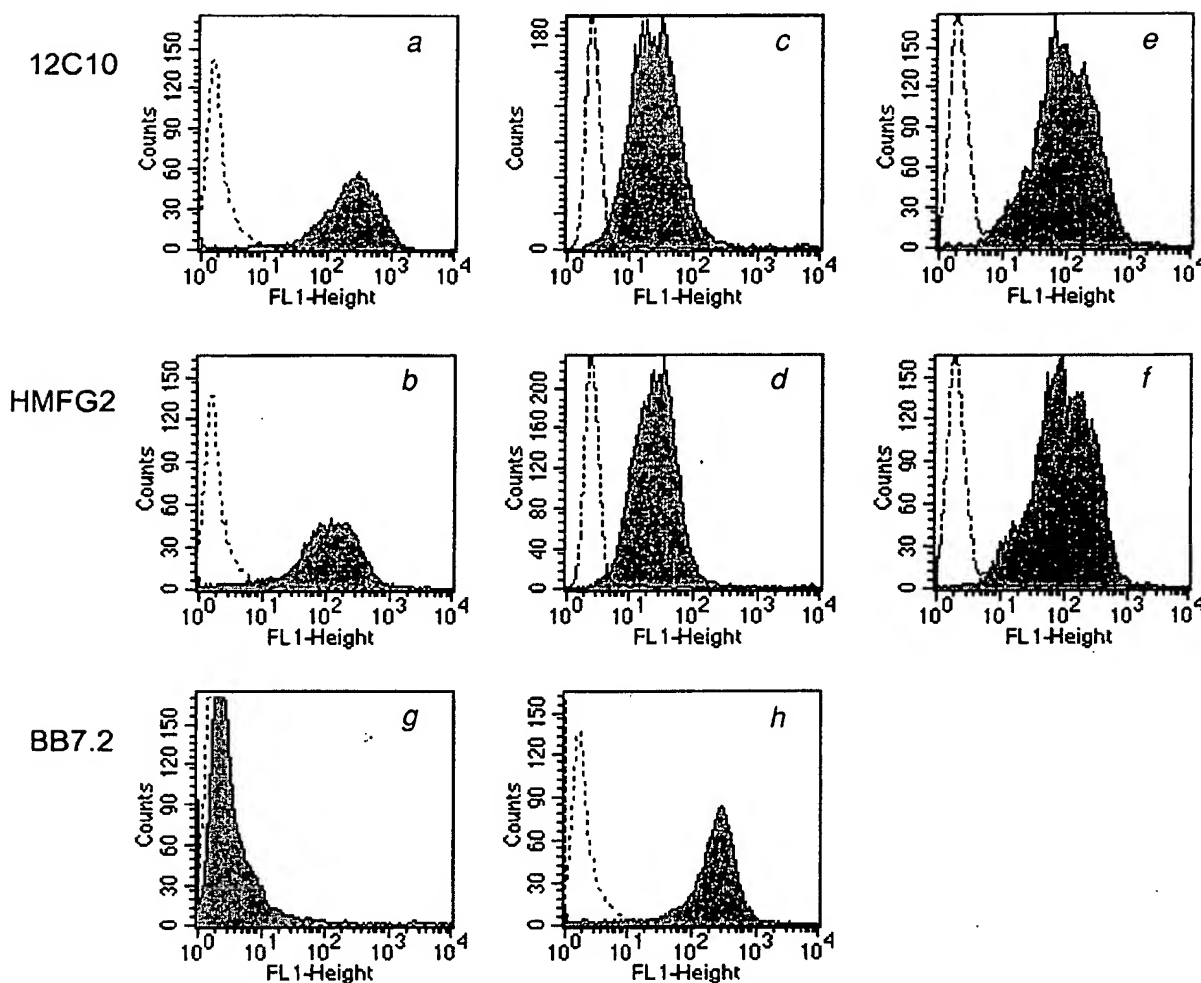
Figure 2 – Surface expression of MUC1 and A2/K^b on B16 F1 transfectants. A stable cell line developed from B16 F1 by transfection of the MUC1 cDNA and the chimeric A2/K^b cDNA construct expresses MUC1 and A2/K^b on the cell surface as detected by flow cytometry. B16-MUC1-A2/K^b (a,b), human cervical carcinoma cell line HeLa (c,d) and human breast carcinoma cell line T47D (e,f) were stained with mAb hybridoma supernatants specific for MUC1 (12C10 and HMFG2). Furthermore, B16-MUC1-A2/K^b was stained for HLA-A*0201 (BB7.2). The A2/K^b expression on B16-MUC1-A2/K^b was increased by treatment of the cell culture with 10u/ml murine IFNγ for 3 days before staining (g,h). Background staining with secondary FITC-labelled mAb alone is shown with a dotted line.

observed for many murine and human tumour cell lines (data not shown). In tumour-take experiments s.c. administration of 10^5 B16-MUC1-A2/K^b cells resulted in 80%–100% tumour take in A2/K^b transgenic mice (data not shown). This tumour dose was used for all further experiments.

To test whether the MUC1-derived HLA-A*0201 binding peptides could protect A2/K^b transgenic mice against tumour challenge, groups of 8 mice were immunised with MUC1 peptides in IFA and subsequently challenged with B16-MUC1-A2/K^b. As a positive control for this experiment, one group of mice was immunised intraperitoneally (i.p.) with 10^8 pfu of a recombinant Vaccinia virus expressing MUC1 (VV-MUC1), a mode of antigen delivery that has been shown previously to protect mice against MUC-1-positive tumours.[29] Immunisation with peptides MUC$_{79-87}$, MUC$_{167-175}$ and MUC$_{264-272}$ as well as with VV-MUC1 induced significant protection of the mice against tumour growth compared with mice immunised with IFA alone ($p = 0.0008, p = 0.005$ and $p = 0.02$, respectively). This finding indicated that the CTL activity raised against these 3 epitopes is capable of eradicating B16-MUC1-A2/K^b tumour cells $in\ vivo$. Peptides MUC$_{13-21}$ and MUC$_{460-468}$, which failed to induce peptide-specific CTL responses (Fig. 1), were also not

able to protect mice against tumour challenge. Mice immunised with these peptides did not survive significantly better than mice that had received IFA alone ($p = 0.536$ and $p = 0.926$, respectively). Furthermore, the rate of tumour growth was not inhibited (Fig. 3).

Vaccination with peptides emulsified in IFA has in certain cases been shown to induce epitope specific tolerance.[25,30] However, presentation of these peptides in an appropriate co-stimulatory context, for instance by loading of the peptides on dendritic cells, was shown to prevent tolerance induction and instead resulted in CTL priming.[25] To exclude the possibility that we might overlook the immunogenic potential of one or more of the MUC1-derived peptides under investigation, in particular peptides MUC$_{13-21}$ and MUC$_{460-468}$, A2/K^b transgenic mice were immunised, prior to tumour challenge, with 5×10^5 peptide-loaded scDC (Fig. 4). This experiment confirmed that peptides MUC$_{264-272}$, MUC$_{79-87}$ and MUC$_{167-175}$ induced significant protection against tumour challenge ($p = 0.006, p = 0.002$ and $p = 0.001$, respectively). Peptides MUC$_{13-21}$ and MUC$_{460-468}$, however, failed to result in significant protection of the mice, even when loaded on DC ($p = 0.122$ and $p = 0.172$, respectively) (Fig. 4).
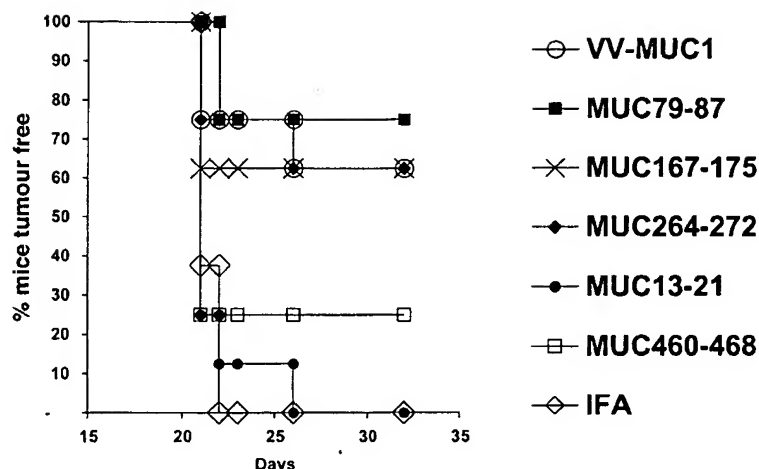
FIGURE 3 – MUC1 peptide vaccination protects A2/K^b transgenic mice against tumour challenge. Groups of eight A2/K^b transgenic mice were immunised s.c. on day −28 and −14 with 100 μg of MUC1 peptide in IFA, IFA alone or with 10^8 pfu rec. VV-MUC1 i.p. All mice were challenged s.c. with 10^5 B16-MUC1-A2/K^b on day 0, 14 days after the last immunisation. Tumour growth was recorded by measuring three dimensions. No changes in tumour status were recorded after the last day shown.
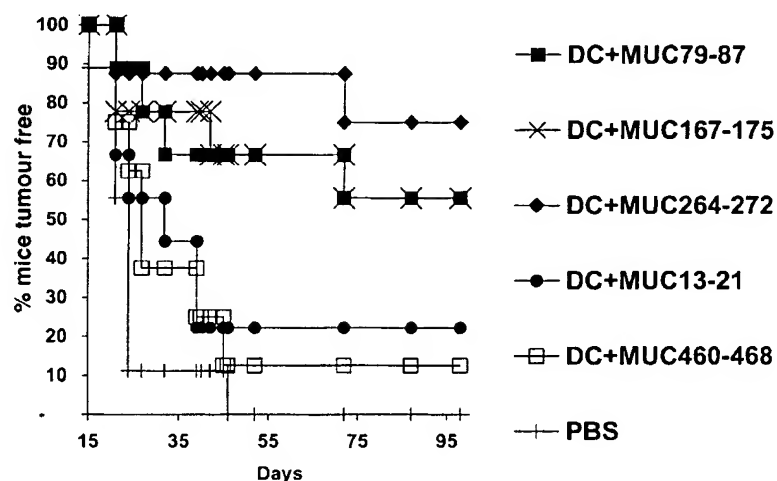

FIGURE 4 – Immunization with peptide-loaded dendritic cells (DC) induces protective cytotoxic T lymphocyte (CTL) immunity against MUC1-over-expressing tumor cells. Groups of 8 A2/K^b transgenic mice were immunised intravenously (i.v.) with 5×10^5 DC per mouse loaded with 10 μg/ml of the indicated MUC1 peptide, or with phosphate-buffered saline alone i.v. All mice were challenged subcutaneously (s.c.) with 10^5 B16-MUC1-A2/K^b on day 0, 14 days after the last immunisation. Tumour growth was recorded by measuring 3 dimensions. No changes in tumour status were recorded after the last day shown.

DISCUSSION

The human polymorphic epithelial mucin MUC1 is over-expressed by a number of epithelial and hematological malignancies and therefore is a potential target for T-cell-mediated immunity. Whereas most previous studies have focused on identifying potential CTL epitopes in the VNTR region of MUC1, we have identified 3 MUC1-derived HLA-A*0201-restricted epitopes that map outside the VNTR region, comply with the HLA-A*0201 motif and show strong binding to this molecule. Our studies with A2/K^b transgenic mice show that these peptides are not only immunogenic, but also are capable of protecting the mice against a challenge with MUC1-expressing tumour cells. The tumour-rejection experiments demonstrate that peptides MUC$_{79-87}$, MUC$_{167-175}$ and MUC$_{264-272}$ represent naturally processed CTL epitopes. It is theoretically possible that the naturally processed epitopes would constitute 8- or 10-mer length variants of these peptides, which in view of the C-terminal anchor position would have to share the

same C-terminus. However, CTL raised against the 9-mer peptides effectively recognised and killed the B16-MUC1-A2/K^b tumour cells *in vivo*. In fact, vaccination of A2/K^b transgenic mice with either of the 3 identified peptide epitopes induced equally effective anti-tumour immunity as vaccination with a recombinant Vaccinia construct encoding the entire MUC1 antigen (Fig. 3), indicating that vaccines comprising the 9-mer peptides are powerful inducers of the HLA-restricted anti-tumour CTL response. We therefore did not pursue further studies concerning the epitope length variants. The tumour-rejection experiments were performed in A2/K^b-transgenic mice challenged with A2/K^b-expressing tumours. The chimeric A2/K^b molecule and the wild-type HLA-A*0201 molecule differ in their α$_3$ domain, which is involved in the interaction with the CD8 molecule on the T cell, but are identical with respect to their other domains including those that govern peptide binding and T-cell receptor interaction.[21] Furthermore, MUC1 levels on B16-MUC1-A2/K^b cells are similar to those on human MUC1-

TABLE III – CANDIDATE PEPTIDES FROM THE NON-VNTR REGION OF MUC1 FOR INDUCTION OF HLA-A*0201 RESTRICTED CTL RESPONSES

Sequence of the peptide	Amino acid position in MUC1[1]		Reference
LLLLTVLTV	12–20		Brossart et al.[31]
LLLTVLTVV	13–21 (32–40)[2,3]		Carmon et al.[32]
TLAPATEPA	79–87		This study
ALGSTAPPV	167–175		This study
ALASTAPPV		(226–234)[2]	Carmon et al.[32]
STAPPVHNV	170–178 (950–958)[4]		Brossart et al.[31]
FLSFHISNL	264–272 (323–331)[2]		This study
NLTISDVSV	353–361 (412–420)[2,3]		Carmon et al.[32]

[1]Our numbering is based on the MUC1 cDNA sequence including 2 tandem repeats as published by Gendler and co-workers.[1]–[2]The amino acid numbering used by Carmon et al.[32] differs from our numbering. Since our MUC13–21 peptide matches the MUC32–40 peptide described by Carmon et al.,[32] we conclude that their reference sequence must contain an additional 19 amino acids at the N-terminus. This addition is distinct from the extra 9 residues contained within a previously described splice variant of MUC1.[33] The numbering of the other peptides can be readily aligned with our numbering by assuming the above as well as that the reference sequence used by Carmon et al.[32] contains 4 instead of 2 20-amino-acid long tandem repeats (add 19 + 40 = 59). We were not in fact able to find a MUC1 sequence in the available databases that matched the amino acid numbering by Carmon et al.,[32] so all peptides are listed with numbers from our sequence.–[3]The actual numbering of these peptides in the report by Carmon et al.[32] is 32–41 and 412–421, respectively. We adjusted this numbering to represent 9-mer peptides.–[4]The numbering of the peptides by Brossart et al.[31] is based on a MUC1 sequence containing 39 additional 20 amino acid repeats (add 39 × 20 = 780).

positive tumour cell lines (Fig. 2). Our data therefore indicate that human CTL raised against MUC_{79-87}, $MUC_{167-175}$ and $MUC_{264-272}$ should be equally capable of responding against MUC1-over-expressing, HLA-A*0201-positive human tumours, provided that these tumours express sufficient levels of HLA-A*0201 at their surface.

In 2 recent reports[31,32] a number of MUC1-derived HLA-A*0201-restricted CTL epitopes have been described which, as with the epitopes identified in the present report, map outside the VNTR sequence and are in compliance with the binding motif for HLA-A*0201. Brossart and co-workers[31] identified peptides MUC_{12-20} (LLLLTVLTV) and $MUC_{170-178}$ (STAPPVHNV), as potential targets for CTL-mediated immune attack (Table III). Human CTL raised against these peptides recognise MUC1-expressing tumour cells, indicating that these peptides represent naturally processed epitopes.[31] The fact that independent attempts to identify non-VNTR MUC1-derived HLA-A*0201-restricted T-cell epitopes resulted in the identification of complementary sets of epitopes can be explained best by differences in experimental approach. Brossart and co-workers[31] screened the MUC1 sequence for peptides matching the motif for HLA-A*0201-binding, after which they selected 2 peptides for induction of CTL responses without prior analysis of their capacity to bind to HLA-A*0201. These 2 peptides were in fact among the set of 90 MUC1-derived peptides that we tested for HLA-A*0201 binding. However, they showed only weak binding in our assays, and only peptides showing stronger binding were selected for analysis of immunogenicity.

The report by Carmon et al.[32] describes 3 MUC1-derived potential epitopes: MUC_{13-21} (LLLTVLTVV), $MUC_{167-175}$ (ALASTAPPV) and $MUC_{353-361}$ (NLTISDVSV). As explained

in Table III, one of these peptides ($MUC_{167-175}$) corresponds to one of the peptides we identified as being immunogenic and effective in tumour protection, although it differs by one amino acid from the sequence ALGSTAPPV defined in our experiments. This discrepancy may be explained by usage of a MUC1 sequence that deviates from the one we used. Peptide MUC_{13-21} was also found to bind well to HLA-A*0201 in our experiments, but did not display immunogenicity in vivo (Table I). The third peptide epitope ($MUC_{353-361}$) defined by Carmon et al.[32] as being immunogenic in HLA-A2.1/D^b-β2-microglobulin single chain (HHD) transgenic mice was found by ourselves to be a weak binder to the HLA-A*0201 molecule and was not tested in the in vivo assays. Conversely, the peptide $MUC_{264-272}$ (FLSFHISNL) was found by Carmon et al.[32] to be a weak binder to the hybrid HHD single chain molecule and was not analysed further by those investigators, whereas peptide MUC_{79-87} TLAPATEPA was not selected for testing. This again illustrates that different selection criteria and in vitro binding assays can result in the identification of distinct T-cell epitopes.

In conclusion, our study has resulted in the identification of 3 non-VNTR MUC1-derived HLA-A*0201-restricted epitopes. Two of these peptides, MUC_{79-87} and $MUC_{264-272}$, represents novel epitopes, whereas the epitope corresponding to peptide $MUC_{167-175}$ has also been described by others,[32] albeit with a sequence difference. In addition, the tumour rejection experiments described herein demonstrate that all 3 peptides can serve as constituents of an effective peptide vaccine capable of inducing effective anti-tumor CTL immunity in vivo. Because MUC1 is a tumour-associated auto-antigen that is also expressed by normal epithelia, albeit at lower levels, it cannot be excluded that tolerance for these epitopes and/or auto-immune reaction of MUC1-specific CTL toward normal epithelia would restrict the exploitation of these epitopes for immunotherapy of cancer. Importantly, the detection of MUC1-specific CTL responses in human CTL cultures from healthy individuals and from vaccinated cancer patients,[12,14,31,34,35] as well as the efficacy of MUC1-specific vaccination against MUC1-over-expressing tumours in (human)MUC1-transgenic mice in the absence of detectable auto-immune damage,[36,37] indicate that the issues of tolerance and auto-immunity do not put a general restriction on the use of MUC1 as a target for CTL-mediated immunotherapy of cancer. Similar observations have been made for other tumour-associated auto-antigens such as carcinoembryonic antigen, HER-2/neu and melanocyte antigens (reviewed in: Offringa et al.[38]).

Taken together, there are currently 4 independent and complementary studies aimed at the identification of HLA-A*0201-restricted MUC1 epitopes that have resulted in the identification of 7 distinct immunogenic peptides, one derived from the VNTR sequence[14] and 6 derived from the non-VNTR areas of the MUC1 protein (Table III). Analysis of T-cell immunity against these peptides in cancer patients with MUC1-positive tumours will be required to show which of these peptides constitute targets of the natural and/or vaccine-induced CTL response against MUC1 in humans.

REFERENCES

1. Gendler SJ, Lancaster CA, Taylor Papadimitriou J, Duhig T, Peat N, Burchell J, et al. Molecular cloning and expression of human tumor-associated polymorphic epithelial mucin. J Biol Chem 1990;265:15286–93.
2. Gendler SJ, Spicer AP, Lalani EN, Duhig T, Peat N, Burchell J, et al. Structure and biology of a carcinoma-associated mucin, MUC1. Am Rev Respir Dis 1991;144:S42–7.
3. Zotter S, Hageman PC, Lossnitzer A, Mooi WJ, Hilgers J. Tissue and tumor distribution of human polymorphic epithelial mucin. Cancer Rev 1988;12:55–101.

4. Finn OJ, Jerome KR, Henderson RH, Pecher G, Domenech N, Magarian-Blander J, et al. MUC-1 epithelial tumor mucin-based immunity and cancer vaccines. Immunol Rev 1995;145:61–89.
5. Gendler S, Taylor Papadimitriou J, Duhig T, Rothbard J, Burchell J. A highly immunogenic region of a human polymorphic epithelial mucin expressed by carcinomas is made up of tandem repeats. J Biol Chem 1988;263:12820–3.
6. Girling A, Bartkova J, Burchell J, Gendler S, Gillett C, Taylor Paradimitriou J. A core protein epitope of the polymorphic epithelial

mucin detected by the monoclonal antibody SM-3 is selectively exposed in a range of primary carcinomas. Int J Cancer 1989;43: 1072–6.

7. Noto H, Takahashi T, Makiguchi Y, Hayashi T, Hinoda Y, Imai K. Cytotoxic T-lymphocytes derived from bone-marrow mononuclear-cells of multiple-myeloma patients recognize an underglycosylated form of muc1 mucin. Int Immunol 1997;9:791–8.

8. Miles DW, Taylor-Papadimitriou J. Therapeutic aspects of polymorphic epithelial mucin in adenocarcinoma. Pharmacol Ther 1999;82: 97–106.

9. Brockhausen I, Yang JM, Burchell J, Whitehouse C, Taylor Papadimitriou J. Mechanisms underlying aberrant glycosylation of MUC1 mucin in breast cancer cells. Eur J Biochem 1995;233:607–17.

10. Lloyd KO, Burchell J, Kudryashov V, Yin BWT, Taylor-Papadimitriou J. Comparison of O-linked carbohydrate chains in MUC-1 mucin from normal breast epithelial cell lines and breast carcinoma cell lines. Demonstration of simpler and fewer glycan chains in tumor cells. J Biol Chem 1996;271:33325–34.

11. Agrawal B, Reddish MA, Christian B, VanHeele A, Tang L, Koganty RR, et al. The anti-MUC1 monoclonal antibody BCP8 can be used to isolate and identify putative major histocompatibility complex class I associated amino acid sequences. Cancer Res 1998;58:5151–6.

12. Domenech N, Henderson RA, Finn OJ. Identification of an HLA-A11-restricted epitope from the tandem repeat domain of the epithelial tumor antigen mucin. J Immunol 1995;155:4766–74.

13. Jerome KR, Barnd DL, Bendt KM, Boyer CM, Taylor Papadimitriou J, McKenzie IF, et al. Cytotoxic T-lymphocytes derived from patients with breast adenocarcinoma recognize an epitope present on the protein core of a mucin molecule preferentially expressed by malignant cells. Cancer Res 1991;51:2908–16.

14. Apostolopoulos V, Karanikas V, Haurum JS, McKenzie IF. Induction of HLA-A2-restricted CTLs to the mucin 1 human breast cancer antigen. J Immunol 1997;159:5211–8.

15. Heath WR, Kurts C, Miller JF, Carbone FR. Cross-tolerance: a pathway for inducing tolerance to peripheral tissue antigens. J Exp Med 1998;187:1549–53.

16. Kurts C, Miller JF, Subramaniam RM, Carbone FR, Heath WR. Major histocompatibility complex class I-restricted cross-presentation is biased towards high dose antigens and those released during cellular destruction. J Exp Med 1998;188:409–14.

17. Morgan DJ, Kreuwel HT, Fleck S, Levitsky HI, Pardoll DM, Sherman LA. Activation of low avidity CTL specific for a self epitope results in tumor rejection but not autoimmunity. J Immunol 1998;160:643–51.

18. Ohashi PS, Oehen S, Buerki K, Pircher H, Ohashi CT, Odermatt B, et al. Ablation of "tolerance" and induction of diabetes by virus infection in viral antigen transgenic mice. Cell 1991;65:305–17.

19. Oldstone MB, Nerenberg M, Southern P, Price J, Lewicki H. Virus infection triggers insulin-dependent diabetes mellitus in a transgenic model: role of anti-self (virus) immune response. Cell 1991;65:319–31.

20. Vitiello A, Marchesini D, Furze J, Sherman LA, Chesnut RW. Analysis of the HLA-restricted influenza-specific cytotoxic T lymphocyte response in transgenic mice carrying a chimeric human-mouse class I major histocompatibility complex. J Exp Med 1991;173:1007–15.

21. Graham RA, Burchell JM, Beverley P, Taylor-Papadimitriou J. Intramuscular immunisation with MUC1 cDNA can protect C57 mice challenged with MUC1-expressing syngeneic mouse tumour cells. Int J Cancer 1996;65:664–70.

22. van der Burg SH, Ras E, Drijfhout JW, Benckhuijsen WE, Bremers AJ, Melief CJ, et al. An HLA class I peptide-binding assay based on competition for binding to class I molecules on intact human B cells. Identification of conserved HIV-1 polymerase peptides binding to HLA-A*0301. Hum Immunol 1995;44:189–98.

23. van der Burg SH, Visseren MJ, Brandt RM, Kast WM, Melief CJ. Immunogenicity of peptides bound to MHC class I molecules depends on the MHC-peptide complex stability. J Immunol 1996;156: 3308–14.

24. Ressing ME, Sette A, Brandt RM, Ruppert J, Wentworth PA, Hartman M, et al. Human CTL epitopes encoded by human papillomavirus type 16 E6 and E7 identified through *in vivo* and *in vitro* immunogenicity studies of HLA-A*0201-binding peptides. J Immunol 1995;154:5934–43.

25. Toes RE, van der Voort EI, Schoenberger SP, Drijfhout JW, van Bloois L, Storm G, et al. Enhancement of tumor outgrowth through CTL tolerization after peptide vaccination is avoided by peptide presentation on dendritic cells. J Immunol 1998;160:4449–56.

26. D'Amaro J, Houbiers JG, Drijfhout JW, Brandt RM, Schipper R, Bavinck JN, et al. A computer program for predicting possible cytotoxic T lymphocyte epitopes based on HLA class I peptide-binding motifs. Hum Immunol 1995;43:13–8.

27. Parker KC, Bednarek MA, Coligan JE. Scheme for ranking potential HLA-A2 binding peptides based on independent binding of individual peptide side-chains. J Immunol 1994;152:163–75.

28. van der Burg SH, Visseren MJW, Offringa R, Melief CJM. Do epitopes derived from autoantigens display low affinity for MHC class I? Immunol Today 1997;18:97–8.

29. Acres RB, Hareuveni M, Balloul JM, Kieny MP. Vaccinia virus MUC1 immunization of mice: immune response and protection against the growth of murine tumors bearing the MUC1 antigen. J Immunother 1993;14:136–43.

30. Nieland JD, Da Silva DM, Velders MP, de Visser KE, Schiller JT, Muller M, et al. Chimeric papillomavirus virus-like particles induce a murine self-antigen-specific protective and therapeutic antitumor immune response. J Cell Biochem 1999;73:145–52.

31. Brossart P, Heinrich KS, Stuhler G, Behnke L, Reichardt VL, Stevanovic S, et al. Identification of HLA-A2-restricted T-cell epitopes derived from the MUC1 tumor antigen for broadly applicable vaccine therapies. Blood 1999;93:4309–17.

32. Carmon L, El-Shami KM, Paz A, Pascolo S, Tzehoval E, Tirosh B, et al. Novel breast-tumor-associated MUC1-derived peptides: characterization in D^b-/- x b2 microglobulin (b2m) null mice transgenic for a chimeric HLA-A2.1/D^b-b2m single chain. Int J Cancer 2000;85:391–7.

33. Ligtenberg MJ, Vos HL, Gennissen AM, Hilkens J. Episialin, a carcinoma-associated mucin, is generated by a polymorphic gene encoding splice variants with alternative amino termini. J Biol Chem 1990;265:5573–8.

34. Reddish M, MacLean GD, Koganty RR, Kan-Mitchell J, Jones V, Mitchell MS, et al. Anti-MUC1 class I restricted CTLs in metastatic breast cancer patients immunized with a synthetic MUC1 peptide. Int J Cancer 1998;76:817–23.

35. Kugler A, Stuhler G, Walden P, Zoller G, Zobywalski A, Brossart P, et al. Regression of human metastatic renal cell carcinoma after vaccination with tumor cell-dendritic cell hybrids. Nat Med 2000;6: 332–6.

36. Gong J, Chen D, Kashiwaba M, Li Y, Chen L, Takeuchi H, et al. Reversal of tolerance to human MUC1 antigen in MUC1 transgenic mice immunized with fusions of dendritic and carcinoma cells. Proc Natl Acad Sci U S A 1998;95:6279–83.

37. Acres B, Apostolopoulos V, Balloul JM, Wreschner D, Xing PX, Ali-Hadji D, et al. MUC1-specific immune responses in human MUC1 transgenic mice immunized with various human MUC1 vaccines. Cancer Immunol Immunother 2000;48:588–94.

38. Offringa R, van der Burg SH, Ossendorp F, Toes REM, Melief CJM. Design and evaluation of antigen-specific vaccination strategies against cancer. Curr Opin Immunol 2000;12:576–82.

I. Dendreon Announces Provenge Significantly Improves Survival In Men With Advanced Prostate Cancer

Median survival benefit of 4.5 months is longest ever reported from a Phase 3 study in advanced prostate cancer --

Conference Call Scheduled for Tuesday, February 22, at 9:00 a.m. EST --

ORLANDO, FLA., February 17, 2005 - Dendreon Corporation (Nasdaq: DNDN) announced today that Provenge®, the Company's investigational immunotherapy for the treatment of prostate cancer, significantly improved survival in men with asymptomatic, metastatic androgen-independent (hormone-refractory) prostate cancer when compared to patients receiving placebo. The final data from the D9901 study will be presented by Eric J. Small, M.D., professor of medicine and urology at the University of California, San Francisco, on Saturday, February 19 at the 2005 Multidisciplinary Prostate Cancer Symposium.

According to the final three-year intent-to-treat analysis of the Company's first randomized Phase 3 clinical study, known as Study D9901, patients receiving Provenge had a 4.5 month improvement in their median survival and a greater than 3-fold increase in survival at 36 months when compared to patients receiving placebo.

"The survival benefit seen with Provenge is the largest ever reported in this patient population with any therapy," said Dr. Small. "This survival benefit, combined with a favorable safety profile, has the potential to provide an important new treatment option for prostate cancer patients."

In Study D9901, patients receiving Provenge had a median survival of 25.9 months compared to 21.4 months for patients in the placebo arm, a 4.5 month improvement (p-value = 0.01, hazard ratio = 1.7). This hazard ratio implies that patients receiving placebo have a relative risk of dying that is 70 percent higher than those patients receiving Provenge. In addition, 34 percent of patients receiving Provenge were alive at 36 months compared to 11 percent of patients receiving placebo (p-value = 0.0046). The survival benefit seen with Provenge was independent of a patient's Gleason Score, a common measure of disease severity. Provenge was well tolerated with the most common adverse events reported being fever and chills lasting for one to two days.

Study Details

The D9901 study was a double-blind, placebo-controlled Phase 3 trial evaluating Provenge in men with asymptomatic, metastatic androgen independent prostate cancer. The study was designed to measure time to disease progression and time to development of disease-related pain in men with androgen independent prostate cancer. In addition, a 36 month final survival analysis was required per the study design. The study randomized 127 men to receive three infusions of Provenge or placebo over a four-week period.

About Prostate Cancer

Prostate cancer is the number one non-skin cancer in the United States and the third most common cancer worldwide. More than one million men in the United States have prostate cancer, with an estimated 232,000 new cases of prostate cancer diagnosed each year. More than 30,000 men die each year of the disease.

Conference Call Details

The Company will be hosting a conference call on Tuesday, February 22, 2005 at 9:00 a.m. Eastern Standard Time; 6:00 a.m. Pacific Standard Time. To listen to this conference call, please call 877-502-9276 (domestic) or +1-913-981-5591 (international). A replay of the call will be available for 30 days by phone at 888-203-1112 (domestic) or +1-719-457-0820 (international), Passcode: 5926949. In addition, this call is being webcast and can be accessed via the "Investor/Webcasts & Presentations" section of Dendreon's website at www.dendreon.com.

About Provenge

Provenge is designed to stimulate a patient's immune system against prostate cancer. It is developed through Dendreon's proprietary Antigen Delivery Cassette™ technology, which utilizes a recombinant form of an antigen found in 95 percent of prostate cancers, prostatic acid phosphatase (PAP). Provenge is being further evaluated in an ongoing, pivotal Phase 3 trial (D9902B) under a Special Protocol Assessment agreement with the U.S. Food and Drug Administration. Provenge also has Fast Track designation. The double-blind, placebo-controlled trial is enrolling patients at leading cancer centers around the country. To learn more about the trial, go to www.dendreon.com.

About Dendreon

Dendreon Corporation is a biotechnology company whose mission is to target cancer and transform lives through the development of innovative cancer treatments. In addition to its immunotherapies in clinical and preclinical development for a variety of cancers, Dendreon's product pipeline also includes monoclonal antibody and small molecule product candidates. Dendreon has research and development alliances with Genentech, Inc., Abgenix, Inc. and Dyax Corp. For more information about the company and its programs, visit www.dendreon.com.

Except for historical information contained herein, this news release contains forward-looking statements that are subject to risks and uncertainties surrounding the efficacy of Provenge to treat men suffering from prostate cancer, risks and uncertainties surrounding the presentation of data to the FDA and approval of product applications by the FDA and risks and uncertainties inherent in the process of discovering, developing and commercializing drugs that are safe and effective for use as human therapeutics. Factors that may cause such differences include risks related to our limited operating history, risks associated with completing our clinical trials, the risk that the safety and/or efficacy results of a clinical trial for Provenge will not support an application for a biologics license, the risk that the FDA may interpret data differently than we do or require more data or a more rigorous analysis of data than expected, the risk that the FDA will not approve a product for which a biologics license has been applied, the risk that the results of a clinical trial for Provenge or other product may not be indicative of results obtained in a later clinical trial, risks that we may lack the financial resources and access to capital to fund required clinical trials or commercialization of Provenge, our dependence on the efforts of third parties, including collaborators, and our dependence on intellectual property. Further information on the factors and risks that could affect Dendreon's business, financial condition and results of operations, are contained in Dendreon's public disclosure filings with the U.S. Securities and Exchange Commission, which are available at www.sec.gov.

Contacts:
Monique Greer
Sr. Director, Corporate Communications
Dendreon Corporation
(206) 829-1500

http://investor.dendreon.com/ReleaseDetail.cfm?ReleaseID=156146&Header=IR

Immunotherapy (APC80I5, Provenge®) Targeting Prostatic Acid Phosphatase Can Induce Durable Remission of Metastatic Androgen-Independent Prostate Cancer: A Phase 2 Trial

Patrick A. Burch,[1] Gary A. Croghan,[1] Dennis A. Gastineau,[2] Lori A. Jones,[3] Judith S. Kaur,[1] Jelle W. Kylstra,[3] Ronald L. Richardson,[1] Frank H. Valone,[3] and Stanimir Vuk-Pavlović[4]*

[1]*Division of Medical Oncology, Department of Oncology, Mayo Clinic, Rochester, Minnesota*
[2]*Division of Transfusion Medicine, Department of Laboratory Medicine and Pathology, Mayo Clinic, Rochester, Minnesota*
[3]*Dendreon Corporation, Seattle, Washington*
[4]*Stem Cell Laboratory, Mayo Clinic Cancer Center, Mayo Clinic, Rochester, Minnesota*

BACKGROUND. Prostate cancer is the most commonly diagnosed malignancy in American men, yet treatment of its metastatic androgen-independent form remains inadequate. This mandates development of new therapies such as immunotherapy. In this Phase 2 trial, we determined the efficacy of antigen presenting cells (APCs) loaded with PA2024, a recombinant fusion protein containing prostatic acid phosphatase (PAP) and GM-CSF.

METHODS. We enrolled 21 patients with histologically documented androgen-independent prostate carcinoma that could be evaluated by radionuclide bone scan or computed tomography scan. APC8015 was prepared from a leukapheresis product; it contained autologous CD54-positive PA2024-loaded APCs with admixtures of monocytes, macrophages, B and T cells. APC8015 was infused intravenously twice, 2 weeks apart. Two weeks after the second infusion, patients received three subcutaneous injections of 1.0 mg of PA2024 1 month apart. We monitored patients' physical condition, immune response, and laboratory parameters.

RESULTS. Nineteen patients could be evaluated for response to treatment. The median time to progression was 118 days. Treatment was tolerated reasonably well; most adverse effects were secondary to APC8015 and were NCI Common Toxicity Criteria Grade 1–2. Four of the 21 patients reported Grade 3–4 adverse events. Two patients exhibited a transient 25–50% decrease in prostate-specific antigen (PSA). For a third patient, PSA dropped from 221 ng/ml at baseline to undetectable levels by week 24 and has remained so for more than 4 years. In addition, this patient's metastatic retroperitoneal and pelvic adenopathy has resolved. PBMC collected from patients for at least 16 weeks proliferated upon in vitro stimulation by PA2024. For the patient with responsive disease, PBMC could be stimulated for 96 weeks.

CONCLUSIONS. This study demonstrates a definite clinical response of androgen-independent prostate cancer to APC immunotherapy. Currently we are studying this mode of therapy in Phase 3 trials. *Prostate 60: 197–204, 2004.* © 2004 Wiley-Liss, Inc.

KEY WORDS: antigen presenting cells; clinical response; dendritic cells; metastatic adenopathy; PA2024; prostate-specific antigen; time to disease progression

---

INTRODUCTION

Prostate cancer is the most commonly diagnosed malignancy in American men, with an estimated number of 220,900 new cases and 28,900 expected deaths in 2003 [1]. Treatment of metastatic prostate cancer usually includes androgen ablation by bilateral orchiectomy or by agonists of leuteinizing hormone-releasing hormone with or without concurrent administration of antiandrogens [2]. Initially, most patients respond to such treatment, but virtually all eventually develop progressive androgen-independent disease [3,4]. Management of androgen-independent disease is less well standardized. It often depends on the extent of disease, symptoms, and other concurrent medical problems. Options for management include symptomatic and supportive care, second-line hormonal treatment, chemotherapy, or experimental treatments [5,6]. The limited survival and lack of reliably effective treatments for this stage of prostate cancer mandates development of new therapeutic strategies.

One new approach utilizes recent advances in identification of tumor-associated and tumor-specific antigens and the ability to culture antigen presenting cells (APCs). Among the APCs, dendritic cells are pivotal in the initiation and maintenance of immune responses to infections and tumors [7]. Such cells can be exposed to tissue-associated antigens and activated ex vivo [8,9]. Activated cells can be infused to stimulate the immune system to search for tumor cells and eliminate them; this strategy of cancer immunotherapy is under investigation in a number of tumor types [10].

Prostate cancer presents a unique opportunity for cellular immunotherapy. The prostate and prostate-derived tumors express molecules such as prostate-specific antigen (PSA), prostate-specific membrane antigen (PSMA), and prostatic acid phosphatase (PAP); each of these molecules is currently under clinical investigation as a target antigen [11–16]. PAP is particularly attractive because its expression is more restricted to the prostate than PSA and PSMA [17]. Tissue-specific PAP expression is likely to focus the immune effects on prostate tissue. We have previously fused the *PAP* gene to the granulocyte/macrophage colony stimulating factor (*GM-CSF*) gene, expressed the fused protein (termed PA2024), and used it in Phase 1 clinical studies. There we used autologous APCs loaded with PA2024 (termed APC8015) for therapy of advanced prostate cancer and showed that the treatment is feasible and safe, that it induces cellular immunity, reduces PSA and PAP levels in some patients, and that it may affect time to disease progression [11,17]. Earlier we completed a PA2024 dose escalation Phase 1 trial that demonstrated that PA2024 injections following APC8015 infusions are also safe [12]. These results mandated this Phase 2 study to determine the effects of APC8015 followed by the highest dose of PA2024 on the course of androgen-independent prostate cancer.

PATIENTS, MATERIALS, AND METHODS

Patients

Before enrollment, all patients signed informed consent approved by the Mayo Clinic Institutional Review Board. The patients were eligible when their histologically documented prostate carcinoma progressed despite androgen ablation and antiandrogen withdrawal. Progression had to be documented radiographically (bone scan or CT scan) or by consecutive increases in PSA levels. The tumor had to be evaluable by radionuclide bone scan or computed tomography scan. Gonadal androgen suppression was continued throughout the trial. Prior chemotherapy, radiation therapy, or therapy with other experimental agents was permitted if completed 4 weeks before enrollment, the patient had recovered from any adverse reaction, and further disease progression was documented. Prior immunotherapy or current use of corticosteroids were not allowed. Patients had to exhibit a performance status of 0 or 1 (Eastern Cooperative Oncology Group criteria) and a life expectancy of at least 12 weeks. Other entry criteria included a PSA value above or equal to 5.0 ng/ml and detectable PAP levels in patients who had undergone a prostatectomy or above the upper limit of normal in patients who had not undergone surgery. Further requirements for enrollment included negative serological tests for HIV, human T-cell lymphotrophic virus type I, hepatitis B and hepatitis C, and acceptable hematological, renal, and hepatic function.

Preparation of PA2024

Dendreon Corporation prepared PA2024 for all patients in compliance with current Good Manufacturing Practices. PA2024 consists of human PAP fused through its carboxy terminus to the amino terminus of GM-CSF by a Gly-Ser linker [12]. The GM-CSF portion targets the fusion protein to APCs [18]. Preparation of recombinant PA2024, its expression in a baculovirus system and purification to more than 90% purity has been previously described [12].

Preparation and Administration of APC8015

APC8015 is a product comprised of autologous APCs (CD54-positive cells that include monocytes and dendritic cells) loaded with PA2024. The product also contains macrophages, B and T cells exposed to PA2024 [12]. Mayo Clinic Human Cell Therapy

Laboratory prepared APC8015 for all patients in compliance with current Good Manufacturing Practices for somatic cell therapy. Two days before each APC8015 infusion, patients underwent a standard leukapheresis (1.5–2.0 blood volumes). Leukapheresis products were processed as previously described [12]. Briefly, APC precursors were isolated from the mononuclear cell preparation and cultured for 40 hr. PA2024 was added to the cultures for the entire 40 hr and unbound PA2024 was removed by washing. The final product was transported to the Mayo Clinic Infusion Therapy Center approximately 48 hr after leukapheresis and infused in the outpatient setting.

Treatment and Assessment

APC8015 was administered intravenously to eligible patients twice, in week 0 and week 2. The cells were infused through a large bore intravenous line over 30 min. Patients were then observed for acute adverse effects for 30 additional minutes before discharge. Subsequently they received three subcutaneous injections of 1.0 mg of PA2024 (0.5 mg into each thigh) at weeks 4, 8, and 12.

We monitored patients' physical condition, immune response, and laboratory parameters (including PSA and PAP) every 4 weeks through week 16, and every 8 weeks thereafter until disease progression. Tumor burden was evaluated radiographically at baseline, week 16, week 32, and week 48. Progression was defined as objective enlargement of soft tissue disease or the appearance of two or more new lesions on a radionuclide bone scan. For patients undergoing APC immunotherapy, the correlation of PSA levels and clinical outcome is unknown. Hence, we did not remove from the trial the patients who experienced an increase in PSA in the absence of clinically or radiographically confirmed disease progression. Nonetheless, such patients were free to request removal from the study to initiate other treatments. Adverse events were evaluated for the relationship to treatment with APC8015 and PA2024 and scored according to National Cancer Institute Common Toxicity Criteria (NCI-CTC).

Assessment of Immune Function

To assess immune response to treatment, blood was drawn from patients every 4 weeks from week 0 (baseline) through week 16, then every 8 weeks thereafter until disease progression. Peripheral blood mononucelar cells (PBMCs) were isolated from heparinized blood by buoyant density centrifugation at 1.077 g/ml and 320 mosM. Isolated PBMCs were washed twice with D-PBS (Life Technologies) and suspended in AIM-V (Life Technologies) containing

5.0% human AB serum (Gemini Bioproducts, Calabas, CA) for immediate use or freezing.

Proliferation assays were completed in triplicate 96-well, round-bottom plates (Dynex Technologies, Chantilly, VA) using 1.0×10^5 PBMCs/well. Cell proliferation was evaluated in response to PA2024, PAP (Biodesign International, Kennebunk, ME), and GM-CSF (Leukine, Immunex, Seattle, WA). Each molecule was introduced to cells at 0.4, 2.0, 10, or 50 µg/ml and incubated for 6 days at 37°C and 5% CO_2. Control wells contained no antigen. For the last 16 hr of incubation, each well was treated with 1.0 µCi of ^{3}H-thymidine (Amersham, Piscataway, NJ). The cells were harvested and incorporated radioactivity was measured by a Wallac-LKB Betaplate counter and expressed in counts per minute (cpm). Data are presented as stimulation indices (SI) calculated by dividing the mean radioactivity (of triplicate wells) of stimulated cells by the mean radioactivity measured in control wells.

Titers of serum antibodies specific for PA2024, PAP, and GM-CSF were determined from data obtained by ELISA. Each antigen was immobilized overnight at 4°C in triplicate 96-well plates at 1.0 µg/ml in 100 µl of D-PBS. Plates were washed with PBST and serially diluted serum was added to each well. Pooled human serum was used as the negative control, and sera with high titers of respective antibodies were used as positive controls. The plates were incubated for 1 hr at room temperature and washed with PBST. Antigen-specific antibodies were exposed to horseradish peroxidase-conjugated goat anti-human IgG/IgM and quantified by the extent of o-phenylenediamine dihydrochloride converted into the product absorbing at 492 nm in the course of 12 min. Antibody titer was defined as the highest serum dilution that yielded the 492 nm reading twice above the negative control.

Statistics

This Phase 2 study was designed to obtain preliminary evidence of clinical benefit in the treatment of metastatic, androgen-independent prostate carcinoma. Time to tumor progression was summarized by the Kaplan–Meier method. Clinical response rate equal or above 15% was considered adequate to justify further studies of efficacy. Nineteen subjects were needed to achieve this target. If none of the 19 subjects responded to treatment, the probability that the true response rate is equal to or larger than 15% was $P < 0.05$.

To compare treatment-induced changes in cellular immunity, by maximum likelihood method [19], we fitted a linear mixed model to the natural logarithms of SI values. We analyzed these values for PBMC samples stimulated with PA2024 (10 µg/ml) at weeks 4, 8, 12,

and 16 as only fragmentary data at other time points were available.

RESULTS

Patients

Table I displays the demographics and baseline characteristics of the 21 patients on the study. Each received both infusions of the maximum number of cells manufactured from the respective leukapheresis product. The median number of cells was 2.7×10^9 for the first infusion and 3.2×10^9 for the second infusion. The disease progressed before the first PA2024 injection at week 4 for two patients, after the first injection for one patient, and after the second injection at week 8 for three patients. The remaining 15 patients received all three PA2024 injections and remained on study until at least week 16.

Response to Treatment

Nineteen patients received both infusions of APC8015 and at least one injection of PA2024; thus, they could be evaluated for response to treatment. For these patients the median time to progression was 118 days from the date of registration. In the course of treatment, two patients exhibited a 25–50% transient decrease in PSA, one during tumor progression and the other following the second APC8015 infusion (data not shown). For a third patient, the level of PSA rose from 221 ng/ml at baseline to 251 ng/ml by week 4 and then dropped to undetectable levels by week 24 (Fig. 1a).

The changes in serum levels of PAP closely followed the changes of PSA and dropped to normal levels below detection (data not shown). His PSA level has remained undetectable for 52 months after the beginning of treatment and the metastatic adenopathy has resolved (Fig. 1b). No other patients responded by radiographic criteria. PSA levels in all but four patients increased more than 50% over baseline or nadir values at the time of radiographic progression.

Treatment-Related Toxicity

Overall, treatment was tolerated reasonably well (Table II). The most frequent adverse events after APC8015 infusion were NCI-CTC Grade 1–2 chills and fatigue. Four of the 21 patients reported severe (Grade 3–4) adverse events. These included one episode each of chills, fatigue, fever, malaise, tachycardia, dyspnea, and vomiting after infusion of APC8015. Five patients exhibited Grade 1–2 local reaction following subcutaneous injections of PA2024. One patient experienced a Grade 3 infection, hematuria, and Grade 4 fatigue 2 weeks after the last PA2024 injection, at a time when disease was progressing.

Immune Response

We evaluated antigen-specific cellular immunity in response to treatment with APC8015 and soluble PA2024 for 15 patients every 4 weeks from week 0 (baseline) to week 16 and then every 8 weeks thereafter until disease progression. Response to PA2024 was

TABLE I. Patient Demographics and Baseline Characteristics

Number of patients enrolled	21
Age, years [median (range)]	72 (57–83)
Prostate-specific antigen (PSA), ng/ml [median (range)]	221 (21–1,147)
Prostatic acid phosphatase (PAP), ng/ml [median (range)]	9.2 (0.8–291)
Hemoglobin, g/dl [median (range)]	12.7 (10.5–15.2)
Primary therapy	
Surgery	9[a]
Surgery/hormone ablation	4
Radiation	3
Radiation/hormone ablation	1
Hormones	4
Site of metastases	
Osseous	13
Soft tissue	6
Both	2
Gleason score (n = 19)	
≤ 6	3
7	8
≥ 8	8

[a]Values denote the number of patients in each group.

significant at week 4 ($P < 0.0001$) and persisted for the duration of monitoring (Fig. 2). In the patient with responsive disease, PA2024-specific PBMC proliferation was evaluated until week 138; his PBMCs

a

Time (Months)

b   Before Treatment   After Treatment

c

Time (Weeks)

proliferated upon stimulation with PA2024 until week 96 (Fig. 1c). PAP and GM-CSF stimulated PBMC proliferation only marginally (data not shown). The extent of stimulation differed among patients and was not significant overall.

We measured serum levels of antibodies specific for PA2024, PAP, and GM-CSF. After all treatments, with APC8015 and PA2024, 13 of 15 patients developed antibodies specific for PA2024 with the highest titers measured between week 4 and week 8 (Table III). We also detected antibodies specific for GM-CSF, but not for PAP (Table III). In the patient whose disease fully responded, levels of antibodies specific for PA2024 peaked at week 12 and steadily declined thereafter (Fig. 1c).

DISCUSSION

The median survival time of patients suffering from metastatic androgen-independent prostate cancer is only 12–18 months. Thus, providing an effective treatment for this disease remains a major challenge. Chemotherapy can palliate symptoms and significantly reduce PSA levels, but in many patients the response is brief and side effects can be troublesome [6,20]. Numerous current clinical trials are investigating novel treatments as an alternative to cytotoxic chemotherapy [13]. One promising new avenue is immunotherapy.

In this Phase 2 trial, we evaluated infusions of APC8015 (autologous APCs incubated in the presence of PA2024, recombinant PAP–GM-CSF) followed by injections of soluble PA2024 for the treatment of patients suffering from metastatic androgen-independent prostate cancer. PSA is often used as a surrogate marker of response in androgen-independent prostate cancer [21]. In addition to PSA, we followed disease progression by radiography because the utility of PSA as a marker in the patients treated by immunotherapy is unknown. Therefore, we tested the utility of PSA as an endpoint in immunotherapy with APC8015 by comparing disease progression based on PSA levels with such evaluation based on radiography. In four patients,
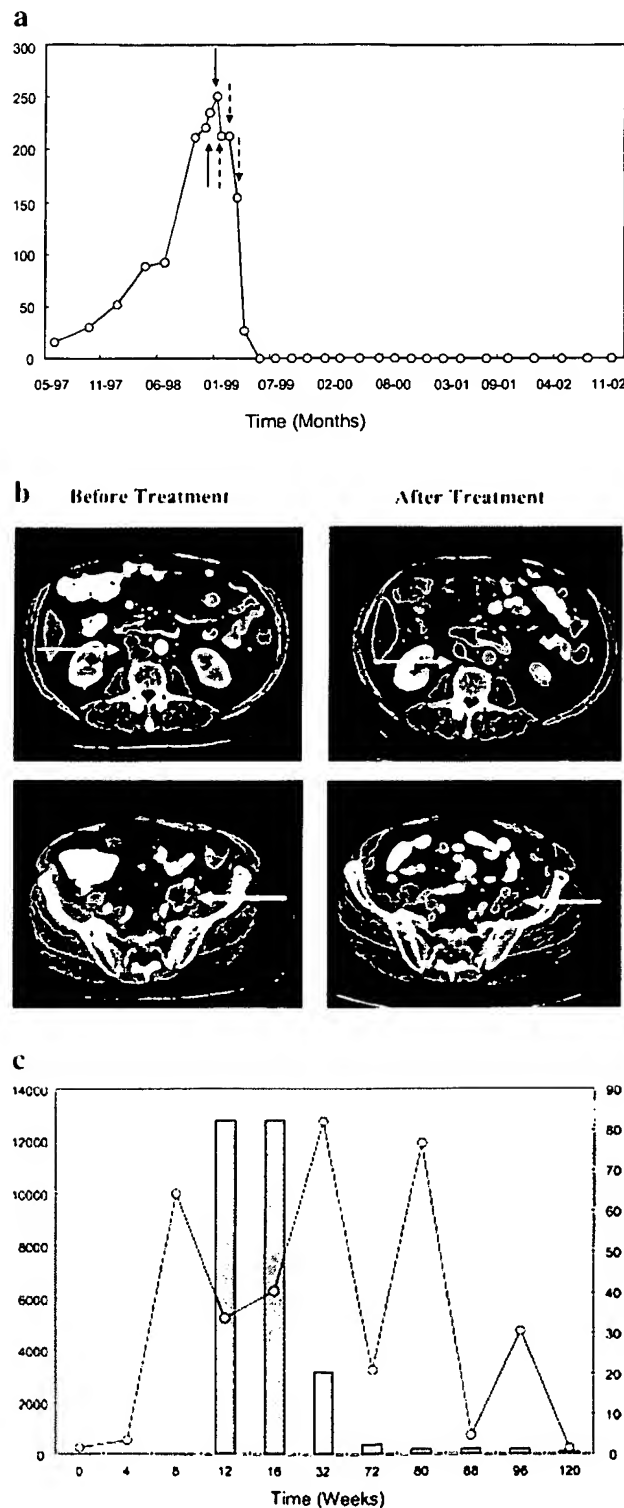
Fig. 1. Treatment-induced clinical and immune effects in the patient 9702-22 who underwent a complete clinical response. a: Change in serum levels of prostate-specific antigen (PSA) as a function of time before and after treatment with APC8015 (full-line arrows) and PA2024 (dashed line arrows). b: **Left**, computerized tomography scans obtained before treatment and, **right**, 22 months after initiation of treatment. Arrows indicate the sites of retroperitoneal lymph nodes (**upper panels**) and pelvic lymph nodes (**lower panels**). c: Titer (reciprocal dilution) of PA2024-specific antibodies (columns, left axis) and PA2024-stimulated PBMC proliferation (stimulation index circles; right axis) as a function of treatment.

TABLE II. Treatment-Related Adverse Effects (NCI CommonToxicity Criteria) in Patients on Study

After APC8015 infusions (42 total infusions)	After PA2024 injections (52 total injections)
Grade 4: dyspnea, 1; vomit, 1	Grade 4: fatigue, 1
Grade 3: tachycardia, 1; chills, 1; malaise, 1; fatigue, 1; fever, 1	Grade 3: infection, 1; hematuria, 1
Grade 2: hypertension, 1; fever, 1; chills, 1; dyspnea, 1	Grade 2: local, 3; anorexia, 2; fatigue, 1; fever, 1
Grade 1: fatigue, 4; fever, 7; chills, 15; pain, 2; dausea, 2; malaise, 1; dyspnea, 1; vomit, 1; diarrhea, 1	Grade 1: local, 10; anorexia, 4; diarrhea, 3; fever, 3; fatigue, 2; chills, 2; nausea, 2; malaise, 1

PSA levels were less than 50% above the baseline or nadir values at the time of disease progression. Similarly to our observation in the Phase 1 trial, one patient exhibited a PSA decline of nearly 50% during disease progression [12]. These findings suggest that PSA alone must be used cautiously as a marker of disease response to immunotherapy.

Treatment with APC8015 and PA2024 induced PA2024-specific immune effector cells (quantified by the extent of PA2024-stimulated in vitro proliferation). These cells were present during the entire 16 weeks of sampling. In one patient who responded to treatment, PA2024-specific cells were detected as long as 22 months from the initiation of treatment. We did not detect any PAP-specific immune effector cells. This

could result if PA2024 is more immunogenic than PAP and competes successfully for the pertinent T cell clones. Alternatively, purified natural PAP used in these assays could have retained some immunosuppressive molecules from the semen [22,23] that would reduce in vitro proliferation. Currently we are attempting to discriminate between these alternatives by comparing the ability of PA2024, PAP from seminal fluid and recombinant PAP to stimulate PBMC. Similarly, we detected antibodies specific for PA2024 and GM-CSF but not for PAP. This may stem from the specificity of the antibodies for the carbohydrate moieties for PA2024 rather than for its protein core. Glycosylation of the baculovirus-expressed PA2024 may differ from glycosylation of human PAP rendering the antibodies raised against PA2024 unreactive towards PAP.

In previous studies, we found that APC8015 was safe and that it effectively stimulated cellular immunity [11,12]. In this study, we confirmed that APC8015 and PA2024 were generally well tolerated and that adverse effects were manageable. This is particularly important in comparison to cytotoxic chemotherapy regimens where adverse effects can be more severe, and where dose reductions and dose interruptions are common [6,20]. Along with manageable adverse effects, we observed a definite clinical response. While in one patient PSA levels dropped during disease progression, in another the decline in PSA levels coincided with stable disease. Particularly significant has been the patient whose PSA initially increased and then became undetectable, while his retroperitoneal and pelvic adenopathy completely resolved. This response has continued well beyond 4 years after completion of treatment. Our evidence that this mode of treatment is clinically active and accompanied by manageable adverse effects complements the evidence obtained at the University of California, San Francisco in a study of APC8015 alone [11]. A comparison of the two studies indicates that the addition of subcutaneous PA2024 injections does not confer apparent immunologic or clinical benefits over and beyond APC8015 alone [12].
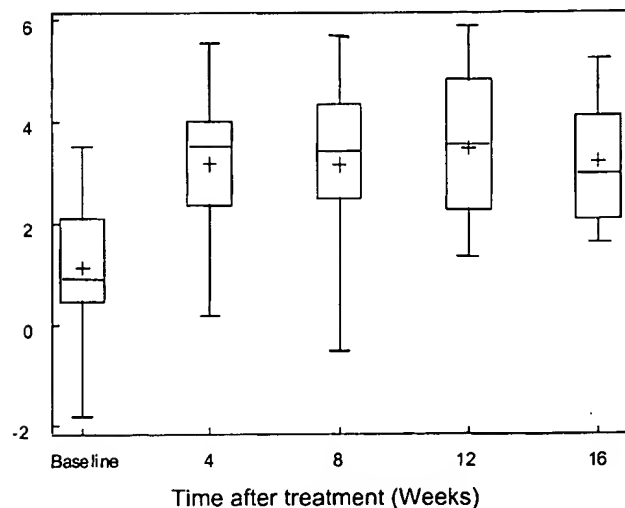
Fig. 2. Time dependence of treatment-induced cellular response against PA2024 in patients treated with APC8015 and PA2024. Each box represents the range from the 25th to the 75th percentile value of the stimulation index (SI), the error bars the range of values, the plus sign the mean value and the horizontal line in the box the median value. The difference between values observed at week 4 and baseline is significant (P < 0.0001).

TABLE III. AntibodyTiters in Patient Sera Before (Week 0) and AfterTreatment (Week 16)

Antigen	Number of evaluable patients	Antibody titer, mean (standard deviation)	Antibody titer, median (range)
Week 0			
PAP	15	1.3 (3.51)	0 (0–10)
PA2024	15	1,370 (5,290)	0 (0–20,480)[a]
GM-CSF	15	2.0 (5.6)	0 (0–20)
Week 16			
PAP	10	2.0 (4.2)	0 (0–10)
PA2024	10	12,810 (8,610)	16,640 (2,560–20,480)
GM-CSF	10	4,790 (8,310)	1,280 (0–20,480)

[a]These values stem from the one patient who displayed PA2024-reactive antibodies before treatment. In all other patients titers were 10 or less.

Consequently, we are currently conducting a multi-center, randomized Phase 3 trial of APC8015 alone for the treatment of patients with asymptomatic, radiographically evaluable, androgen-independent prostate carcinoma.

ACKNOWLEDGMENTS

REFERENCES

1. Jemal A, Thomas A, Murray T, Thun M. Cancer statistics. CA Cancer J Clin 2002;52:23–47.

2. Dowling AJ, Tannock IF. Systemic treatment for prostate cancer. Cancer Treat Rev 1998;24:283–301.

3. Scher HI, Maxumdar M, Kelly WK. Clinical trials in relapsed prostate cancer: Defining the target. J Natl Cancer Inst 1996; 88:1623–1634.

4. Small EJ, Vogelzang NJ. Second-line hormonal therapy for advanced prostate cancer: A shifting paradigm. J Clin Oncol 1997;15:382–388.

5. Oh WK, Kantoff PW. Management of hormone refractory prostate cancer: Current standards and future prospects. J Urol 1998; 160:1220–1231.

6. Kantoff PW, Halabi S, Conaway M, Picus J, Kirshner J, Hars V, Trump D, Winer EP, Vogelzang NJ. Hydrocortisone with or without mitoxantrone in men with hormone-refractory prostate cancer: Results of the cancer and leukemia group B 9182 study. J Clin Oncol 1999;17:2506–2513.

7. Banchereau J, Steinman RM. Dendritic cells and the control of immunity. Nature 1998;392:245–252.

8. Nestle FO, Banchereau J, Hart D. Dendritic cells: On the move from bench to bedside. Nat Med 2001;7:761–765.

9. Dietz AB, Litzow MR, Gastineau DA, Vuk-Pavlovic S. Engineering dendritic cell grafts for clinical trials in cellular immunotherapy of cancer: The example of chronic myelogenous leukemia. Croat Med J 2001;42:427–434.

10. Valone FJ, Small E, MacKenzie M, Burch P, Lacy M, Peshwa MV, Laus R. Dendritic cell-based treatment of cancer: Closing in on a cellular therapy. Cancer J 2001;7:S53–S61.

11. Small EJ, Fratesi P, Reese DM, Strang G, Laus R, Peshwa MV, Valone FH. Immunotherapy of hormone-refractory prostate cancer with antigen-loaded dendritic cells. J Clin Oncol 2000; 18:3894–3903.

12. Burch PA, Breen JK, Buckner JC, Gastineau DA, Kaur JA, Laus RL, Padley DJ, Peshwa MV, Pitot HC, Richardson RL, Smits BJ, Sopapan P, Strang G, Valone FH, Vuk-Pavlovic S. Priming tissue-specific cellular immunity in a phase I trial of autologous dendritic cells for prostate cancer. Clin Cancer Res 2000;6:2175–2182.

13. Eder JP, Kantoff PW, Roper K, Xu GX, Bubley GJ, Boyden J, Gritz L, Mazzara G, Oh WK, Arlen P, Tsang KY, Panicali K, Schlom J, Kufe DW. A phase I trial of a recombinant vaccinia virus expressing prostate-specific antigen in advanced prostate cancer. Clin Cancer Res 2000;6:1632–1638.

14. Salgaller ML, Tjoa BA, Lodge PA, Ragde H, Kenny G, Boynton A, Murphy GP. Dendritic cell-based immunotherapy of prostate cancer. Crit Rev Immunol 1998;18:109–119.

15. Dannull J, Diener PA, Prikler L, Furstenberger G, Cerny T, Schmid U, Ackermann DK, Groettrup M. Prostate stem cell antigen is a promising candidate for immunotherapy of advanced prostate cancer. Cancer Res 2000;60:5522–5528.

16. Simmons SJ, Tjoa BA, Rogers M, Elgamal A, Kenny GM, Ragde H, Troychak MJ, Boynton AL, Murphy GP. GM-CSF as a systemic adjuvant in a phase II prostate cancer vaccine trial. Prostate 1999;39:291–297.

17. Fong L, Brockstedt D, Benike C, Breen JK, Strang G, Ruegg CL, Engleman EG. Dendritic cell-based xenoantigen vaccination for prostate cancer immunotherapy. J Immunol 2001;167:7150–7156.

18. Tao M-H, Levy R. Idiotype/granulocyte-macrophage colony-stimulating factor fusion protein as a vaccine for B-cell lymphoma. Nature 1993;362:755–758.

19. Verbeke G, Molenberghs G. Linear mixed models for longitudinal data. New York: Springer; 2000.

20. Savarese DM, Halabi S, Hars V, Akerley WL, Taplin M, Godley PA, Hussain A, Small EJ, Vogelzang NJ. Phase II study of docetaxel, estramustine, and low-dose hydrocortisone in men with hormone-refractory prostate cancer: A final report of CALGB 9780. J Clin Oncol 2001;19:2509–2516.

21. Bubley GJ, Carducci M, Dahut W, Dawson N, Dalani D, Eisenberger M, Figg WD, Freidlin B, Halabi S, Hudes G, Hussain M, Kaplan R, Myers C, Oh W, Petrylak DP, Reed E, Roth B, Sartor O, Scher H, Simons J, Sinibaldi V, Small EJ, Smith MR, Trump DL, Vollmer R, Wilding G. Eligibility and response guidelines for phase II clinical trials in androgen-independent prostate cancer: Recommendations from the prostate-specific antigen working group. J Clin Oncol 1999;17:3461–3467.

22. Lokeshwar BL, Block NL. Isolation of a prostate carcinoma cell proliferation-inhibiting factor from human seminal plasma and its similarity to transforming growth factor β. Cancer Res 1992; 52:5821–5825.

23. Nocera M, Chu TM. Transforming growth factor beta as an immunosuppressive protein in human seminal plasma. Am J Reprod Immunol 1993;30:1–8.

⊘ Adjuvant autologous renal tumour cell vaccine and risk of tumour progression in patients with renal-cell carcinoma after radical nephrectomy: phase III, randomised controlled trial

Dieter Jocham, Axel Richter, Lothar Hoffmann, Klaus Iwig, Dirk Fahlenkamp, Günther Zakrzewski, Eberhard Schmitt, Thomas Dannenberg, Walter Lehmacher, Jörn von Wietersheim, Christian Doehn

Summary

Background Organ-confined renal-cell carcinoma is associated with tumour progression in up to 50% of patients after radical nephrectomy. At present, no effective adjuvant treatment is established. We aimed to investigate the effect of an autologous renal tumour cell vaccine on risk of tumour progression in patients with stage pT2–3b pN0–3 M0 renal-cell carcinoma.

Methods Between January, 1997, and September, 1998, 558 patients with a renal tumour scheduled for radical nephrectomy were enrolled at 55 institutions in Germany. Before surgery, all patients were centrally randomised to receive autologous renal tumour cell vaccine (six intradermal applications at 4-week intervals postoperatively; vaccine group) or no adjuvant treatment (control group). The primary endpoint of the trial was to reduce the risk of tumour progression, defined as progression or death. All patients were assessed after standardised diagnostic investigations at 6-month intervals for a minimum of 4·5 years.

Findings By preoperative and postoperative inclusion criteria, 379 patients were assessable for the intention-to-treat analysis. At 5-year and 70-month follow-up, the hazard ratios for tumour progression were 1·58 (95% CI 1·05–2·37) and 1·59 (1·07–2·36), respectively, in favour of the vaccine group (p=0·0204, log-rank test). 5-year and 70-month progression-free survival rates were 77·4% and 72%, respectively, in the vaccine group and 67·8% and 59·3%, respectively, in the control group. The vaccine was well tolerated, with only 12 adverse events associated with the treatment.

Interpretation Adjuvant treatment with autologous renal tumour cell vaccine in patients with renal-cell carcinoma after radical nephrectomy seems to be beneficial and can be considered in patients undergoing radical nephrectomy due to organ-confined renal-cell carcinoma of more than 2·5 cm in diameter.

Department of Urology, University of Lübeck Medical School, Ratzeburger Allee 160, 23538 Lübeck, Germany (Prof D Jocham MD, C Doehn MD); **Department of Urology, Klinikum St Georg, Leipzig** (A Richter MD); **Department of Urology, Wald-Klinikum Gera, Gera** (L Hoffmann MD); **Department of Urology, Klinikum Meiningen, Meiningen** (K Iwig MD); **Department of Urology, Ruppiner Kliniken, Neuruppin** (Prof D Fahlenkamp MD); **Department of Urology, Eichsfeld Klinikum (Haus Reifenstein), Reifenstein** (G Zakrzewski MD); **Department of Urology, Kreiskliniken Aschersleben-Staßfurt, Aschersleben** (E Schmitt MD); **Department of Urology, Klinikum Offenbach, Offenbach** (T Dannenberg MD); **Institute for Medical Statistics, Informatics and Epidemiology, University of Cologne Medical School, Cologne** (Prof W Lehmacher PhD); **Department of Psychosomatic Medicine and Psychotherapy, University of Ulm Medical School, Ulm** (Prof J von Wietersheim PhD)

Correspondence to: Prof Dieter Jocham
(e-mail: Prof.Jocham.MUL@t-online.de)

Introduction

Of all malignant tumours in adults, 3% develop in the kidney; in 85% of these cases, the tumour originates from cells of the proximal tubules and is known as renal-cell carcinoma.[1] This disease mainly arises in the 6th and 7th decades of life, with a male to female ratio of 1·6 to 1·0.[2] In 2003, a total of 31 500 new cases of renal-cell carcinoma and renal pelvis cancer and 11 900 deaths from the disease were expected in the USA.[2] Standard treatment of organ-confined renal-cell carcinoma is partial or radical nephrectomy, whereas patients with distant metastasis are usually treated with non-specific immunotherapy.

According to data from the Surveillance, Epidemiology, and End Results Registry (http://www.seer.cancer.gov), renal-cell carcinoma is localised in 54%, regionally advanced in 21%, and distant in 25% of patients; corresponding 5-year survival rates are 89%, 61%, and 9%, respectively. This disease is also staged by the International Union against Cancer (UICC) tumour-node-metastasis classification.[3] 15 years ago, 5-year survival rates after radical nephrectomy varied between 57% and 92% for T2 tumours and between 35% and 77% for T3 tumours.[4–8] In 2002, a risk-group assessment was published that used tumour stage, tumour grade, and performance status to predict tumour progression and survival.[9] On the basis of this model, patients with low-grade T1 tumours and a good performance status have a high probability (91%) of remaining without tumour progression, whereas all patients with T2 or T3 tumours have an intermediate risk (64%).

Despite the important stage-related risk of tumour progression, until now no effective adjuvant treatment after surgery has been established.[10] Various adjuvant protocols—including radiotherapy, interferon alfa, interleukin 2, medroxyprogesterone acetate, and others—failed to improve progression-free survival, overall survival, or both after nephrectomy for renal-cell carcinoma.[11–15] Therefore, active treatment (medical, operative, or radiotherapy) after surgery is only applied in case of local relapse or systemic progression.[10]

In a pilot study, Repmann and colleagues[16,17] investigated adjuvant treatment with an autologous renal tumour cell vaccine after radical nephrectomy for renal-cell carcinoma and showed a progression-free and overall survival benefit for the vaccine group compared with a historical control group. In 1997, we initiated a phase III randomised trial to investigate the effect of an adjuvant autologous renal tumour cell vaccine on risk of tumour progression in patients with renal-cell carcinoma after radical nephrectomy and to assess safety with respect to its side-effects.

Methods

Patients

Between January, 1997, and September, 1998, we enrolled patients from 55 institutions in Germany with a renal tumour who were scheduled for radical nephrectomy. The ethics committee of the University of Lübeck Medical School and local ethics committees of the participating institutions approved the protocol. The trial was undertaken

according to International Conference on Harmonisation Good Clinical Practice guidelines.

Before surgery, all patients were centrally randomised (Quintiles GmbH, Neu-Isenburg, Germany) to receive autologous renal tumour cell vaccine (vaccine group) or no adjuvant therapy (control group) after radical nephrectomy. No placebo was given to individuals in the control group. Some days after surgery, Quintiles informed the hospital and patient about the randomisation result via fax. Therefore, neither the surgeon and hospital staff nor the patient knew about the randomisation results before surgery. Within 2 weeks after surgery, we checked all patients for inclusion and exclusion criteria, and we finally included only those with histologically proven renal-cell carcinoma stage pT2-3b pN0-3 M0.

Postoperative inclusion criteria were: primary renal-cell carcinoma stage pT2-3b pN0-3 M0 (1993 UICC classification) treated by radical nephrectomy; age 18-70 years; Eastern Cooperative Oncology Group (ECOG) performance status 0-2; ability to cooperate; and provision of written informed consent. Exclusion criteria were: no histologically proven renal-cell carcinoma; primary renal-cell carcinoma stage pT1 or pT4 or M1 (1993 UICC classification); surgery other than radical nephrectomy; relapse of renal-cell carcinoma; embolisation or other treatment for renal-cell carcinoma (eg, immuno-therapy, chemotherapy, radiotherapy); immunosuppressive treatment; ECOG performance status 3-4; serious chronic or acute illness such as serious pulmonary or cardiac disease; severe hypertension (diastolic blood pressure ≥ 115 mm Hg); myocardial infarction in the past 3 months; cerebral infarction in the past 6 months; autoimmune disease (eg, inflammatory bowel disease); previous cancer except basal-cell carcinoma; active or chronic infection (eg, HIV, hepatitis); pregnancy or lactation; no contraception in women of child-bearing potential; participation in a clinical trial over the past 30 days; simultaneous participation in another clinical trial; or lack of cooperation.

Procedures

Patients undergoing radical nephrectomy had an ipsilateral regional lymphadenectomy. We obtained a specimen (10 g) from the peripheral zone of the tumour under sterile conditions, placed this sample in tissue-culture medium, and immediately transported it to the laboratory of LipoNova (Hannover, Germany) by courier.[18]

Workers at LipoNova prepared the vaccine as described previously.[16-18] Briefly, tumour tissue was cut into small pieces and passed through a steel sieve to obtain a cell suspension. Cell debris was removed from this suspension by centrifugation with a density gradient. The separated cells were suspended, and characterisation of cells and cell viability was done by established staining methods. Cells were incubated in RPMI 1640 for 3 h at 37°C with interferon γ 1500 IE per vaccine dose (Imukin; Boehringer, Ingelheim, Germany) and tocopherol acetate 750 μg per vaccine dose (E-Vicotrat; Heyl, Berlin, Germany). Some workers have shown that incubation of renal carcinoma cells with interferon leads to increased expression not only of MHC class I and II but also of ICAM1 (intercellular adhesion molecule 1), TAP1 (transporter associated with antigen processing), and LMP2 (low molecular weight peptide), thus increasing the antigenicity of these cells.[19-25] Tocopherol acetate was added as a lipid-soluble radical-scavenging agent to protect inner and outer cell membranes during the incubation process with interferon γ.[26]

After incubation, cells were washed several times to remove interferon γ and tocopherol acetate. They were then suspended in physiological saline containing 0·5% glucose. 1 mL aliquots containing about 5×10^6 renal-tumour cells of the lysate were stored. To devitalise the cells, repeated rapid freezing at -82°C without a cryoprotector and thawing was done. Testing of the devitalisation process was by standard staining procedures. Sterility tests were undertaken by culturing the probes: confirmed sterility of the final product was a release criterion. No antibiotics were present in the media. Until shipping the vaccine was stored at -82°C and then was shipped on dry ice and stored until use at -18°C. The entire production process was done according to good manufacturing practice.

We injected six intradermal applications of the vaccine into the patient's upper arm at 4-week intervals. The vaccine was given in the outpatient department of the hospital or by the urologist in private practice.

The primary endpoint of the trial was to reduce the risk of tumour progression, defined as progression—which we measured by local recurrence or distant metastasis confirmed by physical examination, imaging, or both—or death. Secondary outcome measures were the effect of the vaccine on quality of life; effect of the vaccine production process (total number of cells, percentage of tumour cells) and the number of vaccine doses on patients' outcome and tolerability of autologous renal tumour cell vaccine; and rate of adverse events.

We assessed adverse events with WHO criteria. Adverse events in patients given the vaccine were recorded by their doctor and noted in a standardised way according to the WHO classification: mild (grade I), moderate (grade II), and severe (grade III). We investigated quality of life with the QLQ-C30 questionnaire of EORTC (European Organisation for Research and Treatment of Cancer)[27] and the Lebenszufriedenheit questionnaire (modification of the Munich Quality of Life Dimension List). We gave the questionnaires to patients before surgery and at 6, 24, 36, 48, and 60 months thereafter.

We saw patients every 6 months for physical examination, blood chemistry, ultrasound, chest radiography, and abdominal CT or MRI. Monitoring of the trial was undertaken by local monitors and contract research organisations (Quintiles GmbH, Neu-Isenburg, Germany; Medicore International, Schöndorf, Germany; Pharmcon, Essen, Germany). We followed up all patients for a minimum of 4·5 years. Total observation period was 71 months in the vaccine group and 72 months in the control group.

Statistical analysis

We calculated sample size according to the results of a pilot trial[16,17] that showed a hazard ratio of 2·1 in favour of the vaccine group. According to the protocol, at least 328 patients had to be randomised, including a dropout rate of 20% (two-sided α of 0·05 and power of 0·9).

Data analysis was done by one of us (WL) with Medicore International and DSH statistical reviews (Rohrbach, Germany). We analysed demographic data with Fisher's exact test, Cochran-Mantel-Haenszel test, Wilcoxon test for rank-sums, and Kolmogorov-Smirnov test (for comparison of the histograms of tumour-size distribution). We calculated Störkel score, which predicts survival of patients with renal-cell carcinoma and takes into account different variables like T stage, grading, patient's age, cell type, and growth pattern.[8] For analysis of the primary endpoint, we used a stratified log-rank test, with T stage as a stratification criterion. Also, we calculated the absolute and relative risk reduction of progression-free survival rates at 60 and 70 months and the number needed to treat. We applied a Cox proportional-hazards model to assess the effect of
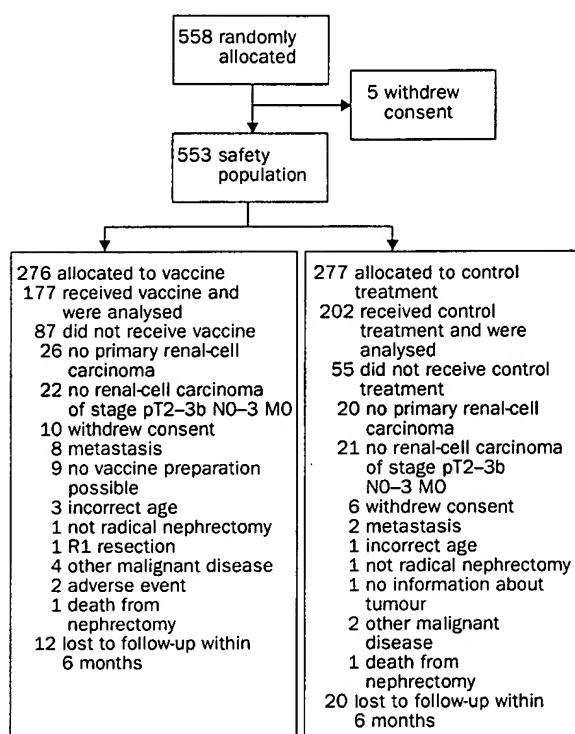
Figure 1: **Trial profile**

Boxes in figure 1:

558 randomly allocated

5 withdrew consent

553 safety population

276 allocated to vaccine
177 received vaccine and were analysed
87 did not receive vaccine
26 no primary renal-cell carcinoma
22 no renal-cell carcinoma of stage pT2–3b N0–3 M0
10 withdrew consent
8 metastasis
9 no vaccine preparation possible
3 incorrect age
1 not radical nephrectomy
1 R1 resection
4 other malignant disease
2 adverse event
1 death from nephrectomy
12 lost to follow-up within 6 months

277 allocated to control treatment
202 received control treatment and were analysed
55 did not receive control treatment
20 no primary renal-cell carcinoma
21 no renal-cell carcinoma of stage pT2–3b N0–3 M0
6 withdrew consent
2 metastasis
1 incorrect age
1 not radical nephrectomy
1 no information about tumour
2 other malignant disease
1 death from nephrectomy
20 lost to follow-up within 6 months

different variables on progression-free survival. Results of the quality of life analysis are given as means and SDs, with 0 being the worst and 100 being the best result. We tested differences between both groups with the Mann-Whitney U test. We analysed all data obtained up to February, 2003.

Role of the funding source
The sponsor of the study—LipoNova (Hannover, Germany)—was involved in development of the study design. Data collection, statistical analysis, and data interpretation were done by external experts. The authors wrote the report.

Results
Of 558 patients who were randomly allocated, five withdrew their written informed consent before surgery; no further data are available on these patients. The remaining 553 patients (276 in the vaccine group and 277 in the control group) are regarded as the safety population (figure 1). Of these patients, 174 were withdrawn because they did not fulfil postoperative inclusion criteria such as histologically proven renal-cell carcinoma, correct tumour stage, or ability to prepare a vaccine (figure 1). Thus, the intention-to-treat population consisted of 379 patients. Of these, 36 were withdrawn due to protocol violation. Therefore, the per-protocol population consisted of 343 patients. Both groups were comparable for variables such as sex, age, ECOG performance status, tumour diameter and location, T stage, lymph-node status (N stage), cell type, and Störkel score (table 1).[8] Here, we only give the results for the intention-to-treat population; however, those for the per-protocol population are closely similar.

At 5-year follow-up, the intention-to-treat population had hazard rates for the primary endpoint of 0·26 in the vaccine group and 0·39 in the control group, resulting in a hazard ratio of 1·58 (95% CI 1·05–2·37) in favour of the vaccine

group (p=0·0204, log-rank test). At 70-month follow-up, hazard rates were 0·33 in the vaccine group and 0·52 in the control group, resulting in a hazard ratio of 1·59 (1·07–2·36) in favour of the vaccine group (p=0·0204). In terms of progression-free survival, an absolute reduction of 12·7% and a relative reduction of 32·6% could be achieved, corresponding to a number of patients needed to treat of eight.

5-year progression-free survival rate for patients at all tumour stages was 77·4% in the vaccine group and 67·8% in the control group (p=0·0204), and 70-month progression-free survival rates were 72% in the vaccine group and 59·3% in the control group (figure 2). Median time to tumour progression was not reached in either group. The time until 25% of patients had progressed was 63·2 months (95% CI 44·9 to not reached) for patients in the vaccine group versus 42·1 months (27·3–58·9) for those in the control group (figure 2).

For patients with T2 tumours, 5-year progression-free survival rates were 81·3% in the vaccine group and 74·6% in the control group (p=0·216, log-rank test), and 70-month progression-free survival rates were 75·9% and 64·2%, respectively (figure 3). Median time to tumour progression was not reached in either group. The time until 25% of patients had progressed was not reached in the vaccine group compared with 58·9 months (95% CI 4·3 to not reached) for those in the control group (figure 3).

	Total (n=379)	Vaccine group (n=177)	Control group (n=202)
Men	246 (65%)	113 (64%)	133 (66%)
Patient age (median [IQR], years)	59 (53–64)	58 (53–64)	59 (53–64)
ECOG status			
0	321 (85%)	151 (85%)	170 (84%)
1	49 (13%)	23 (13%)	26 (13%)
2	7 (2%)	3 (2%)	4 (2%)
Unknown	2 (<1%)	0	2 (1%)
Tumour diameter and location			
Size (median [IQR], cm)	5·5 (4·5–7·7)	6 (4·5–8·0)	5·5 (4·5–7·0)
Right-sided tumours	191 (50%)	87 (49%)	104 (51%)
Left-sided tumours	182 (48%)	88 (50%)	94 (47%)
Bilateral tumours	1 (<1%)	0	1 (<1%)
Tumour stage (1993 classification)			
pT2	264 (70%)	119 (67%)	145 (72%)
pT3	115 (30%)	58 (33%)	57 (28%)
Tumour stage (2003 classification)			
pT1a	49 (13%)	18 (10%)	31 (15%)
pT1b	169 (45%)	84 (47%)	85 (42%)
T2	46 (12%)	17 (10%)	29 (14%)
T3	115 (30%)	58 (33%)	57 (28%)
Lymph-node status			
N0	363 (96%)	169 (95%)	194 (96%)
N1	4 (1%)	3 (2%)	1 (<1%)
N2	7 (2%)	3 (2%)	4 (2%)
Nx	5 (1%)	2 (1%)	3 (1%)
Cell type			
Clear cell renal-cell carcinoma	272 (72%)	134 (76%)	138 (68%)
Chromophobe renal-cell carcinoma	49 (13%)	18 (10%)	31 (15%)
Chromophil renal-cell carcinoma	44 (12%)	17 (10%)	27 (13%)
Other renal-cell carcinoma	14 (3%)	8 (4%)	6 (2%)
Störkel score			
Good prognosis	176 (46%)	72 (41%)	104 (51%)
Intermediate prognosis	194 (51%)	102 (58%)	92 (45%)
Poor prognosis	8 (2%)	3 (2%)	5 (2%)
Unknown	1 (<1%)	0	1 (<1%)

Data are number of patients (%) unless otherwise indicated.

Table 1: **Characteristics of 379 eligible patients (intention to treat)**
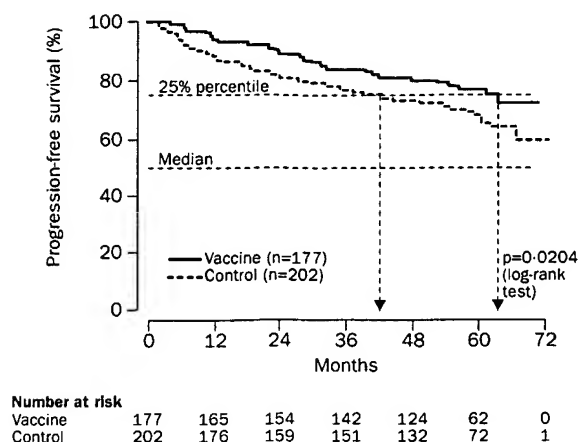
Figure 2: **Progression-free survival for all eligible patients (intention-to-treat population)**

5-year progression-free survival rates for patients with T3 tumours were 67·5% in the vaccine group and 49·7% in the control group (p=0·039, log-rank test); 70-month progression-free survival rates were 66·2% and 46·9%, respectively (figure 4). Median time to tumour progression was 51·5 months in the control group but was not reached in the vaccine group. The time until 25% of patients had progressed was 47·8 months (95% CI 21·8 to not reached) for those in the vaccine group compared with 13·5 months (95% CI 7·3–34·6) for those in the control group (figure 4).

11 patients had positive lymph nodes. Of six in the vaccine group, four had tumour progression. Of five individuals in the control group, two had tumour progression and one patient died. Progression-free survival rates were not calculated for these patients.

The effect of various covariates—vaccine, tumour stage, tumour size, tumour grade, Störkel score, tumour growth pattern, cell type, age, and sex—on progression-free survival was tested with the Cox proportional-hazards model. Table 2 shows the results of the univariate analysis. Because of high intercorrelation between the covariates tumour size, tumour grade, and Störkel score, multivariate analysis including all variables was not meaningful. Therefore, for two of these variables (Störkel score and tumour size), a multivariate analysis was done including treatment, sex, and age. Men were at higher risk than women, as were older
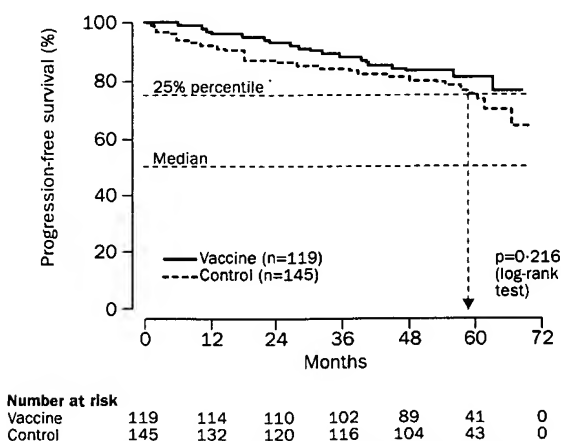
Figure 3: **Progression-free survival for eligible patients with T2 tumours (intention-to-treat population)**
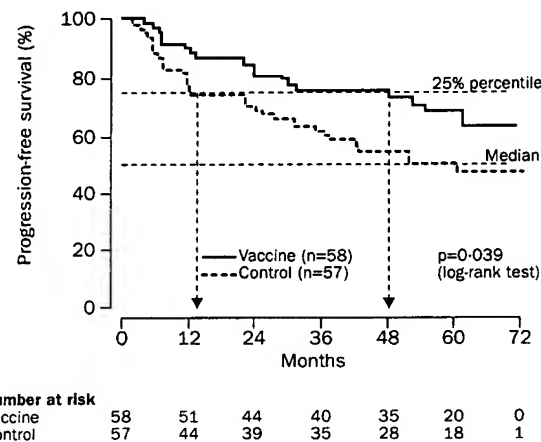
Figure 4: **Progression-free survival for eligible patients with T3 tumours (intention-to-treat population)**

patients (table 2). No significant effect was noted of the total number of cells, percentage of tumour cells, and number of vaccine doses on patients' outcome.

In the intention-to-treat population, 177 patients received a total of 1053 vaccine doses. 12 vaccine-related adverse events of mild to moderate severity were noted in two patients (table 3). The higher number of adverse events and serious adverse events in the control group can be accounted for by the higher number of patients with tumour progression in this group (table 3). Clinically relevant abnormalities in blood chemistry variables or vital signs were not recorded.

Global health status and quality of life (questions 29 and 30 of the QLQ-C30 questionnaire) results were closely similar between the vaccine and control groups before nephrectomy (mean 62·5 [SD 24·0] vs 58·8 [24·7], p=0·2278), at 6 months (69·7 [21·8] vs 69·7 [20·8], p=1·0), 24 months (73·1 [17·9] vs 73·4 [18·4], p=0·8857), 36 months (73 [18·2] vs 75·8 [13·9]), and 48 months (67·1 [27·6] vs 71·2 [19·5], p=0·5108) after nephrectomy. Detailed quality-of-life findings will be reported separately.

Discussion

We have shown that adjuvant treatment with an autologous renal tumour cell vaccine after radical nephrectomy reduces the risk of tumour progression compared with surgery alone in patients with renal-cell carcinoma.

	Hazard ratio (95% CI)	p
Univariate analysis		
Treatment with vaccine (yes vs no)	1·509 (1·02–2·24)	0·0407
Tumour stage (T2 vs T3)	2·164 (1·47–3·18)	<0·0001
Tumour size (1-cm steps)	1·186 (1·11–1·26)	<0·0001
Tumour grade (G1 vs G2 vs G3)	2·134 (1·53–2·98)	<0·0001
Störkel score (good vs intermediate vs poor)	2·529 (1·72–3·73)	<0·0001
Age (1-year steps)	1·043 (1·02–1·07)	0·0016
Sex (male vs female)	0·631 (0·41–0·97)	0·0351
Multivariate analysis (Störkel score)		
Störkel score (good vs intermediate vs poor)	2·510 (1·72–3·66)	<0·0001
Treatment with vaccine (yes vs no)	1·647 (1·11–2·45)	0·0138
Age (1-year steps)	1·036 (1·01–1·06)	0·0089
Sex (male vs female)	0·592 (0·39–0·91)	0·0165
Multivariate analysis (tumour size)		
Tumour size (1-cm steps)	1·200 (1·13–1·28)	<0·0001
Treatment with vaccine (yes vs no)	1·571 (1·06–2·33)	0·0253
Age (1-year steps)	1·041 (1·01–1·07)	0·0028
Sex (male vs female)	0·564 (0·37–0·87)	0·091

Table 2: **Cox proportional-hazards models**

	Total (n=553)	Vaccine group (n=276)	Control group (n=277)
Number of patients with adverse events (%)	233 (42%)	108 (39%)	125 (45%)
Number of patients with drug-related adverse events (%)	2 (<1%)	2 (1%)	0
Number of patients with serious adverse events (%)	154 (28%)	64 (23%)	90 (32%)
Number of adverse events	462	215	247
Number of drug-related adverse events	12	12	0
Number of serious adverse events	264	106	158
Adverse events by frequency			
Progression, surgical intervention	106 (19%)	45 (16%)	61 (22%)
General disorders	59 (11%)	33 (12%)	26 (9%)
Neoplasm	44 (8%)	13 (5%)	31 (11%)
Urinary-system disorders	28 (5%)	15 (5%)	13 (5%)
Gastrointestinal-system disorders	21 (4%)	10 (4%)	11 (4%)
Cardiovascular disorders	14 (3%)	5 (2%)	9 (3%)
Metabolic and nutritional disorders	15 (3%)	9 (3%)	6 (2%)
Musculoskeletal system disorders	15 (3%)	8 (3%)	7 (3%)

Table 3: **Adverse events in 553 patients (safety population)**

During the past century, many vaccines were developed to successfully combat devastating bacterial and viral diseases. In recent years, different vaccine approaches have been developed to treat malignant tumours in adjuvant, second-line, or third-line settings.[28] The main targets are tumour-specific cell epitopes to induce a tumour-specific T-cell response and other pathways of the immune system including natural killer cells. Tumour-specific antigens have been reported in some tumours like melanoma; however, in renal-cell carcinoma only few antigens are as yet known.[29]

In a randomised study by Galligioni and colleagues,[30] 120 patients underwent radical nephrectomy for renal-cell carcinoma stage pT1–3b pN0 or pN+; 60 of these received three adjuvant intradermal vaccinations with 10^7 irradiated tumour cells and the remaining 60 received no adjuvant treatment. For progression-free survival and 5-year overall survival no significant differences were reported between the groups. However, only 120 patients took part in the study, and the sample-size calculation was not given by these authors. This study cannot be compared with our trial since those researchers used a completely different vaccine with irradiated tumour cells that were also stimulated with BCG. Also, fewer applications of the vaccine were given, and there were shorter intervals between the applications, than in our study.

We chose progression-free survival as the primary endpoint because even with surgery for metastatic disease and modern immunotherapy with cytokines—eg, interferon alfa, interleukin 2, or both—survival for most patients is between 12 and 18 months, and fewer than 5% survive longer than 5 years. Furthermore, medical treatment for patients with progression from renal-cell carcinoma has potentially severe side-effects, with 30% of patients not finishing this kind of treatment because of associated toxic effects. Also, nowadays, many patients with metastasis from this cancer will enter clinical trials with several combinations of therapeutic approaches, with a variable effect on individual prognosis. For these reasons, benefit from an adjuvant treatment delaying or preventing progression can be anticipated in patients with renal-cell carcinoma. Therefore, we did not use overall survival as the primary endpoint. Furthermore, our approach has shown only few toxic effects and no negative effect on quality of life versus the control group.

In our trial, all patients were randomly allocated before radical nephrectomy. Therefore, many participants had to be excluded according to histological and postoperative staging results—which showed no renal-cell carcinoma at all, or no cancers of stage T2–T3 N0–3 M0, in 56 of 99 patients in the vaccine group and 43 of 75 in the control group—and for other reasons. This trial design

was chosen to reduce the risk of patient selection bias for the study with respect to postoperative information. All demographic data, including Störkel score, were comparable between both groups in the intention-to-treat analysis. At the time our trial was designed no test for monitoring the immune response was available in a standardised and generally accepted way. Findings of a few studies have suggested that delayed type hypersensitivity might correlate with in-vitro proliferation assays and clinical outcome. However, the fact that this response might not entirely be antigen-specific and other components of the vaccine may contribute to the response—and the fact that delayed type hypersensitivity response is not standardised to compare across studies—limits use of this test.[31] Although some researchers have reported a correlation between delayed type hypersensitivity and tumour response to vaccination in patients with melanoma or colon cancer, Galligioni and colleagues[30] could not show such correlation in patients with renal-cell carcinoma. Therefore, we decided not to use a surrogate variable for monitoring of the immune response in our trial.

Patients with risk factors for tumour progression such as large tumour size, high tumour grade, and high Störkel score had an even greater benefit from adjuvant treatment compared with the entire trial group (data not shown). It is noteworthy that only 12 side-effects from the vaccine were recorded. Also, no differences were noted between both groups in terms of global health status and general quality of life.

We included all patients with renal-cell carcinoma of stage pT2–3b pN0–3 M0, according to the 1993 UICC classification. Since our trial began, this classification has been changed twice. The most important difference is the extension of the upper limit for T1 tumours from 2·5 cm to 7 cm (1997 classification). In the 2003 classification, pT1 tumours are subdivided into pT1a (<4 cm) and pT1b (4–7 cm). We therefore treated patients who would nowadays be classified as renal-cell carcinoma stage pT1a or pT1b.

According to our results, application of an autologous renal tumour cell vaccine can be considered in patients undergoing radical nephrectomy due to organ-confined renal-cell carcinoma of more than 2·5 cm in diameter.

References

1 Figlin RA. Renal cell carcinoma: management of advanced disease.
J Urol 1999; 161: 381–87.

2 Jemal A, Murray T, Samuels A, Ghafoor A, Ward E, Thun MJ.
Cancer statistics, 2003. *CA Cancer J Clin* 2003; 53: 5–26.

3 Spiessl B, Beahrs OH, Hermanek P, et al. TNM atlas: Illustrierter
Leitfaden zur TNMpTNM-Klassifikation maligner Tumoren.
New York: Springer-Verlag, 1993.

4 Dal Bianco M, Arbitani W, Bassi PF, Pescatori E, Pagano F.
Prognostic factors in renal cell carcinoma. *Eur Urol* 1988; 15: 73–76.

5 Dinney CP, Awad SA, Gajewski JB, et al. Analysis of imaging
modalities, staging systems, and prognostic indicators for renal cell
carcinoma. *Urology* 1992; 39: 122–29.

6 Giuliani L, Gilberti C, Martorana G, Rovida S. Radical extensive
surgery for renal cell carcinoma: long-term results and prognostic factors.
J Urol 1990; 143: 468–74.

7 Hermanek P, Schrott KM. Evaluation of the new tumor, nodes and
metastases classification of renal carcinoma. *J Urol* 1990; 144:
238–42.

8 Störkel S, Thoenes W, Jacobi GH, Lippold R. Prognostic parameters in
renal cell carcinoma: a new approach. *Eur Urol* 1989; 16: 416–22.

9 Zisman A, Pantuck AJ, Wieder J, et al. Risk group assessment and
clinical outcome algorithm to predict the natural history of patients with
surgically resected renal cell carcinoma. *J Clin Oncol* 2002; 20: 4559–66.

10 Motzer RJ, Russo P. Systemic therapy for renal cell carcinoma.
J Urol 2000; 163: 408–17.

11 Kjaer M, Frederiksen PL, Engelholm SA. Postoperative radiotherapy in
stage II and III renal adenocarcinoma: a randomized trial by the
Copenhagen renal cancer study group. *Int J Radiat Oncol Biol Physiol*
1987; 13: 665–72.

12 Pizzocaro G, Piva L, Di Fronzo G, et al. Adjuvant medroxyprogesterone
acetate to radical nephrectomy in renal cancer: 5-year results of a
prospective randomized study. *J Urol* 1987; 138: 1379–81.

13 Pizzocaro G, Piva L, Colavita M, et al. Interferon adjuvant to radical
nephrectomy in Robson stages II and III renal cell carcinoma:
a multicentric randomized study. *J Clin Oncol* 2001; 19: 425–31.

14 Messing EM, Manola J, Wilding G, et al. Phase III study of Interferon
alfa-NL as adjuvant treatment for resectable renal cell carcinoma: an
Eastern Cooperative Oncology Group/Intergroup Trial. *J Clin Oncol*
2003; 21: 1214–22.

15 Clark JI, Atkins MB, Urba WJ, et al. Adjuvant high-dose bolus
interleukin-2 for patients with high-risk renal cell carcinoma: a cytokine
working group randomized trial. *J Clin Oncol* 2003; 21: 3133–40.

16 Repmann R, Wagner S, Richter A. Adjuvant therapy of renal cell
carcinoma with active-specific-immunotherapy (ASI) using autologous
tumor vaccine. *Anticancer Res* 1997; 17: 2879–82.

17 Repmann R, Goldschmidt AJ, Richter A. Adjuvant therapy of renal cell
carcinoma patients with an autologous tumor cell lysate vaccine: a 5-year
follow-up analysis. *Anticancer Res* 2003; 23: 969–74.

18 Doehn Ch, Richter A, Lehmacher W, Jocham D. Adjuvant autologous
tumour cell-lysate vaccine versus no adjuvant treatment in patients with
M0 renal cell carcinoma after radical nephrectomy: 3-year interim
analysis of a German multicentre phase-III study. *Folia Biol (Praha)*
2003; 49: 69–73.

19 Gastl G, Ebert T, Finstad CL, et al. Major histocompatibility complex
class I and class II expression in renal cell carcinoma and modulation by
interferon gamma. *J Urol* 1996; 155: 361–67.

20 Hillman GG, Puri RK, Kukuruga MA, Pontes JE, Haas GP. Growth
and major histocompatibility antigen expression regulation by IL-4,
interferon-gamma (IFN-gamma) and tumour necrosis factor-alpha
(TNF-alpha) on human renal cell carcinoma. *Clin Exp Immunol* 1994;
96: 476–83.

21 Angus R, Collins CM, Symes MO. The effect of alpha and gamma
interferon on cell growth and histocompatibility antigen expression by
human renal carcinoma cells in vitro. *Eur J Cancer* 1993; 29A: 1879–85.

22 Hansen AB, Lillewang ST, Andersen CB. Stimulation of intercellular
adhesion molecule-1 (ICAM-1) antigen expression and shedding by
interferon-gamma and phorbol ester in human renal carcinoma cell
cultures: relation to peripheral blood mononuclear cell adhesion.
Urol Res 1994; 22: 85–91.

23 Santarosa M, Favaro D, Quaia M, et al. Expression and release of
intercellular adhesion molecule-1 in renal-cancer patients. *Int J Cancer*
1995; 62: 271–75.

24 Tanabe K, Campbell SC, Alexander JP, et al. Molecular regulation of
intracellular adhesion molecule 1 (ICAM-1) expression in renal cell
carcinoma. *Urol Res* 1997; 25: 231–38.

25 Seliger B, Hammers S, Hohne A, et al. IFN-gamma-mediated
coordinated transcriptional regulation of the human TAP-1 and
LMP-2 genes in human renal cell carcinoma. *Clin Cancer Res* 1997; 3:
573–78.

26 Elmadfa I, Wagner KH. Non-nutritive bioactive food constituents of
plants: Tocopherols (vitamin E). *Int J Vitam Nutr Res* 2003; 73: 89–94.

27 Aaronson NK, Ahmedzai S, Bergmann B, Bullinger M. The European
Organization for Research and Treatment of Cancer QLQ-C30: a
quality of life instrument for use in international clinical trials in
oncology. *J Natl Cancer Inst* 1993; 85: 368–73.

28 Armstrong AC, Hawkins RE. Vaccines in oncology: background and
clinical potential. *Br J Radiol* 2001; 74: 991–1002.

29 Michael A, Pandha HS. Renal-cell carcinoma: tumour markers, T-cell
epitopes, and potential for new therapies. *Lancet Oncol* 2002; 4: 215–23.

30 Galligioni E, Quaia M, Merlo A, et al. Adjuvant immunotherapy
treatment of renal carcinoma patients with autologous tumor cells and
bacillus Calmette-Guerin: five-year results of a prospective randomized
study. *Cancer* 1996; 77: 2560–66.

31 Morse MA, Clay TM, Hobeika AC, Mosca PJ, Lyerly HK. Surrogate
markers of response to cancer immunotherapy. *Expert Opin Biol Ther*
2001; 1: 153–58.

A liposomal MUC1 vaccine for treatment of non-small cell lung cancer (NSCLC); updated survival results from patients with stage IIIB disease
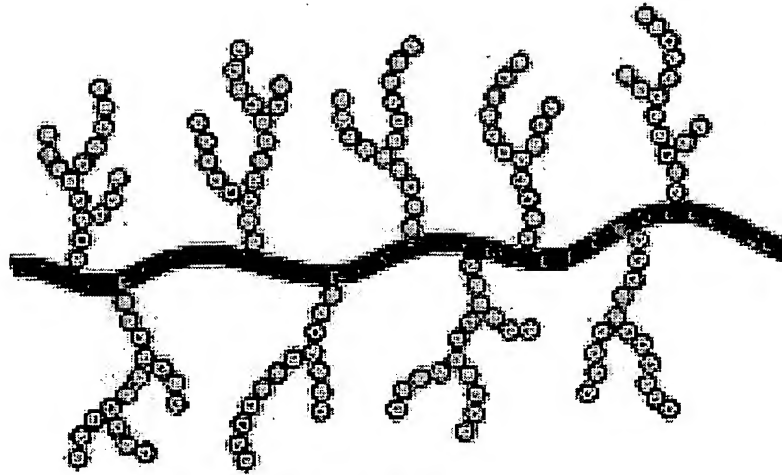
Abstract No: 7037

Author(s): N. Murray, C. Butts, A. Maksymiuk, E. Marshall, G. Goss, D. Soulieres, L-BLP25 Non-Small Cell Lung Cancer Study Group

Abstract: **Background**: The primary analysis results from a randomized, open label phase IIb trial utilizing L-BLP25 (BLP25 Liposome Vaccine) for the immunotherapy of stage IIIB and IV NSCLC patients with stable or responding disease following any first line chemotherapy were reported in April 2004. Patients were randomized 1:1 to best supportive care (BSC) or BSC + L-BLP25 (TX), with survival as the primary endpoint. Treatment arm patients received a single intravenous dose of 300mg/m^2 cyclophosphamide, followed by 8 weekly subcutaneous immunizations with L-BLP25. Maintenance immunizations are then given at 6-week intervals. At primary analysis, the median survival of TX patients in the pre-stratified stage IIIB locoregional (LR) disease subset, had not yet been reached. **Methods:** Updated survival information was obtained as part of a protocol specified follow-up period at two years after enrollment of the last patient. Survival was calculated from the date of randomization into the trial, to the date of death or last contact. **Results:** Of 171 patients enrolled, 65 had IIIB LR disease. Of these, 35 were randomized to TX, and 30 to BSC. The IIIB LR subgroup was well balanced in terms of age and ethnicity. More female and ECOG 0 patients were randomized to TX than BSC (51.4 versus 36.7%, and 40.0 versus 26.7%), and more patients in the TX arm received radiotherapy in addition to . chemotherapy, for cancer treatment prior to trial enrollment (91.4 versus 76.7%). The current median number of vaccinations received by TX patients is 17, with a maximum of 41. Mild injection site reactions occurred in 54.3% of patients. There were no major toxicities. To date, a survival median for TX patients has not yet been reached (54% alive at >24 months). **Conclusion**: A clinically meaningful survival advantage appears likely for patients with stage IIIB NSCLC treated with L-BLP25. Further development of the vaccine is warranted.

Treatment Arm	L-BLP25 + BSC	BSC	Cox p value	Hazard Ratio (95% CI)
Median survival (months)	not reached	13.3	0.0924	0.5652 (0.2908, 1.0985)

A Liposomal MUC1 Vaccine for Treatment of Non–Small Cell Lung Cancer (NSCLC); Updated Survival Results from Patients with Stage IIIB Disease

Nevin Murray, Charles Butts, Andrew Maksymink,

Ernie Marshall, Glenwood Goss, Denis Soulières
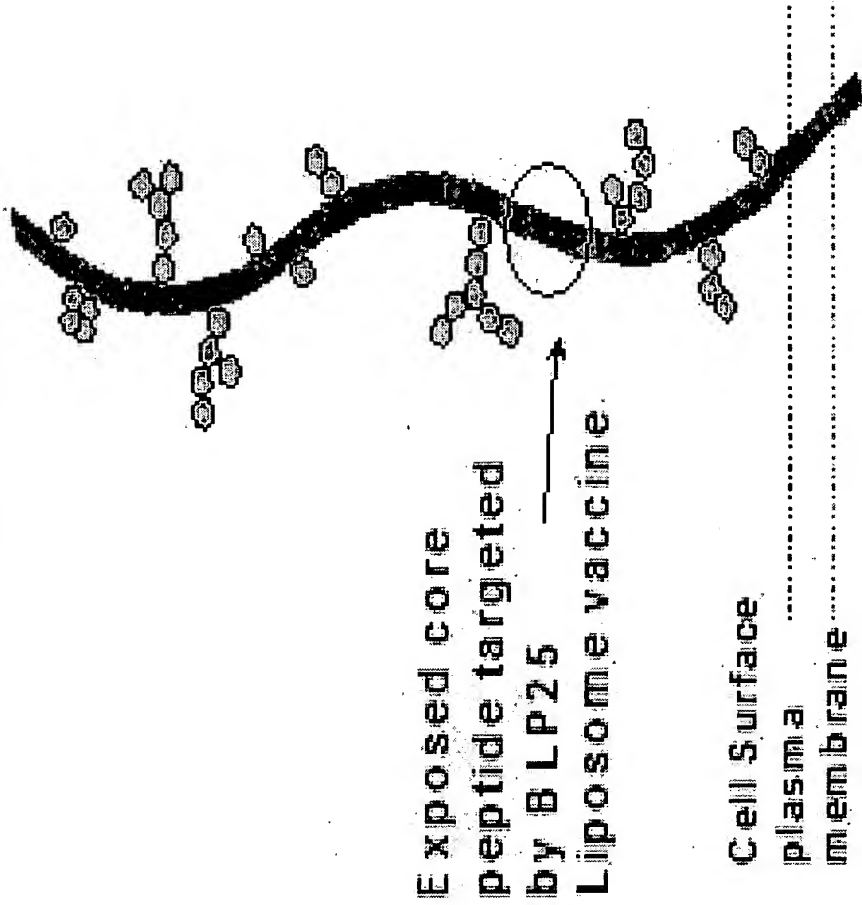
Advanced Non–Small Cell Lung Cancer (NSCLC)

- Prognosis for patients with advanced NSCLC poor

- Platin-based chemotherapy results in modest improvements in survival and QoL

- Addition of maintenance chemotherapy or targeted therapies (EGFR-TKIs, Herceptin®, MMPIs) failed to improve outcomes

- Great need for new, less toxic treatment options that add to current standards

Cancer-Associated Mucins

Normal MUC1 Mucin

MUC1 Cancer Mucin

Exposed core
peptide targeted
by BLP25
Liposome vaccine.

Cell Surface
plasma
membrane

B25-LG-304

```
Stage IIIB/IV
NSCLC
Response or SD
to 1st-line Therapy
```

→

```
R
A
N
D
O
M
I
Z
E
```

→ L-BLP25 +
Best Supportive
Care

→ Best Supportive
Care
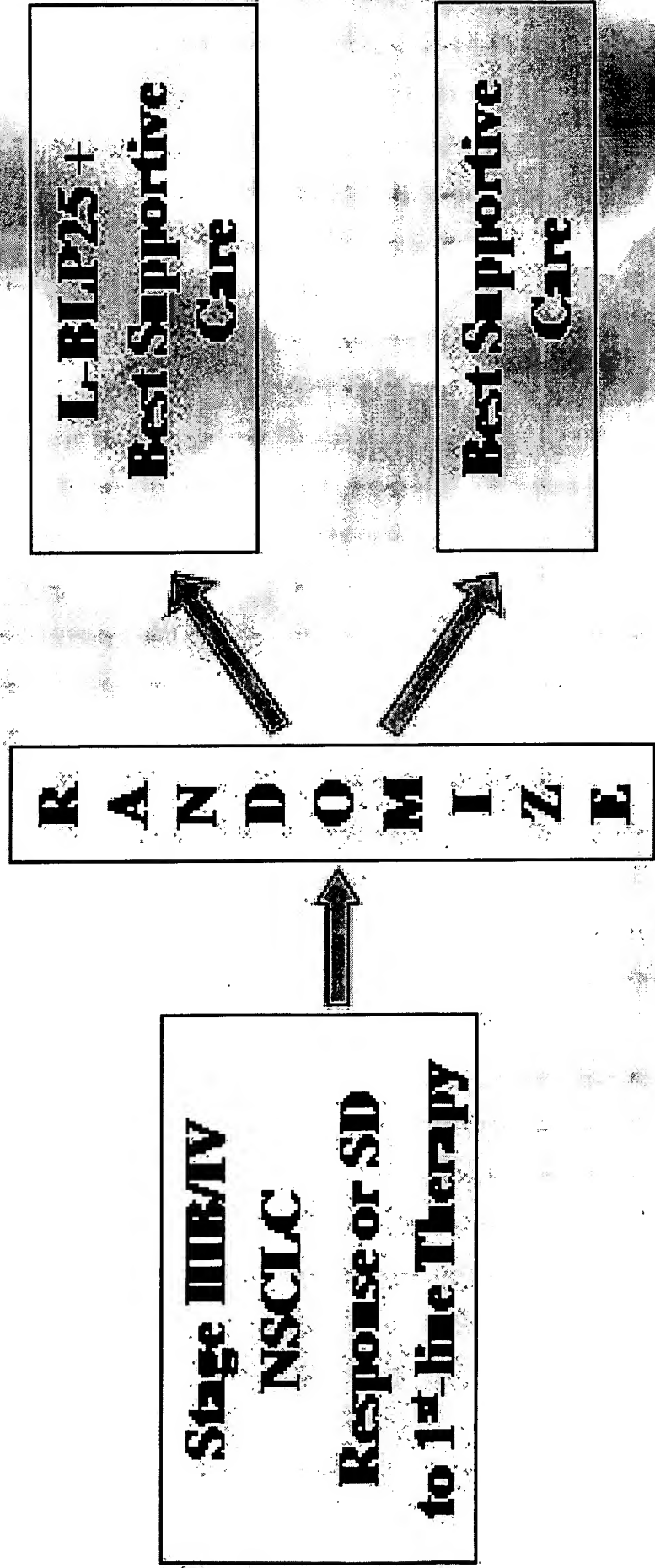
B25-LG-304 Objectives

- **Primary:**

  1. Efficacy- Survival

  2. Safety of L-BLP25

- **Secondary:**

  1. Health-related quality of life (HRQoL)
     - Assessed by FACT-L

  2. Immune response elicited by L-BLP25
     - Assessed by MUC1 proliferative T-cell response

Note: Tumor responses were not expected and therefore was not assessed

B25-LG-304 Study Design

Survival Assessments

1. Cox Proportional Hazard Regression model generating
   - Hazard Ratio; 95% CI; *P*-value
2. Kaplan-Meier survival estimate

Study Assumptions

1. Median Survival
   - BSC arm- 7 months
   - L-BLP25 + BSC arm- 12 months
2. 108 deaths required for 80% power
   - 150 patients required

B25-LG-304 Treatment and Evaluation Schematic
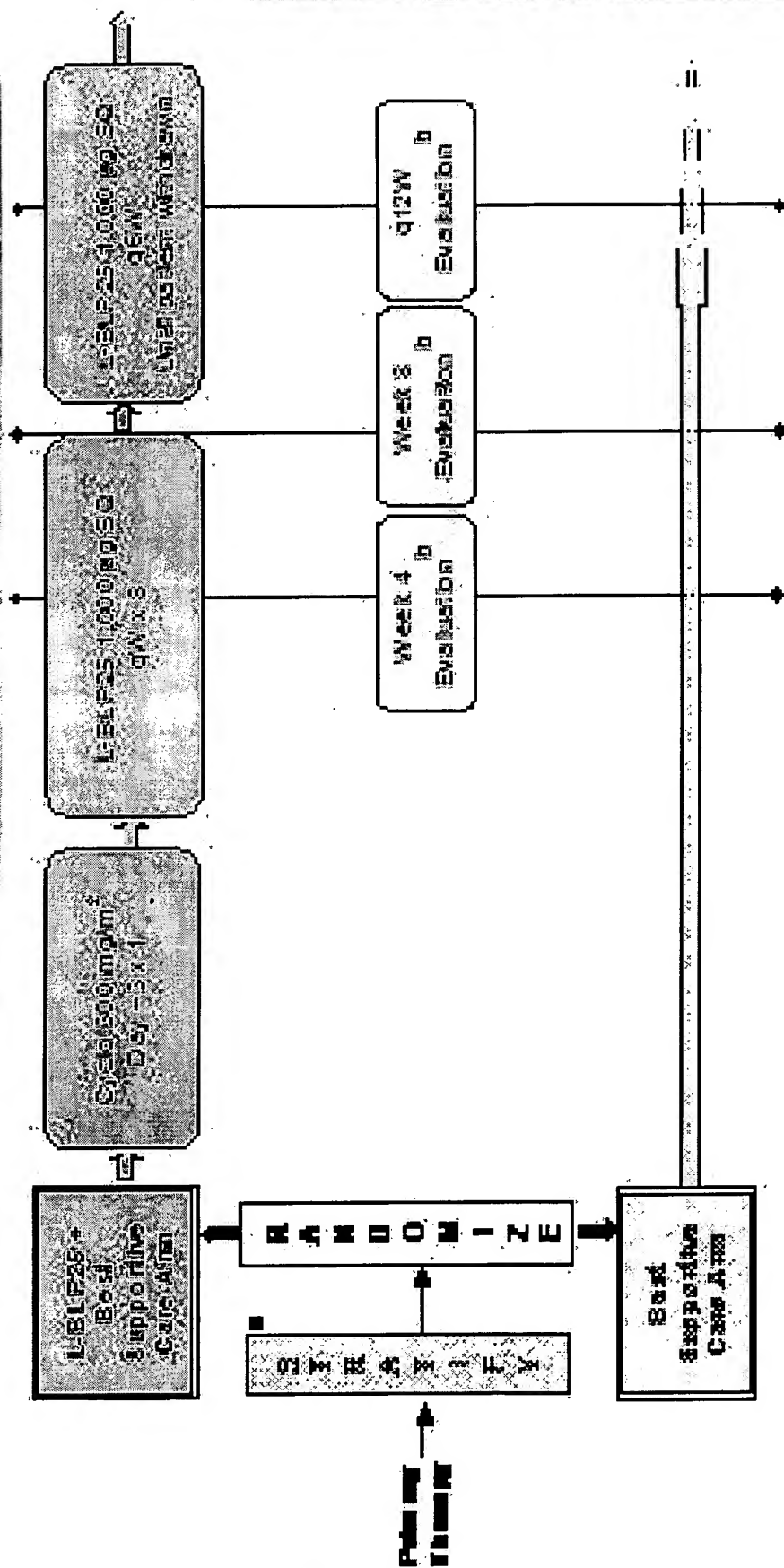
B25-LG-304

Chi-Square Test of Radiotherapy Dosage, by Treatment Arm Stage IIB Longitudinal Population (n=65)

Treatment Group by RT			
RT (Gy)			
Treatment Group	Population (< or = Gy)	Duration	Total
Control			
BL/Pbo			
Total			

Type of RT received in induction = 37

No RT = 28

B25-LG-304 Summary

Stage IIIB LR Survival

- Longer survival for L-BLP25+BSC arm vs BSC arm

  Median not reached vs 13.3 months

  — *Adjusted** HR: 0.565, *P*=0.0924

  — 2-year survival: 60.0% vs 36.7%

*Response to first line treatment

Meeting: 2003 ASCO Annual Meeting
Category: Developmental Therapeutics - Immunotherapy
SubCategory: Vaccines

🖨 Printer Friendly

📖 Bookmark

Clinical trials of a peptide based vaccine targeting telomerase

Abstract No: 666

Author(s):   G. Gaudernack, T. Buanes, M. Meo, S. Aamdal, P. Brunsvig, L. R. Braathen, K. Kernland, M. K. Gjertsen, J. A. Eriksen, M. Moller; Section for Immunotherapy, The Norwegian Radium Hospital, Oslo, Norway; Department of Surgery Ullevaal University Hospital, Oslo, Norway; Department of Clinical Cancer Research, The Norwegian Radium Hospital, Oslo, Norway; Department of Medical Oncology, The Norwegian Radium Hospital, Oslo, Norway; Dermatologische Klinik, Inselspital, Bern, Switzerland; GemVax, Oslo, Norway

Abstract: The reverse transcriptase subunit of human telomerase (hTERT) is a tumor associated antigen expressed in almost all tumors. By re-expressing hTERT, tumor cells escape cellular senescence to become immortal. This makes hTERT uniquely attractive as a target candidate for cancer vaccines. We have identified several new epitopes in hTERT, and designed vaccines aimed at generating both CD4+ and CD8+ tumor-reactive T cells. The present studies were performed to determine safety and immunogenicity of such dual specific peptide vaccines in patients with different types of cancer and to correlate immune responses with the clinical responses observed. In a single center dose escalation study, 47 patients with newly diagnosed, histologically confirmed, non-resectable pancreatic cancer were included. None of the patients received prior or concomitant chemotherapy. The peptide was injected intradermally 8 times over a period of 10 weeks. Selected patients received monthly booster vaccinations thereafter. The vaccine was tested in 3 dose levels, using GM-CSF as an adjuvant. Based on the safety data from this study, two parallel studies were performed in 10 patients with malignant melanoma and 20 with non small cell lung cancer. A total of 505 vaccine injections (up to 18 injections in one patient) were given to 77 patient and no serious adverse events related to the treatment were observed. Specific immune responses measured as DTH and in vitro could be induced in a dose dependent fashion. CTL's specific for several epitopes and Th cells restricted by HLA-DR, -DP and -DQ were obtained from vaccinated patients. In one patient cloned T cells were shown to recognize autologous targets in short term primary cultures from ascites fluid. In the pancreas cancer study which started September 2000, a strong correlation between vaccine dose, number of responders and survival

was observed. In the group of patients who received the low dose 3/10 patients responded compared to 13/17 patients at the intermediate dose level. Median survival of the two groups were 3,5 months vs. 9,8 months. These results demonstrate that immunity to hTERT can be generated safely and effectively in patients and encourage further trials.

# Clinical trials of a peptide based vaccine targeting telomerase

Gaudernack G, Buanes T, Meo AM, Aamdal S, Brunsvig P, Braathen L, Kernland K, Kvalheim G, Markowski-Grimsrud, CJ, Gjertsen MK, Eriksen JA and Møller M
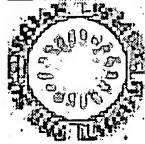
Cancer vaccine: Telomerase = universal tumor antigen?

- Telomere length is maintained by the Telomerase enzyme in germline

- Most somatic cells are telomerase negative, chromosomes are shortened for each cell division $\Rightarrow$ cellular senescence

- Immortalization of somatic cells requires reactivation of telomerase (hTERT) activity:
  - tumors: <90%
  - cell lines: ~100%
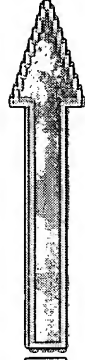 - frequent gene amplification of hTERT locus $\Rightarrow$ increased expression
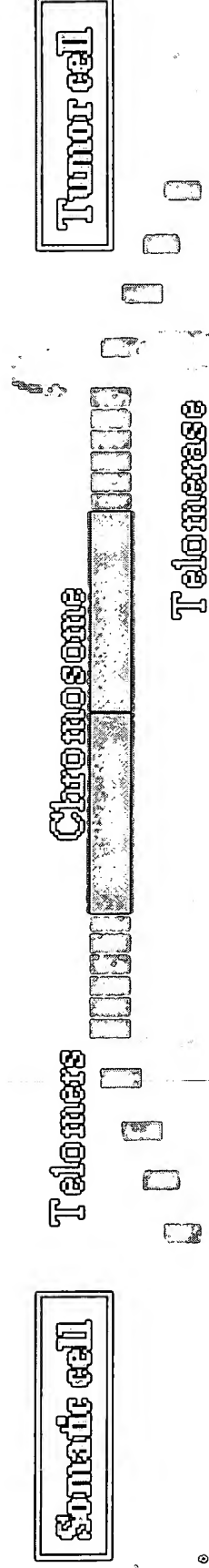
Somatic cell

Telomers   Chromosome   Telomerase

Tumor cell
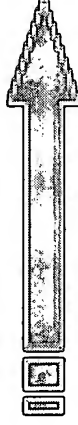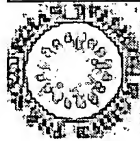
Telomerase

GemVax: Ongoing and finished clinical trials of telomerase vaccines, phase I/II

Study	Indication (No. of patients treated)	Institutions
CTN Telomerase 1/2000	Non-resectable pancreatic cancer (10 + 17 + 20)	Ullevål University Hospital and The Norwegian Radium Hospital
hTERT-101	Malignant melanoma (10)	Dermatologische Klinik Inselspital Bern, Switzerland
CTN ras/telomerase 2/2000	Non-resectable pancreatic cancer (9)	Ullevål University Hospital and The Norwegian Radium Hospital
CTN telomerase 3/2000	Non-small cell lung cancer (25)	The Norwegian Radium Hospital

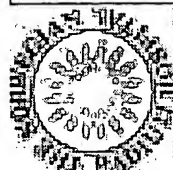# Summary of safety data: all trials

- No evidence of serious adverse effects observed in 85 patients at 3 dose levels

- Immune response correlates with increased survival

- No evidence of effect on BM stem cells

- No evidence of autoimmune disease in long term survivors (>1 year) with immune response who receive monthly booster vaccines
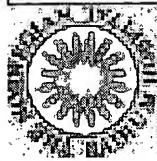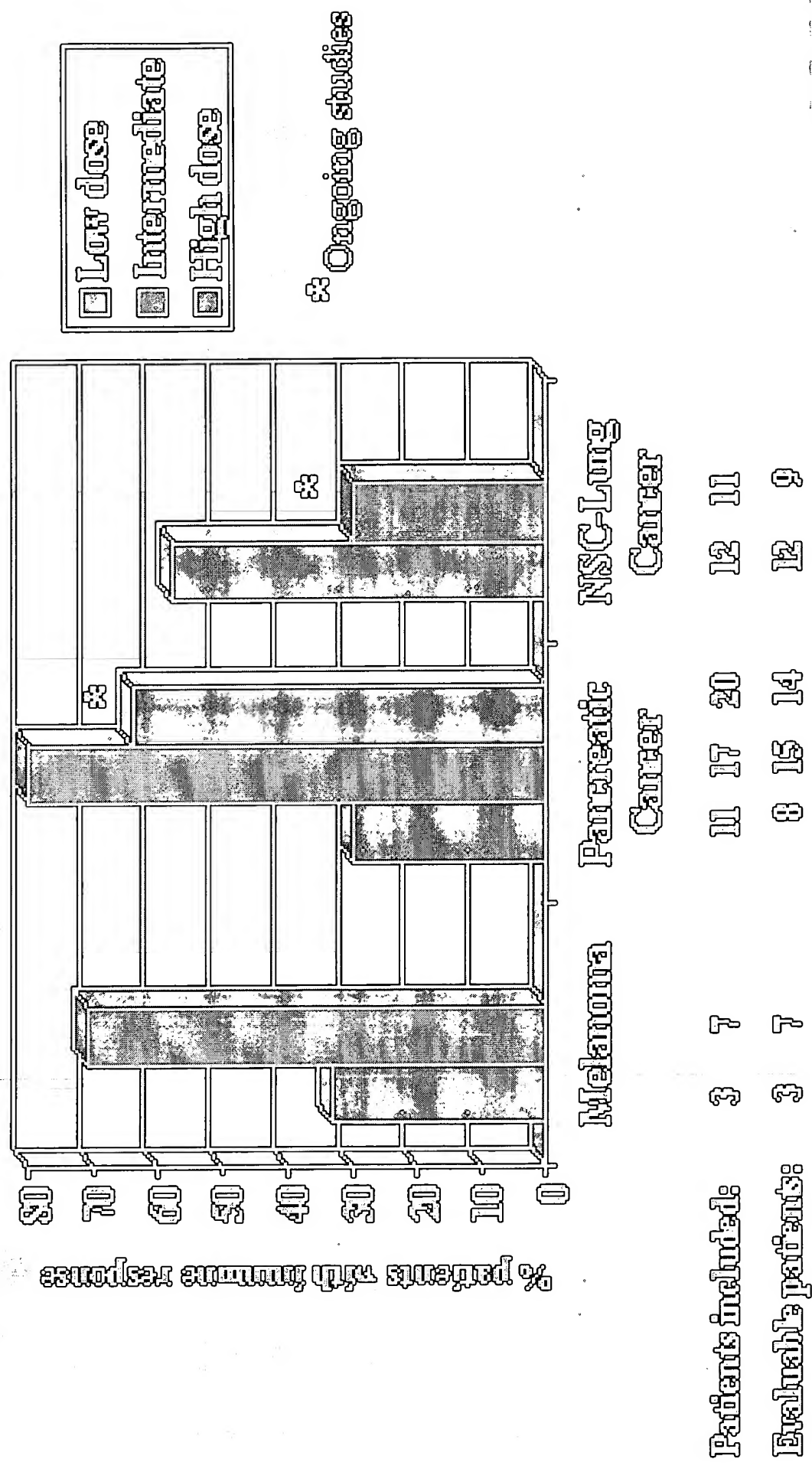
Telomerase 3/200 (NSCLC) Safety:
Progenitor cell activity in BM samples

Patient	CFU-gm/ 1000cells before	CFU-gm/ 1000cells after	CFU-e/ 1000cells before	CFU-e/ 1000cells after	LTC-IC/ 100000cell before	LTC-IC/ 100000cell after
704	4.0	3.5	7.6	7.6	4.8	4.6
708	3.9	1.6	4.7	4.2	4.3	3.4
711	2.1	2.0	2.6	2.8	0.6	0.6
712	2.6	1.9	3.5	2.9	5.1	6.3

BM samples taken 4 mo apart from patients with immune response against the vaccine

Summary immune response:
ASO 50 vaccine doses in 78 patients

Legend: ☐ Low dose ▨ Intermediate ▦ High dose ✲ Ongoing studies

% patients with immune response

y-axis: 80 75 60 45 50 45 30 20 10 0

	Melanoma		Pancreatic Cancer			NSC-Lung Cancer	
Patients included:	3	7	11	17	20	12	11
Evaluable patients:	3	7	8	15	14	12	9

GERVAX

AG 89
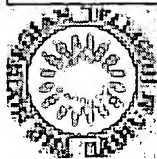
GV1001 vaccination of patients with advanced pancreatic cancer - survival of evaluable patients

percent survival

Log-rank test: P=0.0076

days from start of vaccination

0 25 50 75 100 125 150 175 200 225 250 275 300 325 350 375 400 425 450 475 500

100 90 80 70 60 50 40 30 20 10 0
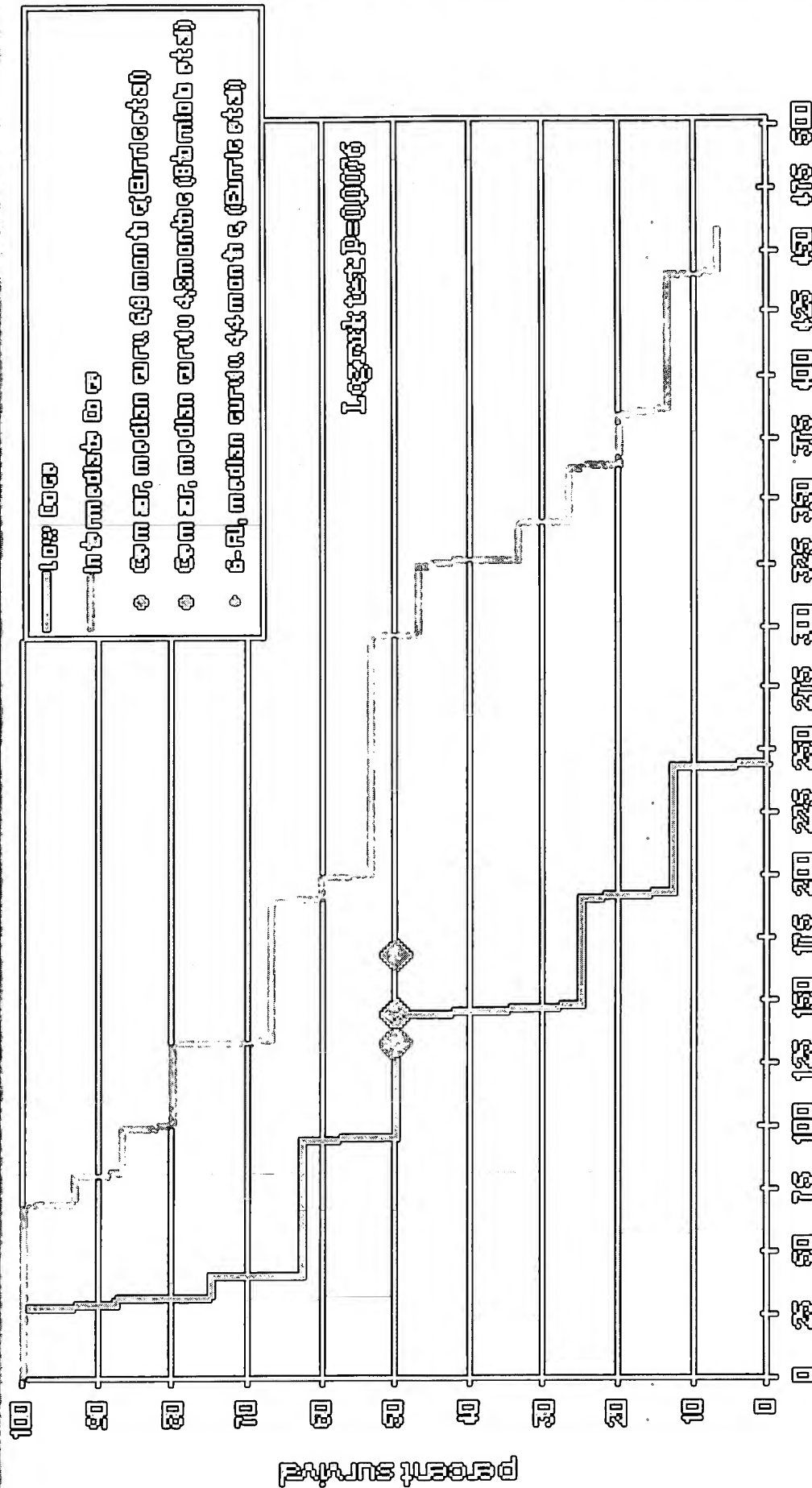
GV1001 – survival of patients with advanced pancreatic cancer vaccinated with intermediate dose

percent survival

days from start of vaccination

0 25 50 75 100 125 150 175 200 225 250 275 300 325 350 375 400 425 450 475 500

Immune Responders (n=13)
Non Responders (n=9)
Censor, median surv 8.9 months (Imm total)
Censor, median surv 4.3 months (Nonimm total)
S-RU median surv 4.4 months (Imm total)
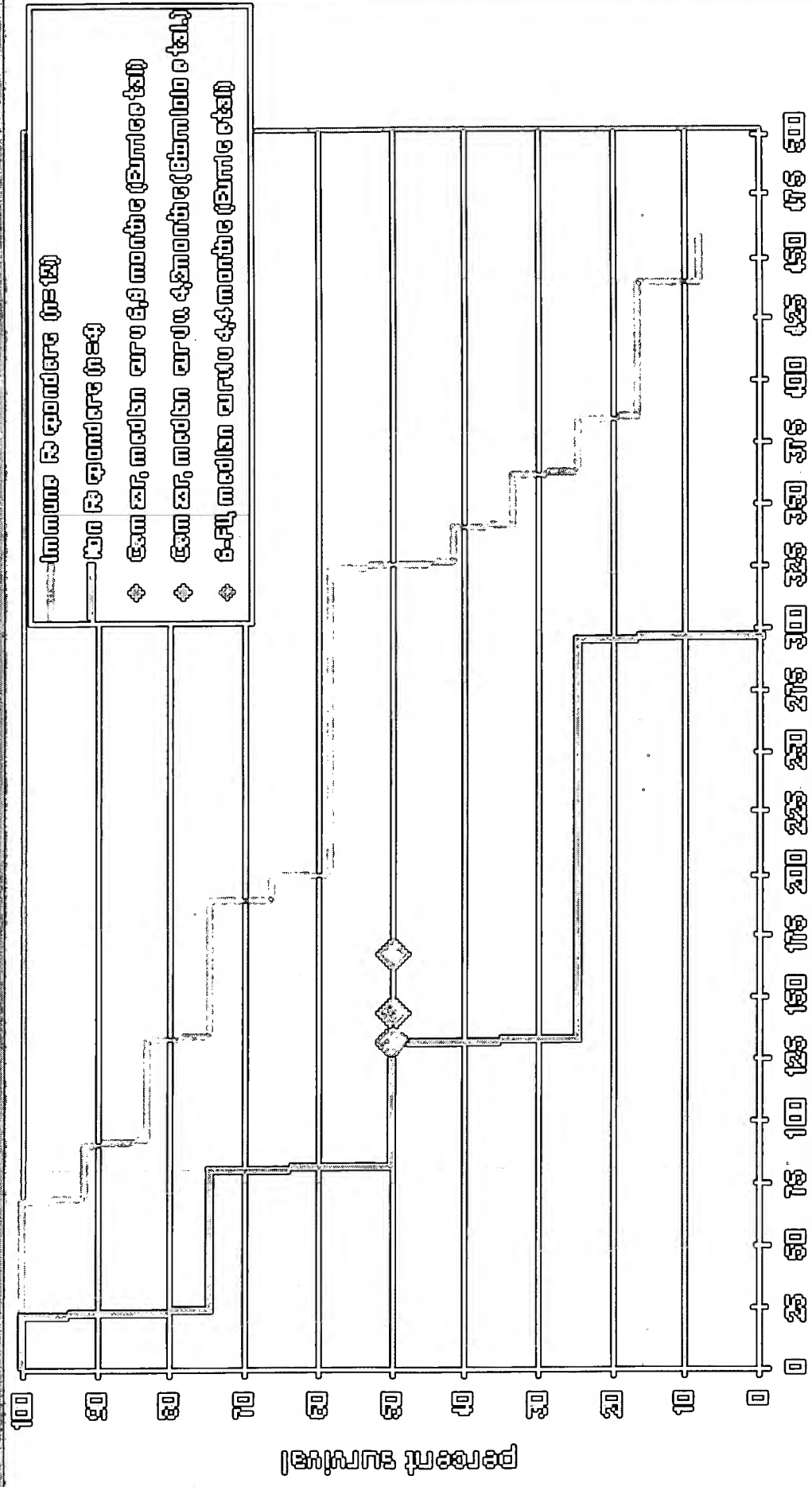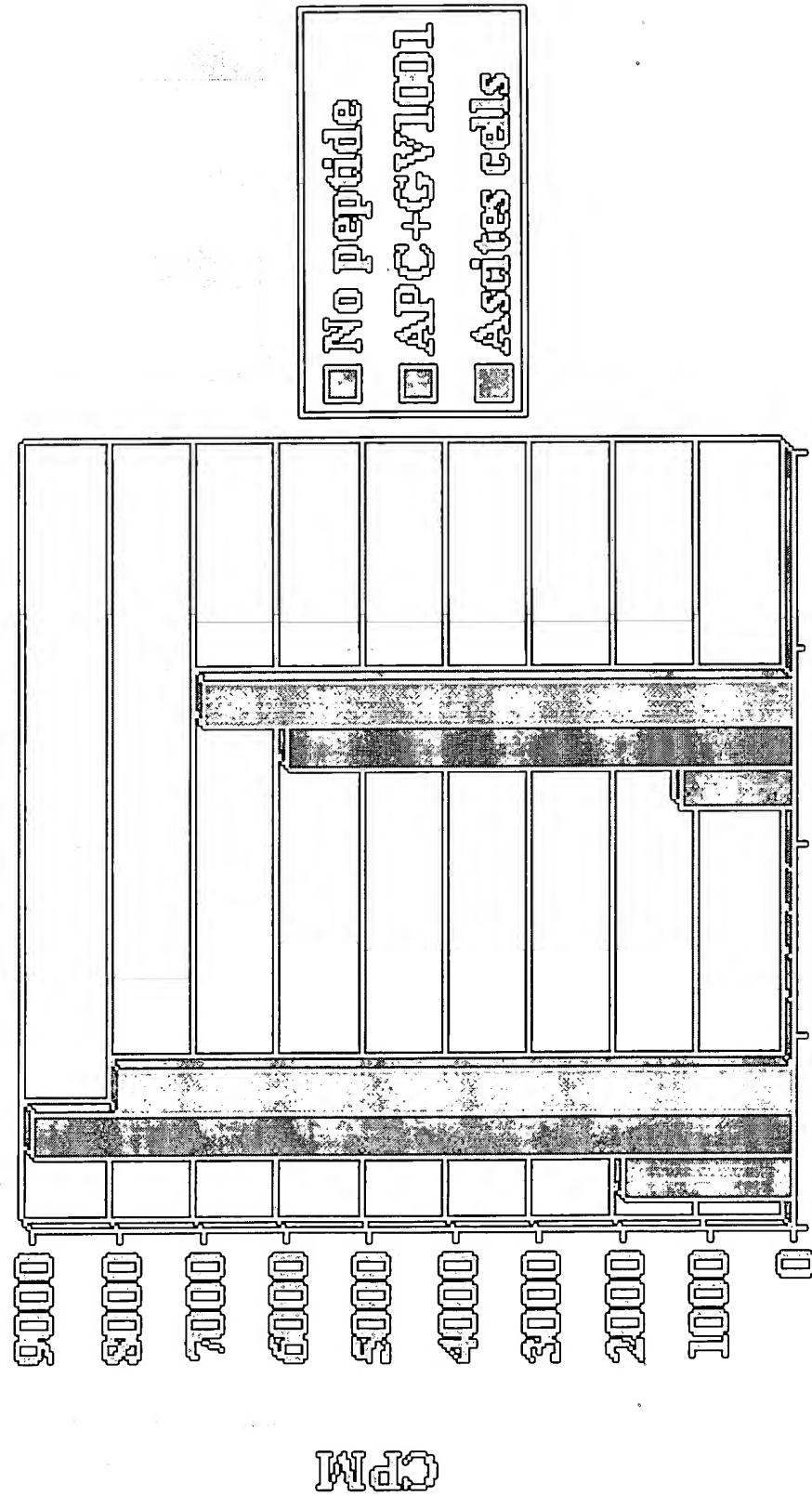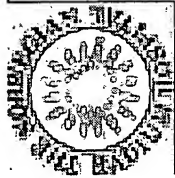
Recognition of autologous ascites cells by CD4+ T cell clones derived from pancreas cancer patient vaccinated with GV1001

Clone:#49 (HLA-DP*0401) #25 (HLA-DQ*0601) (HLA-DP*0401) (HLA-DQ*0601)

Legend:
- No peptide
- APC+GV1001
- Ascites cells

Y-axis: CPM
Y-axis values: 0, 1000, 2000, 3000, 4000, 5000, 6000, 7000, 8000, 9000

CTL clone TRM76 specific for a GV1001 fragment

Patient #11 NSCLC protocol (CTN3/2000)

Legend: P601, P613, P614, P615

GV1001: EARNLLLSRPGGK
RH: EARNLLLS
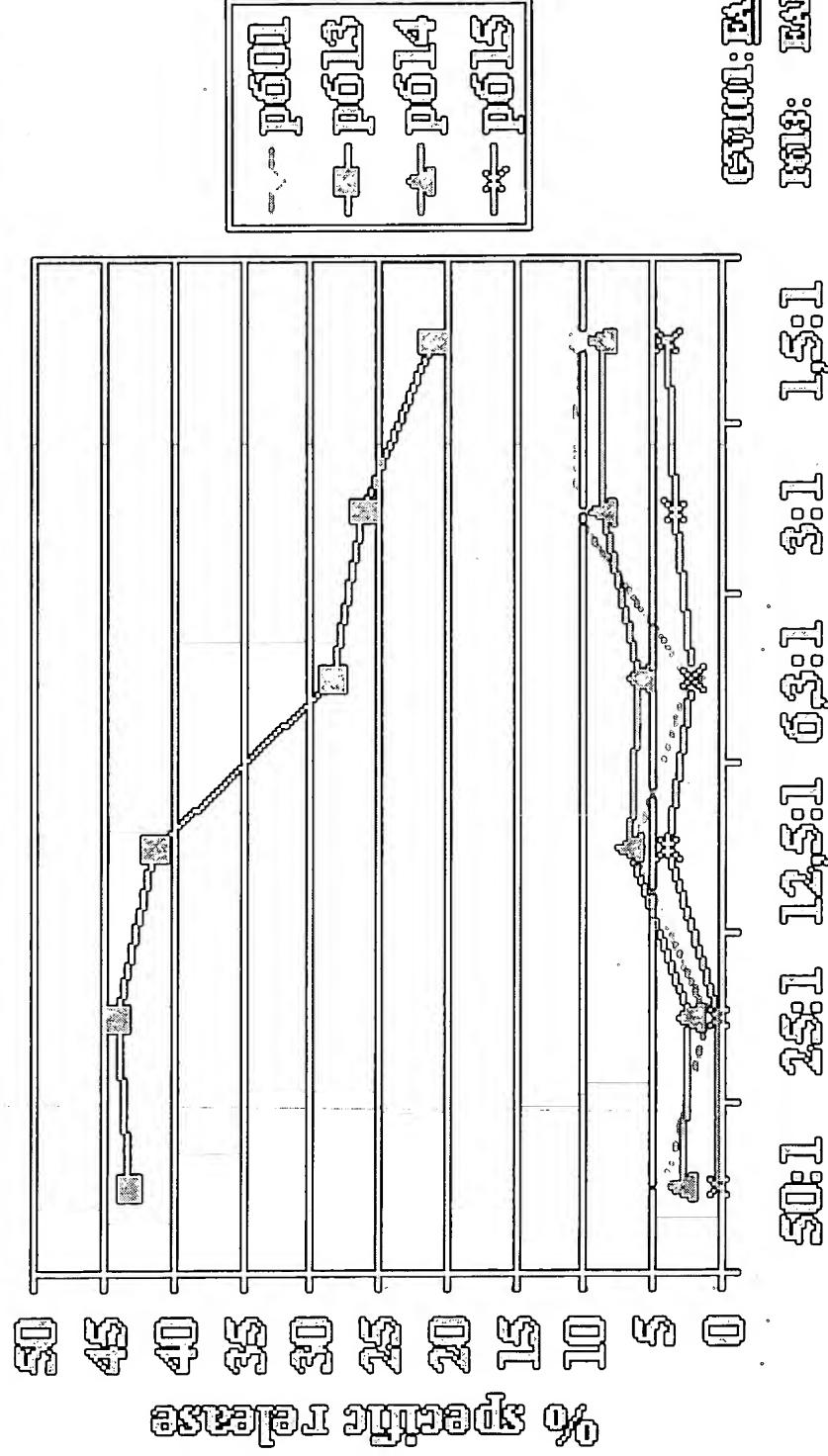
Target cells: Peptide pulsed autologous EB blasts

X-axis: E:T ratio — 50:1 25:1 12.5:1 6.3:1 3:1 1.5:1

Y-axis: % specific release — 0, 5, 10, 15, 20, 25, 30, 35, 40, 45, 50

GenVax

Conclusions – GV1001

- The telomerase vaccine GV1001 is well tolerated

- GV1001 induces both T-helper and cytotoxic T cells that may contribute to an anti-tumor effect

- The number of immune responding patients is dose related

- In advanced pancreatic cancer patients a dose related survival benefit is observed

- Immune responders live longer than non-responders

Collaborators

Vaccine development

GemVax AS, Oslo

The Norwegian Radium Hospital, Oslo
M.K. Gjertsen
S.Sæbøe-Larssen
C. Markowski-Grimsrud
K. Lislerud
S. Trachsel
E.Fossheim
J.Roe
G.Gaudernack

Clinical Collaborators

Ullevål University Hospital, Oslo
T.Buanes
A.M.Mæo

The Norwegian Radium Hospital, Oslo
S. Aamdal
P. Brunsvig
G. Kvalheim

Inselspital, Bern
L. Braathen
K.Kernland

Karolinska Institute Stockholm
R. Kiessling
M. Petterson

University of Tromsø
Ø. Rekdal

Immune and Clinical Responses in Patients with Metastatic Melanoma to CD34+ Progenitor-derived Dendritic Cell Vaccine[1]

Jacques Banchereau,[2,3] A. Karolina Palucka,[2] Madhav Dhodapkar,[2] Susan Burkeholder, Nicolas Taquet, Alexandre Rolland, Sybil Taquet, Sebastien Coquery, Knut M. Wittkowski, Nina Bhardwaj, Luis Pineiro, Ralph Steinman, and Joseph Fay

Baylor Institute for Immunology Research, Dallas, Texas 75204 [J. B., A. K. P., S. B., N. T., A. R., S. T., S. C., L. P., J. F.]; Laboratory of Cellular Physiology and Immunology, The Rockefeller University, New York, New York 10021-6399 [M. D., N. B., R. S.]; and General Clinical Research Center, The Rockefeller University Hospital, New York, New York 10021-6399 [K. M. W.]

ABSTRACT

Immunization to multiple defined tumor antigens for specific immune therapy of human cancer has thus far proven difficult. Eighteen *HLA A*0201*+ patients with metastatic melanoma received injections s.c. of CD34+ progenitor-derived autologous dendritic cells (DCs), which included Langerhans cells. DCs were pulsed with peptides derived from four melanoma antigens [(MelAgs) MelanA/MART-1, tyrosinase, MAGE-3, and gp100], as well as influenza matrix peptide (Flu-MP) and keyhole limpet hemocyanin (KLH) as control antigens. Overall immunological effects were assessed by comparing response profiles using marginal likelihood scores. DC injections were well tolerated except for progressive vitiligo in two patients. DCs induced an immune response to control antigens (KLH, Flu-MP) in 16 of 18 patients. An enhanced immune response to one or more MelAgs was seen in these same 16 patients, including 10 patients who responded to >2 MelAgs. The two patients failing to respond to both control and tumor antigens experienced rapid tumor progression. Of 17 patients with evaluable disease, 6 of 7 patients with immunity to two or less MelAgs had progressive disease 10 weeks after study entry, in contrast to tumor progression in only 1 of 10 patients with immunity to >2 MelAgs. Regression of >1 tumor metastases were observed in seven of these patients. The overall immunity to MelAgs after DC vaccination is associated with clinical outcome ($P = 0.015$).

INTRODUCTION

Molecular identification of human cancer antigens in the last decade (1–3) has ushered in a new era of antigen-specific cancer immunotherapy specifically targeting these antigens (4–7). However, several such approaches (*e.g.*, peptides, DNA vaccines, and viral vectors) have thus far met with little or no success in the clinic (7–9). In particular, it has proved difficult to immunize humans simultaneously with multiple tumor antigens. In the case of melanoma, in which most such antigens have been defined, the immune system may be tolerized to these "self" antigens because they are also expressed on normal tissues (*e.g.*, melanocytes). Additional obstacles may include tumor-induced tolerance and global immunosuppression in advanced cancer (7–9). Unfortunately, most human tumor vaccine studies have not included control CD8+ T-cell antigens (*e.g.*, viral CD8+ epitopes), making it difficult to distinguish among these possibilities.

DCs[4] are antigen-presenting cells specialized to initiate and regulate immune responses (10, 11). Their clinical use as adjuvants has been aided by the development of methodologies to generate large numbers of these cells in culture from blood monocytes (12, 13) or CD34+ progenitors (14). In contrast to Mo-DCs, DCs derived from CD34+ cells consist of two phenotypically and functionally distinct populations (15). One subset is similar to the epidermal LCs, and the other termed "interstitial/dermal DCs" is similar to those derived from blood monocytes (15). Immune responses to these unique LC-containing preparations need to be evaluated in humans. Here we describe the safety and immunogenicity of antigen-bearing CD34-DCs in patients with stage IV melanoma.

MATERIALS AND METHODS

Study Design, Patients Characteristics, and Eligibility Criteria

Eighteen *HLA-A201*+ patients with metastatic melanoma received injections of CD34-DCs (Fig. 1; Table 1). Four patients (patients 1, 9, 12, and 13) had CNS involvement treated by surgery and radiation before entry into the trial, four patients (2, 4, 5, and 16) had received prior chemotherapy, and five patients (2, 4, 6, 9, and 15) had received prior biological therapy without a clinical or immune response (Table 1). Three patients (3, 13, and 20) progressed before completing the trial. Inclusion criteria were: biopsy-proven American Joint Committee on Cancer stage IV metastatic melanoma; age, ≥18 years; Karnofsky performance status, >80%; *HLA-A*0201* phenotype; intradermal skin test positivity to mumps, histoplasmosis, or streptokinase antigen; normal blood CD4 and CD8 T-cell numbers by flow cytometry; and normal quantitative immunoglobulin levels. Exclusion criteria were: prior chemotherapy or biologicals <4 weeks before trial entry; untreated CNS lesions; bulky hepatic metastatic lesions; pregnancy; or concurrent corticosteroid/immunosuppressive therapy. Patients with history of asthma, venous thrombosis, congestive heart failure, autoimmune disease, or active infections, including viral hepatitis, were also excluded. All of the patients were presented with several treatment alternatives, including surgery, high-dose cytokines, chemotherapy, or alternative immunotherapy. Patients were unlikely to be cured with surgery because of the presence of visceral metastases in most patients, including CNS involvement. Patient 10 had recurrent disease close to a prior biopsy site and refused further surgery. All of the patients gave a written informed consent, and the study was approved by the Food and Drug Administration, the NCI, and the Institutional Review Board. Patients received a 6-week outpatient vaccination course with antigen-loaded CD34-DCs given s.c. every 14 days for a total of four vaccinations. DCs were administered in a dose-escalation design at the dose level per cohort of 0.1, 0.25, 0.5, and 1×10^6 DCs/kg/injection. The calculated DC dose was the actual number of CD1a+ and CD14+ cells in the cell preparation (see below).

Preparation and Administration of the DC Vaccine

Harvest of DC Progenitors. The patients received recombinant granulocyte-CSF (Neupogen) 10 μg/kg/day s.c. for 5 days, for peripheral blood stem cell mobilization, and then underwent leukapheresis for 2 consecutive days to
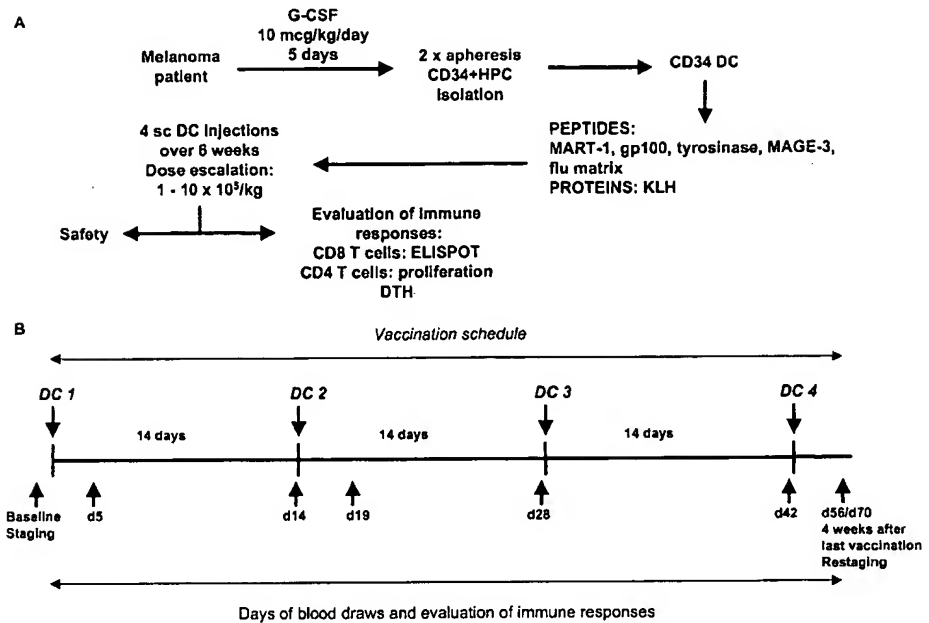
Fig. 1. Study design and vaccination schedule.

collect mobilized CD34$^+$ HPCs. The cells were processed using the CE-PRATE SC stem cell concentration system (CellPro Inc., Seattle, WA) to obtain an enriched population of CD34$^+$ HPCs (purity, 62 ± 17%; recovery, 158 ± 133 × 10^6 mean ± SD), which were then cryopreserved.

Preparation of DC Vaccine. All procedures were performed according to Good Laboratory Practice standards. CD34-DCs were generated from CD34$^+$ HPC by culture at a concentration of 0.5 × 10^6/ml culture medium (X-VIVO-15; BioWhittaker) supplemented with autologous serum, 10^{-5} M 2-β-mercaptoethanol and 1% L-glutamine. The following human recombinant cytokines, approved for clinical use, were used: GM-CSF (50 ng/ml; Immunex Corp.),

FLT3-L (100 ng/ml; Immunex Corp.), and TNF (10 ng/ml; CellPro, Inc.). Cultures were conducted in a humidified incubator at 37°C and 5% CO$_2$ with a separate incubator being assigned to each patient. On day 8 of culture, all of the cells were pulsed overnight with KLH (2 μg/ml; Intracell), 20% of the cells were pulsed separately with HLA-A*0201 restricted Flu-MP GILG-FVFTL$_{58-66}$ (2.5 μg/ml), and 80% of the cells were pulsed overnight with a mix of four HLA-A201 restricted peptides (2.5 μg/ml) derived from MelAgs (MelanA/MART-1$_{27-35}$: AAGIGILTV; gp100$_{g209-2}$ M: IMDQVPFSV; tyrosinase$_{368-376}$: YMDGTMSQV; and MAGE-3$_{271-279}$: FLWGPRALV). After overnight loading, all of the DCs were washed three times with sterile saline

Table 1 *Patient characteristics and disease status on entry and post-DC vaccine*

Pt. I.D.[a]	Age/sex	Months from diagnosis to stage IV/previous therapy	Status and measurable disease on entry	Early clinical outcome restaging at 10 wk (4 wk after last DC vaccine)
1	59/M	36/Surgery and radiation of CNS lesion	Retroperitoneal mass by CT scan (2 cm), positive PET scan	No evidence of measurable disease by CE, CT, and PET scan
2	55/M	24/Chemotherapy, IL-2, & IFN-α	Skin, LN, CNS, liver (4 cm), lung (3 cm)	PD: all sites enlarged
3	43/F	6/Surgery	Skin, LN, bones, and liver	PD: progression at all sites, early death from melanoma
4	42/F	82/Chemotherapy, IL-2, & IFN-α	PD: subcarinal LN mass by CT (6 cm)	Pulmonary nodule (2.8 cm) and subcarinal LN mass (7 cm) stable
			Pulmonary nodule by CT (3.2 cm)	Progressive vitiligo on chest, neck, back. No new lesions
5	45/M	10/Chemotherapy, IL-2, & IFN-α	PD: spleen nodule (3.5 cm), liver nodules (2.5 cm), and pulmonary nodules (1 cm) by CT scan	Spleen nodule 1 cm by CT scan, pulmonary, and liver nodules stable
6	36/M	30/Surgery, high-dose IL-2	PD: skin nodules (1.5–2.5 cm) and LN	PD: disappearance of 3 s.c. nodules but several new lesions
8	61/F	69/Surgery and radiation	Skin nodule by CE and CT scan (3 cm), liver nodule (4.5 cm), LDH 249, AP 261, AST 71, ALT 120	Regression of skin nodule by CE and CT, liver lesion stable (4.3 cm), normalization of liver enzymes: LDH 193, AP 196, AST 26, ALT 36; progressive vitiligo chest and arms
9	44/M	10/Melanoma cell vaccine, surgery, and radiation of CNS lesion	3-cm axillary LN mass by CE	No axillary LN mass, no evidence of measurable disease by CE and CT scan
10	50/M	144/Surgery	2-cm femoral LN next to biopsy-proven LN mass	No palpable LN mass, no evidence of measurable disease by CE and CT scan
12	56/F	35/Surgery, radiation CNS lesions	Skin nodule (2 cm)	50% regression of skin nodule, no new lesions by CE and PET scan
13	50/M	1/Surgery, radiation CNS lesion	2-cm axillary LN by physical examination	PD: progression in CNS after 2 DC vaccinations
15	43/F	1/Surgery and adjuvant IFN-α	LN, lung, and spleen	PD: progression, new lesion in spleen
16	73/M	96/Chemotherapy	PD: retroperitoneal LN (8 cm), liver (10 cm)	PD: progression
17	57/F	40/Surgery	Lung nodule by CT scan (1 cm)	No evidence of progression by CT scan and CE
18	70/F	3/Surgery	Pericardial nodule by CT (2 cm), 7.5-mm lesion in vaginal wall proximal to biopsy-proven lesion	Regression of pericardial nodule by CT scan and of vaginal metastases by CE
19	66/M	6/Radiation	Parotid nodule 2 cm by PET scan.	Nonevaluable for clinical outcome (no PET scan postvaccination)
20	40/M	44/Surgery	LN, liver and chest wall	PD: progression, early death from melanoma
21	66/M	1/Surgery	Liver lesion by MRI (1.8 cm)	Liver lesion stable by MRI (1.9 cm)

[a] Pt. I.D., patient identification number; CT, computed tomography; PET, positron emission tomography; LN, lymph node; LDH, lactate dehydrogenase; AP, alkaline phosphatase; AST, aspartate aminotransferase; ALT, alanine aminotransferase; CE, clinical examination; MRI, magnetic resonance imaging.

and were counted and resuspended in 10 ml of sterile saline containing melanoma peptides (1 μg/ml). After 2-h incubation at 22°C, the cells were centrifuged and resuspended in 9 ml of sterile saline for injection. All of the peptides were Good Manufacturing Practice (GMP) quality and were either obtained from the NCI (MelanA/MART-1, gp100, and tyrosinase) or purchased (Flu-MP and MAGE-3; MultiPeptide Systems, San Diego, CA). Vaccine release criteria included: (a) negative bacterial culture 48 h prior to DC injection; (b) negative Gram's staining after antigen pulsing; (c) DC morphology on Giemsa-stained cytospins performed 2 h before DC administration, (d) cell viability >80%; and (e) a minimum of 20% DCs (CD1a+ and CD14+) in cell preparation as determined by phenotypic analysis. The remaining cells contained DC precursors as well as cells with the ability to induce mixed lymphocyte reaction (not shown). Further quality testing of each DC batch included: (a) reactivity with a panel of monoclonal antibodies; and (b) determination of their stimulatory capacity in mixed lymphocyte reactions.

Administration of Vaccine. Vaccination was administered s.c. in three injection sites (both thighs and the upper arm). Limbs from which draining lymph nodes had been surgically removed and/or irradiated were not injected. DCs were injected using a long spinal-cord needle and were spread over a 6- to 8-cm distance.

Clinical Monitoring

Adverse events were graded according to the NCI Common Toxicity Criteria. All of the patients underwent assessment of tumor status at baseline and 4 weeks after the fourth DC vaccination (10 weeks from trial entry). Disease progression was defined as >25% increase in target lesions and/or the appearance of new lesions.

Immunological Monitoring

PBMCs samples from at least two time points before vaccination, as well as 5 and/or 14 days after each vaccination and 14 or 28 days after the fourth vaccination, were harvested and frozen. Pre- and postimmunization PBMCs were frozen in aliquots, coded, thawed and assayed together in a blinded fashion.

Antigen-specific Proliferation

PBMCs (10^5 cells/well) were cultured in triplicate wells in the absence or presence of graded doses of KLH at 1-10 μg/ml, and as a positive control, in the presence of SEA. Assays were pulsed overnight with [^{3}H]thymidine on day 3 (SEA) or day 5 (KLH) of culture and harvested 16 h later.

ELISPOT Assay for IFN-γ Release from Single Antigen-specific T Cells

ELISPOT assay for the detection of antigen-specific IFN-γ-producing T cells was performed as described previously (16, 17). Briefly, PBMCs (2 × 10^5 cells/well) were added to plates precoated with 10 μg/ml of a primary anti-IFN-γ monoclonal antibody (Mabtech, Stockholm, Sweden) in the presence or absence of 10 μg/ml peptide antigens. The antigens were the same HLA A*0201-restricted peptides (four melanoma peptides and Flu-MP) used in the DC vaccine. HLA A*0201-restricted gag peptide was used as a negative control, and SEA as a positive control for T-cell function. For some experiments, depending on the cell yield, influenza virus-infected PBMCs (MOI 2) were used as APCs. Antigen-specific SFCs were calculated after subtracting the background obtained with control peptide. Immune responses were scored as positive if the postimmunization measurements for antigen-specific SFCs were >2-fold higher than the baseline and >10 SFC/2 × 10^5 cells (16).

Antigen-specific Recall T-cell Responses

To evaluate the ability of antigen-specific T cells to proliferate and differentiate in culture, pre- and postimmunization PBMCs were thawed together and cocultured (2 × 10^5 cells/well) for 7 days with autologous mature DCs (PBMC:DC ratio, 30:1) pulsed with 1 μg/ml peptides. After 7 days, cells were transferred to an ELISPOT plate and cultured overnight with (T-cell:APC ratio, 20:1) irradiated (3000 rads) T2 cells with or without specific antigen. Antigen-specific SFCs were calculated after subtracting the background obtained with unpulsed T2 cells.

DTH Reactions

CD34-DCs (10^5), pulsed separately with each antigen, were injected intradermally on the patient's back and induration at the injection site was measured at 48 h.

Statistical Analysis

The sign test for discretized data were used to demonstrate the presence of specific immune response to KLH and Flu-MP (18). Because the role of different MelAgs with regard to protective immunity is not known, we integrated postvaccination responses to all four MelAgs, as measured by both direct and recall assays, into an immunity score using a nonparametric method based on the marginal likelihood approach (19, 20). To score n individuals according to their immune response profiles, one computes all rankings (permutations of numbers 1 . . . n) that are compatible with all pairwise orderings. An immune response is considered higher if it is at least as high for each of the eight variables and higher for at least one variable. A patient's immunity score is the average of the corresponding ranks among the compatible rankings minus the expected score. All of the immunized patients were included in the analysis in an "intent to treat" approach.

RESULTS

DC Vaccine. Fresh DCs were generated from granulocyte-CSF mobilized blood CD34+-HPCs for each vaccination. Frozen/thawed CD34+-HPCs cultured for 9 days with GM-CSF, TNF-α, and FLT3-L yielded MHC class I+, HLA-DR+, CD80+, CD86^{low}, and CD83^{low} DCs (not shown). Although CD83^{low}, these DCs are not considered immature because they are generated in the presence of TNF-α (a well-established DC maturation factor) and routinely induce proliferation of allogeneic CD8 T cells (not shown). The DCs included CD1a+CD14- LCs as well as CD1a$^{\pm}$CD14+ interstitial DC precursors (intDC). The LC phenotype was confirmed by confocal microscopy revealing Langerin staining in CD1a+ DCs (not shown; 21). The mean proportion of CD1a+CD14- cells was 9 ± 3% (range, 4-17%; median, 9%) and that of CD1a$^{\pm}$CD14+ cells was 32 ± 9% (range, 19-52%; median, 30%). The composition of DC vaccine for each patient is given in Table 3.

Responses to Control Antigens. DC vaccination primed KLH-specific immune responses in 16 of 18 patients (all except patients 3 and 13; P = 0.00007 in the exact sign test; Fig. 2A). There is no indication that higher DC doses induced greater KLH-specific proliferation. Fifteen patients (all except patients 3, 13, and 20) were evaluated for DTH after they completed the vaccination protocol (four DC vaccines). Thirteen of these patients (all except patients 1 and 19) developed DTH to KLH (median, 10 mm; range, 6-47 mm). Of the 17 patients injected with Flu-MP-pulsed DCs (all except patient 18 with a history of allergy to flu vaccine), enhancement of Flu-MP-specific memory T-cell responses by at least one assay was observed in 15 patients (all except patients 3 and 13; Table 2; Fig. 2B). The elicited T cells also recognized the naturally processed antigen from flu-infected PBMCs (not shown). The finding that all except two patients responded to both KLH and Flu-MP-pulsed DCs indicates that patients with metastatic melanoma enrolled in our study were immunocompetent.

In Vivo Expansion of Melanoma-specific Blood CD8 T Cells

Responses in Uncultured T Cells. Except for patient 8, only a few MelAg-specific IFN-γ-producing cells were detected in baseline blood samples (Table 2; Fig. 3). The response was considered as enhanced if there was a >2-fold increase and a minimum of 10 MelAg-specific ELISPOTs (after subtracting the values obtained from control wells) in postimmunization samples. After DC vaccination, enhanced responses to ≥1 MelAgs were detectable in uncultured T
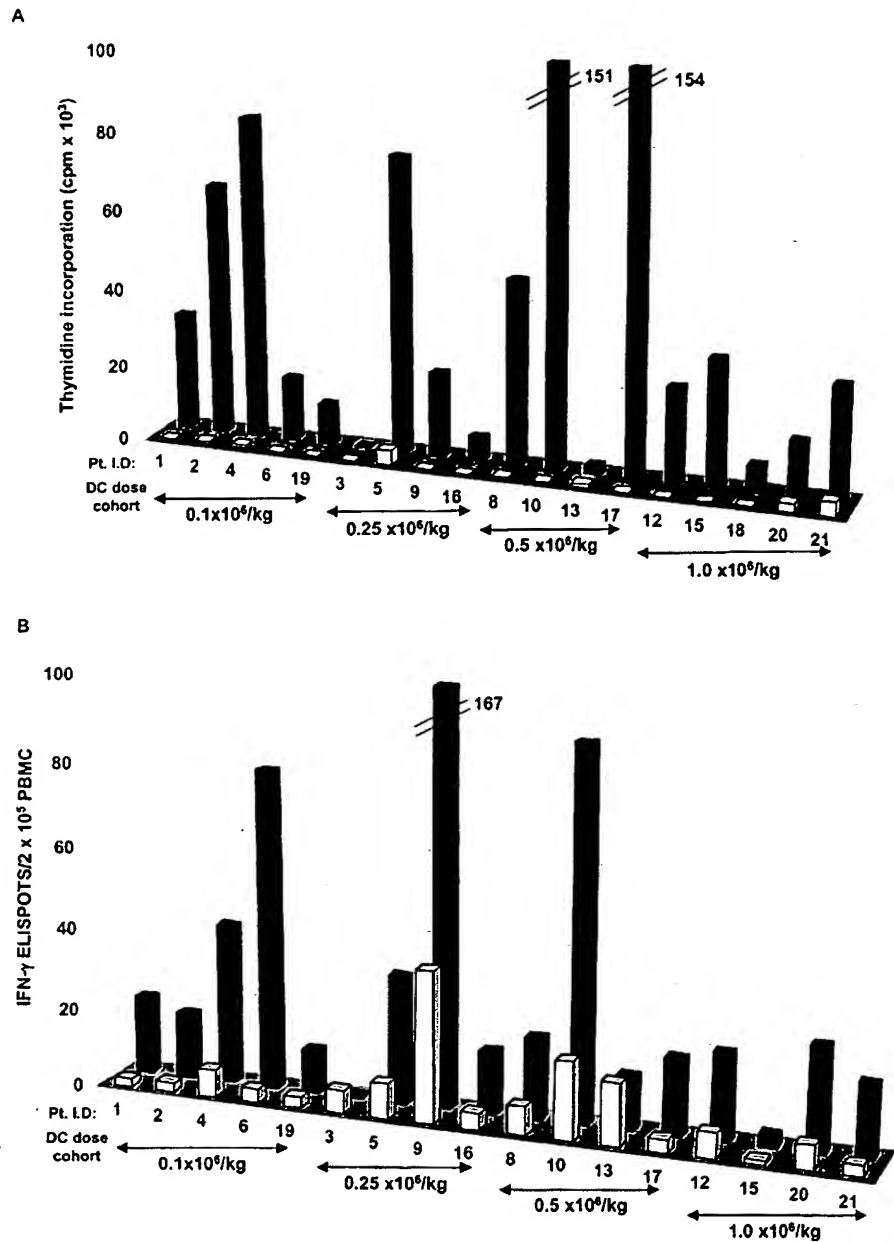
A

Fig. 2. Responses to control antigens. *A*, KLH-dependent proliferative responses: pre/postimmunization PBMCs are cultured with 10 µg/ml KLH for 5 days. KLH-specific T-cell proliferation is determined based on [³H]thymidine incorporation. *B*, Flu-MP responses. PBMCs obtained at baseline and after four DC vaccinations are cultured overnight with 10 µM Flu-MP peptide. Antigen-specific IFN-γ-secreting cells are quantified using an ELISPOT assay and expressed as number of IFN-γ ELISPOTs/2 × 10⁵ PBMCs. The numbers obtained in control wells are subtracted (median, 1 spot/2 × 10⁵ PBMCs; range, 0–8).

B

cells in 8 of 18 patients (Table 2). Five patients showed increased responses to MAGE-3, four to MelanA/MART-1, five to gp100, and seven to tyrosinase peptide (Table 2; Fig. 3*A*). There is no indication that higher DC doses induce greater melanoma-specific immunity. We conclude that MelAg-pulsed CD34-DCs lead to enhancement of MelAg-specific circulating effectors in melanoma patients.

Responses in Cultured T Cells. Next, we determined the capacity of blood CD8 T cells to mount melanoma-specific responses after 1-week culture with melanoma peptide-pulsed autologous DCs. Most patients had low levels of MelAg-specific memory cells in preimmunization samples (except for patient 21). However, in 14 of 15 evaluated patients, an increased response to at least one melanoma peptide was found after DC vaccination, (Table 2; Fig. 3*B*), and 5 of these patients (patients 1, 5, 9, 16, and 17) responded to all four melanoma peptides.

Overall Response to MelAgs

Overall, enhanced immunity to ≥1 MelAgs by at least one assay was observed in 16 of 18 patients after DC vaccination. Of these, enhanced immunity to two, three, or all four MelAgs was seen by at least one assay in patients 3, 4, and 6, respectively. Thus, vaccination with melanoma-peptide-pulsed CD34-DCs leads to enhanced immunity to several MelAg peptides in melanoma patients.

DTH

Ten of 14 evaluated patients developed DTH to at least one peptide after repeated DC vaccination. Thus, DTH to DCs pulsed with: (*a*) MART-1 was observed in all 10 patients (median induration, 7.5 mm); (*b*) MAGE-3 in 8 of 10 patients (median induration, 9.5 mm); (*c*) tyrosinase in 8 of 10 patients (median induration, 8 mm); and (*d*)

Table 2 *Number of peptide-specific IFN-γ ELISPOTS/10^5 PBMCs in pre/postvaccination samples: circulating effectors (direct ELISPOT, D) and memory T cells (recall ELISPOT, R)*

DC dose	Pt. I.D.[a] %CD3+CD8+[b]	Flu	MAGE	MART	Tyr	Gp100	No. of MelAgs
0.1 × 10^6/kg	1	D: 2/19	1/8	3/3	1/6	1/8	0
	16%	R: 1/276	3/40	5/59	5/45	6/40	4
		T2: 2/4	0/2	0/2	0/2	0/2	
	2	D: 2/16	1/4	1/0	0/2	0/8	0
	31%	R: 3/12	3/2	0/14	1/9	2/14	2
		T2: 0/6	0/3	4/1	3/4	1/0	
	4	D: 7/39	0/36	3/25	3/27	0/33	4
	27%	R: ND	ND	ND	ND	ND	
	6	D: 3/77	1/2	0/1	0/2	0/2	0
	25%	R: ND	1/3	ND	1/7	5/13	1
		T2: ND	10/10	ND	11/14	6/9	
	19	D: 2/10	2/6	0/1	0/4	0/1	0
	36%	R: 89/164	5/20	4/14	6/8	11/14	2
		T2: 3/1	1/1	1/4	1/1	2/2	
0.25 × 10^6/kg	3	D: 5/0	0/0	0/0	0/0	0/0	0
	ND	R: 0/0	0/0	0/0	0/0	0/0	0
		T2: 0/0	0/0	0/0	0/0	0/0	
	5	D: 8/31	1/23	10/13	5/24	1/25	3
	12%	R: 272/1019	4/178	13/55	4/110	1/59	4
		T2: 8/81	0/2	0/33	0/6	2/8	
	9	D: 37/167	0/12	0/12	0/10	0/18	4
	27%	R: 61/256	1/20	11/29	2/21	1/23	4
		T2: 14/9	6/7	7/4	6/4	6/9	
	16	D: 4/15	2/1	0/2	0/1	0/1	0
	7%	R: 50/225	7/38	0/47	1/45	13/48	4
		T2: 21/23	25/23	23/32	19/39	25/25	
0.5 × 10^6/kg	8	D: 7/19	7/20	12/39	5/15	4/5	3
	26%	R: ND	ND	ND	ND	ND	
	10	D: 19/89	1/4	4/0	2/0	0/0	0
	30%	R: 62/730	0/0	0/15	0/54	0/35	3
		T2: 1/70	0/23	0/23	0/21	0/31	
	13	D: 15/13	0/0	0/0	0/0	0/0	0
	3%	R: 9/4	3/1	1/0	1/0	5/10	0[c]
		T2: 0/0	0/0	1/1	1/0	0/66	
	17	D: 3/18	1/9	1/12	1/10	1/7	2
	25%	R: 34/441	3/37	13/64	4/51	12/44	4
		T2: 5/12	5/18	8/19	7/23	7/27	
1.0 × 10^6/kg	12	D: 6/21	0/3	3/8	0/13	1/4	1
	17%	R: 28/100	0/0	6/20	1/36	0/36	3
		T2: 0/0	0/1	8/0	0/10	0/0	
	15	D: 1/3	0/0	1/0	0/1	0/10	1
	14%	R: 40/155	1/4	5/6	0/6	6/70	1
		T2: 25/0	17/7	37/1	3/0	3/14	
	18	D: 5/13	0/2	0/1	0/1	0/1	0
	15%	R: 35/43	5/18	13/9	0/2	0/16	2
		T2: 0/1	0/1	4/2	0/0	0/3	
	20	D: 6/25	0/0	0/0	1/0	1/2	0
	ND	R: 267/326	9/5	12/10	2/14	13/22	1
		T2: 13/4	15/8	15/3	17/3	19/9	
	21	D: 3/17	1/15	1/9	1/10	1/10	3
	32%	R: 241/473	21/37	30/44	23/20	16/36	1
		T2: 21/37	12/16	10/15	4/7	11/11	

[a] Pt. I.D., patient identification number; ND, not done.
[b] Percentages of CD3 + CD8 + T cells in lymphocyte gate.
[c] Because of unusually high background, we did not consider this as a positive response.

gp100 in 9 of 10 patients (median induration, 8 mm). In three patients, there was reactivity to unpulsed DCs (erythema without induration (8 mm). There was no correlation between the responses in blood and DTH.

Toxicity of DC Injection

Safety and tolerability were assessed with each DC vaccination and 1 month after the fourth vaccination. No patients developed injection site erythema/irritation or systemic toxicity. Two patients (patients 4 and 8) with mild preexisting vitiligo developed progressive vitiligo during the course of DC therapy (Table 1). Rheumatoid factor and antithyroid antibodies were negative throughout the trial. The antinuclear antibody titer of patient 8 was negative before the first DC injection but increased to 1:80 after the fourth injection. No clinical manifestations of autoimmune disease developed in this patient.

Clinical Outcome. Seven of 17 evaluable patients experienced tumor progression (PD, Table 1). The remaining 10 patients did not progress at this time point (10 weeks from study entry). Among these, three patients (4, 17, and 21) had neither new lesions nor progression of measurable disease; four patients (5, 8, 12, and 18) with multiple lesions on entry experienced regression at one or more disease sites; and three patients (1, 9, and 10), who had only limited disease on entry, cleared any evidence of disease. Nonprogressing patients have received additional DC vaccinations on a subsequent study; therefore, we cannot assess the durability of these responses. Patient 5 has received additional immunotherapy at another institution.

Correlation of Immunological Responses and Clinical Outcome

We first used >2-fold increase and ≥10 antigen-specific IFN-γ ELISPOTS in the postvaccination assays as an indicator of immune

Fig. 3. Melanoma-specific responses. *A*, circulating melanoma-specific effector cells. PBMCs obtained at baseline and after four DC vaccinations are cultured overnight with each of the four melanoma peptides (*MAGE-3*, MelanA/*MART-1*, *Tyrosinase*, and gp100 (*Gp-100*) used for vaccination (10 μM). The specific T-cell response in each of the evaluated patients is expressed as the number of IFN-γ ELISPOTS/2 × 10^5 PBMCs. The values obtained with control gag peptide or in the wells with no peptide are subtracted (on average one spot/2 × 10^5 PBMC; range, 0–8). *B*, expansion of MelAg-specific memory effector cells. PBMCs obtained at baseline and after four DC vaccinations are cultured for 7 days with mature melanoma-peptide-pulsed autologous Mo-DCs. The T cells are harvested and peptide induced IFN-γ release is measured in the overnight culture with melanoma-peptide pulsed T2 cells. Numbers of IFN-γ ELISPOTS/10^5 peripheral blood lymphocytes. The values obtained with unpulsed T2 cells are subtracted; *MAGE-3*: median number of spots pre/post vaccine 1/7; range, 0–25/0–23; *MART-1*: median number of spots pre/post vaccine 5/3; range, 0–37/0–33; *Tyrosinase*: median number of spots pre/post vaccine 2/4; range, 0–19/0–39; gp100 (*Gp-100*): median number of spots pre/post vaccine 2/9; range, 0–25/0–33.
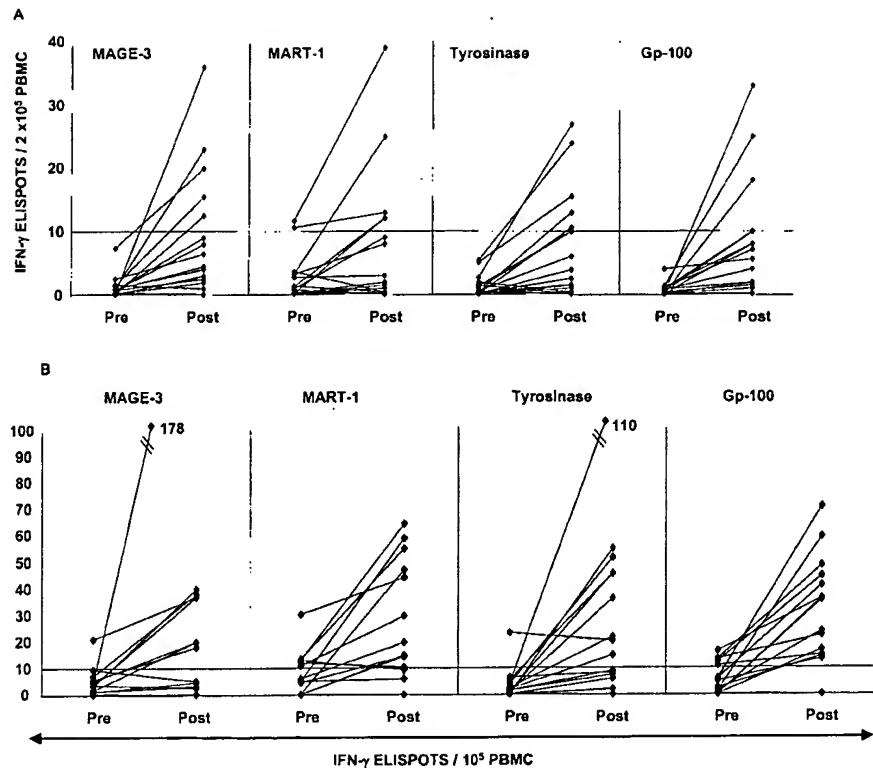
response (16). Two patients (3 and 13) who failed to respond to either the control or MelAgs by any assay, experienced rapid tumor progression and could not complete the planned therapy. Of 17 patients with evaluable disease, 6 of 7 patients who responded to zero, one, or two MelAgs had PD on restaging 10 weeks after study entry (Table 3). In contrast, tumor progression was seen in only 1 of the 10 patients who responded to three or all four MelAgs (P = 0.002, Fisher exact test). Regression of >1 tumor metastases were observed in seven of these patients.

To obtain an overall assessment of antitumor immunity after the DC vaccination, we integrated data for absolute immune responses to all four antigens by direct and recall assays into a tumor immunity

score (from −8.5 to +8.5), as described earlier (19, 20). By this comprehensive analysis, tumor immunity is associated with clinical outcome (P = 0.015). Six of the eight patients with a negative score, but only 1 of the 9 patients with a positive score, progressed (Fig. 4). Omitting data from the MAGE-3 epitope, which is thought to require an immunoproteasome for presentation, yields similar results (P = 0.009).

DISCUSSION

Our results indicate that vaccination of stage IV melanoma patients with antigen-pulsed CD34-DCs is well tolerated and results in en-

Table 3 *DC vaccine, immune responses, and clinical outcome*

	DC vaccine		Immune responses				Clinical outcome
			Control antigens		Melanoma antigens		
Pt. I.D.[a]	Dose × 10^6/kg	CD1a+CD14−/CD1a±CD14+ mean % of positive cells	FLU	KLH	n	>2 Ag	Early evaluation at 10 wk
1	0.1	4/25	Yes	Yes	4	Yes	NP
2	0.1	6/28	Yes	Yes	2	No	PD
4	0.1	7/38	Yes	Yes	4	Yes	NP
6	0.1	6/42	Yes	Yes	1	No	PD
19	0.1	10/40	Yes	Yes	2	No	NE
3	0.25	5/44	No	No	0	No	PD
5	0.25	17/20	Yes	Yes	4	Yes	NP
9	0.25	9/32	Yes	Yes	4	Yes	NP
16	0.25	7/25	Yes	Yes	4	Yes	PD
8	0.5	14/33	Yes	Yes	3	Yes	NP
10	0.5	11/42	Yes	Yes	3	Yes	NP
13	0.5	10/36	No	No	0	No	PD
17	0.5	8/27	Yes	Yes	4	Yes	NP
12	1.0	13/24	Yes	Yes	3	Yes	NP
15	1.0	10/52	Yes	Yes	1	No	PD
18	1.0	11/20	ND	Yes	2	No	NP
20	1.0	12/19	Yes	Yes	1	No	PD
21	1.0	8/30	Yes	Yes	3	Yes	NP

[a] Pt. I.D., patient identification; Ag, antigen; NP, ●●●; NE, ●●●.

6456

Fig. 4. Correlation of immune response and clinical outcome. Immune responses from both direct and recall assays for all four MelAgs were ranked and integrated into a tumor immunity score (from −8.5 to +8.5). Data are plotted as tumor immunity score (Y axis) versus clinical response (X axis). Each number on horizontal axis, the patient identification (Pt I.D.). Four groups of patients are depicted: patients with regression of one or more lesions postvaccination (Regression, white bars); patients with stable disease (Stable, thin hatched bars); patients whose disease progressed at 10 weeks (PD, black bars); and patients who experienced early progression (before evaluation at 10 weeks, Early PD, thick hatched bars).
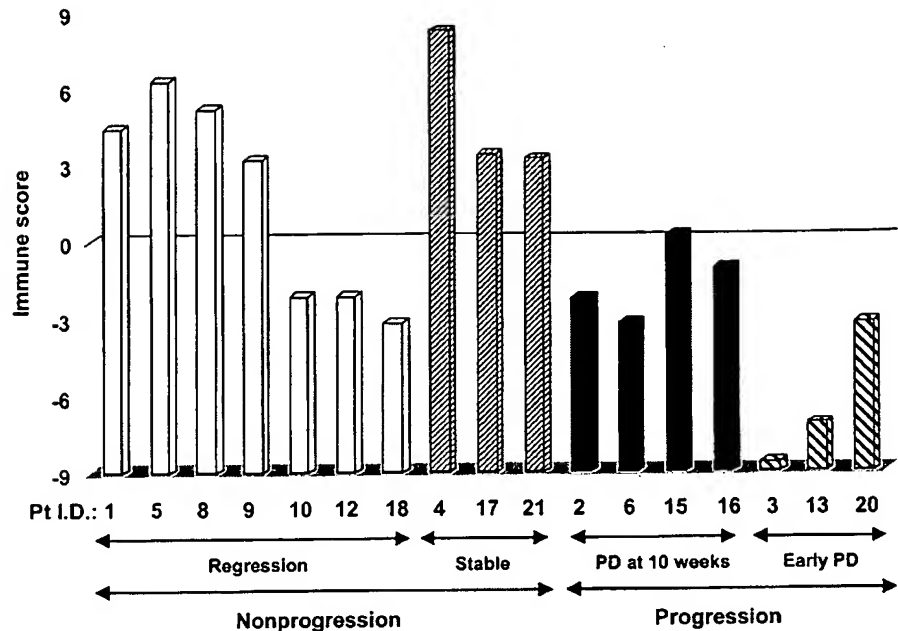
hanced immunity to a viral antigen as well as to several MelAgs. Our findings emerged from a Phase I study designed to evaluate the tolerability of this new source of DC vaccine containing LCs. Administration of CD34-DCs leads to no major systemic toxicity. The development of progressive vitiligo in two patients came as an early demonstration that the DC vaccine may enhance immunity to the melanocyte differentiation antigens. Nevertheless, several secondary outcomes with respect to immunogenicity and clinical efficacy were also evident. Our patients, despite prior chemotherapy in some of them and advanced stage of disease, clearly showed immune competence when challenged with two non-MelAgs: the KLH protein to evaluate priming of CD4 T cells and the influenza matrix peptide to test boosting of CD8+ T cells. Immune competence in stage IV melanoma was also noted by Thurner et al., demonstrating T-cell proliferation and DTH to tetanus toxoid delivered on mature Mo-DCs (22).

Injection of peptide-pulsed DCs correlates with enhanced immunity to multiple defined tumor antigens. The MelAg-specific T cells that were elicited after DC vaccine are functional and are detectable in effector T-cell assays without the need for prior ex vivo expansion. They are also capable of proliferation and effector function after short-term (1 week) coculture with antigen-bearing DCs, without the need for exogenous cytokines or multiple restimulations with antigen. The feasibility of eliciting immune response to multiple MelAgs suggests that tolerance to these self antigens, if present, may only be partial (23, 24).

The ability of DCs to elicit immune response to multiple tumor antigens in vivo may be clinically important. The development of T-cell response to multiple tumor antigens on peptide-pulsed DCs in this study was associated with a favorable early clinical outcome. Prior studies using chemical adjuvants have failed to reliably elicit immunity to MelAgs (25). Improved results were obtained more recently with the use of modified peptides combined with IL-2 (26). However, in most studies, limited clinical responses are observed, which may be attributable to targeting a limited number of epitopes.

We chose to test CD34-DCs because they are composed of two distinct DC subsets, LCs and interstitial DCs (15). This contrasts with

Mo-DCs, which are devoid of LCs (27). Mo-DCs have been shown to act as immune adjuvants in healthy volunteers and in stage IV melanoma (16, 17, 22, 28). Injection of MAGE-3-pulsed Mo-DCs were recently shown to enhance circulating MAGE-3-specific active effectors in melanoma patients (29). However, no clinical responses were observed, which may be attributable to the choice of the immunizing epitope or targeting of a single epitope. Others have reported that CD34-DCs can be more efficient than Mo-DCs in activating CTLs in vitro (30, 31). In the circumstances like the induction of tumor-specific CTLs, CD34-DCs could thus be advantageous. Another recent study evaluated CD34-DCs in advanced melanoma and found little clinical or immunological efficacy (32). However, the DCs were cultured in the presence of IL-4 (which inhibits LC development; Ref. 27) and administered i.v. Controlled studies are needed to compare the immunogenicity of this new form of DCs (and their subsets) to those derived from blood monocyte precursors.

Although these data provide encouragement for targeting MelAgs using DCs in the clinic, additional studies are needed to establish and optimize their clinical efficacy. The patients who experienced favorable clinical outcome had relatively limited disease and no history of chemotherapy, which supports the concept of testing DC vaccines earlier, e.g., in a surgical adjuvant setting. Optimizing variables such as peptide loading, vaccine schedule, and DC maturation may further improve the immunogenicity of these DCs.

ACKNOWLEDGMENTS

REFERENCES

1. Knuth, A., Wolfel, T., Klehmann, E., Boon, T., and Meyer zum Buschenfelde, K. H. Cytolytic T-cell clones against an autologous human melanoma: specificity study and definition of three antigens by immunoselection. Proc. Natl. Acad. Sci. USA, *86:* 2804–2808, 1989.
2. van der Bruggen, P., Traversari, C., Chomez, P., Lurquin, C., De Plaen, E., Van den Eynde, B., Knuth, A., and Boon, T. A gene encoding an antigen recognized by cytolytic T lymphocytes on a human melanoma. Science (Wash. DC), *254:* 1643–1647, 1991.
3. Rosenberg, S. A. Cancer vaccines based on the identification of genes encoding cancer regression antigens. Immunol. Today, *18:* 175–182, 1997.
4. Celluzzi, C. M., Mayordomo, J. I., Storkus, W. J., Lotze, M. T., and Falo, L. D., Jr. Peptide-pulsed dendritic cells induce antigen-specific CTL-mediated protective tumor immunity. J. Exp. Med., *183:* 283–287, 1996.
5. Zitvogel, L., Mayordomo, J. I., Tjandrawan, T., DeLeo, A. B., Clarke, M. R., Lotze, M. T., and Storkus, W. J. Therapy of murine tumors with tumor peptide-pulsed dendritic cells: dependence on T cells, B7 costimulation, and T helper cell 1-associated cytokines. J. Exp. Med., *183:* 87–97, 1996.
6. Sogn, J. A. Tumor immunology: the glass is half full. Immunity, *9:* 757–763, 1998.
7. Gilboa, E. The makings of a tumor rejection antigen. Immunity, *11:* 263–270, 1999.
8. Pardoll, D. M. Cancer vaccines. Nat. Med., *4:* 525–531, 1998.
9. Fong, L., and Engleman, E. G. Dendritic cells in cancer immunotherapy. Annu. Rev. Immunol., *18:* 245–273, 2000.
10. Steinman, R. M. The dendritic cell system and its role in immunogenicity. Annu. Rev. Immunol., *9:* 271–296, 1991.
11. Banchereau, J., Briere, F., Caux, C., Davoust, J., Lebecque, S., Liu, Y., Pulendran, B., and Palucka, K. Immunobiology of dendritic cells. Annu. Rev. Immunol., *18:* 767–811, 2000.
12. Romani, N., Gruner, S., Brang, D., Kampgen, E., Lenz, A., Trockenbacher, B., Konwalinka, G., Fritsch, P. O., Steinman, R. M., and Schuler, G. Proliferating dendritic cell progenitors in human blood. J. Exp. Med., *180:* 83–93, 1994.
13. Sallusto, F., and Lanzavecchia, A. Efficient presentation of soluble antigen by cultured human dendritic cells is maintained by granulocyte/macrophage colony-stimulating factor plus interleukin 4 and downregulated by tumor necrosis factor α. J. Exp. Med., *179:* 1109–1118, 1994.
14. Caux, C., Dezutter-Dambuyant, C., Schmitt, D., and Banchereau, J. GM-CSF, and TNF-α cooperate in the generation of dendritic Langerhans cells. Nature (Lond.), *360:* 258–261, 1992.
15. Caux, C., Massacrier, C., Vanbervliet, B., Dubois, B., Durand, I., Cella, M., Lanzavecchia, A., and Banchereau, J. CD34$^+$ hematopoietic progenitors from human cord blood differentiate along two independent dendritic cell pathways in response to granulocyte-macrophage colony-stimulating factor plus tumor necrosis factor α. II. Functional analysis. Blood, *90:* 1458–1470, 1997.
16. Dhodapkar, M. V., Steinman, R. M., Sapp, M., Desai, H., Fossella, C., Krasovsky, J., Donahoe, S. M., Dunbar, P. R., Cerundolo, V., Nixon, D. F., and Bhardwaj, N. Rapid generation of broad T-cell immunity in humans after a single injection of mature dendritic cells. J. Clin. Investig., *104:* 173–180, 1999.
17. Dhodapkar, M. V., Krasovsky, J., Steinman, R. M., and Bhardwaj, N. Mature dendritic cells boost functionally superior CD8(+) T-cell in humans without foreign helper epitopes. J. Clin. Investig., *105:* R9–R14, 2000.
18. Wittkowski, K. M. Versions of the sign test in the presence of ties. Biometrics, *54:* 789–791, 1998.
19. Kalbfleisch, J. D., and Prentice, R. L. Marginal likelihoods based on Cox's regression and life model. Biometrika, *60:* 267–278, 1973.
20. Wittkowski, K. M. Friedman-type statistics and consistent multiple comparisons for unbalanced designs. J. Am. Stat. Assoc., *83:* 1163–1170, 1988.
21. Valladeau, J., Ravel, O., Dezutter-Dambuyant, C., Moore, K., Kleijmeer, M., Liu, Y., Duvert-Frances, V., Vincent, C., Schmitt, D., Davoust, J., Caux, C., Lebecques, S., and Saeland, S. Langerin. A novel C-type lectin specific to Langerhans cells, is an endocytic receptor that induces the formation of Birbeck granules. Immunity, *12:* 71–81, 2000.
22. Thurner, B., Haendle, I., Roder, C., Dieckmann, D., Keikavoussi, P., Jonuleit, H., Bender, A., Maczek, C., Schreiner, D., von den Driesch, P., Brocker, E. B., Steinman, R. M., Enk, A., Kampgen, E., and Schuler, G. Vaccination with mage-3A1 peptide-pulsed mature, monocyte-derived dendritic cells expands specific cytotoxic T cells and induces regression of some metastases in advanced stage IV melanoma. J. Exp. Med., *190:* 1669–1678, 1999.
23. Romero, P., Dunbar, P. R., Valmori, D., Pittet, M., Ogg, G. S., Rimoldi, D., Chen, J. L., Lienard, D., Cerottini, J. C., and Cerundolo, V. Ex vivo staining of metastatic lymph nodes by class I major histocompatibility complex tetramers reveals high numbers of antigen-experienced tumor-specific cytolytic T lymphocytes. J. Exp. Med., *188:* 1641–1650, 1998.
24. Lee, P. P., Yee, C., Savage, P. A., Fong, L., Brockstedt, D., Weber, J. S., Johnson, D., Swetter, S., Thompson, J., Greenberg, P. D., Roederer, M., and Davis, M. M. Characterization of circulating T cells specific for tumor-associated antigens in melanoma patients. Nat. Med., *5:* 677–685, 1999.
25. Wolchok, J. D., Livingston, P. O., and Houghton, A. N. Vaccines and other adjuvant therapies for melanoma. Hematol. Oncol. Clin. North Am., *12:* 835–848, 1998.
26. Rosenberg, S. A., Yang, J. C., Schwartzentruber, D. J., Hwu, P., Marincola, F. M., Topalian, S. L., Restifo, N. P., Dudley, M. E., Schwarz, S. L., Spiess, P. J., Wunderlich, J. R., Parkhurst, M. R., Kawakami, Y., Seipp, C. A., Einhorn, J. H., and White, D. E. Immunologic and therapeutic evaluation of a synthetic peptide vaccine for the treatment of patients with metastatic melanoma. Nat. Med., *4:* 321–327, 1998.
27. Caux, C., Massacrier, C., Dubois, B., Valladeau, J., Dezutter-Dambuyant, C., Durand, I., Schmitt, D., and Saeland, S. Respective involvement of TGF-β and IL-4 in the development of Langerhans cells and non-Langerhans dendritic cells from CD34$^+$ progenitors. J. Leukoc. Biol., *66:* 781–791, 1999.
28. Nestle, F. O., Alijagic, S., Gilliet, M., Sun, Y., Grabbe, S., Dummer, R., Burg, G., and Schadendorf, D. Vaccination of melanoma patients with peptide- or tumor lysate-pulsed dendritic cells. Nat. Med., *4:* 328–332, 1998.
29. Schuler-Thurner, B., Dieckmann, D., Keikavoussi, P., Bender, A., Maczek, C., Jonuleit, H., Roder, C., Haendle, I., Leisgang, W., Dunbar, R., Cerundolo, V., von Den Driesch, P., Knop, J., Brocker, E. B., Enk, A., Kampgen, E., and Schuler, G. Mage-3 and influenza-matrix peptide-specific cytotoxic T cells are inducible in terminal stage HLA-A2.1+ melanoma patients by mature monocyte-derived dendritic cells. J. Immunol., *165:* 3492–3496, 2000.
30. Mortarini, R., Anichini, A., Di Nicola, M., Siena, S., Bregni, M., Belli, F., Molla, A., Gianni, A. M., and Parmiani, G. Autologous dendritic cells derived from CD34$^+$ progenitors and from monocytes are not functionally equivalent antigen-presenting cells in the induction of melan-A/Mart-1(27–35)-specific CTLs from peripheral blood lymphocytes of melanoma patients with low frequency of CTL precursors. Cancer Res., *57:* 5534–5541, 1997.
31. Ferlazzo, G., Klein, J., Paliard, X., Wei, W. Z., and Galy, A. Dendritic cells generated from CD34$^+$ progenitor cells with flt3 ligand, c-kit ligand, GM-CSF, IL-4, and TNF-α are functional antigen-presenting cells resembling mature monocyte-derived dendritic cells. J. Immunother., *23:* 48–58, 2000.
32. Mackensen, A., Herbst, B., Chen, J. L., Kohler, G., Noppen, C., Herr, W., Spagnoli, G. C., Cerundolo, V., and Lindemann, A. Phase I study in melanoma patients of a vaccine with peptide-pulsed dendritic cells generated *in vitro* from CD34(+) hematopoietic progenitor cells. Int. J. Cancer, *86:* 385–392, 2000.

Cytotoxic T lymphocytes derived from bone marrow mononuclear cells of multiple myeloma patients recognize an underglycosylated form of MUC1 mucin

Hisaya Noto, Tohru Takahashi, Yusuke Makiguchi, Toshiaki Hayashi, Yuji Hinoda and Kohzoh Imai

First Department of Internal Medicine, Sapporo Medical University School of Medicine S-1, W-16, Chuo-ku, Sapporo 060, Japan

Abstract

MUC1 is a highly immunogenic epithelial mucin and serves as a tumor-associated antigen in breast, pancreatic and ovarian carcinomas. We previously reported the expression of MUC1 on myeloma cells and the establishment of an HLA-unrestricted cytotoxic T lymphocyte (CTL) line TN that recognized MUC1 from peripheral blood mononuclear cells in a multiple myeloma patient. In this study, we attempted to induce such CTL from six other multiple myeloma patients consecutively in order to show that the induction of the CTL line TN had not resulted from some idiosyncrasy of the first patient. Bone marrow mononuclear cells were used to induce CTL, because they contain myeloma cells that might stimulate the autologous lymphocytes. Bulk CTL lines were induced from two out of six patients. The CTL line TS was CD8$^+$ cell dominant and KY was CD4$^+$ cell dominant. Both CTL lines lysed MUC1$^+$ myeloma and breast carcinoma cell lines. The cytotoxicity of the CTL lines was inhibited by anti-CD3, anti-αβ TCR and anti-MUC1 mAb. It was also inhibited by a MUC1 transfectant, but not by a mock transfectant in cold target inhibition assays. MUC1 was transfected into a human colonic carcinoma cell line. The reactivity of anti-MUC1 core protein mAb and the cytotoxicity of the CTL against the transfectant was enhanced by the treatment of the cells with an O-glycosylation inhibitor. Thus it is generally accepted that the HLA-unrestricted CTL which directly recognize the underglycosylated form of MUC1 using their TCR could be induced from a certain proportion (~30%) of untreated multiple myeloma patients.

Introduction

MUC1 is a mucin molecule produced by ductal epithelial cells of a variety of tissues and also by tumors derived from these tissues. It is a type I transmembrane glycoprotein with unique extracellular domains mostly consisting of tandem repeats of 20 amino acids (1–3). The number of tandem repeats is 25–100 or more and varies among individuals or derived tissues. MUC1 contains a lot of O-linked glycosylation sites, and the level of glycosylation varies among different tissues and between normal and malignant cells. The cytoplasmic tail of MUC1 contains tyrosine phosphorylation sites and tyrosine phosphorylated MUC1 directly interacts with the SH2 domain of the adaptor protein Grb2 (4). It has thus been suggested to have a role in intracellular signaling.

MUC1 is highly immunogenic—autoantibodies against it have been detected not only in sera of cancer patients but also in sera of ulcerative colitis patients (5–7). Moreover, CTL against MUC1 have also been induced in pancreas, breast and ovarian cancer patients (8–10). Interestingly, these CTL directly recognized MUC1 molecules in an HLA-unrestricted manner unlike conventional CTL. It was proposed that normally cryptic CTL epitopes on the MUC1 core protein were unmasked by underglycosylation in tumor cells and the highly multivalent epitopes of tandemly repeated peptides on a single MUC1 molecule cross-linked the TCR of anti-MUC1 CTL.

MUC1 was also detected in non-epithelial cells as epithelial

membrane antigen (EMA), especially in lymphoid malignancies (11). We previously reported the expression of MUC1 on myeloma cells and the detection of circulating MUC1 molecules in ~50% of our multiple myeloma patients (12). We have established an anti-myeloma CTL line TN from peripheral blood mononuclear cells (PBMC) in a stage III multiple myeloma patient. TN recognized MUC1 in an HLA-unrestricted manner. This suggested that the precursors of HLA-unrestricted CTL reacting with MUC1 could exist in multiple myeloma patients, though the supposition that the CTL line was accidentally induced because of some idiosyncrasy of that patient is a possibility which still has to be eliminated. Moreover, a more efficient way to induce the CTL from multiple myeloma patients will be required if this is to be used clinically in immunotherapy for multiple myeloma on the basis of anti-MUC1 immunity.

To address these issues, we performed allogeneic mixed leukocyte tumor cell culture (MLTC) to induce the CTL in six consecutive non-treated multiple myeloma patients, with bone marrow mononuclear cells instead of PBMC as a source of MLTC in this study. We expected that bone marrow mononuclear cells would be the better source because they contained myeloma cells that might stimulate the autologous lymphocytes. Moreover, it was also expected that the bone marrow lymphocytes might be pre-sensitized by myeloma cells more often than peripheral blood lymphocytes. CTL were consequently induced in two out of six myeloma patients. These CTL showed HLA-unrestricted cytotoxicity· and their target molecule appeared to be MUC1. Moreover, we showed exposure of the CTL epitope on MUC1 by an O-glycosylation inhibitor, with the cytotoxicity being markedly enhanced. These findings may confer meaning in the design of immunotherapy of multiple myeloma.

Methods

Cell lines and cell culture

Cell cultures were maintained in RPMI 1640 supplemented with 25 mM HEPES, 25 mM sodium bicarbonate, 200 mg/l ampicillin, 100 mg/l kanamycin and 10% (v/v) FCS. MDA-MB-231, SK-BR-3 and MRK-nu-1 are breast carcinoma cell lines. JRST and Kato III are gastric carcinoma cell lines. CHCY1 and DLD-1 are colonic carcinoma cell lines. RPMI8226, KR4, KR12 and TAPC were myeloma cell lines. RPMI1788 is a B cell line. CEM is a T cell line. K562 is an erythroleukemic cell line. EJ-NIH-3T3 is a mouse fibroblast cell line transfected with human activated H-ras gene.

MUC1$^+$-EJ-NIH-3T3 is a sense MUC1 gene transfectant and MUC1$^-$-EJ-NIH-3T3 is an anti-sense MUC1 gene tranfectant as previously described (12). HLA allelic typing of tumor cell lines was performed by PCR-RFLP, PCR-SSOP or PCR-SSP methods at the Shionogi Biomedical Laboratory, Osaka, Japan as described elsewhere (13–17).

Establishment of CTL lines

Mononuclear cells of six consecutive multiple myeloma patients were separated from heparinized bone marrow blood by Ficoll-Paque (Pharmacia, Pisctaway, NJ). Bone marrow mononuclear cells were cultured in the medium described

above supplemented with heat-inactivated human AB serum instead of FCS. We did not add tumor cells in initial culture because contaminating myeloma cells could be stimulator cells for lymphocytes. Three days after the onset of the culture, recombinant IL-2 (a gift from Takeda Pharmaceutical, Osaka, Japan) was added at a final concentration of 5 IU/ml. The cultured cells were stimulated with RPMI8226 cells at a lymphocyte:stimulator ratio of 20:1 on day 7. A different tumor cell line was used for the second stimulation in order to minimize the induction of allo-reactive T cells. The cells were re-stimulated on day 14 with MDA-MB-231, on day 21 with KR12 and on day 28 with RPMI1788. Cell culture was expanded in proportion to proliferation of the lymphocytes. The lymphocytes used in this study were >4 weeks old grown in vitro. Tumor cell lines were treated with mitomycin C (50 mg/ml; Sigma, St Louis, MO) at 37°C for 30 min and washed three times with culture medium before use.

Cell-mediated cytotoxicity assay

Cell-mediated cytotoxicity was assessed with ^{51}Cr release assay as previously described (12). Briefly, ~1×10^6 target cells were suspended in 1 ml of culture medium and labeled with 100 mCi of ^{51}Cr (New England Nuclear, Boston, MA) for 45–60 min at 37°C and washed three times. Then 5×10^3 labeled cells were seeded into each well of 96-well U-bottomed tissue culture plates (Costar, Cambridge, MA). Effector cells were added at various E:T ratios and assays were performed in triplicate. The plates were incubated for 4 h at 37°C in a 5% CO$_2$ atmosphere. Supernatants were harvested with a Skatron harvesting system (Skatron, Stering, VA) and assayed in a γ-counter. Percent specific lysis was calculated as: (experimental release – spontaneous release)/ (maximum release – spontaneous release)×100. Spontaneous release was measured by incubating target cells in the medium alone and maximum release was obtained by adding 1% (v/v) Triton X-100 (Katayama Chemical, Osaka, Japan) in PBS to target cells.

For cold target inhibition assays, unlabeled inhibitor cells (cold targets) were seeded in plates at various cold to hot target ratios. Effector cells were then added and incubated for 30 min at 37°C before labeled target cells (hot targets) were added. Cytotoxicity was assessed as described above. Percent inhibition was calculated as: (% specific lysis without cold target – % specific lysis with cold target)/(% specific lysis without cold target)×100.

Antibodies

mAb T4 (anti-CD4), mAb T8 (anti-CD8) and MSIgG (control antibody) were obtained from Coulter Immunology (Hialeah, FL). mAb UCHT1 (anti-CD3), W6/32 (anti-HLA class I), DK22 (anti-HLA DR) and E29 (anti-EMA; anti-protein core epitope of MUC1) were purchased from Dakopatts (Glostrup, Denmark). mAb MUSE11 recognizes a protein core epitope of MUC1 (18) and was purified using a Protein A column (MAPS II system; BioRad, Richmond, CA). mAb against CD16, αβ TCR and γδ TCR were obtained from T cell Science (Boston, MA). mAb TCR Pan αβ used for the blocking assay was purchased from Immunotech (Marseille, France). .

For target blocking assays, antibodies W6/32, DK22, MUSE11, E29 or MSIgG were added to the wells in which

^{51}Cr-labeled target cells had been seeded. The effector cells were added after the plates had been incubated for 30 min at room temperature. For effector blocking assays, mAb UCHT1, TCR Pan αβ, T4, T8 or MSIgG were added to the wells in which lymphocytes had been seeded. The target cells were added after the cells had been incubated for 30 min at room temperature. Then the cytotoxicity assays were performed as described above.

For determination of cell surface phenotype of TS and KY cells, indirect immunofluorescent assays were performed as previously described (19). Briefly, cells were incubated with a saturating amount of mAb for 30 min on ice, washed twice with PBS and then incubated with FITC-conjugated rabbit anti-mouse Ig (Dakopatts) for 30 min on ice. After washing twice with PBS, cells were analyzed by flow cytometry (Epics Profile II, Coulter Electronics).

Establishment of MUC1-transfected cells and inhibition of glycosylation with benzyl-α-GalNAc

Transfection of MUC1 gene into a human colonic carcinoma cell line CHCY1 was performed as previously described (12). A mammalian expression vector pHβAPr-1-neo containing the full-length MUC1 cDNA (20) and a vector containing antisense MUC1 cDNA were kindly provided by Dr Richard S. Metzgar, Duke University. Liposome–DNA mixture was made of 20 μg of the plasmid DNA and 60 μl of Transfectace (Gibco/BRL, Grand Island, NY) in 6 ml of DMEM. CHCY1 cells were washed twice with DMEM and then incubated with 6 ml of the liposome–DNA mixture over night. Then, 6 ml of DMEM supplemented with 20% FCS (v/v) was added and the cells were incubated for 24 h. The media were then replaced with DMEM with 10% FCS (v/v) and they were then incubated for another 72 h. G418 (Geneticin; Gibco/BRL) was added in the culture at a concentration of 800 μg/ml. The transfectants were cloned by limiting dilution. MUC1$^+$-CHCY1 is a sense MUC1 gene transfectant and MUC1$^-$-CHCY1 an anti-sense MUC1 gene tranfectant.

For inhibition of glycosylation, MUC1$^+$-CHCY1 cells and MUC1$^-$-CHCY1 cells were incubated in 10% FCS/RPMI 1640 supplemented with 5 mM benzyl-GalNAc (Sigma) for 5 days. Benzyl-GalNAc is a competitive inhibitor of mucin glycosylation (21).

Results

Establishment and characterization of CTL lines TS and KY

Bone marrow lymphocytes stimulated with allogeneic MUC1-positive cells proliferated for at least 3 weeks, though four out of six cultured cells declined in number after having been cultured for a longer time. Two out of six cultured cells proliferated up until 10 weeks, and the CTL lines TS and KY were established. The analysis of KY cells was limited because we could not obtain sufficient CTL from the small number of initially cultured bone marrow cells.

Cytotoxicity of TS and KY cells was investigated using a panel of human tumor cell lines (Table 1). TS cells showed definite cytotoxicity against two of three breast carcinoma cell lines, four of four myeloma cell lines, two of two gastric carcinoma cell lines, two of two colonic carcinoma cell lines

and against a B cell line. KY cells showed less broad activity, though one of three breast carcinoma cell lines and three of three myeloma cell lines were lysed. All the cell lines lysed by the CTL lines expressed MUC1 mucin as judged by mAb (data not shown). HLA-allelic typing of the tumor cell lines lysed by the CTL disclosed no apparent HLA-A, -B, -C or -DR restriction (Table 2). NK/LAK cell-sensitive K562 cells were not killed by either TS or KY cells at all, thus the broad reactivity of these CTL lines is not explained by a non-specific NK/LAK cell-like activity.

Cell surface phenotypes of the CTL lines were analyzed by flow cytometry (Fig. 1). CTL lines TS and KY expressed CD3 and TCR αβ chains, but not γδ TCR or a NK cell marker, CD16. Other NK cell markers CD56 and CD57 were also negative (data not shown). TS cells mainly consisted of CD8$^+$ (86.2%). On the contrary, most KY cells were positive for CD4 (89.3%).

Characterization of lysis mediated by the CTL

Blocking assays using mAb were performed to investigate the mechanism of recognition of target cells. As shown in Fig. 2(A and C), the cytotoxicity of TS and KY cells was inhibited by an anti-CD3 mAb, though no significant inhibition by an anti-CD4 mAb nor by an anti-CD8 mAb were observed in effector blocking assays. In target blocking assays, no definite inhibition by anti-HLA mAb were observed (Fig. 2B and D). These results were in agreement with our previous report about the HLA-unrestricted CTL line TN. Together with the HLA-allelic typing DATA, HLA is not likely to be the target molecule recognized by TS and KY cells.

Both CTL lines were considered to have used their CD3–TCR complex for recognition of the target antigen. The TCR usage of TS cells was confirmed by a separate experiment using an anti-αβ TCR mAb (Fig. 3). The cytotoxicity of TS cells was clearly inhibited by an anti-αβ TCR mAb as well as by an anti-CD3 mAb in a dose-dependent manner.

Target antigen for TS and KY cells

To investigate the target molecule of the CTL lines, an H-ras-transformed mouse fibroblast cell line, EJ-NIH-3T3, was transfected with a sense MUC1 gene and an anti-sense MUC1 gene. We anticipated that accidental HLA matching would be precluded by using the mouse cell line. LAK cells equally killed both the transfectants (data not shown). Thus, the transfection of the MUC1 gene did not affect the suscepti-bility of the cells to non-specific effector cells. TS cells showed significant cytotoxicity against MUC1$^+$-EJ-NIH-3T3, but only marginal cytotoxicity was observed against MUC1$^-$-EJ-NIH-3T3 (Fig. 4A). Thus, MUC1 is considered to be the target molecule of TS cells. The cytotoxicity of TS cells against the myeloma cell line RPMI8226 was clearly inhibited by MUC1$^+$-EJ-NIH-3T3, but not by MUC1$^-$-EJ-NIH-3T3, in cold target inhibition assays (Fig. 4B). Therefore, TS cells can recognize myeloma cells through the MUC1 molecule.

As shown in Fig. 4(C), KY cells did not lyse either MUC1$^+$-EJ-NIH-3T3 or MUC1$^-$-EJ-NIH-3T3. As the cytotoxicity of KY cells against RPMI8226 was clearly inhibited by MUC1$^+$-EJ-NIH-3T3 but not by MUC1$^-$-EJ-NIH-3T3 (Fig. 4D); however, KY cells also appeared to be able to recognize MUC1 on myeloma cells.

Table 1. Cytotoxicity of CTL lines TS and KY against a panel of cell lines determined by ^{51}Cr-release assay

Cell type	Cell line	Specific lysis of TS (%)			Specific lysis of KY (%)		
		20[a]	10	5	20	10	5
Myeloma	KR4	44	22	22	_[b]	–	–
	KR12	117	104	82	45	33	19
	RPMI8226	48	44	33	78	71	50
	TAPC	107	95	76	36	13	4
Breast	MDA-MB-231	65	45	28	42	18	9
	SK-BR-3	44	21	5	7	4	3
	MRK-nu-1	2	–1	0	8	7	4
Gastric	JRST	19	13	5	4	13	11
	Kato III	75	69	52	–	–	–
Colonic	DLD-1	65	45	28	1	0	2
	CHCY1	29	15	8	–	–	–
B cell	RPMI1788	28	20	14	–	–	–
T cell	CEM	6	3	4	–	–	–
Erythroid	K562	4	2	–4	2	1	–2

[a]E/T ratio.
[b]Not done.

Table 2. HLA allelic typing of cell lines lysed by CTL

Cell line	HLA-A	HLA-B	HLA-C	HLA-DR
KR-4	A*0201/0201	B*1801/1801	Cw*0701/0701	DRB1*1104/1104
RPMI8226	A*3001/6802	B*1503/1510	Cw*0202/0304	DRB1*0301/0301
TAPC	A*0207/2402	B*1518/4601	Cw*0102/0704	DRB1*0401/08032
MDA-MB-231	A*0201/0217	B*4002/4101	Cw*0202/1701	DRB1*0701/1305
JRST	A*2402/2402	B*1501/1501	Cw*0303/0303	DRB1*0403/0403
Kato III	A*0201/0207	B*1501/4601	Cw*0102/0303	DRB1*08032/1501
DLD-1	A*0201/2402	B*0801/3501 or 3507	Cw*0401/0701	DRB1*0301/1401
CHCY1	A*6802/6802	B*1503/1503	Cw*0802/1203	DRB1*0102/0102
RPMI1788	A*0201/3301	B*1401 or 1402/0705	Cw*0802/1505	DRB1*04051/0701

A blocking assay of TS cells was also performed using anti-MUC1 mAb. As shown in Fig. 5, anti-MUC1 mAb MUSE11 and E29 clearly inhibited the cytotoxicity of TS cells; the epitope of the CTL was thus considered to exist in the protein core of MUC1.

Inhibition of glycosylation affects recognition by antibody and CTL

The MUC1 gene was transfected into a human colonic carcinoma cell line CHCY1 which expressed MUC1 weakly. As shown in Fig. 6, MUC1^{+}-CHCY1 cells showed only a minor augmentation of reactivity to an anti-MUC1 mAb when compared to MUC1^{-}-CHCY1 cells. When the MUC1^{+}-CHCY1 cells were treated with O-glycosylation inhibitor benzyl-α-GalNAc, reactivity of the mAb was strongly increased.

We then investigated the cytotoxicity of TS cells against these above cells to see the effect of O-glycosylation inhibitor. As shown in Fig. 7, susceptibility of lysis by TS cells was strikingly augmented by the O-glycosylation inhibitor treatment of the MUC1 transfectant. On the contrary, no such enhancement of lysis was observed in the mock transfectant. Therefore increase in cytotoxicity could not be due to general cytotoxic effects of benzyl-α-GalNAc. The susceptibility of the cells seemed almost parallel to the reactivity to the mAb.

Discussion

A lot of studies have indicated that the immune repertoire of cancer patients contains B and T cells that recognize antigens expressed by autologous cancer cells. Recently, several genes encoding human tumor rejection antigens of melanoma and breast carcinoma have been identified (22). Those antigens were presented by HLA class I molecules as short peptides and recognized by autologous CD8^{+} CTL. Several studies to identify the epithelial tumor rejection antigens are currently under progression (23–25).

In hematological malignancies, only a few studies have been performed to suggest the existence of tumor rejection antigens recognized by CTL (26–28). Graft-versus-tumor responses without graft-versus-host disease by infusion of donor leukocytes in relapsed leukemia and myeloma patients after bone marrow transplantation were reported (29–31). This was circumstantial evidence supporting the existence of tumor rejection antigens in hematological malignancies.

In the previous study, we established an HLA-unrestricted CTL line TN which reacted with MUC1 from peripheral blood of a multiple myeloma patient with a large tumor burden. As far as we know, no other defined tumor-associated antigens recognized by CTL in multiple myeloma have been reported.
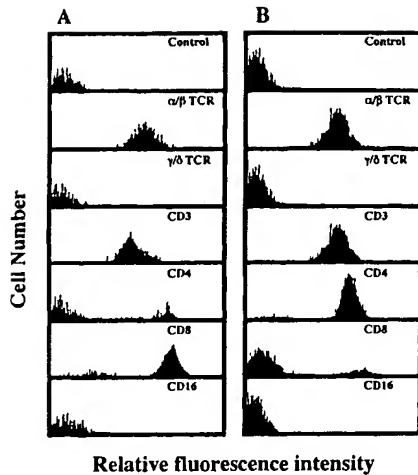
Relative fluorescence intensity

Fig. 1. Flow cytometric analysis of surface antigen expression of CTL. TS cells (A) and KY cells (B) were stained with mAb (corresponding CD numbers are indicated) and analyzed with Epics Profile II flow cytometry. The cells stained without the first antibody were used as a control. Fluorescence intensities are shown on a log scale. The analysis was performed on all the cells in the viable lymphocyte population determined by the forward and 90° light scatter profiles.
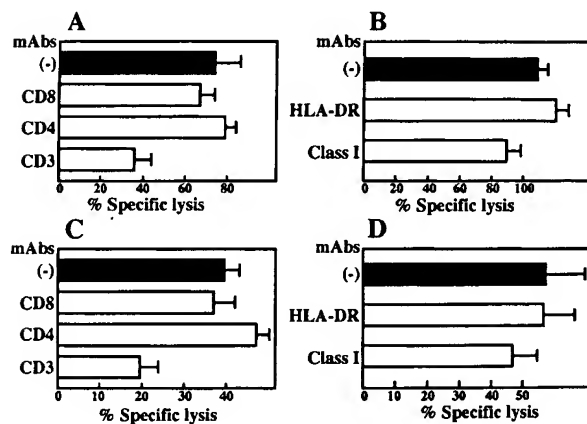

Fig. 3. Involvement of $\alpha\beta$ TCR in recognition of target cells. TS cells were incubated with anti-$\alpha\beta$ TCR mAb, anti-CD3 mAb and MSIgG (control) at various concentrations and then cytotoxicity assays were performed against MDA-MB 231. E:T ratio was 10:1.

Fig. 2. Inhibition of cytotoxicity of CTL by mAb. (A and C) Cytotoxicity assay after incubating effector cells with mAb. TS cells (A) and KY cells (C) were incubated with mAb against CD3, CD4 and CD8, and then cytotoxicity assays were performed against RPMI8226 cells. The final concentration of the mAb was 5 µg/ml. (B and D) Cytotoxicity assay after incubating target cells with mAb. RPMI8226 cells were incubated with anti-HLA class I and DR mAb and then cytotoxicity assays of TS (B) and KY (D) were performed. The final concentration of mAb was 50 µg/ml. E:T ratios were 10:1 (A and B) and 5:1 (C and D). The bars mean ± SE of triplicate samples.

Fig. 4. Target antigen recognition by CTL. (A and C) Cytotoxicity assay of TS cells (A) and KY cells (C) against MUC1$^+$-EJ-NIH-3T3 and MUC1$^-$-EJ-NIH-3T3. (B and D) Cold target inhibition assay. Cytotoxicity assays against a myeloma cell line RPMI8226 were performed after incubating effector cells with unlabeled inhibitor cells. E:T ratios were 10:1 (B) and 5:1 (D).

T cells in bone marrow mononuclear cells of multiple myeloma patients have recently been shown to possess distinct features in terms of susceptibility to CD3 stimulation and cytokine production compared with normal bone marrow T cells and this could be exploited to generate anti-plasma cell activity (32). In this study, we therefore used bone marrow mono-
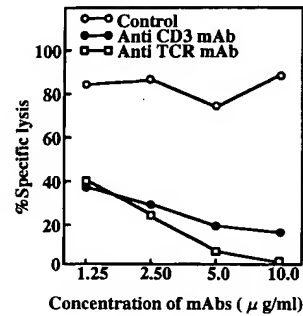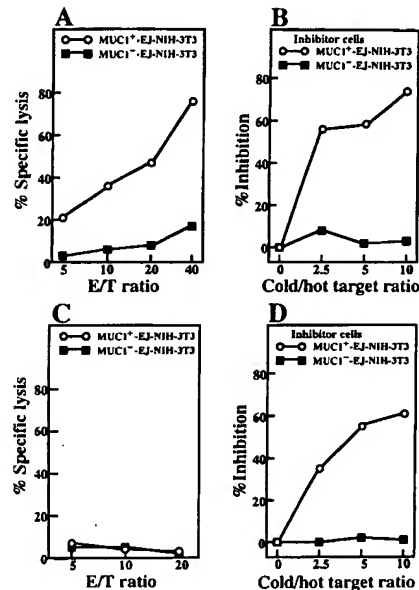
nuclear cells as a source of lymphocytes in the expectation of a more efficient induction of CTL than would be the case by PBMC. Moreover, we tried to induce the CTL from six consecutive untreated multiple myeloma patients to eliminate the possibility that such CTL could have been accidentally induced by an idiosyncratic immune response of the previous patient. Two CTL lines designated as TS and KY were successfully induced from the bone marrow mononuclear cells. The CTL lines showed broad cytotoxicity against MUC1-positive tumor cell lines regardless of the cell type, with the exception of K562 cells which are sensitive to NK/LAK cells. The cytotoxicities were not restricted by HLA-A, -B, -C or -DR
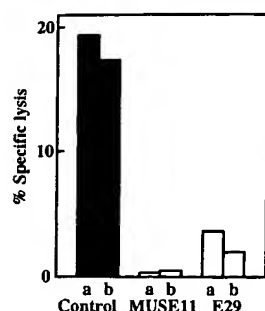
Fig. 5. Blocking of cytotoxicity of TS cells by anti-MUC1 mAb. MDA-MB-231 cells were incubated with mAb MUSE11, mAb E29 or MSIgG (control) and then cytotoxicity assays were performed. E:T ratio was 10:1. Final concentrations of antibodies were (a) 25 μg/ml and (b) 12.5 μg/ml. Percent specific lysis without mAb was 15%.

Fig. 7. Cytotoxicity of TS cells against MUC1 transfectant treated with benzyl-GalNAc. BG denotes treatment with an O-glycosylation inhibitor benzyl-GalNAc for 5 days.

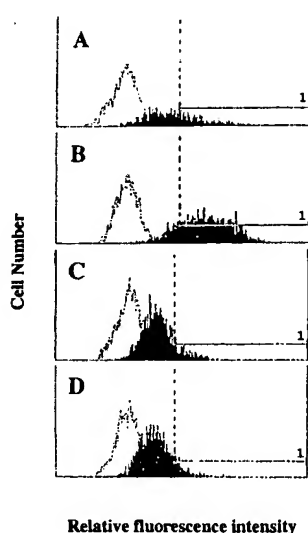

Relative fluorescence intensity

Fig. 6. Effect of benzyl-GalNAc on reactivity of an anti-MUC1 mAb against transfectants. MUC1⁺-CHCY1 cells (A), benzyl-GalNAc-treated MUC1⁺-CHCY1 cells (B), MUC1⁻-CHCY1 cells (C) and benzyl-GalNAc-treated MUC1⁻-CHCY1 cells (D) were stained with mAb MUSE11 or without the first antibody as controls (dotted lines), and analyzed with Epics Profile II flow cytometry. Fluorescence intensities are shown on a log scale. The cells whose fluorescent intensities exceeded vertical broken lines were calculated as positive. Percent positive cells were as follows: (A) control 0.0%, MUSE11 40.4%; (B) control 0.1%, MUSE11 82.3%; (C) control 0.1%, MUSE11 15.6%; (C) control 0.0%, MUSE11 17.9%.

as judged by HLA-allelic typing. The cytotoxicities of both CTL lines were not inhibited by anti-HLA mAb. Anti-MUC1 mAb directly inhibited the cytotoxicity of TS cells. Moreover, inhibition of cytotoxicity against myeloma cells was observed by a mouse cell line transfected with MUC1 cDNA but not by antisense transfectants. Thus, the HLA-unrestricted CTL recognizing MUC1 were demonstrated to be inducible from bone marrow cells of multiple myeloma patients.

The cytotoxicities of the CTL lines were inhibited by anti-CD3 and anti-αβ TCR mAb. Thus the CTL lines were considered to
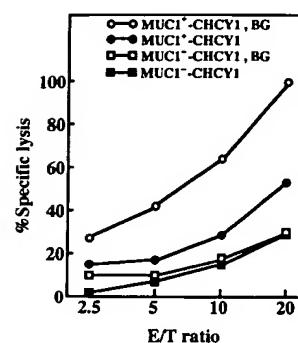
have used their CD3–TCR complex for recognition of the target antigen. However, the contribution of not only TCR but other molecules (CD2, LFA-1 or other adhesion molecules) should be also considered because it is possible that the antibody treatment inhibited the signal from other molecules which bind to MUC1.

Treatment of MUC1-transfected Epstein–Barr virus-transformed B cells or normal mammary epithelial cells using O-glycosylation inhibitor phenyl-GalNAc or benzyl-GalNAc resulted in the exposure of tumor-associated epitopes recognized by anti-MUC1 protein core mAb (33,34) and MUC1 transfected Epstein–Barr virus-transformed B cells treated with the inhibitor became more susceptible to an anti-MUC1 CTL clone than the non-treated cells (35). We also investigated the effect of an O-glycosylation inhibitor on the recognition of MUC1 by the CTL. In this study, we transfected the MUC1 gene into the colon cancer cell line CHCY1. Treatment of the transfectant with O-glycosylation inhibitor benzyl-GalNAc resulted in marked enhancement of reactivity with an anti-MUC1 mAb. Thus, MUC1 in CHCY1 cells is considered to be highly glycosylated and most of the core protein epitopes were masked by carbohydrate chains. The susceptibility to the CTL was also strikingly augmented by the treatment. In agreement with the previous report, our CTL line also recognized a protein core epitope on MUC1 which can be exposed through underglycosylation.

CTL line KY mainly consisted of CD4⁺ T cells and showed less broad cytotoxicity than TS did. KY cells also failed to lyse the MUC1 transfected mouse cell line. However, cytotoxicity against the myeloma cell line RPMI8226 was clearly inhibited by the MUC1 transfectant in a cold target inhibition assay. CD4⁺ CTL preferentially lyse their targets via Fas–Fas ligand interaction, whereas the major cytotoxic effect of CD8⁺ CTL is by perforin and granzymes (36). It was reported that most myeloma cells expressed Fas and RPMI8226 cells showed a high sensitivity to Fas-mediated apoptosis (37). Lack of the human Fas molecule on the mouse cells may explain the resistance of the MUC1 transfectant to KY cells. The less broad cytotoxicity of KY might be due to lack of Fas on the tumor cell lines. However, we could not confirm apoptotic lysis of myeloma cells by CTL line KY because of the limited number of the cells. We also could not

conclude that the CD4$^+$ T cells were responsible for the target cell lysis simply because KY cells mainly consisted of CD4$^+$ T cells.

Multiple myeloma cannot be cured with standard chemotherapy. The use of high doses of chemoradiotherapy followed by hematopoietic stem cell transplantation has shown promise for selected patients with myeloma in some preliminary studies (38). However, multiple myeloma remains incurable at present and innovative treatments should be explored. In addition to the search for better chemotherapeutic regimens, therapies based on immunological modalities for multiple myeloma are under investigation (39–41). Our study indicated that a certain proportion (~30%) of myeloma patients are expected to harbor the CTL precursors against myeloma cells. Thus immunotherapy based on anti-MUC1 immunity such as vaccination using MUC1 transfectant treated with O-glycosylation inhibitor or adoptive transfer of *ex vivo* induced anti-MUC1 CTL might be considered as an alternative modality to chemotherapy in the near future.

Acknowledgement

Abbreviations

benzyl-GalNAc	benzyl-2-acetamido-2-deoxy-α-D-. galactopyranoside
CTL	cytotoxic T lymphocyte
EMA	epithelial membrane antigen
LAK	lymphokine activated killer
MLTC	mixed leukocyte tumor cell culture
PBMC	peripheral blood mononuclear cell

References

1 Hareuveni, M., Tsarfaty, I., Zaretsky, J., Kotkes, P., Horev, J., Zrihan, S., Weiss, M., Green, S., Lathe, R., Keyder, I. and Wreschner, D. H. 1990. A transcribed gene, containing a variable number of tandem repeats, codes for a human epithelial tumor antigen. cDNA cloning, expression of the transfected gene and over-expression in breast cancer tissue. *Eur. J. Biochem.* 189:475.

2 Lan, M. S., Batra, S. K., Qui, W.-N., Metzgar, R. S. and Hollingsworth, M. A. 1990 Cloning and sequencing of a human pancreatic tumor mucin cDNA. *J. Biol. Chem.* 265:5573.

3 Merlo, G. R., Siddiqui, J., Cropp, C., Liscia, D. S., Lidereau, R., Callahan, R. and Kufe, D. 1989. Frequent alteration of the DF3 tumor-associated antigen gene in primary human breast carcinomas. *Cancer Res.* 49:6996.

4 Pandy, P., Kharbanda, S. and Kufe, D. 1995. Association of the DF3/MUC1 breast cancer antigen with Grb2 and Sos/Ras exchange protein. *Cancer Res.* 55:4000.

5 Rughetti, A., Turchi, V., Ghetti, C. A., Scambia, G., Panici, P. B., Roncucci, G., Mancuso, S., Frati, L. and Nuti, M. 1993. Human B-cell immune response to polymorphic epithelial mucin. *Cancer Res.* 53:2457.

6 Kotera, Y., Fontenot, J. D., Pecher, G., Metzgar, R. S. and Finn, O. J. 1994. Humoral immunity against a tandem epitope of human mucin MUC1-1 in sera from breast, pancreatic, and colon cancer patients. *Cancer Res.* 54:2856.

7 Hinoda, Y., Nakagawa, N., Nakamura, H., Makiguchi, Y., Itoh, F., Adachi, M., Yabana, T., Imai, K. and Yachi, A. 1993. Detection of

8 Barnd, D. L., Lan, M. S., Metzgar, R. S. and Finn, O. J. 1989. Specific, major histocompatibility complex-unrestricted recognition of tumor-associated mucins by human cytotoxic T cells. *Proc. Natl Acad. Sci. USA* 86:7159.

9 Jerome, K. R., Barnd, D. L., Bedt, K. M., Boyer, C. M., Taylor-Papadimitriou, J., Mckenzie, I. F., Bast, R. C. and Finn, O. J. 1991. Cytotoxic T-lymphocytes derived from patients with breast adenocarcinoma recognize an epitope present on the protein core of a mucin molecule preferentially expressed by malignant cells. *Cancer Res.* 51:2908.

10 Ioannides, C. G., Fisk, B., Jerome, K. R., Irimura, Wharton, T. J. and Finn, O. J. 1993. Cytotoxic T cells form ovarian malignant tumors can recognize polymorphic epithelial mucin core peptides. *J. Immunol.* 151:3693.

11 Duperry, C., Klein, B., Durie, B. G. M., Zhang, X., Jourdan, M., Poncelet, P., Favier, F., Vincent, C., Brochier, J., Lenoir, G. and Bataille, R. 1989. Phenotype analysis of human myeloma cell lines. *Blood* 73:566.

12 Takahashi, T., Makiguchi, Y., Hinoda, Y., Kakiuchi, H., Nakagawa, N., Imai, K. and Yachi, A. 1994. Expression of MUC1 on myeloma cells and induction of HLA-unrestricted cytotoxic T lymphocytes against MUC1 from a multiple myeloma patient. *J. Immunol.* 153:2102.

13 Yoshida, M., Kimura, A., Numano, F. and Sasazuki, T. 1992. Polymerase chain reaction based analysis of polymorphism in the HLA-B gene. *Hum. Immunol.* 34:257.

14 Felnandez-Vina, M., Lazaro, A. M., Sun, Y., Miller, S., Forero, L. and Stanstny, P. 1995. Population diversity of B-locus alleles observed by high-resolution DNA typing. *Tissue Antigens* 45:153.

15 Bunce, M., O'Neil, C. M., Barnardo, M. C., Krausa, P., Browning, M. J., Morris, P. J. and Welsh, K. I. 1995. Phototyping: comprehensive DNA typing for HLA-A, B, C, DRB1, DRB3, DRB4, DRB5 and DQB1 by PCR with 144 primer mixes utilizing sequence-specific primers (PCR-SSP). *Tissue Antigens* 46:355.

16 Levine, J. E. and Yang, S. S. 1994. SSOP typing of the Tenth International Histocompatibility Workshop reference cell lines for HLA-C alleles. *Tissue Antigens* 44:174.

17 Ng, J., Hurley, C. K., Baxter-Lowe, L. A., Chopek, M., Coppo, P. A., Hegland, J., KuKuruga, D., Monos, D., Rosner, G., Schmeckpper, Yang, S. S., Dupont, B. and Hartzman, R. J. 1993. Large-scale oligonucleotide typing for DRB1/3/4/ and HLA-DQB1 is highly accurate, specific, and reliable. *Tissue Antigens* 43:473.

18 Hinoda, Y., Nakagawa, N., Ohe, Y., Kakiuchi, H., Tsujisaki, M., Imai, K. and Yachi, A. 1990. Recognition of the polypeptide core of mucin by monoclonal antibody MUSE11 against an adenocarcinoma-associated antigen. *Jpn. J. Cancer Res.* 81:1206.

19 Takahashi, T., Imai, K., Sugiyama, T., Sasaki, T. and Yachi, A. 1990. Preparation of anti-T idiotype monoclonal antibody reacting with human T leukemic cell lines and with a small percentage of peripheral T lymphocytes. *Clin. Exp. Immunol.* 82:590.

20 Batra, S. K., Kern, H. F., Worlock, A. J., Metzgar, R. S. and Hollingsworth, M. A. 1991. Transfection of the human Muc 1 mucin gene into a poorly differentiated human pancreatic tumor line, Panc1: integration, expression and ultrastructural changes. *J. Cell Sci.* 100:841.

21 Kuan, S.-F., Byrd, J. C., Basbaum, C. and Kim, Y. S. 1989. Inhibition of mucin glycosylation by aryl-N-acetyl-α-galactosamides in human colon cancer cells. *J. Biol. Chem.* 264:19271.

22 Houghton, A. N. 1994. Cancer antigens: immune recognition of self and altered self. *J. Exp. Med.* 180:1.

23 Nakao, M., Yamana, H., Imai, Y., Toh, Y., Kimura, A., Yanoma, S., Kakegawa, T. and Itoh, K. 1995. HLA A2601-restricted CTL recognize a peptide antigen expressed on squamous cell carcinoma. *Cancer Res.* 55:4284.

24 Slingluff, C. L., Cox, A. L., Stover, J. M., Moore, M. M., Hunt, D. F. and Engelhard, V. H. 1994. Cyotoxic T-lymphocyte response to autologous human squamous cell cancer of the lung: epitope reconstruction with peptides extracted from HLA-Aw68. *Cancer Res.* 54:2731.

25 Wolfel, T., Herr, W., Coulie, P., Schmitt, U., Meyer zum Buschenfelde, K.-H. and Knuth, A. 1993. Lysis of human pancreatic adenocarcinoma cells by autologous HLA-class I-restricted cytolytic T-lymphocyte (CTL) clones. *Int. J. Cancer* 54:636–644.

26 Fisch, P., Weil-Hillman, G., Upperkamp, M., Hank, J. A., Chen, B. P., Sosman, J. A., Bridges, A., Colamonici, O. R. and Sondel, P. M. 1989. Antigen-specific recognition of autologous leukemia cells and allogeneic class-I MHC antigens by IL-2 activated cytotoxic T cells from a patient with acute T-cell leukemia. *Blood* 74:343.

27 Sosman, J. A., Oettel, K. R., Smith, S. D., Hank, J. A., Fisch, P. and Sondel, P. M. 1990. Specific recognition of human leukemic cells by allogeneic T cells: II. Evidence for HLA-D restricted determinants present on unrelated nonleukemic cells. *Blood* 75:2005.

28 Faber, L. M., van Luemburg-Heijs, S. A. P., Willemze, R. and Falkenburg, J. H. F. 1992. Generation of leukemia-reactive cytotoxic T lymphocytes clones from HLA-identical bone marrow donor of a patients with leukemia. *J. Exp. Med.* 176:1283.

29 Kolb, H. J., Mittermuller, J., Clemm, Ch., Holler, E., Ledderose, G., Brehm, G., Heim, M. and Wilmanns, W. 1990. Donor leukocyte transfusion for treatment of recurrent chronic myelogenous leukemia in marrow transplant patients. *Blood* 76:2462.

30 Mackinnon, S., Papadopoulos, E. B., Carabasi, M. H., Reich, L., Collins, N. H., Boulad, F., Castro-Malaspina, H., Childs, B. H., Gillio, A. P., Kernan, N. A., Small, T. N., Young, J. W. and O'Reilly, R. J. 1995. Adoptive immunotherapy evaluating escalating doses of donor leukocytes for relapse of chronic myeloid leukemia after bone marrow transplantation: separation of graft-versus-leukemia responses from graft-versus-host disease. *Blood* 86:1261.

31 Tricot, G., Vesole, D. H., Jagannath, S., Hilton, J., Munshi, N. and Barlogie, B. 1996. Graft-versus-myeloma effect: proof of principle. *Blood* 87:1196.

32 Massaia, M., Attisano, C., Peola, S., Montacchini, L., Omede, P., Corradini, P., Ferrero, D., Boccadoro, M., Bianchi, A. and Pileri, A. 1993. Rapid generation of antiplasma cell activity in the bone marrow of myeloma patients by CD3-activated T cells. *Blood* 82:1787.

33 Jerome, K. R., Bu, D. and Finn, O. J. 1992. Expression of tumor associated epitopes on EBV-immortalized B cells and Burkitt's lymphomas transfected with epithelial mucin cDNA. *Cancer Res.* 52:5985.

34 Burchell, J. and Taylor-Papadimitriou, J. 1993. Effect of modification of carbohydrate side chains on the reactivity of antibodies core-protein epitopes of the MUC1 gene product. *Epith. Cell. Biol.* 2:155.

35 Jerome, K. R., Domenech, N. and Finn, O. J. 1993. Tumor-specific cytotoxic T cell clones from patients with breast and pancreatic adenocarcinoma recognize EBV-immortalized B cell transfected with polymorphic epithelial mucin complementary DNA. *J. Immunol.* 151:1654.

36 Hahn, S., Gehri, R. and Erb, P. 1995. Mechanism and biological significance of CD4-mediated cytotoxicity. *Immunol. Rev.* 146:57.

37 Hata, H., Matsuzaki, H., Takeya, M., Yoshida, M., Sonoki, T., Nagasaki, A., Kuribayashi, N., Kawano, F. and Takatsuki, K. 1995. Expression of Fas/Apo-1 (CD95) and apoptosis in tumor cells from patients with plasma cell disorders. *Blood* 86:1939.

38 Barlogie, B., Jagannath, S., Vesole, D. and Tricot, G. 1995. Autologous and allogeneic transplantation for multiple myeloma. *Semin. Hematol.* 32:31.

39 Anderson, K. C., Anderson, J., Soiffer, R., Freeman, A. S., Takvorian, T., Rabinowe, S. N., Robertson, M. J., Spector, N., Blake, K., Murray, C., Freeman, A., Coral, F., Mauch, P., Marcus, K. C., Nadler, N. M. and Ritz, J. 1993. Monoclonal antibody purged bone marrow transplantation therapy for multiple myeloma. *Blood* 82:2568.

40 Kwak, L. W., Taub, D. D., Duffy, P. L., Bensinger, W. I., Bryant, E. M., Reynolds, C. W. and Longo, D. L. 1995. Transfer of myeloma idiotype-specific immunity from an actively immunized marrow donor. *Lancet* 345:1016.

41 Goldmacher, V. S., Bourret, L. A., Levine, B. A., Rasmussen, R. A., Pourshadi, M., Lambert, J. M. and Anderson, K. C. 1994. Anti-CD38-blocked ricin: an immunotoxin for the treatment for multiple myeloma. *Blood* 84:3017.

This Page is Inserted by IFW Indexing and Scanning Operations and is not part of the Official Record

BEST AVAILABLE IMAGES

Defective images within this document are accurate representations of the original documents submitted by the applicant.

Defects in the images include but are not limited to the items checked:

☐ **BLACK BORDERS**

☐ **IMAGE CUT OFF AT TOP, BOTTOM OR SIDES**

☐ **FADED TEXT OR DRAWING**

☑ **BLURRED OR ILLEGIBLE TEXT OR DRAWING**

☐ **SKEWED/SLANTED IMAGES**

☐ **COLOR OR BLACK AND WHITE PHOTOGRAPHS**

☐ **GRAY SCALE DOCUMENTS**

☑ **LINES OR MARKS ON ORIGINAL DOCUMENT**

☐ **REFERENCE(S) OR EXHIBIT(S) SUBMITTED ARE POOR QUALITY**

☐ **OTHER:** _____

IMAGES ARE BEST AVAILABLE COPY.
As rescanning these documents will not correct the image problems checked, please do not report these problems to the IFW Image Problem Mailbox.